The Role of CDCA7 in Akt-mediated Myc-Dependent Apoptosis and Proliferation

Tim Gabor

A dissertation submitted to the Faculty of Graduate Studies

In partial fulfillment of the requirements for the degree of

Doctor of Philosophy

Graduate Program in Biology

York University

Toronto, Ontario, Canada

May 2018

Abstract

CDCA7, or cell division cycle associated protein A7, was described in 2001 by Prescott and colleagues as a target of Myc-dependent transcriptional regulation (Prescott et al., 2001). We have identified CDCA7 as associating with the transcription factor Myc and is the target of phosphorylation by the prosurvival serine/threonine kinase Akt. Phosphorylation by Akt at threonine 163 disrupts CDCA7 association with Myc, promotes binding to 14-3-3 and sequestration in the cytoplasm. Coexpression of CDCA7 and Myc in fibroblasts potentiates Myc-dependent apoptosis upon serum withdrawal. In contrast, knockdown of CDCA7 by shRNA abrogated Myc-dependent apoptosis. Myc induced transformation of fibroblasts was reduced in the presence of CDCA7 and significantly inhibited by the expression of the non-Myc binding mutant Δ(156-187) CDCA7. We have shown that CDCA7 enhances the activation of an E-box in a Myc-binding dependent manner. CDCA7 increases Myc occupancy of the proapoptotic BAX promoter, elevates BAX and Cyclin B1 mRNA levels while reducing $p15^{INK4B}$ mRNA levels. This data points to a novel mechanism which implicates Akt phosphorylation of CDCA7 as participating in the dual signal model of Myc of function and thus affecting Myc-dependent growth and transformation.

In this study, we have also shown that expression of CDCA7 reduces proliferation rates and shifts cell cycle distribution towards G2/M phase and that phosphorylation of CDCA7 at T163 occurs strictly in G2/M. CDCA7 phosphorylated at threonine 163 colocalizes with the centrosomal protein marker γ-Tubulin and activated Akt (phospho-serine 473) in mitotic cells. Finally, we have shown that CDCA7 co-associates with monomers of itself which is dependent on amino acids 187-234, adding to the possible mechanisms by which CDCA7 function may be regulated.

Dedication and Acknowledgments

I would like to thank my supervisor, Mike Scheid for his invaluable mentorship and guidance over the course of my graduate studies. Dr. Scheid sparked my interest in molecular biology and gave me the opportunity to pursue and nurture a lifelong long passion. I would like to also extend my sincerest appreciation to my supervisory committee, Dr. Sam Benchimol and Dr. John McDermott for their advice and direction during my graduate school career.

As we are all the product of the sum of our life experience, I would be remiss not to thank all the students and colleagues I have had the pleasure of working with, especially Amber Couzens, Adi Rakowski and Shaon Parial. I sincerely value the friendship and help you have offered me over the years, without it many of the long hours would have felt so much longer. I would like to give a special mention to Monty Gill for bestowing upon me a vast repertoire of protocols, methods and everyday lab-hacks that have helped mold me into the scientist that I am. You taught me that "There's always a reason".

Finally, I would like to extend my greatest appreciation to my family for supporting me and my quest to achieve all the goals I have set before me over the past many years. And to my unconditionally loving wife, Lena Gabor, thank you for your unwavering patience and support while I venture down this long and winding road.

Table of contents

List of figures

Chapter 1: Introduction and Research Objectives

Introduction

The long road to oncogenesis is often hastened by deregulated oncogenes or tumor suppressors which otherwise carefully work to balance the scale between cellular proliferation and apoptosis. This delicate balance is best exemplified by the oncogene Myc, which has been the subject of intense cancer research since its discovery thirty years ago. In its infancy, Myc was described as a transcription factor involved in the expression of genes involved in metabolism, adhesion, cell cycle progression, development and malignant transformation; qualities well suited for a powerful oncogene (Oster et al., 2002, Askew et al., 1991). Myc has been estimated to be active in nearly 70% of human cancers, with mechanism of activation including amplifications, translocations, deregulated translation or protein turnover (Nilsson and Cleveland, 2003). Most notably, Myc has been deemed essential in the progression of Burkitt's lymphoma due to a translocation event which puts Myc under the control of the immunoglobulin heavy locus regulatory element (Spencer and Groudine, 1991). By the early '90s it was becoming obvious that Myc would be a central player in our understanding of cancer, as 1485 papers were published on Myc within ten years of its discovery. However, in 1992 the Myc paradigm would be turned on its head when Evan and colleagues published their seminal paper describing Myc's critical role in apoptosis upon serum withdrawal from constitutive Myc expressing Rat1 fibroblasts. The group showed that as Myc levels increased, Rat1 cells became proportionally prone to apoptosis upon serum withdrawal. Thus, a paradox was born: how could two diametrically opposed functions be controlled by the same protein? When and how would the scales be tipped towards proliferation or apoptosis in this precarious balance (Evan et al., 1992)? In 1997, Kauffmann-Zeh and colleagues provided a clue when they showed that Myc induced apoptosis could be suppressed by Phosphoinositide-3 kinase

(PI-3K) and Akt activation (Kauffmann-Zeh et al., 1997). These findings were supported by the fact that simultaneously dysregulated Myc and Akt (via overactive receptor tyrosine kinases) can provide the necessary environment to promote oncogenesis (Stambolic et al., 1999). A hypothesis began to emerge which suggested that a built-in safety mechanism was in place to prevent aberrant Myc related proliferation by inducing apoptosis in the absence of survival signals (Evan et al., 1992). This lead to the 'dual-signal' model of Myc activity which postulates that Myc sensitizes cells to apoptosis but prevents their ultimate demise via signaling by survival factors such as platelet-derived growth factor (PDGF) or insulin (Harrington et al., 1994). Since the birth of the dual-signal model, it has become an accepted principle of cancer biology that apoptotic pathways mediated by oncogenes must be sidestepped during tumorigenesis, and only then can a transformed cell outgrow its environment (Schmitt et al., 2002). Therefore, the coupling of apoptotic and proliferative activities by a single oncogene presents a unique opportunity for therapeutic intervention to promote the death of tumor cells.

How Akt prevents Myc induced apoptosis remains a long-standing mystery. Akt may influence pro-apoptotic effectors such as Bad or increase Myc protein levels by indirectly stabilizing it via inhibition of T58 phosphorylation by glycogen synthase kinase 3 (GSK3), a Myc residue which is known to promote its degradation when phosphorylated (Welcker et al., 2004). Adding to the mystery, to date there have been no studies implicating Akt in directly acting upon the Myc/Max transcriptional heterodimer. The recent discovery of a Myc and E2F responsive gene known as *cdca7*, the subject of this thesis, may shed some light on the interplay between Myc and Akt and how this interaction affects apoptosis.

MYC

The transcription factor Myc is a part of the family of basic-helix-loop-helix-leucine zipper (bHLH-LZ) transcription factors and is known to both repress and activate target genes by DNA recognition of E box motifs (CACGTG) (Spencer and Groudine, 1991). Myc is encoded by an immediate early response gene which is transactivated by the stimulation of any number of upstream membrane-ligand receptor complexes (Kelly et al., 1983). Expression levels of Myc are faithfully controlled by a host of mechanisms that converge on the transcriptional regulatory motifs found within its promoter region (Levens, 2010). Peak levels of Myc expression occur at the G0-G1 transition of quiescent cells, but remains constant through out the phases of the cell cycle in proliferating cells (Thompson et al., 1985; Rabbitts et al., 1985). Therefore, Myc activity in cycling cells is mediated by mechanisms that are not confined to mRNA or protein levels.

Myc has been associated with the regulation of 15% of all genes, many of which influence functions such as the control of apoptosis, cell growth and cell division (Gearhart et al., 2007). Transactivation via Myc is promoted by heterodimerization with its partner Max (also a bHLH-LZ protein) and recruitment of coactivators along with histone acetyltransferases and ATPase/helicase among others (Nilsson and Cleveland, 2003). Repression is thought to occur when Mad heterodimerizes with Max and competes for identical E box motifs, displacing Myc and recruiting transcriptional corepressors and histone deacetylases (Rottman and Luscher, 2006). Myc activity is also controlled by keeping protein levels transient, as it is indirectly targeted by Akt for proteolytic degradation (Hann and Eisenman, 1984). There is no surprise that healthy cells exert such fine control over Myc activity, as it is often suggested that Myc is at the heart of the cell cycle progression engine. Many of the positive regulators of the cell cycle are encoded by gene targets of Myc, including cyclins, Cdks and the transcription factor E2F. Unsolicited expression

of any number of these regulators could prove to be detrimental. In addition to being directly responsible for the expression of these regulators, Myc can also exert its influence indirectly by hyperactivating cyclin/Cdk complexes by expressing Cdk activating kinase (CAK) and Cdc25 phosphatase. Completion of the cell cycle at mitosis is also influenced by Myc as it is known to bind to origins of replication and expresses genes that are vital to replication initiation (Bretones et al., 2015).

Perhaps the most intriguing discovery from Myc's sphere of influence is the role it plays in the production of induced pluripotent stem cells (iPSC). In 2006, Yamanaka and his colleagues identified Sox2, Oct4, KLF4 and Myc as the four critical factors (dubbed Yamanaka factors) required in reverting fibroblasts back into a pluripotent stem-cell-like state. A feat which would earn the group a Noble Prize. By retroviral integration of the corresponding coding sequences into the genome of terminally differentiated fibroblasts, the Yamanaka lab recapitulated the four hallmarks of pluripotent stem cells: spontaneous differentiation in cell culture, embryoid body formation, teratoma formation and contribution to embryo development (Takahashi et al., 2006). Although a very exciting prospect for regenerative medicine, the contribution of Myc to iPSC generation should come as no surprise as its expression is required for vertebrate development (Stanton et al., 1990).

Molecular Profile of Myc

The transcription factor Myc is encoded by the MYC gene which produces a polypeptide that is 57-65 kDa in size. Transcription can initiate at one of three start codons: a canonical AUG, an upstream CUG or a downstream AUG (Blackwood et al., 1994). Expression from the non-canonical start codons results in versions of Myc for which there is little information regarding form or function. Myc transcribed from the canonical AUG has been thoroughly investigated and

is the subject of the review here. This isoform of Myc contains an N-terminal transcriptional regulatory domain located up stream of a nuclear localization signal (NLS). This domain has been shown to form complexes with a variety of proteins including GCN5, TBP and TRRAP, all of which promote transcriptional activity primarily via epigenetic modifications such as histone acetylation (Dang, 2012). The C-terminus contains a basic DNA-binding domain followed by a helix-loop-helix-leucine zipper (bHLH-LZ) motif that is critical for Myc's ability to heterodimerize with Max (Spencer and Groudine, 1991). Monomers of the Myc-Max heterodimer make contact with target genes via their DNA binding domains at E-box motifs (5'-CACGTG3') (Park et al., 2004). Both the basic DNA-binding domain and bHLH-LZ region have been shown to be required for transformation (Dang et al., 1989; Stone et al., 1987). Although Myc seems committed to binding Max in order to interact with DNA, Max has the ability to heterodimerize with other members of the Mxd family via their bHLH-LZ domains. For example, Mad can compete with Myc for Max binding, thereby forming Mad-Max heterodimers which bind DNA at E-boxes and repress activation by recruitment of histone deacetylases (Ayer et al., 1993).

Myc and Cell Proliferation

In normal tissue, Myc is abundantly expressed during development and it is ubiquitous in adult tissues which have high proliferative potential, such as the gut and epidermis (Schmid et al., 1989). On the contrary, Myc is not detected in cells which have left the cell cycle (Davis et al., 1993). Current estimates suggest that activation of Myc occurs in approximately 70% of cancers, indicating this lesion is a perquisite for tumorigenesis. Myc activation can occur through all conceivable means including translocations, increased translation, amplification and improved protein stability (Sears et al., 1999). Elevated expression of Myc has been detected in various types of cancer including myeloid leukaemia, melanoma, glioblastomas, osteosarcomas, small lung

carcinomas, colon, cervical and breast (Khan and Pelengaris, 2007). Gain of function mutations within Myc have been reported, however most examples of Myc activation are a result of unsolicited errors within the signalling pathways that control Myc transcription (Bhatia et al., 1993). Aware of the ubiquitous nature of Myc expression in tumors, early Myc researchers focused on the correlation between elevated levels of Myc and the risk of transformation and neoplasia. Investigations using transgenic mice models for Myc-induced tumorigenesis have shown that brief inactivation of Myc causes regression of tumors and induction of apoptosis. This suggests that sustained expression of Myc is required to preserve the transformed state (Jain et al., 2002). Finally, Myc expression has been shown to be essential in angiogenesis during proper development and during tumorigenesis (Baudino et al., 2002). The sum of this data, although only a cross section, helped shed light on why Myc activation was so prevalent in cancer.

Initial research revealed that constitutive expression of Myc was adequate to induce and maintain cell proliferation that was independent of mitogen stimulation (Cavalieri and Goldfarb, 1987). Enforced expression was also shown to be sufficient to inhibit terminal differentiation and enforce unchecked proliferation (Maruyama et al., 1987). Activated Myc has been shown to shorten the length of G1 phase, while studies knocking out or repressing Myc expression suggest that the oncogene is critical for entry into S phase (Heikkila et al, 1987). Since these studies, Myc has been shown to regulate the cell cycle by both positive and negative means. For example, Myc can directly repress the expression of cyclin-dependent kinases (Cdk) inhibitors, or indirectly inactivate them by sequestration and degradation. Myc can promote cell cycle progression by positive means through transcription of cyclins D1, D2, E1 and A2, in addition to Cdk4, CDC25A, E2F1 and E2F2 (Meyer and Penn, 2008).

Myc and Apoptosis

The legacy of Myc as an oncogene contributing to malignancy was fully cemented in the first ten years of its study. It was in 1987 when Wyllie and his colleagues produced a study which would implicate Myc in apoptosis, an unexpected result of a transcription factor associated with proliferation and cell cycle progression. When the group expressed *ras* and Myc in rat fibroblasts they observed an increased rate of cell death compared to cells expressing *ras* alone (Wyllie et al., 1987). In 1991, Neiman and his associates would corroborate Myc's role in apoptosis when they showed that premalignant B lymphocytes expressing ectopic viral Myc were more susceptible to cell death via radiation compared to cells not expressing Myc. However, this Myc-mediated sensitivity to apoptosis was not observed in cells after malignant transformation, suggesting the existence of a mechanism by which cancerous cells side step Myc's role in apoptosis (Neiman et al., 1991). Three months later, the Askew lab broadened our mechanistic understanding of Myc's contribution to apoptosis with their studies of interleukin 3 (IL-3) dependent myeloid cells. Upon IL-3 withdrawal, these cells undergo a downregulation of Myc, arrest in G1 phase and eventually apoptosis. When these cells constitutively expressed Myc, removal of IL-3 resulted in a rapid initiation of programmed cells death independent of cell cycle status (Askew et al., 1991). These early investigations revealed some surprising insights into the dual nature of Myc, most notably the cell's binary response to elevated Myc levels based on environmental cues: a) Cells cultured in the presence of growth factors will rapidly proliferate when Myc is over expressed or b) these same cells will undergo apoptosis upon depletion of growth factors. This binary nature of the most infamous pro-proliferative transcription factor was codified by Evan in 1992. The research group recapitulated Myc's affect on apoptosis in Rat1 cells constitutively expressing Myc, resulting in a propensity to undergo apoptosis when cultured in low serum conditions. The study also revealed

that the region of Myc required for its apoptotic function directly overlaps with regions that are vital for cotransformation, autoregulation and inhibition of differentiation (Evan et al., 1992). Early results from these seminal investigations into Myc's apoptotic function gave rise to the notion that oncogenes may possess dormant tumor suppressor traits as a safety mechanism against unwarranted cell proliferation (Lowe et al., 2004). Our understanding of cell death enhanced by Myc expression has grown to include apoptosis via chemotherapy, radiation, DNA damage, hypoxia, glucose starvation, heat shock and chemotoxins (Soucie et al., 2001). Since elevated levels of Myc are a normal occurrence in most human cancers, a vast amount of interest as been devoted to the development of treatments which hope to tip the scales of oncogenic Myc activity from cell proliferation to cell death (Schmitz et al., 2014).

Our understanding of the dual nature of Myc has grown to encompass the interplay between the oncoprotein and various effectors of the apoptotic machinery. Key to that understanding is unravelling the events that occur at the arbiter of cell death, the mitochondrion. As with Myc, mitochondria have assumed a monolithic legacy, often being dubbed the 'powerhouse of the cell', tasked with simply producing ATP. However, with time we have come to realize that mitochondria also lead a dual existence, primed to secrete an array of proapoptotic factors that are critical in committing the cell to programmed death (Harris and Thompson, 2000). The apoptotic program which converges on the mitochondria can be categorized into three phases: induction, decision and execution. Apoptosis is initiated via a variety of inducers such as extrinsic mechanisms independent of death receptors including survival factor withdrawal, chemotherapeutics and metabolic inhibitors. Intrinsic inducers include activation of death receptors such as CD95 and tumor necrosis factor receptor. The subsequent signal cascades lead to the decision phase of apoptosis which is in large part managed by the Bcl-2 family of pro and anti-apoptotic regulators

(Bcl-2, Bad, Bax, Bak among others). Members of this family use protein-protein interactions and subcellular localization to decide whether the apoptotic program will proceed or not. Briefly, inhibition of proapoptotic Bak and Bax is lifted when their heterodimeric partner Bcl-2 is sequestered by Bad, allowing Bak and Bax to localize at the mitochondrial outer membrane where they form pores that allow the secretion of cytochrome *c*. The execution phase is defined by the activation of caspases upon compromise of the mitochondrial membrane, formation of the apoptosome and eventual indiscriminate proteolysis of cellular proteins (Soucie et al., 2001). Within this signalling axis, the mitochondrial secretion of the proapoptotic factor cytochrome *c* has become a node of great interest because stimulation of which is stimulated by the activation of Myc (Juin et al., 1999).

Many efforts have been made to find a means by which Myc can influence apoptosis via the Bcl-2 family of pro and anti-apoptotic proteins. For example, human germinal center B-cell lymphomas, supraglottic squamous cell carcinoma and acute lymphoblastic leukemia contain elevated Myc levels and are often accompanied by overexpression of Bcl-2, a potent oncoprotein and mediator of pro-survival (Martin-Subero et al., 2005; Ozdek et al., 2004; Berger et al., 1996). This genetic environment has been replicated in *bcl-2/*Myc double transgenic mice which die within a few days of birth due to immature lymphoblastic leukemia (Strasser et al., 1990). On the contrary, transgenic mice expressing only Myc have a better prognosis and develop lethal lymphomas within five months of birth (Harris et al., 1988). Finally, researchers have reported significant levels of apoptosis in transgenic mice expressing Myc in a Bcl-2 -/- background. These studies support the notion that overexpression of Bcl-2 is required for cells to overcome the apoptotic affects of oncogenic Myc (Letai et al., 2004). The affects seen here also extends to other members of the Bcl-2 pathway, including BAG-1, which is a chaperone of Bcl-2 with prosurvival

functions. Loss of a single BAG-1 allele results in decreased tumor formation in animal models, hypothesized to be the result of increased levels of apoptosis (Takayama et al., 1995). Zhang and colleagues have shown that Myc-dependent induction of BAG-1 is crucial in diminishing the dormant apoptotic effects of oncogenic Myc (Zhang et al., 2011).

Despite the informative results linking Myc to known members of the apoptotic machinery, what remains unclear is how cells differentiate between Myc that is stimulated by normal mitogenic cues and oncogenic Myc. In normal cells, Myc is required for cell proliferation and cell cycle progression. Therefore, Myc's dormant tumor suppressor activity can only be prompted when Myc signalling has become oncogenic in normal cells. In the context of cancer prevention, these dormant tumor suppressor activities must be initiated to prevent damaged cells from propagating. Only when these tumor suppressor pathways are repressed can cancer begin to develop. Therefore, cells must initiate apoptotic programs as a response to oncogenic, rather then normal growth cues (Murphy et al., 2008). What complicates the situation is the means by which Myc contributes to oncogenesis, either by overexpression or dysregulation. In the case of overexpression, tumors with elevated Myc levels are often identified as more advanced and aggressive. This has been hypothesised to be a result of forced Myc occupancy of low affinity promoters resulting in the transactivation of novel genes. However, dysregulation of Myc not concurrent with overexpression is often adequate to side-step a cell's requirement for mitogens during normal proliferation while simultaneously abrogating tumor suppressor responses. This scenario could be a result of ill-sustained transactivation of the standard subset of Myc target genes (Fernandez et al., 2003). Although there is some uncertainty regarding Myc expression and dysregulation, it is known that apoptosis induced by Myc depends on dimerization with Max, Myc's N-terminal transcriptional

activation domain and subsequent DNA binding. This suggests that Myc induces apoptosis as a product of variations in target gene expression (Shiio et al., 2006).

In 2008, Murphy and colleagues set out to decouple the effects of dysregulated and overexpressed Myc using genetic models that allows for the controlled expression of a constitutively active form of Myc. The group's results indicate that low level expression of dysregulated Myc is sufficient to drive proliferation and is tumorigenic. However, overexpression of dysregulated Myc beyond a certain threshold was required to activate apoptosis and the ARF/p53 tumor surveillance pathway. This would indicate that maintaining low levels of oncogene expression is critical in avoiding the activation of tumor supressing pathways during the onset of tumorigenesis (Murphy et al., 2008). These results threaten the concept of Myc as a monolithic driver of cell proliferation and point to an intrinsic safety mechanism that aims to balance proliferation with antiproliferative programs. It is this balance which is now commonly thought to prevent spontaneous tumorigenesis (Lowe et al., 2004).

The binary nature of Myc activity and the complexities involved in a cell's decision to live or die would suggest that Myc is most likely working in concert with other oncogenes/tumor suppressors to tip the scales. One of these candidate proteins is the tumor suppressor p53, which is recruited during one of many stress response pathways to induce apoptosis (Levine and Oren, 2009). One such response occurs during genotoxic threats that increase the likelihood of transformation if apoptosis is not initiated. Although the p53 response to DNA damage has been of great interest to researchers, the elucidation of p53's contributions to apoptosis effector mechanisms has garnered considerable attention. p53 influences apoptosis by regulating the transcription of members of the BCL family of proapoptotic proteins, specifically BAX, BAK and PUMA. BCL family members can also be functionally regulated by p53 via protein-protein interactions which has the affect of

altering their prosurvival to proapoptotic ratio (Haupt et al., 1997). The result is targeting of proapoptotic BCL family members to the mitochondrial outer membrane, leading to a breakdown of mitochondrial membrane permeability and release of caspase activating molecules. The proteolytic activity of caspase molecules has earned them the title of 'executioners' of the apoptotic program as they indiscriminately cleave proteins. The signalling pathways leading to p53 stimulated apoptosis can also be initiated by the activation of oncogenes such as Myc. For example, growth signalling by oncogenic Myc results in p53 activation by enhancing the function of the tumor suppressor ARF, which abrogates the p53 inhibitor MDM2. The compounding effects of the loss of p53 and oncogenic Myc signalling are of substantial interest since the apoptotic functions of Myc heavily depend on the activation of p53 (Zindy et al., 1998). This is obvious in the case of Eμ-Myc transgenic mice which serve as a model for B cell lymphoma which develop tumors resulting in the death of 90% of mice within 5 months of birth (Harris et al., 1988). Young mice show evidence of high apoptosis rates in their B-lymphocyte compartment, possibly as a means of preventing tumorigenesis. This would suggest that within the 5 month incubation period, a second genetic lesion must be acquired to inhibit Myc induced apoptosis. It turns out that in Eμ-Myc mice, 28% of tumors harbor a p53 loss of function and 24% sustain loss of ARF function, while others expressed MDM2 at elevated levels (Eischen et al., 1999). Although only one of many examples, the Eμ-Myc model convincingly shows that the apoptotic qualities of Myc are intimately linked to the ARF/p53 pathway. Research into Myc activated apoptosis via p53 has ironically sparked interest in apoptotic programs that do not rely on p53. For example, in transformed cells with activated Myc and loss of p53 function, there maybe an opportunity to rouse Myc's dormant apoptotic qualities outside of the ARF/p53 signalling axis. This has been observed in myeloid cells from p53 null mice with deregulated Myc expression. These cells undergo

apoptosis upon IL-6 treatment independent of p53 function (Amanullah et al., 2000). This is of considerably interest since many human cancers are a product of the loss of p53 function, and yet they may still poses potent apoptotic potential via dysregulated Myc. Therefore, the potential for therapeutic intervention is an exciting prospect.

The obvious question that arises from the data presented here is whether cell cycle progression or apoptosis is the primary result of Myc activation. Considering that apoptosis is overcome and tumors flourish only when changes to the apoptotic machinery arise, there is evidence to suggest our classical understanding of Myc is severely flawed. As presented here, some of these changes include upregulation of the oncogenes BCL-2, BAG-1 and MDM2 or loss of p53 and ARF function. Recent advances in the targeted inhibition of BCL-2 and MDM2, coupled with our understanding of apoptosis and Myc thresholds in tumors, may allow us to intelligently restore the apoptotic potential of affected cells (Vassilev, 2004; Tse et al., 2008; Murphy et all 2008). By the same token, inhibition of Myc by small molecule inhibitors should give pause for concern considering the potent apoptotic potential of overexpressed Myc (Mertz et al., 2011). This is of considerable note when inhibition of Myc may be coupled with treatments intended to induce cell death, such as radiation and chemotherapy.

Notwithstanding the volume of data produced by investigations into Myc induced apoptosis, its exact mechanistic details have not been fully elucidated. As a consolation, three possible scenarios describing Myc's involvement in cell death have been proposed; they are the conflict, dual signal and modified dual signal models of Myc function. The conflict model is a default definition of Myc function that does not extend beyond a role in cell proliferation and hypothesizes that apoptosis is indirect downstream response to oncogenic Myc. The dual signal model suggests that Myc is simultaneously executing distinct proliferation and apoptosis programs, with the later being

suppressed by survival signals (Harrington et al., 1994). This is well illustrated in the case of apoptosis upon serum withdrawal from Rat1 cells overexpressing Myc (Evan et al., 1992). However, there is evidence to suggest that apoptosis and proliferation via Myc can not be completely separated as independent and distinct programs. For example, both apoptosis and proliferation rely on DNA binding upon Max association with Myc (Amati et al., 1993). Therefore, we are forced to consider the hypothesis that Myc concurrently primes both proliferation and apoptosis. This notion is at the heart of the modified dual signal model which proposes that priming of apoptosis and proliferation are a result of a single pathway, while triggering of apoptosis is achieved via a second pathway. Priming of apoptosis would be achieved by transcriptional regulation of target genes, and triggering would be a product of death signaling converging on the primed target gene products (Prendergast, 1999). In both iterations of the dual signal model of Myc, apoptosis is kept at bay by the availability of survival factors such as those found in serum or cytokines such as insulin-like growth factor (IGF-1). There has been limited research devoted to categorizing the subset of survival factors, cytokines and their respective signalling pathways which are directly implicated in preventing Myc driven apoptosis. One such study by Rohn and colleagues points to activation of Akt kinase by IGF-1 stimulation as a potent suppressor of Myc induced apoptosis via the CD95 death receptor pathway (Rohn et al., 1998). Although Akt's influence on apoptosis is well documented, the exact mechanisms by which it prevents Myc specific apoptosis is unknown. There is some indication that Akt may directly target pro-apoptotic BAD for phosphorylation, resulting in binding of BAD to 14-3-3 and sequestering of BAD away from Bcl-2 (Du and Montminy, 1998). Other studies have shown that activation of the PI3k/Akt pathway by insulin stimulation up regulates Myc-mediated transcription by phosphorylation and degradation of Mad1 (Zhu et al., 2008).

In the thirty years since Myc's discovery, an enormous volume of data has been collected which describes the many functions of this prolific oncogene. A deep understanding of this pleiotropic transcription factor will arm researchers and clinicians of the future with powerful, novel opportunities to treat afflictions associated with Myc; not the least of which is cancer. Although there have been advances in targeted small molecule inhibitors, targeting of oncogenes with latent apoptotic abilities deserves extra attention. Exploiting these apoptotic abilities cannot come at the expense of silencing the very oncogene which sensitizes the cell to apoptosis. Myc has certainly earned its reputation as a powerful oncogene, but in many cases additional lesions are required for tumorigenesis to take hold. Next, we turn our attention to Akt kinase, a powerful mediator of survival, growth and apoptosis, and is often dysregulated in Myc-tumors (Zhu et al., 2008).

Phosphoinositide-3 Kinase and Akt

Akt kinase is a serine/threonine kinase that mediates crucial cellular functions in response to extracellular stimuli and growth factors. These functions include cell cycle progression, gene expression, differentiation and cell growth by transducing signals from the plasma membrane to the nucleus. Akt belongs to a family of serine/threonine kinases that include Akt1, Akt2 and Akt 3, all of which are highly homologous in mammalian cells (Jones et al., 1991; Cheng et al., 1992; Brodbeck et al., 1999). Akt activation occurs downstream of phosphoinositide-3 kinase (PI3K), which is tasked with phosphorylating the membrane lipid phosphatidylinositol-4,5-P_2 (PIP_2) at the 3' position of the inositol ring to generate PI(3,4,5)P_3 (PIP_3). Generation of PIP_3 allows for the serine/threonine protein kinase Akt to be targeted to the membrane via its Pleckstrin Homology domain, where it can be subsequently activated by phosphorylation via phosphoinositide dependent kinase 1 (PDK1) (Stephens et al., 1998). Activated Akt is free to act upon over 50 known substrates, many of which influence processes such as proliferation, angiogenesis, motility,

metabolism and survival. It is known that the dysregulation of any of these cellular processes, via oncogenes such as Akt, can be a primary contributing factor in the pathogenesis of various diseases, including type-2 diabetes and cancer (Fresno Vara et al., 2004). For example, upon survival-factor stimulation, Akt promotes the survival of cells by inhibiting the function of the pro-apoptotic protein BAD. The up regulation of Akt could thus prove to be a critical step in oncogenesis (Datta et al., 1997). Akt can also be dysregulated by the tumor suppressor PTEN which dephosphorylates PIP_3 at the 3' position, converting the PI3K product back to PIP_2 (Maehama and Dixon, 1998). In cases where this gene is inactivated, high levels of PIP_3 cause the aberrant activation of Akt as seen in many advanced human cancers (Lin et al., 1998) and is correlated with neoplasia (Haas-Kogan et al., 1998).

Molecular Profile of Akt

Akt kinases 1, 2 and 3 are members of the AGC kinase family which include protein kinase A, G and C. All three members of the Akt family share a conserved structure which includes an N-terminal pleckstrin homology (PH) domain, a kinase domain and a C-terminal hydrophobic motif which serves as a regulatory domain. The 100 amino acid PH domain found in Akt allows the kinase to be targeted to the cell membrane by interacting with membrane bound phosphatidylinositol (3, 4, 5) triphosphate (PIP_3). This membrane targeting ability is shared by other signaling molecules that interact with 3-phosphoinositides (Lietzke et al., 2000), including the domain's namesake found in plecsktrin, which is a target of phosphorylation by PKC in platelets (Tyers et al., 1988).

The centrally located kinase domain is conserved between members of the AGC kinase family and contains a threonine residue at position 308 which can partially activate Akt upon phosphorylation (Alessi et al., 1996). Full activation of Akt requires phosphorylation of T308 and serine 473 which

is located down stream of the kinase domain and within the C-terminal regulatory domain. This region of approximately 40 amino acids contains the F-X-X-F/Y-S/T-Y/F hydrophobic motif, which is a hallmark of the AGC kinase family. Phosphorylation of the serine or threonine residue within this motif is required for full activation and is a requites shared by all AGC kinases. Deletion of the hydrophobic motif eliminates enzymatic activity of all Akt isoforms (Peterson and Schreiber, 1999; Andjelkovic et al., 1997).

Phosphorylation of T308 and S473 occurs as a response to stimulation by growth factors and is dependent on a PI3K and PH domain mediated membrane translocation event. Translocation of Akt to the membrane follows activation of PI3K by G protein-coupled receptors and tyrosine kinase receptors (Wymann et al., 2003). Akt is targeted to the membrane by high affinity binding to PIP_3 via its PH domain resulting in a conformational change that precipitates phosphorylation of T308 by the phosphoinositide-dependent kinase-1 (PDK1) (Andjelkovic et al., 1997; Stephens et al., 1998). Phosphorylation of T308 depends on co-localization of Akt and PDK1 at membrane (Anderson et al., 1998).

The source of S473 phosphorylation has not been unanimously agreed upon, however it is known that its phosphorylation is dependent on both PI3K and T308. Because of this relationship, PDK1 has been suggested to be the kinase responsible for S473 phosphorylation (Balendran et al., 1999). Disagreement stems from studies using PDK1 -/- ES cells which showed that S473 phosphorylation in these cells was similar to wild-type cells, while T308 phosphorylation was absent (Williams et al., 2000). This result was countered by researchers that showed an increase in S473 phosphorylation when they transiently overexpressed PDK1 in HEK293 cells (Hill et al., 2001). Phosphorylation of S473 has also been linked to the mammalian target of rapamycin complex 2 (mTORC2) following growth factor stimulation (Sarbassov et al., 2005). DNA damage

has also been shown to result in S473 phosphorylation via DNA-dependent protein kinase (DNA-PK) (Bozulic et al., 2008)). Finally, there have been studies suggesting that Akt has an innate ability to autophosphorylate S473 (Toker and Newton, 2000).

Complete activation of Akt by phosphorylation of T308 and S473 allows Akt to transmit signals from the plasma membrane to various effectors of the PI3K pathway. Substrates of Akt are subject to inhibitory and stimulatory phosphorylation with implications on cell survival and apoptosis.

Akt and Cell Survival

Cell survival is commonly discussed in terms of a cell's ability to balance apoptosis with proliferation. This balancing act is at the heart of the Akt signaling pathway, allowing cells to tolerate apoptotic stimuli by engaging cell survival signals via activated Akt (Yao and Cooper, 1995). As a downstream effector of the PI3K pathway, Akt can influence cell survival either by direct means, via transcriptional control or by metabolic regulation (Song et al., 2005).

Direct control of cell survival is carried out by Akt primarily via the blocking of apoptosis. This is accomplished by Akt mediated phosphorylation of some of the critical regulators and effectors of the apoptotic process. For example, upon receptor tyrosine kinase activation, Akt is stimulated to directly phosphorylate the pro-apoptotic protein BAD at S136 (del Peso et al., 1997). Phosphorylation of Bad disrupts BAD/Bcl-2 heterodimers by promoting the binding of BAD to the 14-3-3 adapter protein. As a result, Bcl-2 is free to inhibit apoptosis by heterodimerizing with pro-apoptotic Bax or Bak which are otherwise responsible for the formation of pores in the outer mitochondrial membrane. Therefore, phosphorylation of BAD at S136 by Akt can inhibit the release of cytochrome *c* which when allowed, is a critical step in committing a cell towards apoptosis (Datta et al., 1997).

Akt can phosphorylate direct effectors of the apoptotic cascade as a means of survival. This is evident in the case of pro-caspase-9, which is considered an initiator caspase and is activated upon the release of cytochrome *c* from the mitochondria. Akt has been shown to phosphorylate pro-caspase-9 at S196, thereby minimizing its activity by unknown means (Cardone et al., 1998). Although inhibition of pro-caspase-9 by Akt has been seen in human cells, this residue is not conserved in monkey, mouse or rat despite evidence suggesting that Akt has a means to abrogate apoptosis down stream of cytochrome *c* release. This would suggest the existence of other Akt targets yet to be identified (Allan and Clarke, 2009).

Influence on cell survival can also come in the form of transcriptional regulation by way of Akt phosphorylation of transcription factors. For example, Akt is known to phosphorylate all four isoforms of the FoxO family of transcription factors whose target genes code for pro-apoptotic proteins such as CD95 ligand (CD95L) and TNF-related apoptosis inducing ligand (TRAIL). Both of these ligands activate the apoptosis program upon binding with their death receptors (CD95 is discussed above in regard to Myc). Phosphorylation of FoxO transcription factors results in 14-3-3 binding and sequestration in the cytoplasm, thereby inhibiting the effects of apoptosis mediated by these target genes (Burgering and Medema, 2003). A reoccurring theme within Akt function is the association of 14-3-3 proteins with targets of Akt phosphorylation. The genesis of this correlation has not yet been determined, however it can be attributed in part to overlap between 14-3-3 binding and Akt phosphorylation consensus sites. 14-3-3 is known to bind at phosphorylated serine or threonine residues within what is known as the mode I motif: R-S-X-pS/pT-X-P (where X is any amino acid, A is arginine, R is serine, T is threonine, P is proline and p indicates a phosphorylated residue). This conforms well with the minimal Akt motif which requires A-X-X-S/T to be present in order to produce the phosphorylated serine/threonine residue

required for 14-3-3 binding (Smith et al., 2011). Both motifs share an arginine at -3 relative to their respective pS/T residues. As we shall see in the data presented at the heart of this thesis, Akt and 14-3-3 binding will once again implicate themselves in mediating apoptosis.

Another example of Akt's ability to influence transcription is by its impact on the transcription factor p53, albeit indirect in this case. p53 is a critical player in DNA damage-induced apoptosis and is partly regulated by the E3 ubiquitin ligase Mdm2, which targets the transcription factor for degradation. Activation of the PI3K pathway results in phosphorylation of Mdm2 at ser166 and 186 by Akt, resulting in its targeting to the nucleus and upregulation of its ubiquitin ligase activity. As a consequence, p53 levels are reduced, which lead to an inhibition of p53 mediated transcription and apoptosis (Mayo and Donner, 2001; Gottileb et al., 2002; Ogawara et al., 2002).

The Akt Signalling Pathway and Cancer

The examples above illustrate the extent to which Akt plays a role in critical cell processes that promote cell survival. With Akt's great power comes great responsibility, which when unchecked, often contributes to tumorigenesis. Perturbations in Akt and PI3K signalling pathway activity can result in uncontrolled cell growth by a variety of means. These include amplification and overexpression of Akt, hyperactivation of Akt or unsolicited activity of members of the PI3K pathway upstream or downstream of Akt (Altomare and Testa, 2005). Because of the ubiquitous nature of these lesions in human cancers, members of the PI3K pathway are an attractive target of therapeutic intervention. However, as with the case of Myc outlined above, careful consideration must be placed in avoiding off target effects that can render these efforts useless (Thorpe et al., 2015).

The very first examples of lesions to the Akt gene came in 1992 when Cheng and colleagues identified an amplification and overexpression of Akt2 in a relatively small sample of ovarian carcinoma cell lines and tumors (Cheng et al.,1992). Overexpression of Akt2 mRNA has also been reported in ovarian carcinomas in the absence of Akt2 amplification, although the means of this mRNA overexpression has not been identified. The amplification and/or overexpression of Akt2 has been hypothesized to contribute to tumorigenesis by sensitizing cells to negligible levels of growth factors (Bellacosa et al., 1996).

Amplification and overexpression of Akt2 has also been observed in pancreatic carcinomas and pancreatic cell lines such as PANC1. In this cell line, 50-fold amplification of Akt2 was reported, most likely contributing to the abnormally high levels of Akt2 protein and mRNA in these cells. In an attempt to investigate the possibility of therapeutic intervention of abnormal Akt2, the Cheng lab transfected PANC1 cells with antisense Akt2 RNA. Expression of Akt2 in cells transfected with Akt2 antisense RNA was significantly lower when compared to control transfections. The tumorigenicity of these cells in nude mice was significantly reduced as was their invasiveness in rat tracheal xenotransplant assays (Cheng et al., 1996). These results were some of the first to highlight the possibility of intervening in tumor progression driven by dysregulated Akt2.

Amplification of the Akt1 isoform has not been observed as commonly as Akt2. The first example occurred in early investigations by Stephen Staal of gastric carcinomas which revealed only one instance of Akt1 amplification in 225 samples (Staal, 1987). Likewise, only a single example of amplification and overexpression of Akt1 was reported in a screen of 103 malignant gliosarcomas (Knobbe and Reifenberger, 2003). Despite few examples of Akt1 amplification, there have been reports of elevated Akt1 protein levels in some types of tumors. In the case of

immunohistochemical analysis of 280 breast tumors, elevated Akt1 staining was observed in 24% of tumors while only 4% were markedly positive for Akt2 (Stål et al., 2003).

The effects of overexpressed Akt on transformation has also been demonstrated in cell culture. Retroviral overexpression of Akt2 in NIH3T3 cells results in transformation as per growth in soft agar and tumor formation in nude mice (Cheng et al., 1997). Overexpression of wild-type Akt1 failed to recapitulate this result in NIH3T3 cells. Only when constitutively active Akt1 was expressed in these cells were they able to grow in soft agar and produce tumors in nude mice (Sun et al., 2001).

Dysregulation of Akt has also been reported as a product of hyperactivation and has been documented in various human cancers including thyroid, gastric, pancreatic, ovarian and breast carcinomas (Bellacoas et al., 2005). This is of considerable importance since Akt activation has been correlated with poor prognosis and advanced disease in some cancers. This was pointed out in a study by Sun and colleagues who showed that of tumors with activated Akt1, 80% of them were high grade and stage III/IV carcinomas (Sun et al., 2001). Despite these alarming statistics, phosphorylated and active Akt expression has been reported in precancerous conditions such as bronchopulmonary dysplasia. This would suggest that activation of Akt in some cases may precede tumorigenesis and therefore might be a target for early intervention as a means of preventing tumor formation (Tsao et al., 2003).

The nature of Akt as a transducer of PI3K signalling means that any number of perturbations upstream of Akt could result in dysregulated signalling. This could manifest as a loss of PTEN activity resulting in an abundance of PIP_3 and therefore hyperactivation of Akt. This was found to be the case in 35% of endometrial cancers studied by Terakawa and colleagues (Terakawa et al.,

2003). PI3K can also generate a surplus of PIP_3 via overstimulation of receptor tyrosine kinases (Di Cristofano and Pandolfi, 2000; Altomare and Testa, 2005). Similarly, overexpression of wild-type growth factor receptors may sensitize cells to otherwise negligible levels of growth factors (Hanahan and Weinberg, 2000). Examples of mutant receptors have also been reported to result in constitutive activation of PI3K signalling (Sordella et al., 2004). In one of the most intriguing examples of a mutant protein activating Akt occurs in over 95% of chronic myeloid leukemia (CML) cases. A reciprocal translocation between chromosome 9 and 22 generates a fusion gene known as BCR-ABL that codes for a constitutively active tyrosine kinase. This mutant tyrosine kinase activates PI3K via binding of its p85 regulatory subunit, which consequently results in the aberrant activation of Akt (Skorski et al., 1997). This same p85 regulatory subunit of PI3K has been found to be mutated in T-cell lymphoma cell lines, colorectal and ovarian tumors, colon cancer cell lines, colon carcinoma, ovarian cancer cell lines and ovarian carcinomas. In each case, a truncated form of the p85 regulatory subunit results in constitutively active PI3K (Jucker et al., 2002; Philip et al., 2001)

PI3K and Akt Inhibitors as Therapeutic Intervention

Interest in inhibiting PI3K and Akt as a means of cancer treatment has resulted in three generations of compounds targeting these potent oncogenes. Despite these efforts, none of these inhibitors have been introduced into clinical use, while hopes of more advance compounds are driving progress in next generation inhibitors of PI3K and Akt.

Early attempts in inhibiting PI3K resulted in the development of compounds like Wortmannin and LY294002. These compounds are considered ‘pan-inhibitors’ because of their ability to inhibit all isoforms of class I PI3Ks. Despite this, neither Wortmannin or LY294002 have been approved for clinical use due to their poor pharmacodynamics. The utility of these compounds has not been lost

on researchers as they have become critical in helping us develop our understanding of the PI3K pathway (Martini et al., 2013). Attempts to create a second generation of PI3K inhibitors has focused on increasing isoform selectivity. These are currently being tested in clinical trials on patients with genitourinary cancers and include PI3Kα specific GDC-0032 and PI3Kβ specific GSK2636771 (Porta and Figlin, 2009; Laplante and Sabatini, 2012). Finally, the third and most recent generation of compounds has been dubbed the 'dual PI3K/mTOR inhibitors' which seeks to leverage the high degree of sequence homology within the catalytic sites of PI3K and Akt. Although efficacy of compounds such as NVP-BEZ235 have yet to be proven *in vivo*, there is hope that simultaneous targeting of PI3K and mTOR may improve outcomes for cancer patience in which both of these molecules are dysregulated (Martelli et al., 2012).

Compounds specifically targeting Akt have focused on its ATP binding site, pleckstrin homology domain and substrate site as a means of inhibition. The number of Akt inhibiting compounds that have entered clinical development is far outweighed by those targeting PI3K and mTOR (Pal et al., 2010). The most promising of Akt inhibitors is Miltefosine, however its use has not been approved for the treatment of cancer. However, the compound has completed phase III trials and has been approved in India, Columbia and Germany for treatment in patients co-infected with visceral or cutaneous leishmaniasis and HIV (Leonard et al., 2001; Dorlo et al., 2012). Visceral leishmaniasis (VL) is the most severe form of black fever which is caused by a single celled protozoan of the *Leishmania* genus and is the second most lethal parasite after malaria (Desjeux, 2001). VL often occurs in patience afflicted with HIV, and requires specific treatment strategies to overcome resistance to other drugs. Miltefosine inhibits Akt in macrophages expressing HIV viral Tat protein, which is a potent activator of the pro-survival PI3K pathway. Apoptosis can then be specifically induced in these cells upon treatment with secondary compounds, thereby

preventing viral production without harming healthy cells (Chugh et al., 2008). Although VL and HIV are obviously not implicated in uncontrolled cell growth, the development of Miltefosine is a wonderful example of how our knowledge of signaling transduction can be of benefit to researchers and clinicians outside the sphere of oncology.

Although promising breakthroughs abound in small molecule inhibitors of PI3K/Akt, none of the drugs described here have been able to achieve the gold standard of complete remission in cancer patients. The inability to do so is usually attributed to the onset of resistance, the molecular basis of which has been hypothesized to include activation of redundant yet latent pathways, secondary target lesions or amplification of downstream effectors in the same pathway (Tan and Yu, 2013). The ability for cancer to adapt in the face of treatment is just one of many obstacles that needs to be overcome if we are to successfully treat this disease the way we have treated other diseases in the 21st century.

CDCA7 – MYC Associated Protein and Target of Akt

In the onset of our investigation into CDCA7, very little was known about this novel cell cycle associated protein. Prior to our publication in 2013, CDCA7 was the focus of only three articles, two of which were published by the same group. Bellow is a summary of what was known prior to 2013 which served as the foundation for our initial investigation, followed by a review of the latest literature regarding CDCA7.

CDCA7 – 2001-2006

In 2001 Prescott and colleagues identified JPO1/CDCA7 as a novel Myc target gene, which encodes a nuclear protein 47 kDa in size, consisting of 371 amino acids and is conserved across many species including human, mouse, rat and *Xenopus*. CDCA7 mRNA is highly expressed in

human colon, thymus and small intestinal tissue, in contrast to bone marrow, spleen and peripheral leukocytes where it is marginally detected. When stably overexpressed in Rat1a cells, CDCA7 has limited transforming ability and does increase the clonogenicity of CB33 human lymphoblastoid cells, although not to the same extent as Myc. However, Prescott was able to establish that CDCA7 is involved in transformation and anchorage-independent growth by demonstrating its complementation with a transformation-defective Myc Box II mutant. The data presented by this group suggests that CDCA7 is one of many Myc target genes that synergistically work with Myc towards tumorigenesis (Prescott et al., 2001).

Investigations into the relationship between CDCA7 and Myc were consequently probed by Osthus and colleagues in 2005, which was the same group to first shed light on CDCA7. Using hybridization arrays containing a variety of solid tumor and blood samples, the group showed that elevated CDCA7 levels are correlated with high levels of Myc in solid tumors, while increased mRNA levels were detected in patients with acute myeloid leukemia (AML) and blast crisis-staged chronic myeloid leukemia (CML). Osthus and colleagues were the first to probe the effects of CDCA7 in an animal model. Their results showed that transgenic mice expressing CDCA7 have elevated incidences of blood and solid tumors over their control littermates. Consequently, the group hypothesized that their observations, in light of the data presented by Prescott et al., indicate that CDCA7 may be implicated in Myc-mediated tumorigenesis (Osthus et al., 2005).

In 2006, a group led by Yuya Goto at Meiji University in Tokyo would shed light on the transcriptional regulation of CDCA7 as well as its own transcriptional abilities. In addition to being a Myc responsive gene, Goto and colleagues showed that CDCA7 is a direct transcriptional target of the transcription factor E2F1. CDCA7 was also able to induce transcriptional activity in mammalian one-hybrid assays. This was not surprising as the C-terminal cysteine rich region of

CDCA7 is homologous to the transcriptional regulatory domain of the closely related JPO2. E2F1 is known to be involved in pathways regulating DNA replication and cell cycle progression (Goto et al., 2006), therefore it is important to note that CDCA7's expression peaks at the G_1 to S phase transition (Osthus et al., 2005). CDCA7 has thus been characterized as an E2F1-mediated member of the cell division cycle-associated family of genes (CDCA), whose members exhibits expression patterns correlating with those of cell cycle genes such as CDC2/7 and cyclins (Goto et al., 2006).

CDCA7 – Gill, Gabor, Couzens and Scheid (2013)

Although there have been no studies probing the nature of a possible physical interaction between CDCA7 and Myc, Penn and colleagues have shown that JPO2 (a related family member of CDCA7) binds Myc at its N-terminal domain, an association which promotes Myc-dependent transformation (Huang et al., 2005). At the amino acid level, JPO2 and CDCA7 share a C-terminal cysteine rich region (Goto et al., 2006) which may confer DNA binding and promoter specificity of Myc-CDCA7 complexes. Figure 1.1 and 2.1 outlines various conserved motifs within CDCA7 and their proposed functions, including a consensus Akt substrate site, a 14-3-3 binding domain as well as a bi-partite nuclear localization sequence (Obenauer et al., 2003; Madiera et al., 2015). In light of CDCA7's novel role in Myc-mediated oncogenic pathways and its E2F1-mediated expression, it is becoming increasingly clear that CDCA7 may play an important role in cancer. In 2013 our research group published a report (Gill et al., 2013; Chapter 2 of this thesis) that implicated CDCA7 as a Myc binding protein, whose interaction with Myc is mediated by phosphorylation at T163 by Akt, promoting dissociation from Myc and binding of 14-3-3, resulting in its sequestration to the cytoplasm. Knockdown of *cdcA7* abrogated Myc-dependent apoptosis, while over expression repressed growth rates and promoted Myc-dependent apoptosis. Our research was the first to suggest that CDCA7 may be directly involved in the Myc-apoptosis

paradox. Chapters 3 and 4 of this thesis further explore the mechanistic details contributing to the phenotypes described in our 2013 publication.

CDCA7 – 2014-2017

In the years following our 2013 publication, four articles explicitly focusing on CDCA7 have been published, yet none of them address the relationship between CDCA7 and Myc. For the most part, these investigations have focused on CDCA7's contribution to development or its role in a condition known as Immunodeficiency, Centromeric Instability and Facial Anomalies (ICF) syndrome. Although not completely related to the topic of Myc-mediated apoptosis, below is a review of these most recent findings regarding CDCA7, some of which sheds light on CDCA7's role in DNA-centric activities.

ICF is a heterogeneous autosomal recessive disorder whose hallmarks include facial anomalies, developmental delay and immunodeficiency often leading to respiratory and gastrointestinal infections that are frequently lethal. All ICF patients present with hypomethylated juxtacentromeric heterochromatin and centromeric instability. The disease was initially characterized by mutations in two ICF genes, although only 50% of cases were explained by mutations in ICF1 (DNA methyltransferase 3B or DNMT3B) and 30% were attributed to mutations in ICF 2 (zinc-finger and BTB domain containing 24 or ZBTB24). While mutations to DNMT3B resulted in reduced methyltransferase activity, the function of ZBTB24 was unknown until recently. Therefore, approximately 20% of ICF cases cannot not be explained by mutations in one of these two ICF genes. In 2015, Thijssen and colleagues combined homozygosity mapping with whole-exome sequencing to identify novel homozygosity in five patients who do not harbour mutations in DNMT3B or ZBTB24. The group identified 4 homozygous variants of CDCA7 in these patients, each containing missense mutations within the c-terminal z-finger domain. These

include R274C, R274H, G294V and R304H. The group subsequently knocked down CDCA7 in mouse embryonic fibroblasts, resulting in hypomethylation of CpG centromeric repeats the likes of which is found in all human cases of ICF (Thijssen et al., 2015).

In 2016, a study by Wu and colleagues focused on ZBTB24 and its contributions to ICF etiology. The group found that CDCA7 expression is significantly reduced in mouse embryonic stem cells that are homozygous for a loss of function ZBTB24 mutant. Expression of CDCA7 was restored in these cells upon ectopic expression of wild-type ZBTB24. Furthermore, CDCA7 expression was also shown to be reduced in ICF patients harbouring ZBTB24 nonsense mutations. Finally, the group demonstrated that ZBTB24 occupies the CDCA7 promoter and may function as a regulator of CDCA7 expression (Wu et al., 2016). The results published by Thijssen et al. and Wu et al. establish a relationship between two of the four ICF genes at the transcriptional level and sheds some light on the activity of CDCA7 outside of cell survival paradigm we have largely focused on thus far.

In studies unrelated to ICF, CDCA7 has been identified as a major transcriptional target of Notch signalling during human embryonic stem cell hematopoietic differentiation (Guiu et al., 2014). Conversely, repression of CDCA7 expression by the transcription factor Pax6 has been shown to be critical for normal corticogenesis (Huang et al., 2017). Although research into CDCA7 is still very early in its infancy, the publications summarized here indicate that CDCA7 most likely plays an important role in normal cell survival and development. The influence of any protein on Myc-mediated functions is usually justification for substantial investments of time and research funds. Our research group is not an exception to this line of thinking. The research presented here is a product of eight years of research, culminating in voluminous data that has been distilled down to the most pertinent results.

Significance of Research and Research Objectives

The evidence presented by Prescott et al., Osthus et al. and Goto et al. suggests that CDCA7 may play an important role in Myc-mediated transformation. This is enforced by the following:

- CDCA7 is a Myc and E2F1 target gene.
- CDCA7 rescues a transformation deficient mutant of Myc
- Elevated levels of CDCA7 are correlated with elevated levels of Myc in solid tumors
- CDCA7 has transcriptional activity
- CDCA7 expression peaks at the G1-S transition
- CDCA7 contains an Akt consensus site, 14-3-3 binding site and a nuclear localization signal

In light of these results and the importance of Myc in many critical cellular processes, it would be prudent to develop a molecular profile of CDCA7 to define the nature of CDCA7's relationship with Myc. The possibility that CDCA7 may be a target of Akt phosphorylation is intriguing because of the fact that simultaneously dysregulated Myc and Akt (via overactive receptor tyrosine kinases) have been shown to provide the necessary environment to promote oncogenesis (Stambolic et al., 1999). This molecular profile of CDCA7 may also shed light on the Myc-apoptosis paradox as Kauffmann-Zeh and colleagues have demonstrated that Myc induced apoptosis could be suppressed by Phosphoinositide-3 kinase (PI-3K) and Akt activation (Kauffmann-Zeh et al., 1997). The following research objectives have been addressed in the thesis presented here:

Research Objective 1: Investigate Consensus Sites within CDCA7's Amino Acid Sequence

Figure 1 shows some of the interesting consensus sites found within the CDCA7 amino acid sequence, such as an Akt phosphorylation site, 14-3-3 binding site and bi-partite nuclear localization sequence (NLS) (Obenauer et al., 2003; Madiera et al., 2015). These sites should be

investigated and confirmed or rejected as conforming to the consensus sites in question. These consensus sites are of particular interest because they are localized in and around threonine 163, making way for the possibility that phosphorylation by Akt mediates 14-3-3 binding and alters sub-cellular localization. This paradigm has been observed in the case of the transcription factor FoxO4 (Obsilova et al., 2005) and if confirmed, would shed light on CDCA7's post-translational regulation and /or function.

Research Objective 2: Does CDCA7 Interact with the Oncogene Myc?

Huang and colleagues have shown that JPO2 (a related family member of CDCA7) can associate directly with Myc, resulting in its transforming abilities in medulloblastoma cells (Huang et al., 2005). Investigating if CDCA7 also interacts with Myc could shed light on any contributions this novel protein might have in Myc-dependent cellular processes, including proliferation, apoptosis or gene expression. This can be approached using *in vivo* association assays via co-immunoprecipitation or *in vitro* association assays using bacterially expressed and purified proteins. The exact region of CDCA7 interaction with Myc can be determined using targeted deletion mutants that focus on areas of interest within CDCA7. Lack of association upon deletion of a region may suggest its involvement in direct protein-protein interactions.

Research Objective 3: Map the Subcellular Localization of CDCA7

Subcellular localization of a protein can help us understand the function and regulation thereof. Using immunohistochemistry will allow us to investigate where CDCA7 is located during various phases of the cell cycle and how a multitude of treatment conditions may affect subcellular localization. The presences of a consensus bipartite NLS suggests that CDCA7 subcellular localization may be confined to the nucleus. However, research objective 1 may reveal a

mechanism which can mediate nuclear localization by means of T163 phosphorylation and therefore contribute to a potential dynamic means of controlling CDCA7 function.

Research Objective 4: How Does CDCA7 Affect Apoptosis and Proliferation?

Since 1992 it has been well known that Myc plays an important role not only in proliferation, but apoptosis as well (Evan et al., 1992). The mechanism behind Myc's non-mutually exclusive influence on proliferation and apoptosis has remained a mystery. Investigating whether CDCA7 contributes to this paradox may help explain how Myc can contribute to two diametrically apposed cellular processes.

Research Objective 5: Does CDCA7 Exist as a Monomer or a Homodimer?

Within the highly conserved C-terminal region of CDCA7 there is a potential zinc-finger, which in many cases allows proteins to either homo or heterodimerize (Ou et al, 2006). Determining whether CDCA7 exists natively as a dimer or monomer will help develop the overall molecular profile of CDCA7 in addition to learning more about how its function may be regulated.

Research Objective 6: How Does CDCA7 Affect Gene Expression?

The CDCA7 family member JPO2 has been shown to associate with Myc; an association which promotes Myc-dependent transformation (Huang et al., 2005). CDCA7 and JPO2 share a C-terminal cysteine rich region (Goto, et al., 2006), which may allow for DNA binding and promoter specificity of a Myc-CDCA7 complex. Identifying the potential subset of genes which are affected by CDCA7 may allow for the dissection of CDCA7's influence on a genetic level. The most notable genes to probe would be those involved with proliferation and apoptosis, such as cyclins, CDKs or members of the Bcl-2 family of pro/anti-apoptotic proteins.

Research Objective 7: How Does CDCA7 Affect the Cell Cycle?

Goto and colleagues have shown that CDCA7 is a gene target of the transcription factor E2F1. It is important to note that E2F1 plays a regulating role in cell cycle progression and DNA replication, perhaps contributing to the temporal expression of CDCA7 at the G_1 to S phase transition. How this temporal expression affects progression through the cell cycle is yet to be seen.

Research objectives 1-4 have been addressed in a manuscript published in 2013 by Molecular and Cellular Biology and is appended in the following section. Research objectives 5-7 are addressed in chapters 3 and 4.

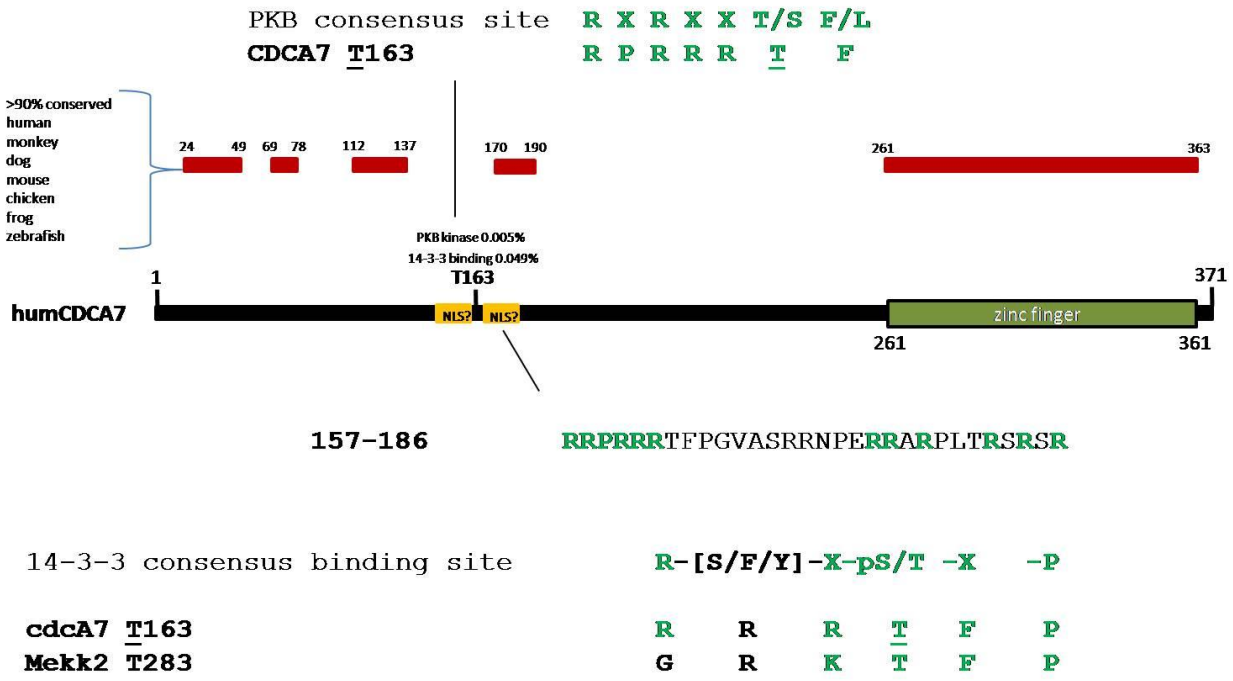

Figure 1.1 CDCA7 conserved areas and regions of interest. The area around T163, 158-181, contains three notable consensus motifs: a Akt substrate site, a 14-3-3 binding motif and a bi-partite nuclear localization sequence. The c-terminal portion of CDCA7 also contains a putative zinc-finger. Areas in red show a greater then 90% conservation amongst species (Obenauer et al., 2003; Madiera et al., 2015).

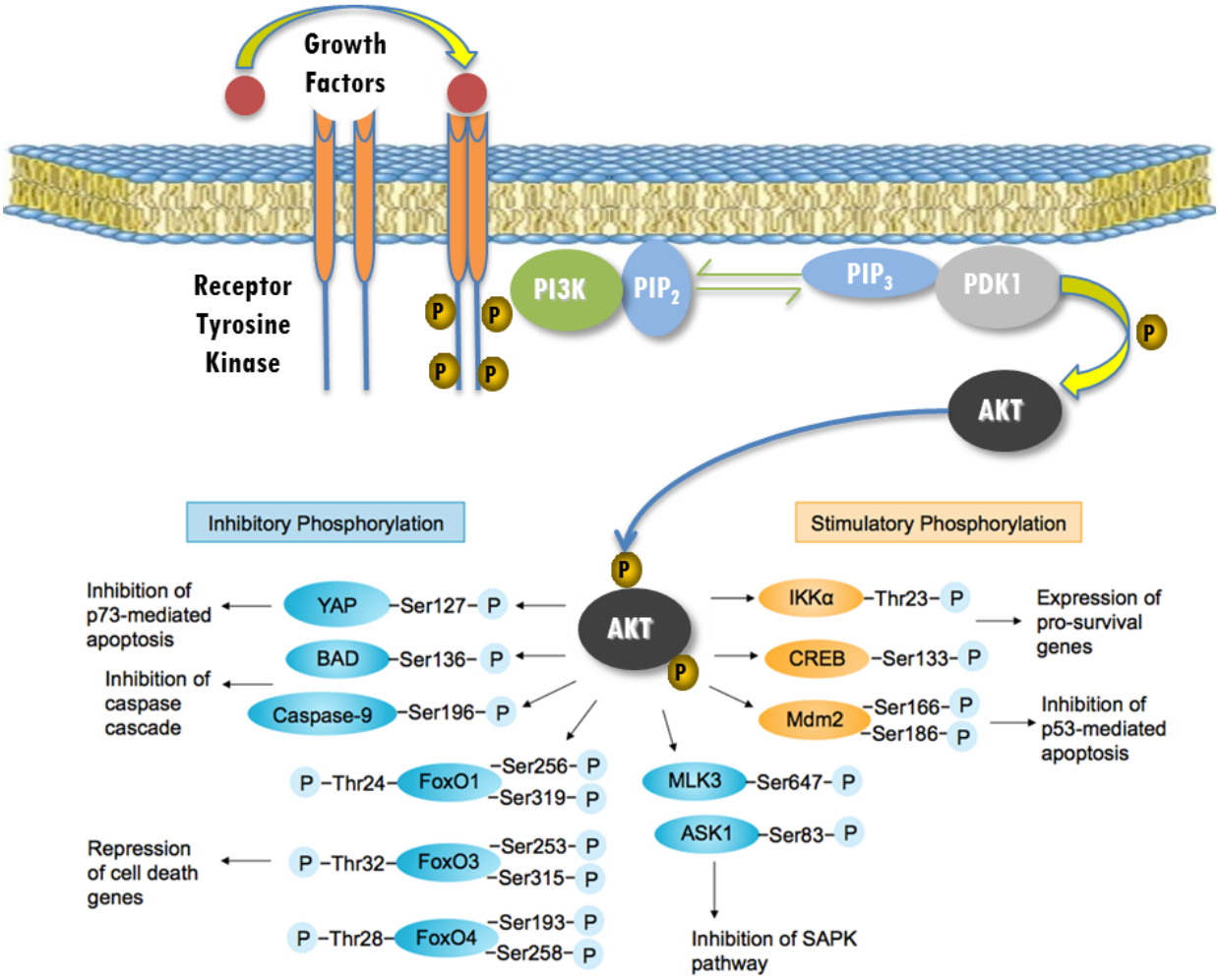

Figure 1.2 PI3K pathway activation and Akt function. Akt activation occurs downstream of phosphoinositide-3 kinase (PI3K), which is tasked with phosphorylating the membrane lipid phosphatidylinositol-4,5-P_2 (PIP_2) at the 3' position of the inositol ring to generate PI(3,4,5)P_3 (PIP_3). Generation of PIP_3 allows for the serine/threonine protein kinase Akt to be targeted to the membrane via its Pleckstrin Homology domain, where it can be subsequently activated by phosphorylation via phosphoinositide dependent kinase 1 (PDK1) (Stephens et al., 1998). Activated Akt is free to act upon over 50 known substrates, many of which influence processes such as proliferation, angiogenesis, motility, metabolism and survival.

Chapter 2: The MYC-associated protein CDCA7 is phosphorylated by Akt to regulate MYC-dependent apoptosis and transformation

R. Montgomery Gill, Timothy V. Gabor, Amber L. Couzens and Michael P. Scheid

Department of Biology, York University, Toronto, Ontario, Canada, M3J 1P3

Michael P. Scheid, PhD
York University
Department of Biology
Toronto, Ontario, Canada
M3J1P3
Tel: 416 736 2100 x40069
Fax: 416 736 5698
Email: mscheid@yorku.ca

This research was originally published in Molecular and Cellular Biology (2013) 33(3): 498-513

Personal Contributions:

The following is a list of the figures from the above publication to which I directly contributed, by either carrying out the experiment therein or by generating critical cell lines used within those experiments:

2 (B and E), 3 (A-D), 4 (A-C), 5 (A, C, E and F), 6 (A and B), 7 (D, F and E), 8 (D), 9 (A), 10 (A-G) and 11 (C and D).

In addition to these figures, I am personally responsible for generating all FLAG-CDCA7 vectors and their mutant permutations, shRNA vectors and vectors involved in sub-cellular localization experiments.

Abstract

Cell division control protein A7 (CDCA7) is a recently identified target of MYC-dependent transcriptional regulation. We have discovered that CDCA7 associates with MYC and that this association is modulated in a phosphorylation-dependent manner. The pro-survival kinase Akt phosphorylates CDCA7 at threonine 163, promoting binding to 14-3-3, dissociation from MYC, and sequestration to the cytoplasm. Upon serum-withdrawal, induction of CDCA7 expression in the presence of MYC sensitized cells to apoptosis, whereas CDCA7 knockdown reduced MYC-dependent apoptosis. Transformation of fibroblasts by MYC was reduced by co-expression of CDCA7, while the non-MYC interacting protein Δ(156-187)-CDCA7 largely inhibited MYC-induced transformation. These studies provide insight into a new mechanism by which Akt signaling to CDCA7 could alter MYC-dependent growth and transformation, contributing to tumorigenesis.

Introduction

The transcription factor MYC is a proto-oncogene that regulates the expression of hundreds of genes involved in cell cycle progression, adhesion, metabolism, and apoptosis (24, 35, 36, 40). Over-expression of MYC is a hallmark of human cancer, contributing to the expression of numerous groups of genes involved in transformation, metastasis, and overall poor prognosis (58, 59). MYC has been estimated to be active in nearly 70% of human cancers, with the mechanisms of activation including amplification, translocation, deregulated translation, and protein turnover (1, 39). As such, MYC has been the subject of extensive study in the search for treatment modalities (reviewed in (23, 36, 53)).

Activation of MYC is induced by mitogenic stimuli to promote cell cycle progression (2, 5, 9, 20, 25, 33, 49). To prevent aberrant MYC expression from driving unsafe proliferation in the animal, a safeguard has evolved whereby MYC activation in the absence of mitogenic survival signals is opposed by cellular responses of apoptosis and/or cell cycle arrest, depending on the cellular context and p53 status (3, 17, 18, 26, 27, 45, 46, 61). Despite these observations of almost 20 years ago, and the realization that other growth-promoting transcription factors, such as E1A and E2F1 act similarly (38, 47, 48, 60), the mechanism of MYC-induced apoptosis and cell cycle arrest is still poorly understood.

Expression of pro-survival oncogenes, with the earliest example being Bcl-2, have previously been shown to counteract the death function of MYC (4, 19, 55). Additionally, activation of PI3K and its downstream target Akt can protect against apoptosis induced by MYC (29). PI3K and Akt were shown in the mid-1990's to convey a strong pro-survival signal downstream of receptor tyrosine kinases (15, 30, 31) by impacting the apoptosis machinery directly (11, 12, 50, 62), and by regulating FOXO transcription factors (6-8, 13, 51). Furthermore, loss of the tumor suppressor MMAC1/PTEN results in constitutive PI3K signals (32, 54) and can lead to tumors in humans (10, 14). Thus, aberrant MYC activation together with overactive Akt, a condition that is often achieved in tumor cells, can provide the cooperative growth and anti-apoptotic signals necessary to promote tumorigenesis.

A recently identified protein, CDCA7 (also called JPO1), is expressed from the MYC- and E2F-responsive gene *cdca7* (22, 41, 44). MYC and E2F1 bind to the promoter of *cdca7* to drive CDCA7 expression (22, 44), causing CDCA7 mRNA to be widely expressed with high levels in the colon, thymus and small intestine, and lower levels in the testis, stomach and bone marrow (44). High levels of CDCA7 mRNA have been found in patients with AML and blast crisis-staged CML (41),

while solid tumors displaying high levels of MYC were also shown to be positive for CDCA7 (41). While CDCA7 had weak transformation properties when expressed alone, co-expression rescued transformation of a transformation-defective MYC with a MYC-Box II deletion (44). Furthermore, recent work by Penn and colleagues have shown that JPO2, a protein with some homology with CDCA7, can directly associate with MYC, and this increases MYC-dependent transformation (28). Both CDCA7 and JPO2 contain a highly conserved carboxyl-terminal cysteine rich region that might allow binding to DNA (22). However, it is unknown if CDCA7 also associates with MYC.

In the present study, we show that CDCA7 and MYC physically interact. We have mapped the domains of interaction and have discovered that Akt phosphorylates CDCA7 near this contact region, leading to loss of its association with MYC, binding to 14-3-3 proteins and exclusion from the nucleus. Co-expression of CDCA7 with MYC sensitized cells to serum-withdrawal induced apoptosis and this pro-apoptotic activity required the MYC-binding region. Short hairpin RNAi-mediated knockdown of CDCA7 rescued cells from MYC-dependent apoptosis following removal from serum. These finding point to a feed-forward loop whereby MYC activation up-regulates CDCA7, with Akt activity controlling the accessibility of CDCA7 to nuclear MYC proportionate to growth factor signaling.

Methods and materials

Cell lines and cell culture

HEK 293 and Rat1 cells were obtained from the American Type Culture Collection and maintained in Dulbecco's modified Eagle's medium supplemented with 10% fetal bovine serum and antibiotics at 37°C and 5% CO_2. Akt 1/2 null mouse embryonic fibroblasts (52) were a gift from

Dr. Veronique Nogueira of the University of Illinois at Chicago. Rat1-MYC cells were obtained by stable transfection of Myc and selection in 600 μg/ml G418 and 20% fetal bovine serum. Clones expressing both wild-type and mutant CDCA7 were established using the Tet-ON advanced inducible gene expression system from Clontech. Specifically, stable clones expressing a tet-induced transactivator (rtTA) were obtained by stable transfection of Rat1 and Rat1-MYC cells, respectively, with pIREShyg3-rtTA, followed by selection in 200μg/ml hygromycin. Subsequently the rtTA-Rat1 and rtTA-Rat1-MYC cells were co-transfected with a 100:1 ratio of pTRE-tight-3xFLAG-CDCA7 plasmid and linearized puromycin plasmid, followed by selection in 2μg/ml puromycin. All Rat1-MYC derived inducible lines were maintained in 20% fetal bovine serum while Rat1-CDCA7 derived inducible lines were maintained in 10% fetal bovine serum.

Antibodies and Reagents

Mouse monoclonal M2 anti-flag (A2220) and rabbit polyclonal anti-CDCA7 (HPA005565) were purchased from Sigma-Aldrich. Rabbit polyclonal anti-CDCA7 (Ab69609) was purchased from Abcam. Mouse monoclonal anti-14-3-3β (SC-1657) and 9E10 mouse monoclonal anti-MYC (SC-40) were purchased from Santa Cruz. Rabbit polyclonal anti-Myc (5605), rabbit polyclonal anti-pan Akt (9272) and mouse monoclonal anti p-Ser473 Akt (4051) were purchased from Cell Signaling Technologies. An anti-p-Thr163 CDCA7 rabbit polyclonal antibody was generated by Genscript Corporation (California). Akt inhibitor VIII (A6730) and LY294002 (L9908) were purchased from Sigma-Aldrich.

Cloning

The CDCA7coding region was ligated into the p3XFLAG-CMV10 mammalian expression vector (Sigma-Aldrich) to introduce an amino terminal FLAG epitope. Mutagenesis of p3XFLAG-

CMV10-CDCA7 was performed using the QuikChange kit (Stratagene), and the various mutations were sequence-verified. Amino-terminal and internal deletions were created by introducing silent mutations coding for unique restriction sites, followed by digestion and re-ligation. Carboxyl terminal deletions were created by introducing stop codons. All deletions were sequence verified. CDCA7 containing the 14-3-3-binding R18-peptide PHCVPRDLSWLDLEANMCLP or the control non-14-3-3-binding peptide PHCVPRDLSWLKLKANMCLP were created by ligating a double-stranded oligonucleotide to replace amino acids 139-164 of CDCA7 in the 3XFLAG-CMV10 vector. The C-terminal His-tagged Myc plasmid was created by cloning the Myc coding region into pEcoli-C-terminal 6xHN (Clontech).

For transient and stable expression of cDNA in cells, HEK 293, mouse 3T3, or Rat1 cells were plated onto 100-mm-diameter dishes at 80% confluency and transfected with 5 μg of plasmid using Lipofectamine 2000 (Invitrogen) following the manufacturer's protocol. Transfection medium was removed and replaced with complete Dulbecco's modified Eagle's medium overnight.

For retroviral expression of CDCA7 in Rat1 cells, 3X-FLAG-CDCA7 or CDCA7 with various mutations were cloned into the pQCXIH retroviral vector (Clontech) upstream of an IRES sequence and the hygromycin resistance gene. Either empty pQCXIH or pQCXIH-CDCA7-IRES-Hygro retroviral vectors were transfected into the ecotropic-envelope protein packaging cell line EcoPack 2-293 (Clontech). Viral particles were collected 48 hours later and concentrated using Retro-X concentrator (Clontech).

shRNA Cloning and qRT-PCR

Oligonucleotides

(5'-GATCCCCAATGAAGTTCCCAGCACGATTCAAGAGATCGTGCTGGGAACTTCATTTTTTTA-3'),

(5’-GATCCCCAGTTCCCAGCACGAAATACTTCAAGAGAGTATTTCGTGCTGGGAACTTTTTTA-3’)

(5’-GATCCCCCTGTGGACGGCTATATGAATTCAAGAGATTCATATAGCCGTCCACAGTTTTTA-3’)

targeting rat CDCA7 at nucleotides 212, 220 and 658 respectively, were annealed, ligated into the pSuper vector, and transfected into Rat1-MYC cells. Several colonies of each targeting region were isolated following puromycin selection.

Total RNA was purified and cDNA synthesized using NEB’s ProtoScript® M-MuLV First Strand cDNA Synthesis Kit. Quantification of shRNA knockdown and screening of clones was performed using SA Bioscience’s RT² SYBR® Green qPCR Master mix and Applied Biosystems’ 7500 Fast RT-PCR system.

Cell Lysis, Immunoprecipitation, and Immunoblotting

Cells were lysed in either RIPA lysis buffer (10mM NaPO4, pH 7.6, 150mMNaCl, 5mM EDTA, 0.1% sodium dodecyl sulphate, 0.25% deoxycholic acid, 1% triton X-100, plus protease and phosphatase inhibitors) or Triton X-100 lysis buffer (50mMHepes, pH 7.9, 250mMNaCl, 0.1% Triton X-100, 10% glycerol, plus protease and phosphatase inhibitors). Ten μl of anti-FLAG M2 agarose conjugated beads (Sigma Aldrich) were added to lysates and incubated overnight at 4°C. The beads were washed five times with lysis buffer, and proteins were eluted with 200 μl of lithium dodecyl sulfate sample buffer and heated to 70°C for 10 min. Portions of the lysates prior to immunoprecipitation were also reserved and boiled with lithium dodecyl sulfate-containing sample buffer. Lysates and immunoprecipitations were fractionated by SDS-PAGE, transferred to a PVDF membrane, blocked in 5% skim milk for 30 min, and probed with the appropriate antibody overnight at room temperature. Primary antibodies were decorated with IR700 anti-mouse and/or

IR800 anti-rabbit secondary antibodies (Li-Cor Biosciences) for 3 hours at room temperature and visualized using the infrared laser scanning (Odyssey, Li-Cor Biosciences).

Microscopy

Rat1, NIH3T3 or HEK 293cells were plated at 80% confluency on no. 1 glass coverslips. Following the desired treatment, the coverslips were washed twice in PBS and then fixed and permeabilized in 3:1 methanol:acetic acid for 25 minutes. The coverslips were then washed three times in PBS followed by blocking in 1% BSA in PBS. Primary antibodies at varying concentrations were applied for 1.5 hours in a humidified chamber at room temperature. Coverslips were washed three times in PBS prior to applying secondary antibodies for 2 hours in a humidified chamber at room temperature and in the dark. The slips were washed three times in PBS before mounting with Invitrogen's ProLong Gold antifade reagent with DAPI. The slides were viewed on an Olympus microscope and images were taken via a QImaging 2000R camera and Q-Capture pro software.

Live cell imaging was performed on an inverted Olympus microscope equipped with an Ultraview ERS spinning disc unit, 37C heated stage and 60X heated objective. NIH 3T3 cells were transfected on number-1 coverslip chambers overnight, serum starved for 4 hours, and stimulated with PDGF. Confocal images were taken every 5 minutes for the duration of the time course and analyzed with Perkin Elmer Ultraview ERS software.

Peptide Competition Assay

The Thr163 peptide (CDSKSPRRRTFPG) and phosphopeptide (CDSKSPRRR(p)TFPG) corresponding to the sequence surrounding Thr163 were synthesized by Genscript. Triton-X100 lysates containing FLAG-CDCA7 were immunoprecipitated with anti-FLAG M2 agarose

conjugated beads overnight at 4°C. Following washing, beads were incubated at 4°C for 1 hour with various concentrations of peptide or phosphopeptide where indicated. The beads were washed three times, and proteins were eluted and resolved by SDS-PAGE. Co-immunoprecipitated 14-3-3 was detected using rabbit polyclonal anti-14-3-3β antibody.

In vitro pull-down assay

HEK293 cells were transfected overnight with FLAG-CDCA7and various mutants. Cells were lysed in RIPA lysis buffer and immunoprecipitated with FLAG-M2 agarose conjugated beads overnight at 4°C. Agarose beads were washed 3 times with RIPA lysis buffer and then 3 times with Triton X-100 lysis buffer. Immunoprecipitates were then eluted by incubation at 4°C with 20μM FLAG peptide in Triton X-100 lysis buffer.

For generation of recombinant MYC, 6xHN-MYC-expressing DH5α bacteria were cultured overnight in 100ml Terrific broth (TB) at 37°C with shaking overnight. The following day 1L of TB was inoculated from the overnight culture. Cells were stimulated with 1 mM IPTG when the OD_{600} reached 1.0. The culture was then incubated at 16°C overnight. Cells were pelleted by centrifugation and resuspended in 60mL of binding buffer (50mM Tris, pH 7.5, 500mM NaCl, 5mM Imidazole). Cells were lysed by sonication at 30% amplitude, 2 seconds on, 3 seconds off, for a total of 2 minutes. Insoluble precipitates were removed by centrifugation and the supernatant was bound to Ni-Nta beads at 4°C, for 20 minutes with gentle rocking. Ni-Nta beads were washed with 10 column volumes of wash buffer (50mM Tris, pH 7.5, 500 mM NaCl, 30 mM Imidazole). 6xHN-MYC was eluted in 5 mL fractions with elution buffer (50 mM Tris, pH 7.5, 500 mM NaCl, 250 mM Imidazole). Purified 6xHN-MYC was dialyzed against three changes of HKG buffer (20 mM HEPES, pH 7.4, 125 mM KCl, 20% (v/v) glycerol).

For pull-down experiments, 500 ng of purified His-MYC protein was bound to Ni-NTA agarose beads and incubated with purifiedFLAG-CDCA7 protein for 4hoursat 4°C in Triton X-100 lysis buffer. Beads were washed 5 times and proteins were proteins were eluted with 200 μl of lithium dodecyl sulfate sample buffer heated to 70°C for 10 min. Portions of the input protein prior to binding were also boiled with lithium dodecyl sulfate-containing sample buffer. Input and bound protein were fractionated by SDS-PAGE.

Apoptosis assays

For annexin assays, cells were harvested with EDTA-free trypsin and washed twice at 4°C with ice cold PBS and stained by resuspension in 200μl Annexin binding buffer (10 mM HEPES, pH 7.4, 140mMNaCl, 2.5 mM $CaCl_2$) containing 5ml Annexin V-alexa488 conjugate and 1μg/ml propidium iodide. The proportion of apoptotic cells (Annexin-V positive, propidium iodide negative) was determined using a FACScan flow cytometer and Cell-Quest software (Becton Dickinson). Caspase assays were performed by scraping approximately 10^6 cells in caspase assay buffer (25 mM HEPES pH 7.4, 5 mM EDTA, 2 mM DTT, 137 mM NaCl, 10% glycerol). Cells were sonicated at low power, and insoluble materials pelleted by centrifugation. 150μl of lysate was incubated at 37C with 10μM DEVD substrate (N-Acetyl-Asp-Glu-Val-Asp-7-amido-4-methylcoumarin, Sigma). Samples were read every 15 minutes at 380nm excitation, 450nm emission and caspase-3 activity was normalized to total protein as determined by Bradford assay.

Metabolic Labeling

HEK293 cells were transfected overnight with FLAG-CDCA7, washed and incubated in phosphate free medium containing 1 mCi/ml ^{32}P-labeled orthophosphate for 4 hours. Cells were lysed in 1ml RIPA and FLAG-CDCA7 was immunoprecipitated with pre-bound monoclonal M2

anti-Flag beads overnight at 4°C. Immunoprecipitates were fractionated by 8% SDS-PAGE, Coomassie stained and ^{32}P-labeled CDCA7 was detected by autoradiography.

Tryptic mapping

^{32}P-labeled CDCA7 was isolated as described above, excised from the gel and digested with 10μg/ml tosylphenylalanylchloromethyl ketone-treated trypsin (Promega) in 50mM $(NH_4)HCO_3$, pH 7.8, overnight at 37°C. Isolation of peptides was performed as described elsewhere (34).

In vitro Akt phosphorylation assay

FLAG-tagged CDCA7 was immunoprecipitated from cell lysates with 25 μl FLAG M2 monoclonal antibody conjugated to agarose (Sigma–Aldrich). Immunoprecipitates were washed three times in RIPA buffer, followed by an additional two times in reaction buffer containing 40 mM MOPS-NaOH pH 7.0, 1 mM EDTA. The samples were then resuspended in reaction buffer plus 0.5 ug of active Akt (S472D) (Millipore). The kinase reaction was started by the addition of an ATP mixture containing 8 μM magnesium acetate, 10 μM ATP and 1μCi of [^{32}P]ATP. Samples were incubated for 20 minutes at 30°C, the supernatant was then removed to fresh tubes and CDCA7 immunoprecipitates were washed three times with reaction buffer and finally resuspended in 1x LDS sample buffer. The supernatant containing Akt and the CDCA7 immunopreciptates were resolved by SDS-PAGE. [^{32}P]CDCA7 was visualized with a phosphoimager (Bio-Rad Laboratories).

Soft-agarose colony formation assay

Rat1 cells were infected with retrovirus generated by the pQCXIH-CDCA7-IRES-Hygro vector. After 5-7 days selection in hygromycin (200 μg/ml), resistant pools were counted and plated in

complete medium containing 0.3% agarose and hygromycin over a bottom layer of complete medium containing 0.7% agarose and hygromycin. Fresh medium with serum was added to the plates every two days, and after two weeks plates were stained with crystal violet, destained, and visualized by infrared scanning on an Odyssey laser scanner. Macroscopic colonies were counted using ImageJ software.

Results

CDCA7 binds to the carboxyl terminus of MYC

Figure 2.1A depicts the various regions of CDCA7 and their postulated biological roles, which includes a C-terminal zinc finger domain that could interact with DNA, a leucine zipper (LZ) region that could promote hetero- and homo-dimerization, and a putative nuclear localization signal between amino acids 170 and 190 of human CDCA7. Conservation within this region is very high between species. We performed co-precipitation experiments, and deletions of both N-terminal and C-terminal segments of CDCA7 revealed that a small region of CDCA7, amino acids 146-170, was essential for interaction with MYC (Figure 2.1B,C). In reciprocal experiments we found that CDCA7 lost association with MYC harboring a deletion of the C-terminal region (Δ274-440), but not MYC lacking the N-terminal MYC Box (MB) I and II domains (Δ5-149), or the central region of MYC containing the MBIII domain (Δ151-274) (Figure 2.1D). Finally, immunoprecipitation of endogenous MYC led to co-precipitation of endogenous CDCA7, indicating interaction of physiological levels of these proteins (Figure 2.1E).

The region of CDCA7 that associates with MYC is remarkable for several reasons. First, there appears to be a putative bipartite NLS domain spanning amino acids 160-190 (Figure 2.1A). Secondly, threonine 163 conforms to the consensus Akt phosphorylation site with an arginine at -

5 and -3, and a bulky hydrophobic at +1. Furthermore, there is a proline at +2, and this same arrangement of residues is present in other Akt substrates that bind to the phospho-adapter proteins 14-3-3, including FOXO3α (7, 8, 51). Based on these initial observations, we formulated the hypothesis that MYC and CDCA7 association could be regulated in a transient manner though phosphorylation at Thr163 by Akt and binding to 14-3-3.

To test whether Thr163 is a site of phosphorylation, we performed phosphotryptic mapping of CDCA7 isolated from cells labeled with ^{32}P-orthophosphate (Figure 2.2A). One spot co-migrated with a synthetic phosphotryptic peptide for this residue, which disappeared upon mutation of Thr163 to alanine. Next, we generated a phospho-specific antibody to this site. The anti-phospho-Thr163 antibody reacted with wildtype CDCA7 but not T163A CDCA7 (Figure 2.2B). Treatment of CDCA7 with calf intestinal phosphatase resulted in significant reduction in immunoreactivity (Figure 2.2B). These data establish that Thr163 is phosphorylated in cells.

Next, we immunoprecipitated CDCA7 and found that it co-precipitated endogenous 14-3-3 in a phospho-Thr163-dependent manner (Figure 2.2C). Addition of a molar excess of a synthetic Thr163-containing phosphopeptide, but not the corresponding unphosphorylated peptide, caused a loss of 14-3-3 binding (Figure 2.2D). We mutated each residue surrounding Thr163 starting at -7 to alanine and examined for 14-3-3 binding and reactivity to the phosphospecific antibody. Both the -5 and -3 arginine's, Arg158 and Arg160, were absolutely required for 14-3-3 binding and phosphorylation of Thr163 (Figure 2.2E). Mutation of phenylalanine 164 and proline 165 resulted in loss of phospho-Thr163 reactivity and loss of 14-3-3 binding. Interestingly, mutation of Arg161 or Arg162 to alanine caused an increase in 14-3-3 binding and an apparent increase in Thr163 phosphorylation.

Binding of 14-3-3 is known to alter numerous biological functions of their target proteins, including subcellular localization (21). In cells grown in 10% serum, over-expressed wildtype CDCA7 resided primarily in the nucleus and, to a lesser extent, cytoplasm (Figure 2.3A). In contrast, T163A CDCA7 was entirely nuclear with no cytoplasmic localization. Conversely, the R161A CDCA7 mutation caused both cytoplasmic and nuclear staining, correlating with the increased binding to 14-3-3 seen in Figure 2.2E. P165A mutation, which abolished 14-3-3 binding, likewise resulted in entirely nuclear localization. We quantified these observations by calculating the ratio of the fluorescence intensity of the cytoplasm (Fc) to nucleus (Fn) for each mutation. R161A CDCA7, as expected had the highest Fc/Fn ratio, which was similar to wildtype CDCA7 stimulated with FGF. T163A, F164A and P165A all had low Fc/Fn ratios, consistent with their predominantly nuclear staining seen in Figure 2.3A and their low level of 14-3-3 binding seen in Figure 2.2E.

Next, we asked if constitutive 14-3-3 binding independent of Thr163 phosphorylation could regulate localization. To test this, we substituted the 20 amino acids surrounding Thr163 with the R18 peptide (PHCVPRDLSWLDLEANMCLP). This peptide was isolated from a phage-display screen for peptides that bind strongly to 14-3-3, where the underlined D and E residues form contacts with 14-3-3 and substitute for phospho-amino acids (56). We found that DE-CDCA7 bound to 14-3-3, and resulted in cytoplasmic CDCA7 (Figure 2.3C, D). As a control, we generated a protein in which the D and E residues were substituted with lysine. KK-CDCA7 did not bind to 14-3-3 and was entirely nuclear (Figure 2.3C, D). Thus, the binding of 14-3-3 at Thr163 of CDCA7 appeared to be responsible for its shift to the cytoplasm in cells.

Amino Acids 160-176 is a bipartite nuclear localization signal

To account for the shift in localization due to Thr163 phosphorylation and 14-3-3 binding, we searched CDCA7 for a proximal NLS domain that could be influenced by 14-3-3. The presence of basic arginine residues at 160, 161, 162, and another cluster at 170, 171, 175 and 176 resembled the bipartite NLS domains of RB and SWI5 (Figure 2.4A). To test this, we asked whether the isolated region spanning amino acids 157–188 of CDCA7 could import a large cargo protein. We juxtaposed our test region between GFP and β-galactosidase, which created a 140-kDa protein. A *bona fide* NLS isolated from SV40 caused the GFP-β-gal fusion protein to localize to the nucleus (Figure 2.4B). Introduction of a point mutation within the SV40 NLS resulted in cytoplasmic localization, validating this model for testing NLS activity. Insertion of amino acids 157-188 of CDCA7 resulted in nuclear localization, similar to the NLS of SV40 (Figure 2.4B). In contrast, subdivision of the full 157-188 region into smaller regions surrounding just the 14-3-3 binding site, amino acids 157-167, or the second cluster of arginine's from 167-188, led to entirely cytoplasmic localization (Figure 2.4B). This suggests that the entire region of 157 through 188 is needed for the nuclear import of the GFP-β-galactosidase fusion protein.

We next tested the importance of the specific arginine residues within the putative NLS. Mutation of Arg160, 161 or 162 shifted the localization of the fusion protein to the cytoplasm (Figure 2.4C). Similarly, mutation of Arg171 or Arg176 individually to glutamic acid shifted the balance of localization from nucleus to cytoplasm, while the double mutation of R171E/R176E led to complete nuclear exclusion (Figure 2.4C). Finally, mutation of Arg182 or Arg184 had no effect on localization (Figure 2.4C). These results indicate that arginine's 160, 161, 162, 171 and 176 compose the critical basic residues of a potential bipartite NLS within CDCA7.

Akt phosphorylates Thr163 of CDCA7

Next, we asked whether Thr163 phosphorylation changed in cells treated with mitogenic stimuli. We expressed CDCA7 in 3T3 fibroblast cells followed by stimulation with PDGF, and found that Thr163 phosphorylation increased rapidly and remained sustained for several hours (Figure 2.5A). Furthermore, we found that PDGF stimulation led to increased cytoplasmic localization that lagged behind phosphorylation of Thr163 (Figure 2.5B). Finally, GFP-CDCA7 was visualized in live cells over a time course of PDGF stimulation (Figure 2.5C,D). This experiment showed that cytoplasmic GFP-CDCA7 signal increased approximately 3-fold, which agreed well with the kinetics observed by immunoblotting in Figure 2.5B.

We then expressed CDCA7 or T163A CDCA7 in 3T3 cells and performed immunofluorescence with anti-phospho-Thr163 antibody (Figure 2.5E). This showed that there was a small amount of primarily nuclear phospho-Thr163 signal in unstimulated cells. Stimulation with PDGF for 15 and 60 minutes resulted in an increase in both nuclear and cytoplasmic phospho-Thr163 signal, corresponding to the appearance of cytoplasmic CDCA7. Finally, we isolated nuclear and cytoplasmic fractions of cells expressing CDCA7 following treatment with LY-294002, a PI3K inhibitor (Figure 2.5F). Cytoplasmic CDCA7 was present in cells maintained in serum, but was abolished upon treatment with LY-294002. The T163A CDCA7 mutation caused very little detectable cytoplasmic CDCA7.

We were able to detect endogenous CDCA7 in 3T3 cells by immunofluorescence using an antibody raised against CDCA7 (Abcam). This experiment showed that under serum-starved conditions endogenous CDCA7 was predominantly nuclear with some cytoplasmic staining (Figure 2.6A). Stimulation with PDGF for 30 minutes caused a pronounced shift to the cytoplasm.

Pre-treatment of cells with LY294002, wortmannin, or Akt inhibitor VIII, each potent inhibitors of PI3K and Akt, completely reversed the cytoplasmic localization of endogenous CDCA7 in response to PDGF, with pronounced staining of endogenous CDCA7 in the nucleus. Moreover, stimulation of cells with PDGF caused an increase in the amount of detectable endogenous Thr163 phosphorylation (Figure 2.6B). This was different from ectopically expressed CDCA7 and GFP-CDCA7: rather than being localized to the nucleus and cytoplasm, endogenous phospho-CDCA7 signal was detected primarily in the cytoplasm at 60 minutes. This might be a result of the lower amount of endogenous CDCA7 protein compared with over-expressed CDCA7, which could overwhelm the cells resources to shuttle phospho-CDCA7 from the nucleus. Pre-treatment with LY-294002 abolished the elevated Thr163 phosphorylation induced by PDGF (Figure 2.6B).

The observations that LY294002 could block the phosphorylation of endogenous Thr163, and reduce the cytoplasmic localization of CDCA7, suggested that a downstream effector of PI3K, such as Akt, might phosphorylate CDCA7 at this site. Treatment of cells with LY294002 reduced Thr163 phosphorylation (Figure 2.7A). To test if this was a result of loss of Akt activation, we co-expressed gag-Akt, a membrane bound, constitutively active form with wildtype CDCA7 or T163A CDCA7. Gag-Akt caused an elevation of Thr163 phosphorylation of CDCA7 and 14-3-3 binding (Figure 2.7B) that was lost upon mutation of Thr163 to alanine. Active recombinant Akt directly phosphorylated CDCA7, but not T163A CDCA7, *in vitro* (Figure 2.7C). Inhibition of Akt in cells with Akt inhibitor VIII blocked phosphorylation of CDCA7 in cells (Figure 2.7D). Co-expression of gag-Akt with CDCA7 caused a redistribution of wildtype CDCA7 from the nucleus to the cytoplasm, but not T163A CDCA7 (Figure 2.7E). Finally, expression of CDCA7 in mouse embryonic fibroblasts in which Akt1 and Akt2 were deleted by homologous recombination resulted in diminished Thr163 phosphorylation (Figure 2.7F). PDGF-stimulated phosphorylation

of Thr163 was reduced in Akt1/2 -/- MEFs compared with wildtype MEFs, which was similar to the reduction of total Ser473 phosphorylation detected for the remaining endogenous Akt3 (Figure 2.7G). Together, these experiments provide strong evidence that Akt catalyzes Thr163 phosphorylation.

Binding of 14-3-3 regulates CDCA7 – MYC interaction

Since Akt phosphorylates CDCA7 and promotes 14-3-3 binding very near the residues required for MYC interaction, we thought that phosphorylation-dependent 14-3-3 binding could cause a change in association between CDCA7 and MYC. When we compared wildtype CDCA7 and T163A CDCA7 for their ability to co-immunoprecipitate MYC from cells, we found that more MYC bound to T163A CDCA7 than the equivalent amount of wildtype CDCA7 (Figure 2.8A). Using purified proteins in pull-down experiments, we found that DE-CDCA7, which binds to 14-3-3 constitutively, immunoprecipitated less MYC, similar to the loss of MYC interaction seen with Δ(156-187)-CDCA7 (Figure 2.8B). On the other hand, the non-14-3-3 interacting control protein, KK-CDCA7, did bind to MYC, about as well as wildtype CDCA7.

If 14-3-3 directly competes with MYC for sites of association on CDCA7, then recombinant 14-3-3 should compete with MYC for CDCA7 binding. So, we incubated recombinant MYC with purified FLAG-CDCA7 stripped of endogenous 14-3-3 by SDS treatment, together in the presence or absence of recombinant 14-3-3 (Figure 2.8C). We rationalized that a fraction of the purified CDCA7 binding to MYC would be phosphorylated at Thr163, and if 14-3-3 competes with MYC then addition of 14-3-3 should break this interaction. This was found to be the case, as 14-3-3 dramatically reduced the amount of Thr163-phosphorylated CDCA7 co-precipitating with MYC (Figure 2.8C). Together, these experiments indicate that 14-3-3 competes with MYC for binding

to CDCA7. Furthermore, when co-expressed in Rat1 cells, MYC co-localizes with non-14-3-3 binding CDCA7 mutants T163A and KK, while MYC co-localized to a lesser degree with wildtype CDCA7 and the 14-3-3 binding DE mutant containing the R18 peptide substitution (Figure 2.8D). Together these results show that 14-3-3, by competing with MYC, alters CDCA7 location in the cell, and therefore its degree of interaction with MYC.

CDCA7 expression sensitizes cells to serum withdrawal-induced apoptosis

We next established Rat1 fibroblast cells expressing MYC under a constitutive CMV promoter (termed MYC-Rat1). These cells underwent apoptosis following 4-24 hours of serum withdrawal, reproducing the findings of Evan et al. (18). In order to investigate if CDCA7 altered MYC-dependent apoptosis, we expressed CDCA7 under the control of a doxycycline-inducible promoter in either parental Rat1-TET-ON or MYC-Rat1-TET-ON fibroblasts. Several independent clones were isolated from each and all showed a low level of CDCA7 expression when grown in serum supplemented with 10 ng/ml doxycycline (Figure 2.9A). When doxycycline was increased to 1000 ng/ml, the level of expression of CDCA7 increased approximately 100-fold (Figure 2.9A). Interestingly, we were not able to generate T163A-CDCA7-MYC-Rat1 cells. Colonies that were isolated were either negative for MYC expression or negative for T163A CDCA7, indicating a possible prohibitive condition for co-expression.

To see if there was an effect on apoptosis upon up-regulation of CDCA7, we pre-treated CDCA7-Rat1 or CDCA7-MYC-Rat1 with doxycycline for 18 hours, followed by 4 hours of serum withdrawal. The CDCA7-MYC-Rat1 cells were sensitized to apoptosis with increasing concentration of doxycycline (Figure 2.9C). Only a minor increase in apoptosis was observed with up-regulation of CDCA7 in the absence of ectopic MYC expression (Figure 2.9C). Next, we asked

if the non-MYC binding CDCA7, Δ(156-187)-CDCA7 would alter MYC-dependent apoptosis (Figure 2.9D). Here we treated CDCA7-MYC-Rat1 or Δ(156-187)-CDCA7-MYC-Rat1 cells with doxycycline for 18 hours and then serum starved for 4 hours. This result showed that despite a high level of MYC expression (Figure 2.9B), the Δ(156-187)-CDCA7-MYC-Rat1 cells were no longer susceptible to serum-withdrawal induced apoptosis, suggesting that Δ(156-187)-CDCA7 was acting as a dominant negative and repressing MYC-induced apoptosis.

Loss of CDCA7 expression reduces MYC-dependent apoptosis.

Endogenous CDCA7 mRNA levels in MYC-Rat1 cells were between 2- and 5-fold higher compared to Rat1 cells not expressing ectopic MYC (data not shown), consistent with an earlier report that the *cdca7* promoter is a target of MYC (44). Since we have shown that elevated levels of ectopic CDCA7 sensitized MYC-Rat1 cells to apoptosis upon serum withdrawal, we hypothesized that the elevated levels of both CDCA7 and MYC in the MYC-Rat1 cells may act together to cause the higher levels of apoptosis seen in these cells. In addition, the loss of apoptosis as a result of expression of Δ(156-187)-CDCA7 suggested that CDCA7 was necessary for MYC-sensitized apoptosis. To test this, we created MYC-Rat1 lines expressing shRNA sequences targeting endogenous CDCA7. This resulted in a knockdown of endogenous CDCA7 messenger RNA compared to a control line expressing scrambled shRNA (Figure 2.10A). These Rat1-MYC-sh lines maintained high levels of MYC as detected by immunoblot (Figure 2.10B). When cultured in 0.2% serum overnight, Rat1-MYC-sh cells exhibited less morphological evidence of apoptosis when compared to their MYC-Rat1 parental lines (Figure 2.10D), and experienced less cell death measured by trypan blue exclusion (Figure 2.10E), and less apoptosis when measured by Annexin

V-binding assay (Figure 2.10C), or by caspase-3 activity (Figure 2.10F, G). Together, these result show that CDCA7 is necessary for MYC to promote apoptosis upon serum withdrawal.

CDCA7 expression alters MYC-dependent transformation

We next asked whether CDCA7 alters MYC-induced transformation. We assessed this by expressing CDCA7 in the MYC-Rat1 cells and evaluating soft agarose colony formation. To overcome the negative selection of prolonged expression of T163A CDCA7 and MYC, we introduced CDCA7 and mutants into the MYC-Rat1 cells by retroviral infection, followed by a short selection period and analysis of the polyclonal pools. These results showed that both wildtype and T163A CDCA7 reduced the number of macroscopic colonies resulting from MYC expression, indicating that increased expression of CDCA7 interferes with MYC-induced transformation (Figure 2.11A,B). Surprisingly, Δ(156-187)-CDCA7 expression largely inhibited MYC-dependent colony formation, suggesting that this protein was acting as a dominant negative, similar to its effects on MYC-dependent apoptosis. Parental Rat1 cells did not form colonies (Figure 2.11A), and we found no effect of CDCA7 expression alone in Rat1 (data not shown), in agreement with pervious results of Prescott and coworkers (44). Finally, stable knockdown of CDCA7 also reduced the number of macroscopic colonies formed compared to Rat1-Myc cells expressing scrambled shRNA (Figure 2.11C,D). Together, these results suggest that CDCA7 is a necessary co-factor for Myc-induced transformation and apoptosis.

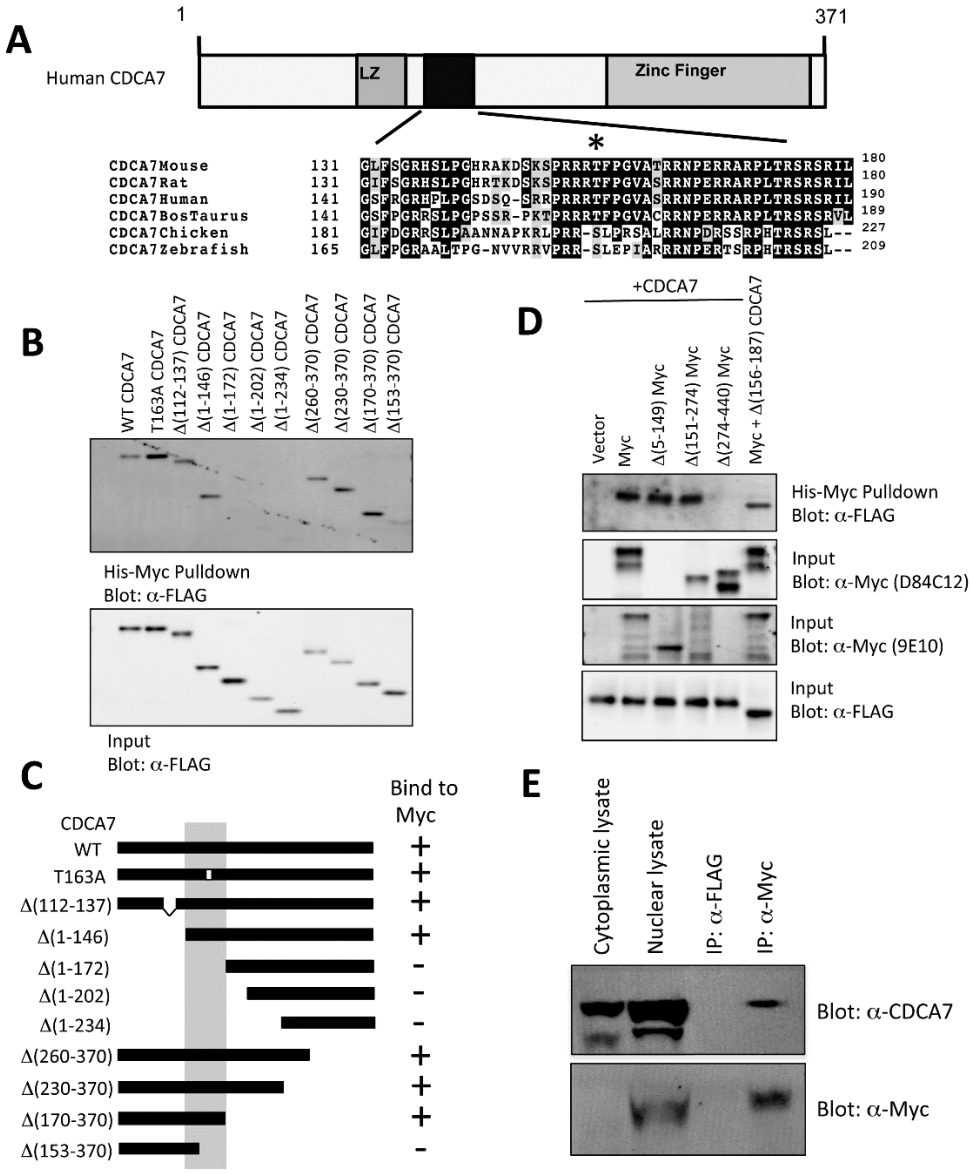

Figure 2.1. Mapping of CDCA7 and MYC association. A. Sequence alignment of CDCA7 within amino acids 131 and 180 of human CDCA7 and from various other species. The asterisk indicates the position of a putative Akt phosphorylation/14-3-3 binding site. **B**. Purified CDCA7 or various truncations were incubated with His-MYC and subjected to pulldown with Ni-Agarose, followed by immunoblotting with anti-FLAG antibody (upper panel). A reserved portion of the input CDCA7 was also immunoblotted with anti-FLAG (lower panel). **C**. Schematic diagram of the region of interaction. **D**. Purified full length His-MYC or containing various truncations were incubated with purified FLAG-CDCA7 or □156-187-CDCA7 and subjected to pull-down with Ni-agarose and immunoblotted with anti-FLAG antibody. Input His-MYC was detected with an N-terminal anti-MYC antibody (D84C12) or a C-terminal antibody (9E10). **E**. Endogenous MYC was immunoprecipitated from HEK293 cells and endogenous CDCA7 was detected by immunoblotting with anti-CDCA7 (Sigma). Anti-FLAG antibody was used as a non-specific immunoprecipitation control.

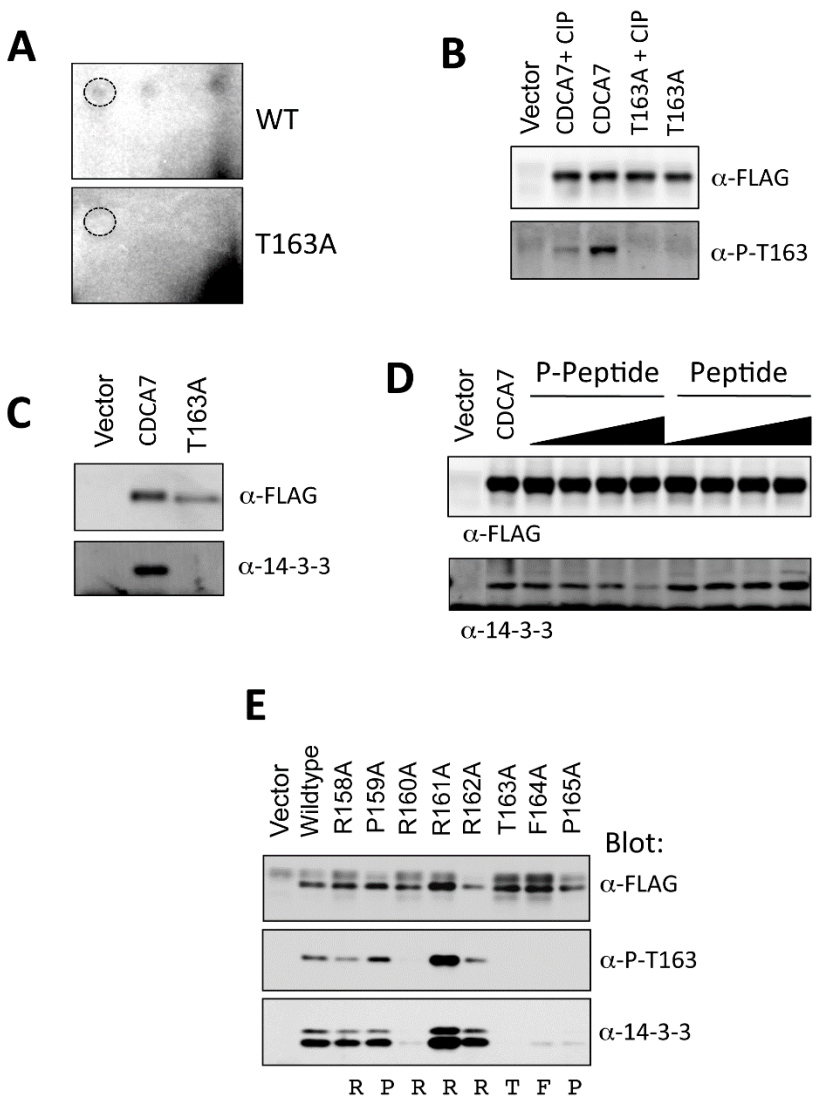

Figure 2.2. CDCA7 is phosphorylated at Thr163 and binds to 14-3-3. A. Two-dimensional tryptic maps of wildtype and T163A-CDCA7. Dotted circle indicates the position of cold synthetic Thr163 tryptic peptide co-migrated with 32P-labelled peptides. **B**. A phosphor-specific antibody raised against phosphor-Thr163 peptide was used to immunoblot CDCA7, CDCA7 pretreated with calf intestinal phosphatase, or T163A-CDCA7. **C.** CDCA7 or T163A-CDCA7 was expressed in cells and immunoprecipitated with anti-FLAG-agarose. Co-immunoprecipitated proteins were detected with anti-FLAG or anti-14-3-3 immunoblotting to detect endogenous 14-3-3. **D.** 14-3-3 bound to CDCA7 was competed with increasing concentrations of the synthetic phospho-Thr163 peptide or the unphosphorylated peptide. Following several washes, proteins were resolved by PAGE and immunoblotted with anti-FLAG or anti-14-3-3 antibodies to detect co-immunoprecipitated endogenous 14-3-3. **E.** CDCA7 containing the indicated mutations was immunoprecipitated and proteins were immunoblotted with anti-FLAG, anti-phospho-Thr163 or anti-14-3-3.

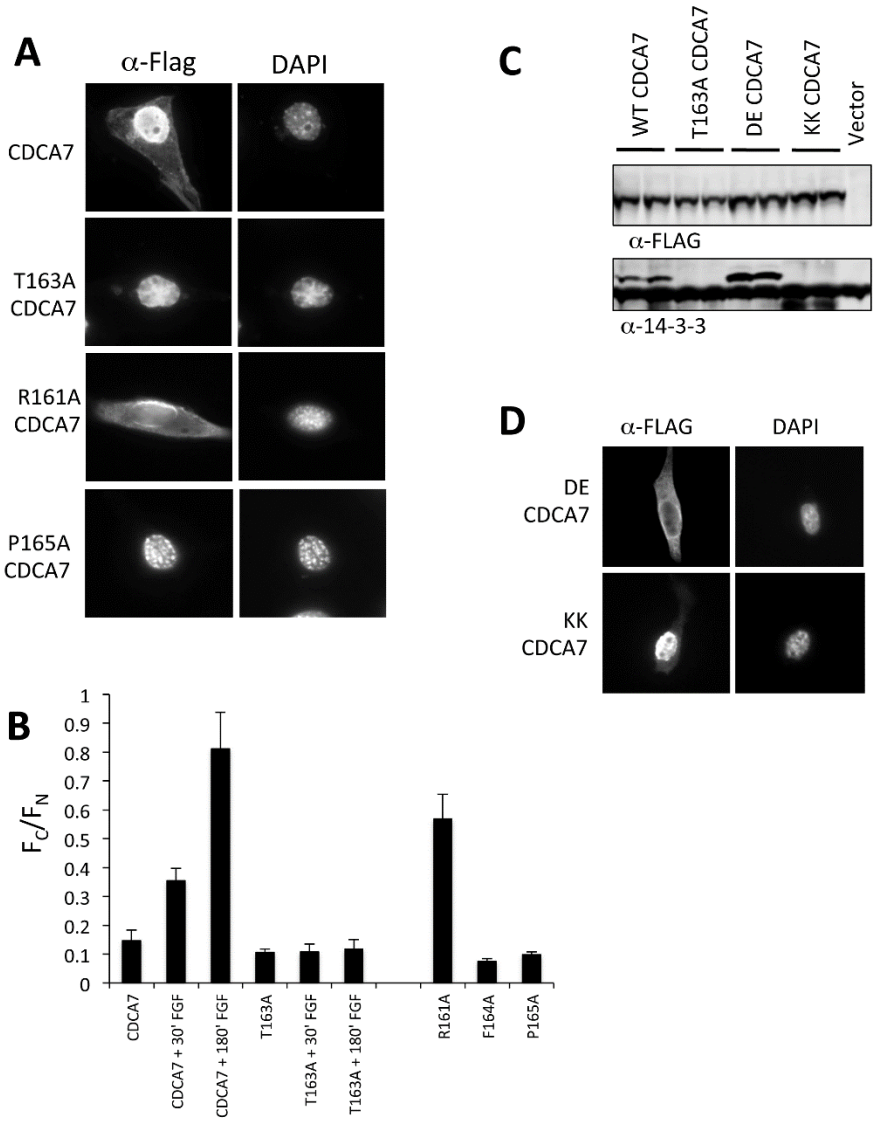

Figure 2.3. Thr163 phosphorylation alters CDCA7 localization. A. NIH3T3 cells were transfected with FLAG-CDCA7 containing the indicated mutations on coverslips. After 24 hours, cells were fixed in methanol and immunofluorescence microscopy was performed to detect CDCA7. **B**. NIH 3T3 cells were transfected with various FLAG-CDCA7 cDNA's for 24 hours, followed by stimulation of some samples with FGF for the indicated times. Cells were fixed, stained with anti-FLAG and visualized by confocal microscopy. The fluorescence intensity of the cytoplasm (Fc) and the nucleus (Fn) were measured in a blind analysis for each sample, and the ratio Fc/Fn was calculated. Error bars represent the standard error of the mean for a minimum of 30 cells for each sample. **C**. Cells expressing CDCA7, T163A-CDCA7, DE-CDCA7 or KK-CDCA7 were lysed and CDCA7 was immunoprecipitated with anti-FLAG M2 agarose. Co-immunoprecipitated endogenous 14-3-3 was detected by anti-14-3-3 immunoblotting. **D.** NIH 3T3 cells were plated on coverslips and transfected with FLAG-DE-CDCA7 or FLAG-KK-CDCA7. After 24 hours, cells were fixed, stained with anti-FLAG antibody, and immunofluorescence microscopy was performed.

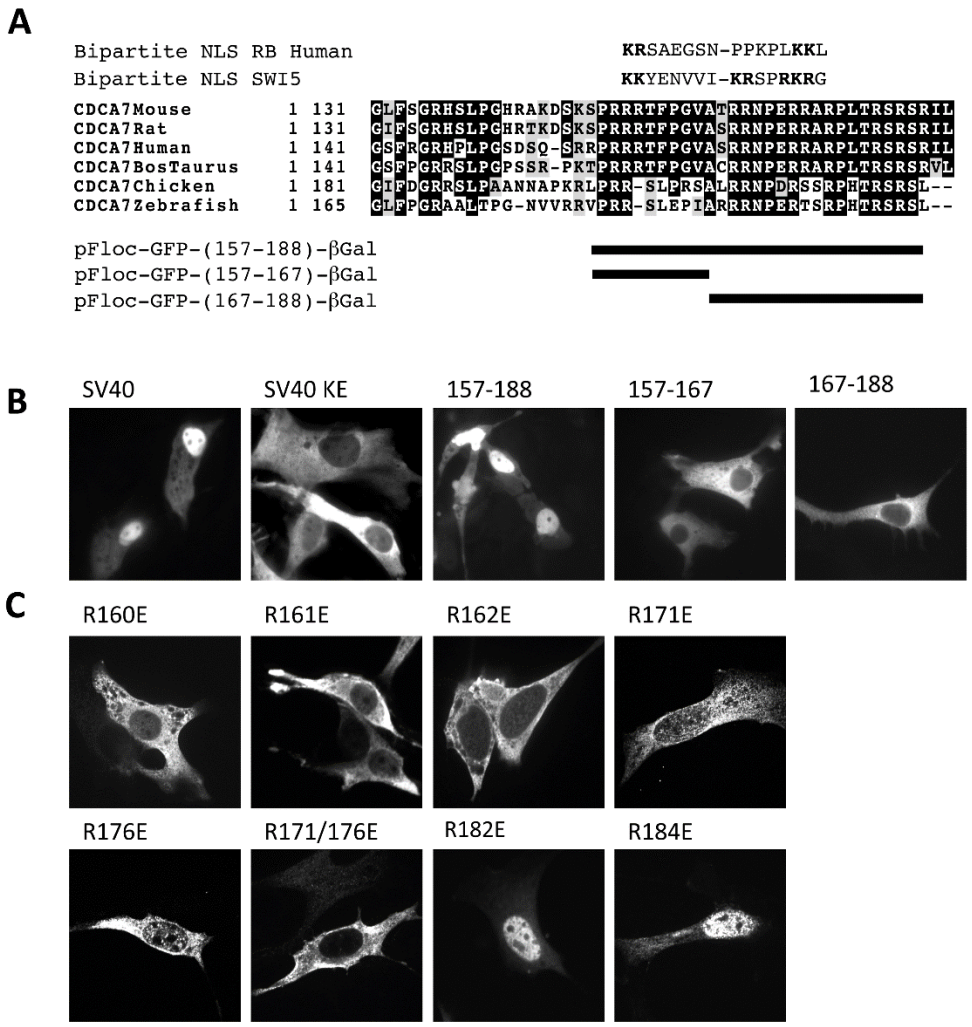

Figure 2.4. Amino acids 167-188 of CDCA7 comprise a putative bipartite NLS. ***A.*** Sequence alignment of CDCA7 with the bipartite NLS domains of human RB protein and SWI5 protein. ***B.*** NIH3T3 cells were transfected on glass coverslips with a vectors expressing pFloc-GFP-SV40-β-gal, pFloc-GFP-SV40KE-β-gal, or pFloc-GFP-CDCA7peptide-β-gal containing various regions of CDCA7 as indicated for 24 hours. The following day GFP signal in live cells were visualized by fluorescence microscopy. ***C***. pFloc-GFP-CDCA7peptide-β-gal containing amino acids 156-188 of CDCA7 and the indicated mutations were transfected into NIH3T3 cells plated on coverslips. The next day, cells were fixed with methanol and visualized by confocal microscopy.

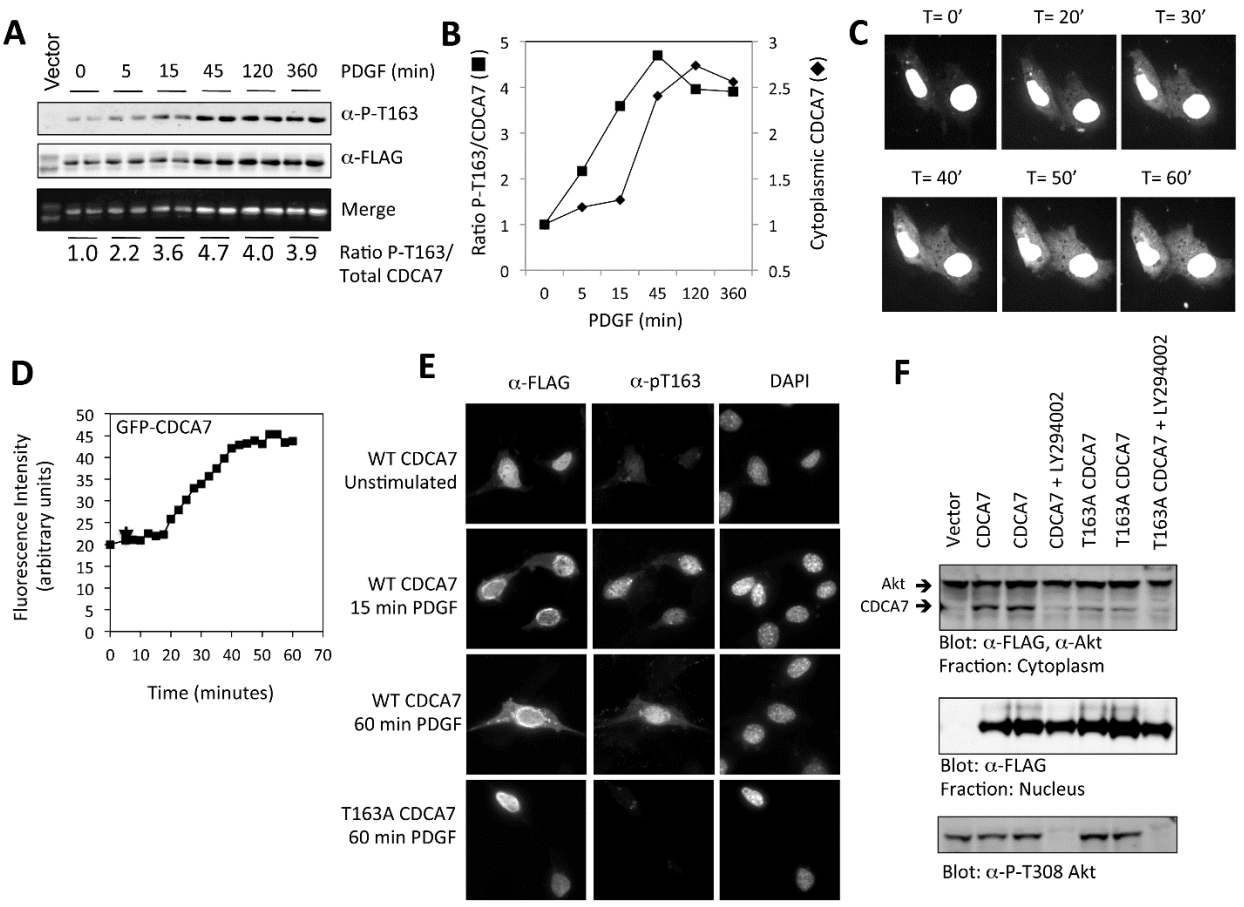

Figure 2.5. PDGF stimulates CDCA7 phosphorylation at Thr163 and cytoplasmic translocation. ***A***. NIH3T3 cells were transfected with FLAG-CDCA7, and the following day were starved of serum for 6 hours and stimulated with PDGF for the indicated times. Cells were then solubilized in 0.25% NP-40 buffer and nuclei were removed by centrifugation. Lysates were probed with anti-phospho-Thr163 and anti-FLAG and both signals were detected simultaneously on an Odyssey infrared scanner. The dual colored image represents the merge of the phospho- (680 nm) and FLAG- (800 nm) signals with ratios of intensities shown beneath. ***B.*** Graphical representation of *A*. ***C***. NIH3T3 cells were transfected with GFP-CDCA7 on a No.1 glass bottom chamber. After 24 hours, the cells were starved of serum for 6 hours and visualized on a Spinning Disc Confocal microscope. At T=0', PDGF was added and the cells were captured every 5 minutes for one hour. ***D***. Cytoplasmic fluorescent intensity was determined using Ultraview software (Perkin Elmer) and plotted against time of PDGF stimulation. The intensity of the nuclei was also measured and decreased by approximately 5% over the time period (not shown). ***E.*** NIH3T3 cells were transfected on glass coverslips with FLAG-CDCA7 or T163A-CDCA7 for 24 hours. Following a 6 hour of serum starvation, cells were stimulated with PDGF for the indicated times, fixed with methanol, and visualized with anti-FLAG and anti-phospho-Thr163 immunofluorescence microscopy. ***F.*** NIH 3T3 cells were transfected with CDCA7 or T163A CDCA7, and the following day were incubated with 50 mM LY294002 for 1 hour before nuclear and cytoplasmic extracts were isolated. CDCA7, endogenous Akt and P-Thr308 Akt were detected by immunoblotting with α-FLAG , α-Akt and α-P-Thr308 Akt antibodies.

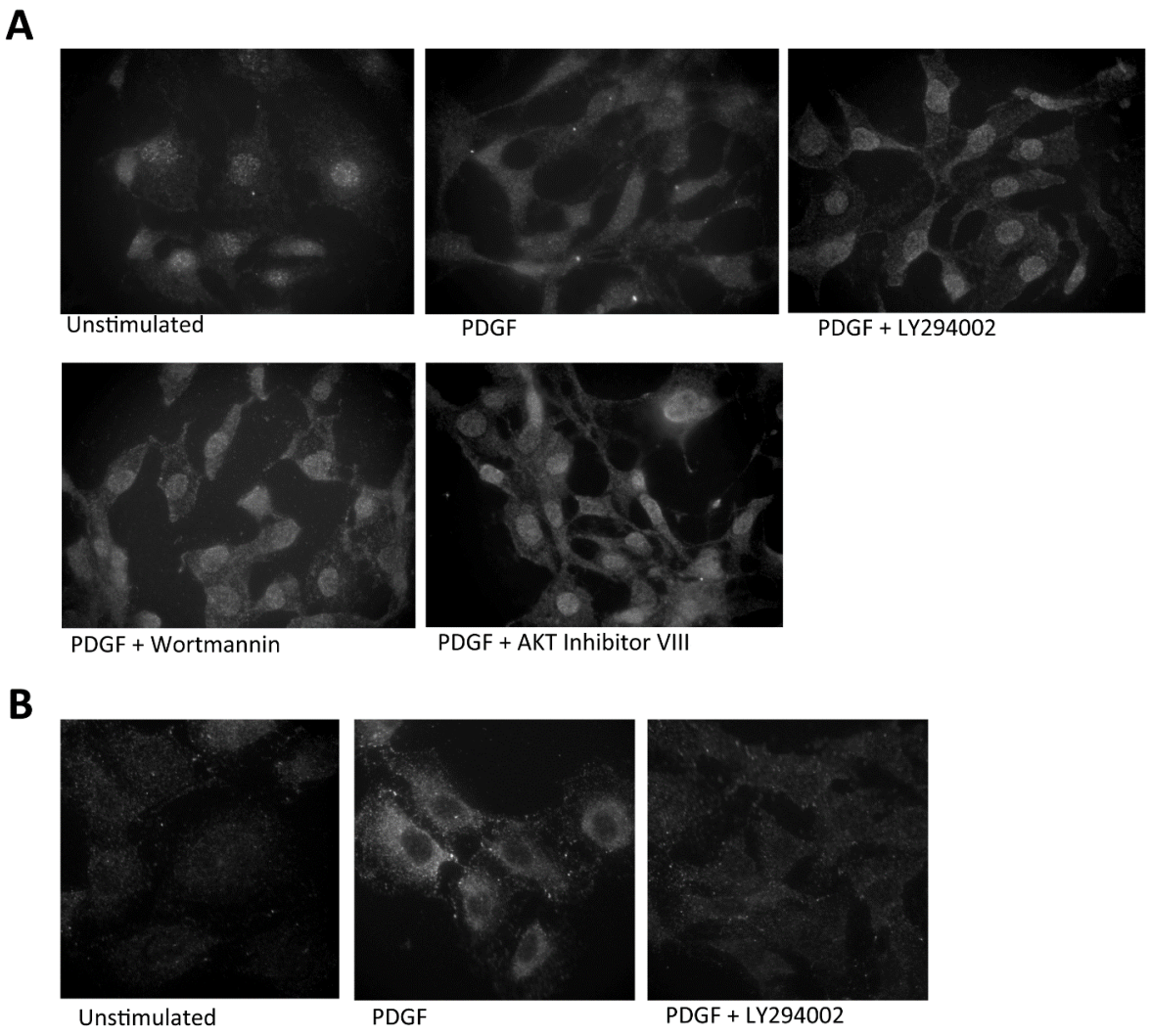

Figure 2.6. Endogenous CDCA7 is phosphorylated at Thr163 and translocates to the cytoplasm upon PDGF stimulation. ***A***. NIH3T3 cells were plated on glass coverslips and starved of serum for 6 hours. PDGF was added for one hour together with LY294002 (25 μM), Wortmannin (100 nM), Akt Inhibitor VIII (2.5 μM) or vehicle where indicated. Cells were fixed in methanol and stained with anti-CDCA7 and DAPI, and visualized by florescence microscopy. ***B***. Similar experiment as in *A*, except that cells were stained with anti-phospho-Thr163.

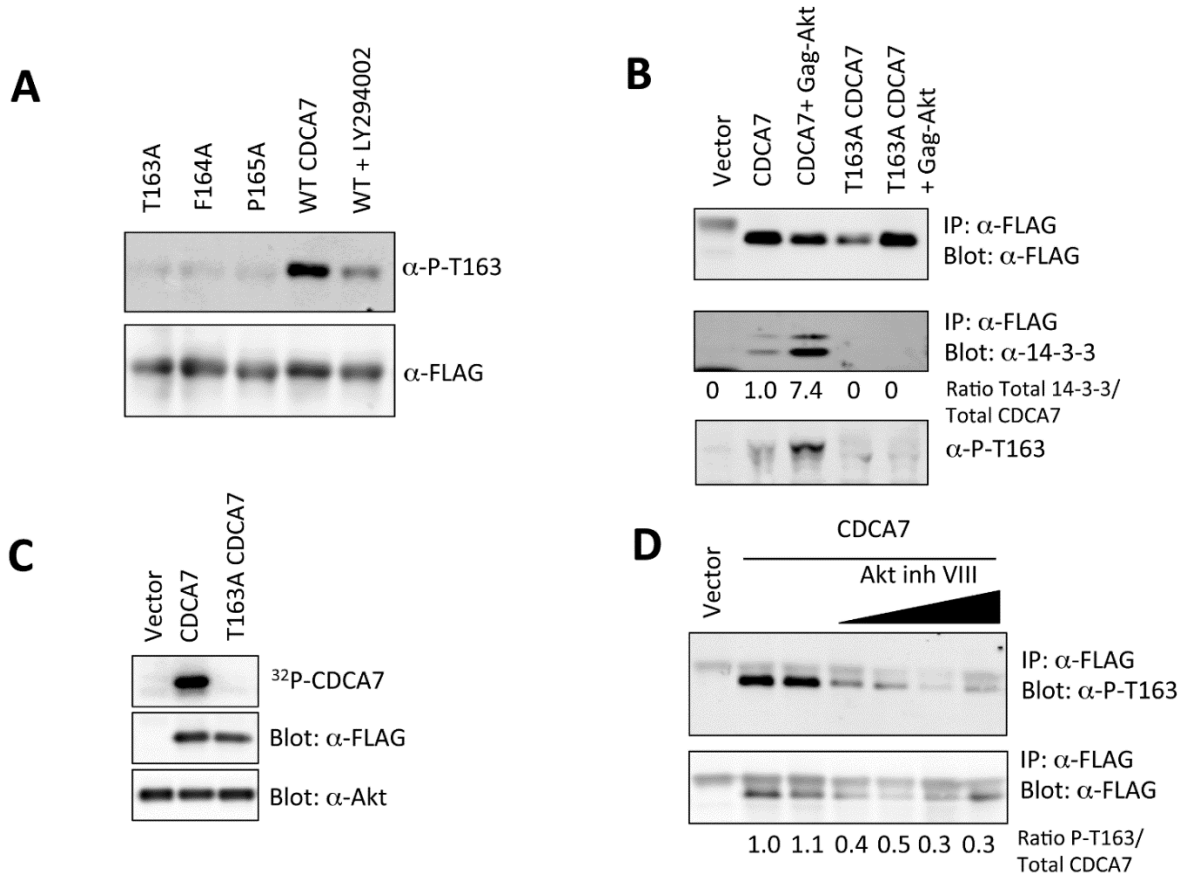
A
T163A
F164A
P165A
WT CDCA7
WT + LY294002
α-P-T163
α-FLAG
B
Vector
CDCA7
CDCA7+ Gag-Akt
T163A CDCA7
T163A CDCA7 + Gag-Akt
IP: α-FLAG
Blot: α-FLAG
IP: α-FLAG
Blot: α-14-3-3
0 1.0 7.4 0 0
Ratio Total 14-3-3/ Total CDCA7
α-P-T163
C
Vector
CDCA7
T163A CDCA7
32P-CDCA7
Blot: α-FLAG
Blot: α-Akt
D
CDCA7
Vector
Akt inh VIII
IP: α-FLAG
Blot: α-P-T163
IP: α-FLAG
Blot: α-FLAG
1.0 1.1 0.4 0.5 0.3 0.3
Ratio P-T163/ Total CDCA7
E
Control
Gag-Akt
α-Flag
α-p-S473
α-Flag
α-p-S473
WT CDCA7
T163A CDCA7

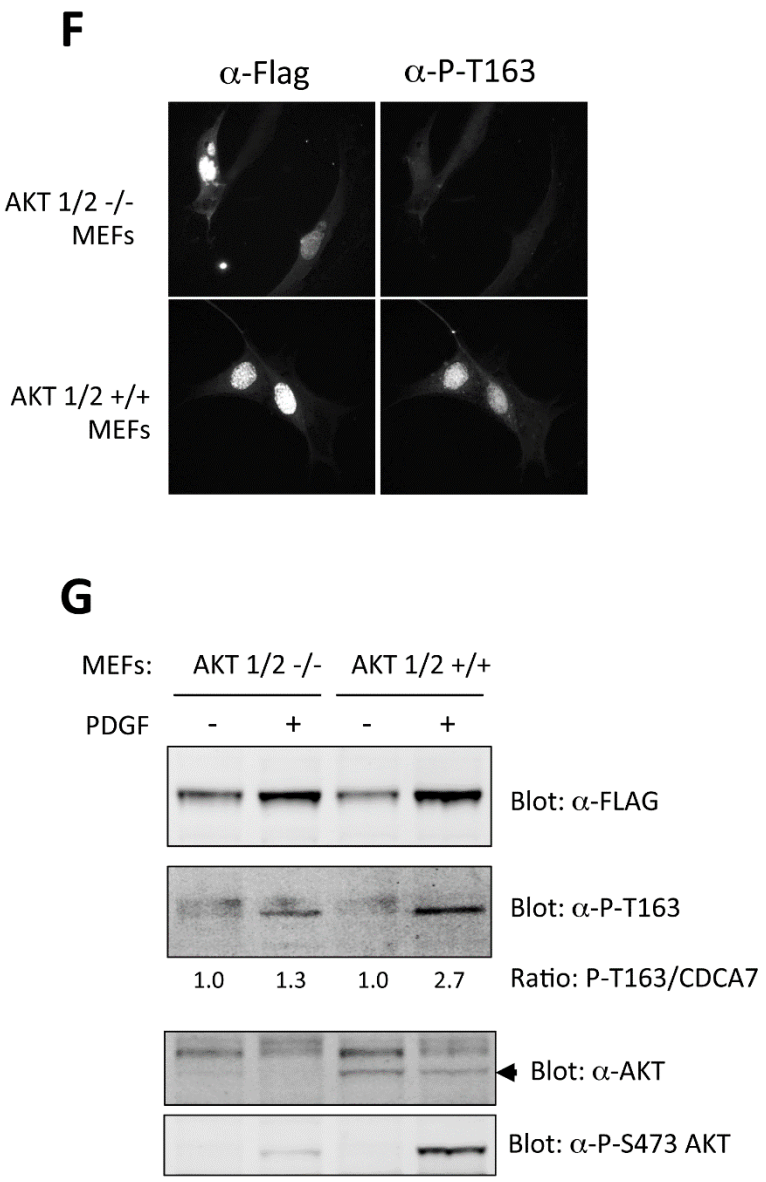

Figure 2.7. Akt phosphorylates CDCA7 at Thr163. ***A***. Cells expressing CDCA7 were treated with the PI3K inhibitor LY294002 for 1 hour, lysed and immunoblotting was performed to detect Thr163 phosphorylation and total CDCA7. ***B***. 293 cells were transfected with CDCA7 together with empty vector or Gag-Akt. 24 hours later CDCA7 was immunoprecipitated and phosphorylation of Thr163 and co-immunoprecipitated endogenous 14-3-3 were visualized by immunoblotting. ***C***. Purified CDCA7 was phosphorylated *in vitro* with recombinant active (S473D)-Akt and ^{32}P-γ-ATP. Proteins were resolved by PAGE and visualized by autoradiography. Total CDCA7 and Akt were detected by immunoblotting. ***D***. Cells expressing CDCA7 were treated with the Akt inhibitor VIII (0.5 and 2.5 μM) for 20 min, lysed, and phosho-Thr163 and total CDCA7 were detected by immunoblotting. ***E***. NIH3T3 cells were transfected with WT CDCA7 or T163A CDCA7 together with vector or Gag-Akt. The next day cells were fixed and stained with anti-FLAG (for total CDCA7) and anti-phospho-S473 (for active Akt). ***F*.** Akt 1/2 +/+ and -/-

MEFs were transfected with CDCA7 on glass coverslips overnight in the presence of serum, fixed with methanol, stained with α-FLAG and α-P-Thr163 and visualized by immunofluorescence microscopy. ***G***. Akt 1/2 +/+ and -/- MEFs were transfected with CDCA7 for 24 hours, starved of serum overnight, and then stimulated with PDGF for 1 hour. CDCA7 was detected by immunoblotting with α-FLAG and α-p-Thr163 antibodies. The numbers beneath each lane represent the ratio of p-Thr163/FLAG signals obtained by direct immunofluorescence detection on an Odyssey infrared imager. Lysates were also probed with α-pan-Akt (Cell Signaling Technology; which detects Akt 1, 2 and 3; arrow indicates Akt band), and a-P-S-473 Akt (Cell Signaling Technology).

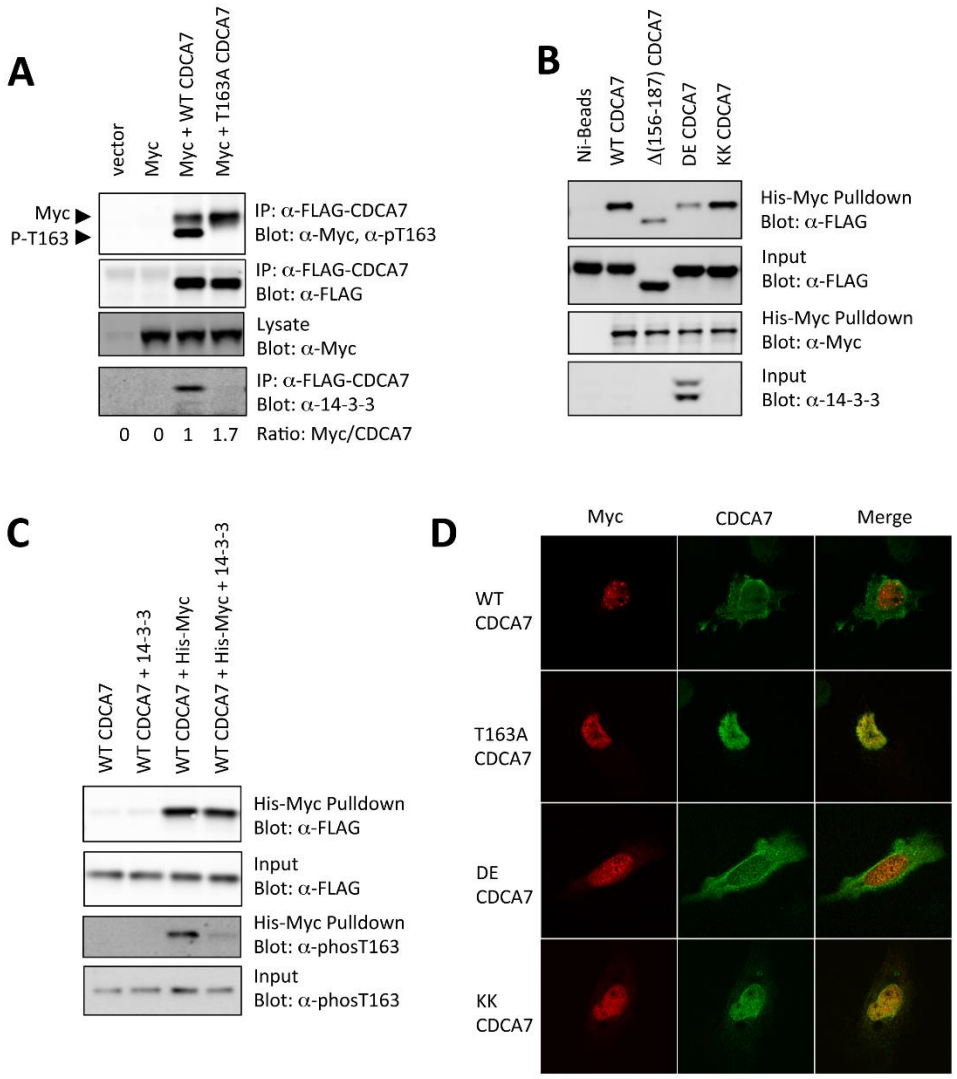

Figure 2.8. 14-3-3 competes with MYC for binding to CDCA7. ***A***. 293 cells were transfected with MYC together with empty vector, FLAG-CDCA7 or FLAG-T163A CDCA7. Detergent solubilized cell extracts were prepared and FLAG-CDCA7 was immunoprecipitated with anti-FLAG M2 antibody. ***B***. Recombinant His-MYC was purified on Ni-Agarose, and wildtype CDCA7, Δ153-188 CDCA7, DE-CDCA7 or KK-CDCA7 were added, the beads rotated 1 hour, washed and boiled in sample buffer. Co-precipitated CDCA7 was detected by FLAG immunoblotting. ***C.*** CDCA7 was immunoprecipitated from cells and incubated with recombinant His-MYC with and without recombinant 14-3-3. CDCA7 bound to MYC was precipitated by Ni-agarose. 14-3-3 specifically reduced the amount of phospho-Thr163 CDCA7 bound to MYC. ***D.*** Rat1 fibroblasts were co-transfected with FLAG-CDCA7 and CMV-MYC plasmids, immunostained, and localization was visualized by confocal florescence microscopy. MYC co-localizes with CDCA7 in the nucleus when Thr163 was mutated to alanine, or with the non-14-3-3 binding R18 peptide (KK) but not with wildtype CDCA7 or the 14-3-3 binding CDCA7 containing the R18 peptide (DE).

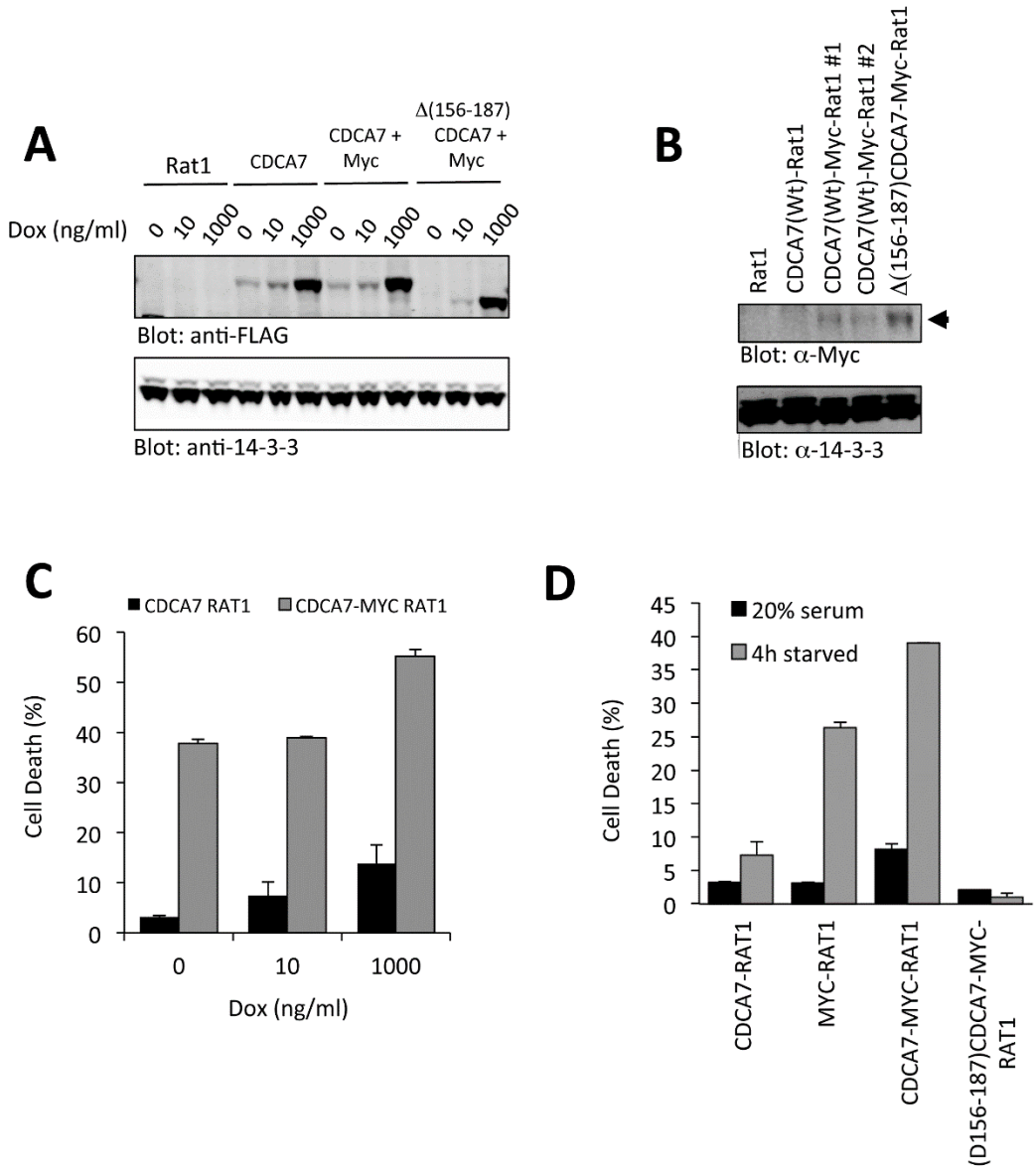

Figure 2.9. CDCA7 increases MYC-induced apoptosis. ***A***. Rat1 cells or Rat1 cells expressing MYC were established with CDCA7 expression under the control of a doxycycline-inducible promoter as described in Experimental Procedures. After 24 hours of doxycycline treatment at various concentrations, cells were lysed and CDCA7 was detected by immunoblotting. ***B***. Various cell lines from *A* were immunoblotted for the presence of ectopically expressed MYC, indicated by arrow. ***C.*** CDCA7-Rat1 and CDCA7-MYC-Rat1 cells were treated with the indicated concentrations of doxycycline for 18 hours, followed by serum starvation for 4 hours. Apoptosis was measured by Annexin-V labeling and flow cytometry. The error bars represent the range of duplicate samples, and are representative of three independent experiments. ***D***. MYC-Rat1, CDCA7-Rat1, CDCA7-MYC-Rat1 and Δ(156-187)-CDCA7-MYC-Rat1 cells were cultured for 18 hours in 10 ng/ml doxycycline, followed by serum starvation for 4 hours. Apoptosis was determined by Annexin-V labeling and flow cytometry. The error bars represent the range of duplicate samples, and are representative of three experiments.

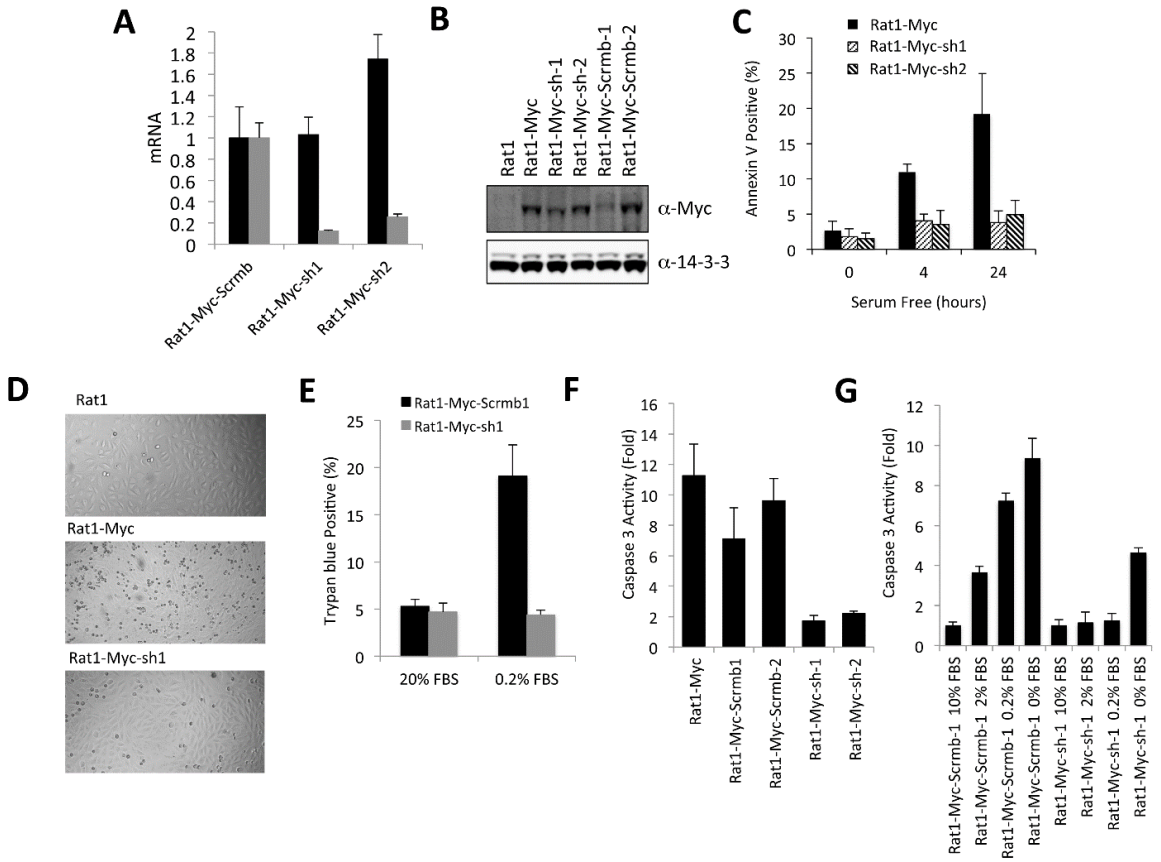

Figure 2.10. Knockdown of CDCA7 rescues Rat1-MYC cells from serum-withdrawal induced apoptosis. shRNA-expressing Rat1 cell lines in which endogenous CDCA7 was knocked down were established in the presence of ectopic MYC as described in Materials and Methods (Rat1-MYC-sh1, Rat1-MYC-sh2). Additionally, control lines were established using a scrambled version of the CDCA7 targeting sequence (Rat1-MYC-scrmb). ***A***. Quantitative RT-PCR of ectopic MYC (black bars) and endogenous CDCA7 (gray bars) was performed on scrambled shRNA-expressing Rat1-MYC cells, or Rat1-MYC cells expressing shRNA-targeted CDCA7. Quantitative RT-PCR was performed in triplicate for each clone. ***B.*** MYC levels of shRNA Rat1-MYC lines were determined by immunoblotting. ***C***. Rat1-MYC, Rat1-MYC-sh1 and Rat1-MYC-sh2 cells were serum starved for 4 or 24 hours and apoptosis was measured by Annexin-V labeling and flow cytometry. Error bars represent the standard deviation of triplicate samples. ***D***. Rat1, Rat1-MYC, or Rat1-MYC-sh1 cells grown to 40% confluency were placed in 0.2% serum overnight. DIC images were captured using bright field microscopy. ***E.*** Rat1-MYC-Scrmb1 or Rat1-MYC-sh1 cells were plated as in *D* and the following day trypan blue-positive cells were counted as a percentage of total cells using a hemocytometer. ***F.*** Rat1-MYC cells as well as two scrambled lines, and two lines expressing shRNA-targeted CDCA7 were plated in triplicate, starved in 0.2% serum for 4 hours, and assayed for caspase-3 activity. ***G.*** Rat1-MYC-scrmb-1 cells and Rat1-MYC-sh1cells were plated in triplicate in various serum concentrations for 4 hours, and assayed for caspase-3 activity.

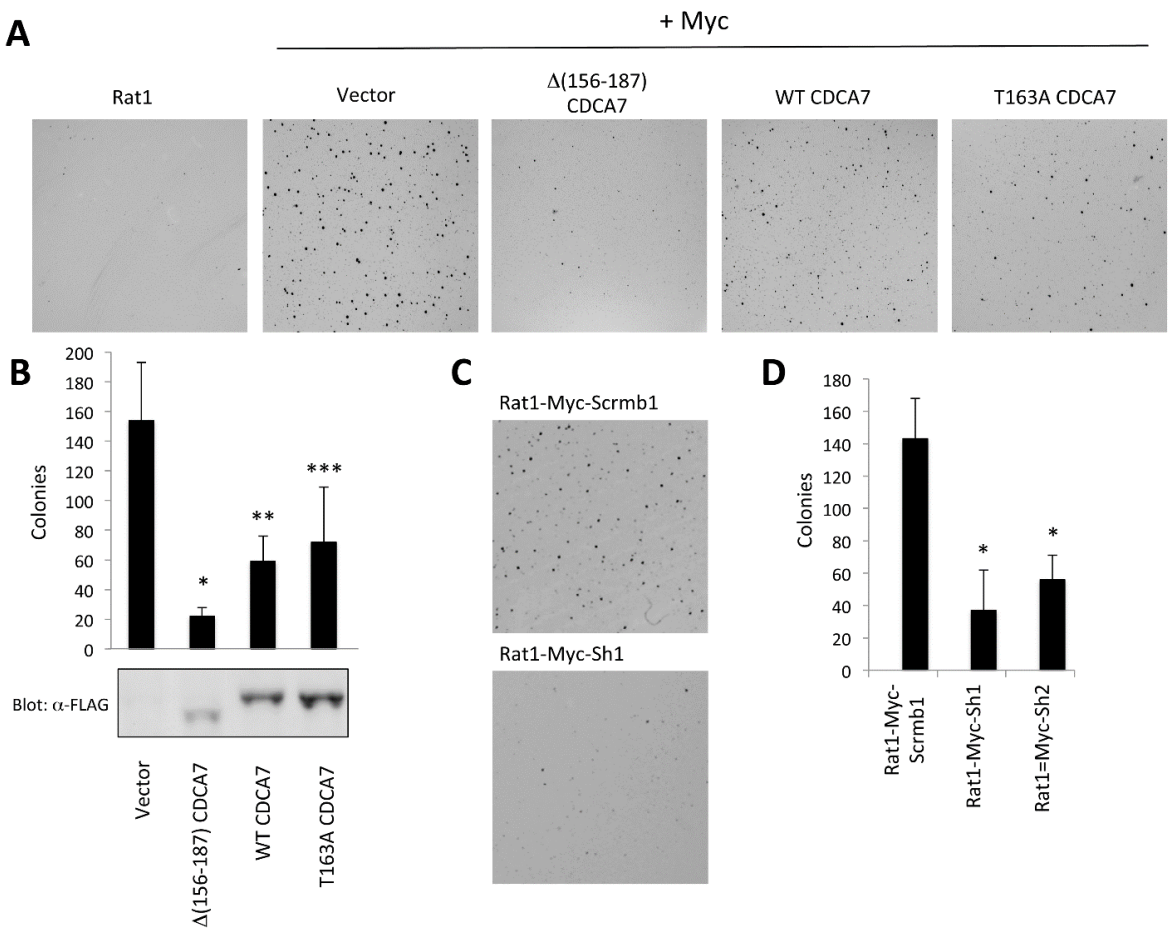

Figure 2.11. CDCA7 influences MYC-induced transformation. ***A.*** Rat1 cells or Rat1 cells stably expressing MYC were infected with retrovirus containing either empty vector, wildtype CDCA7, Δ(156-187)-CDCA7 or T163A-CDCA7. Hygromycin-resistant pools were isolated after 5 days of selection and 5 x 10^3 cells were plated in complete medium containing 0.3% agarose over a 0.7% agarose bottom layer, as described in *Materials and Methods*. Two weeks later colonies were stained with crystal violet, destained with water, and imaged on an Odyssey infrared scanner using a 4 mm offset and 41 μm resolution setting. ***B.*** Colonies were counted using ImageJ software, with the error bars representing the standard deviation of 6 individual wells. The * indicates a significant difference with WT CDCA7 (p=0.0005), while ** indicates a significant difference with vector alone (p=0.0003) and *** indicates a significant difference with vector alone (p=0.004). Lysates of the hygromycin-resistant pools were immunoblotted with α-FLAG. ***C.*** Rat1-MYC-scrmb or Rat1-MYC-sh cells were plated as in *A*, and colonies were stained after two weeks with crystal violet. ***D.*** Macroscopic colonies were counted using ImageJ from 4 individual wells, with error bars representing the standard deviation. The * indicates a significant difference with Rat1-MYC-scrmb (P=0.001).

Discussion

Aberrant proliferation induced by MYC is opposed by apoptosis and/or cell cycle arrest, providing cells with a safety mechanism against the onset of MYC-induced hyper-proliferation and tumorigenesis (57). During normal development, proliferative signals result in activation of pathways that instruct the cell to co-operate with MYC and divide. Phosphoinositide 3-OH kinase is at the apex of one important pathway activated by mitogenic stimuli and one of its main effectors, Akt, cooperates with MYC to suppress pro-apoptotic gene expression while simultaneously instructing the cell towards division (29). Given the important roles of both Akt and MYC in cancer pathology, there is an urgent need to understand the mechanism of cooperative signaling between these two regulators.

In this report, we found that the transcriptional regulator CDCA7 was phosphorylated by Akt and this caused its disengagement from MYC and sequestration to the cytoplasm by binding to 14-3-3. The binding of 14-3-3 to CDCA7 appeared to be competitive for MYC binding, as addition of recombinant 14-3-3 led to reduced co-precipitation of phospho-Thr163 CDCA7 and MYC. In addition, we found that this region harbored nuclear localization activity. Mutation of predicted consensus sites derived from the bipartite NLS domains of RB (16) and SWI5 (37) led to loss of nuclear localization of a large cargo protein. Mutation of two of these sites, Arg161 and Arg162, led to enhanced cytoplasmic localization of CDCA7, which was accompanied by increased phosphorylation of Thr163 and 14-3-3 binding.

When CDCA7 was ectopically expressed with MYC there was a sensitization to serum-withdrawal apoptosis. Surprisingly, the Δ(156-187)-CDCA7 mutation reduced serum-withdrawal induced apoptosis, suggesting that this protein was acting as a dominant negative and interfering with the pro-apoptotic function of MYC. Conversely, knockdown of endogenous CDCA7 rescued MYC-

expressing cells from apoptosis following serum withdrawal. These results argue that CDCA7 is an important co-factor in the ability of MYC to regulate target gene expression and, under physiological conditions, CDCA7 may be important for the normal regulation of MYC-target genes. On the other hand, dysregulation of this pathway becomes pro-apoptotic under pathophysiological conditions.

Consistent with this, transformation of fibroblasts by MYC was also influenced by CDCA7. Co-expression of CDCA7 reduced anchorage-independent colony growth, indicating that over-expression of CDCA7 interferes with the process of MYC-transformation. Importantly, the Δ(156-187)-CDCA7 appeared to act as a dominant negative under these conditions, as this protein greatly reduced colony formation. These results suggest that CDCA7 influences MYC-induced transformation, with high level expression causing interference, possibly by increasing apoptosis within the forming colonies, while expression of Δ(156-187)-CDCA7 interferes by disrupting the association of MYC with either endogenous CDCA7 or other factors that require full length CDCA7 for interaction. In support of this, knockdown of endogenous CDCA7 also reduced the transformation potential of MYC, again arguing that CDCA7 is required for MYC transforming activity. These observations are in general consistent with the earlier findings of Prescott and co-workers (44), who found that CDCA7 rescued transformation by MYC containing a transformation-defective MYC-Box II deletion, supporting the hypothesis of a genetic link between CDCA7 and MYC. While Prescott and coworkers found that CDCA7 co-expression did not significantly increase or decrease MYC-induced transformation (44), the difference between our experiments and those of Prescott and coworkers could be reflected by the levels of expression of MYC, CDCA7, or a combination of both. Future studies will examine if ectopic CDCA7 expression reduces transformation as a direct result of increased apoptosis.

Interestingly, the *cdca7* gene has itself been reported to be a target of MYC (22, 44). In our own experiments, overexpression of MYC in Rat1 cells caused a 2-5 fold increase in *cdca7* mRNA, suggesting that a feed forward loop exists whereby MYC activation leads to elevated CDCA7. We hypothesize that growth factor signals use Akt activity to finely tune the activation of MYC through CDCA7, with loss of Akt activating the pro-death effects of CDCA7/MYC, tipping cell fate towards apoptosis.

An important question remaining is the alteration of global gene expression caused by CDCA7/MYC interaction. The related protein JPO2 was shown to bind to SP1 sites of the MAOA gene via its C-terminal Zinc Finger domain (42). CDCA7 and JPO2 are 77% identical within this region, suggesting that CDCA7 may also bind to similar SP1 elements. MYC-binding E-box sites are preferentially enriched with SP1 elements across the genome (43), suggesting that CDCA7 and MYC might cooperate to regulate these genes. It also remains to be determined what role CDCA7 plays in the context of cell fate determination during early development, where MYC expression is tightly regulated, and also the role that CDCA7 might have with other transcription factors in non-MYC expressing cells.

In summary, we have identified a new target of Akt that is required for the pro-apoptotic and transformation properties of MYC. Akt phosphorylates CDCA7 within a 14-3-3 binding site, disrupting its interaction with MYC and resulting in CDCA7 transit from the nucleus to the cytoplasm. The fine-tuning of CDCA7 and MYC interaction by phosphorylation at Thr163 could represent an important physiological role for Akt, and one that becomes pathophysiological under conditions of an overactive Akt axis.

Acknowledgements

This work was supported by funds from the Canadian Institute of Health Research, an Early Investigator Award (to M.P.S.), and a Canadian Foundation of Innovation Award (to M.P.S.). We thank Dr. Veronique Nogueira of the University of Illinois at Chicago for the kind gift of Akt1/2 null MEFS.

References

1. Hann SR, Eisenman RN. 1984. Proteins encoded by the human c-myc oncogene: differential expression in neoplastic cells. Mol. Cell. Biol.4:2486–2497

2. Meyer N, Kim SS, Penn LZ. 2006. The Oscar-worthy role of Myc in apoptosis. Semin. Cancer Biol. 16:275–287

3. Meyer N, Penn LZ. 2008. Reflecting on 25 years with MYC. Nat. Rev. Cancer 8:976–990

4. Oster SK, Ho CSW, Soucie EL, Penn LZ. 2002. The myc oncogene: MarvelouslY Complex. Adv. Cancer Res. 84:81–154

5. Wolfer A, Ramaswamy S. 2011. MYC and metastasis. Cancer Res. 71:2034–2037

6. Wolfer A, Wittner BS, Irimia D, Flavin RJ, Lupien M, Gunawardane RN, Meyer CA, Lightcap ES, Tamayo P, Mesirov JP, Liu XS, Shioda T, Toner M, Loda M, Brown M, Brugge JS, Ramaswamy S. 2010. MYC regulation of a "poor-prognosis" metastatic cancer cell state. Proc. Natl. Acad. Sci. U. S. A. 107:3698–3703

7. Albihn A, Johnsen JI, Henriksson MA. 2010. MYC in oncogenesis and as a target for cancer therapies. Adv. Cancer Res. 107:163–224

8. Nilsson JA, Cleveland JL. 2003. Myc pathways provoking cell suicide and cancer. Oncogene 22:9007–9021

9. Grandori C, Cowley SM, James LP, Eisenman RN. 2000. The Myc/Max/Mad network and the transcriptional control of cell behavior. Annu. Rev. Cell Dev. Biol. 16:653–699

10. Soucek L, Evan GI. 2010. The ups and downs of Myc biology. Curr. Opin. Genet. Dev. 20:91–95

11. Amati B, Littlewood TD, Evan GI, Land H. 1993. The c-Myc protein induces cell cycle progression and apoptosis through dimerization with Max. EMBO J. 12:5083–5087

12. Born TL, Frost JA, Schonthal A, Prendergast GC, Feramisco JR. 1994. c-Myc cooperates with activated Ras to induce the cdc2 promoter. Mol. Cell. Biol. 14:5710–5718

13. Coller HA, Grandori C, Tamayo P, Colbert T, Lander ES, Eisenman RN, Golub TR. 2000. Expression analysis with oligonucleotide microarrays reveals that MYC regulates genes involved in growth, cell cycle, signaling, and adhesion. Proc. Natl. Acad. Sci. U. S. A. 97:3260–3265

14. Frank SR, Schroeder M, Fernandez P, Taubert S, Amati B. 2001. Binding of c-Myc to chromatin mediates mitogen-induced acetylation of histone H4 and gene activation. Genes Dev. 15:2069–2082

15. Hanson KD, Shichiri M, Follansbee MR, Sedivy JM. 1994. Effects of c-myc expression on cell cycle progression. Mol. Cell. Biol. 14:5748–5755

16. Mateyak MK, Obaya AJ, Adachi S, Sedivy JM. 1997. Phenotypes of c-Myc-deficient rat fibroblasts isolated by targeted homologous recombination. Cell Growth Differ. 8:1039–1048

17. Rudolph B, Saffrich R, Zwicker J, Henglein B, Muller R, Ansorge W, Eilers M. 1996. Activation of cyclin-dependent kinases by Myc mediates induction of cyclin A, but not apoptosis. EMBO J. 15:3065–3076

18. Askew DS, Ashmun RA, Simmons BC, Cleveland JL. 1991. Constitutive c-myc expression in an IL-3-dependent myeloid cell line suppresses cell cycle arrest and accelerates apoptosis. Oncogene 6:1915–1922

19. Eischen CM, Roussel MF, Korsmeyer SJ, Cleveland JL. 2001. Bax loss impairs Myc-induced apoptosis and circumvents the selection of p53 mutations during Myc-mediated lymphomagenesis. Mol. Cell. Biol. 21:7653–7662

20. Evan GI, Wyllie AH, Gilbert CS, Littlewood TD, Land H, Brooks M, Waters CM, Penn LZ, Hancock DC. 1992. Induction of apoptosis in fibroblasts by c-myc protein. Cell 69:119–128

21. Hemann MT, Bric A, Teruya-Feldstein J, Herbst A, Nilsson JA, Cordon-Cardo C, Cleveland JL, Tansey WP, Lowe SW. 2005. Evasion of the p53 tumour surveillance network by tumour-derived MYC mutants. Nature 436:807–811

22. Hermeking H, Eick D. 1994. Mediation of c-Myc-induced apoptosis by p53. Science 265:2091–2093

23. Pusapati RV, Rounbehler RJ, Hong S, Powers JT, Yan M, Kiguchi K, McArthur MJ, Wong PK, Johnson DG. 2006. ATM promotes apoptosis and suppresses tumorigenesis in response to Myc. Proc. Natl. Acad. Sci. U. S. A. 103:1446–1451

24. Qi Y, Gregory MA, Li Z, Brousal JP, West K, Hann SR. 2004. p19ARF directly and differentially controls the functions of c-Myc independently of p53. Nature 431:712–717

25. Zindy F, Eischen CM, Randle DH, Kamijo T, Cleveland JL, Sherr CJ, Roussel MF. 1998. Myc signaling via the ARF tumor suppressor regulates p53-dependent apoptosis and immortalization. Genes Dev. 12:2424–2433

26. Mymryk JS, Shire K, Bayley ST. 1994. Induction of apoptosis by adenovirus type 5 E1A in rat cells requires a proliferation block. Oncogene9:1187–1193

27. Qin XQ, Livingston DM, Kaelin WG, Jr, Adams PD. 1994. Deregulated transcription factor E2F-1 expression leads to S-phase entry and p53-mediated apoptosis. Proc. Natl. Acad. Sci. U. S. A. 91:10918–10922

28. Rao L, Debbas M, Sabbatini P, Hockenbery D, Korsmeyer S, White E. 1992. The adenovirus E1A proteins induce apoptosis, which is inhibited by the E1B 19-kDa and Bcl-2 proteins. Proc. Natl. Acad. Sci. U. S. A. 89:7742–7746

29. Wu X, Levine AJ. 1994. p53 and E2F-1 cooperate to mediate apoptosis. Proc. Natl. Acad. Sci. U. S. A. 91:3602–3606

30. Bissonnette RP, Echeverri F, Mahboubi A, Green DR. 1992. Apoptotic cell death induced by c-myc is inhibited by bcl-2. Nature 359:552–554

31. Fanidi A, Harrington EA, Evan GI. 1992. Cooperative interaction between c-myc and bcl-2 proto-oncogenes. Nature 359:554–556

32. Vaux DL, Cory S, Adams JM. 1988. Bcl-2 gene promotes haemopoietic cell survival and cooperates with c-myc to immortalize pre-B cells.Nature 335:440–442

33. Kauffmann-Zeh A, Rodriguez-Viciana P, Ulrich E, Gilbert C, Coffer P, Downward J, Evan G. 1997. Suppression of c-Myc-induced apoptosis by Ras signalling through PI(3)K and PKB. Nature 385:544–548

34. Dudek H, Datta SR, Franke TF, Birnbaum MJ, Yao R, Cooper GM, Segal RA, Kaplan DR, Greenberg ME. 1997. Regulation of neuronal survival by the serine-threonine protein kinase Akt. Science 275:661–665

35. Kennedy SG, Wagner AJ, Conzen SD, Jordan J, Bellacosa A, Tsichlis PN, Hay N. 1997. The PI 3-kinase/Akt signaling pathway delivers an anti-apoptotic signal. Genes Dev. 11:701–713

36. Khwaja A, Rodriguez-Viciana P, Wennstrom S, Warne PH, Downward J. 1997. Matrix adhesion and Ras transformation both activate a phosphoinositide 3-OH kinase and protein kinase B/Akt cellular survival pathway. EMBO J. 16:2783–2793

37. Datta SR, Dudek H, Tao X, Masters S, Fu H, Gotoh Y, Greenberg ME. 1997. Akt phosphorylation of BAD couples survival signals to the cell-intrinsic death machinery. Cell 91:231–241

38. del Peso L, Gonzalez-Garcia M, Page C, Herrera R, Nunez G. 1997. Interleukin-3-induced phosphorylation of BAD through the protein kinase Akt. Science 278:687–689

39. She QB, Solit DB, Ye Q, O'Reilly KE, Lobo J, Rosen N. 2005. The BAD protein integrates survival signaling by EGFR/MAPK and PI3K/Akt kinase pathways in PTEN-deficient tumor cells. Cancer Cell 8:287–297

40. Zundel W, Giaccia A. 1998. Inhibition of the anti-apoptotic PI(3)K/Akt/Bad pathway by stress. Genes Dev. 12:1941–1946

41. Bouchard C, Marquardt J, Bras A, Medema RH, Eilers M. 2004. Myc-induced proliferation and transformation require Akt-mediated phosphorylation of FoxO proteins. EMBO J. 23:2830–2840

42. Brunet A, Bonni A, Zigmond MJ, Lin MZ, Juo P, Hu LS, Anderson MJ, Arden KC, Blenis J, Greenberg ME. 1999. Akt promotes cell survival by phosphorylating and inhibiting a Forkhead transcription factor. Cell 96:857–868

43. Brunet A, Kanai F, Stehn J, Xu J, Sarbassova D, Frangioni JV, Dalal SN, DeCaprio JA, Greenberg ME, Yaffe MB. 2002. 14-3-3 transits to the nucleus and participates in dynamic nucleocytoplasmic transport. J. Cell Biol. 156:817–828

44. Delpuech O, Griffiths B, East P, Essafi A, Lam EW, Burgering B, Downward J, Schulze A. 2007. Induction of Mxi1-SRα by FOXO3a contributes to repression of Myc-dependent gene expression. Mol. Cell. Biol. 27:4917–4930

45. Singh A, Ye M, Bucur O, Zhu S, Tanya Santos M, Rabinovitz I, Wei W, Gao D, Hahn WC, Khosravi-Far R. 2010. Protein phosphatase 2A reactivates FOXO3a through a dynamic interplay with 14-3-3 and Akt. Mol. Biol. Cell 21:1140–1152

46. Li J, Simpson L, Takahashi M, Miliaresis C, Myers MP, Tonks N, Parsons R. 1998. The PTEN/MMAC1 tumor suppressor induces cell death that is rescued by the Akt/protein kinase B oncogene. Cancer Res. 58:5667–5672

47. Stambolic V, Suzuki A, de la Pompa JL, Brothers GM, Mirtsos C, Sasaki T, Ruland J, Penninger JM, Siderovski DP, Mak TW. 1998. Negative regulation of PKB/Akt-dependent cell survival by the tumor suppressor PTEN. Cell 95:29–39

48. Dahia PL, Aguiar RC, Alberta J, Kum JB, Caron S, Sill H, Marsh DJ, Ritz J, Freedman A, Stiles C, Eng C. 1999. PTEN is inversely correlated with the cell survival factor Akt/PKB and is inactivated via multiple mechanisms in haematological malignancies. Hum. Mol. Genet. 8:185–193

49. Di Cristofano A, Pandolfi PP. 2000. The multiple roles of PTEN in tumor suppression. Cell 100:387–390

50. Goto Y, Hayashi R, Muramatsu T, Ogawa H, Eguchi I, Oshida Y, Ohtani K, Yoshida K. 2006. JPO1/CDCA7, a novel transcription factor E2F1-induced protein, possesses intrinsic transcriptional regulator activity. Biochim. Biophys. Acta 1759:60–68

51. Osthus RC, Karim B, Prescott JE, Smith BD, McDevitt M, Huso DL, Dang CV. 2005. The Myc target gene JPO1/CDCA7 is frequently overexpressed in human tumors and has limited transforming activity in vivo. Cancer Res. 65:5620–5627

52. Prescott JE, Osthus RC, Lee LA, Lewis BC, Shim H, Barrett JF, Guo Q, Hawkins AL, Griffin CA, Dang CV. 2001. A novel c-Myc-responsive gene, JPO1, participates in neoplastic transformation. J. Biol. Chem. 276:48276–48284

53. Huang A, Ho CS, Ponzielli R, Barsyte-Lovejoy D, Bouffet E, Picard D, Hawkins CE, Penn LZ. 2005. Identification of a novel c-Myc protein interactor, JPO2, with transforming activity in medulloblastoma cells. Cancer Res. 65:5607–5619

54. Skeen JE, Bhaskar PT, Chen CC, Chen WS, Peng XD, Nogueira V, Hahn-Windgassen A, Kiyokawa H, Hay N. 2006. Akt deficiency impairs normal cell proliferation and suppresses oncogenesis in a p53-independent and mTORC1-dependent manner. Cancer Cell 10:269–280

55. Matitau AE, Scheid MP. 2008. Phosphorylation of MEKK3 at threonine 294 promotes 14-3-3 association to inhibit nuclear factor κB activation.J. Biol. Chem. 283:13261–13268

56. Freeman AK, Morrison DK. 2011. 14-3-3 proteins: diverse functions in cell proliferation and cancer progression. Semin. Cell Dev. Biol.22:681–687

57. Wang B, Yang H, Liu YC, Jelinek T, Zhang L, Ruoslahti E, Fu H. 1999. Isolation of high-affinity peptide antagonists of 14-3-3 proteins by phage display. Biochemistry 38:12499–12504

58. Wasylishen AR, Penn LZ. 2010. Myc: the beauty and the beast. Genes Cancer 1:532–541

59. Efthymiadis A, Shao H, Hubner S, Jans DA. 1997. Kinetic characterization of the human retinoblastoma protein bipartite nuclear localization sequence (NLS) in vivo and in vitro. A comparison with the SV40 large T-antigen NLS. J. Biol. Chem. 272:22134–22139

60. Moll T, Tebb G, Surana U, Robitsch H, Nasmyth K. 1991. The role of phosphorylation and the CDC28 protein kinase in cell cycle-regulated nuclear import of the S. cerevisiae transcription factor SWI5. Cell 66:743–758

61. Ou XM, Chen K, Shih JC. 2006. Monoamine oxidase A and repressor R1 are involved in apoptotic signaling pathway. Proc. Natl. Acad. Sci. U. S. A. 103:10923–10928

62. Parisi F, Wirapati P, Naef F. 2007. Identifying synergistic regulation involving c-Myc and sp1 in human tissues. Nucleic Acids Res. 35:1098–1107

Chapter 3: CDCA7 Co-association and 14-3-3 Binding

Introduction

Since their discovery in 1967, 14-3-3 proteins have gained notoriety as being regulators of signaling pathways that effect a wide variety of cellular processes including apoptosis, metabolism, cell cycle regulation and general protein trafficking. 14-3-3 is a highly conserved protein which has been detected in all eukaryotic organisms to date but has yet to be identified in prokaryotes. This ~30KDa acidic polypeptide binds specific phosphoserine/threonine motifs (RSXpSXP or RXXXpSXP) on client proteins. 14-3-3 exerts its function by either inducing conformational change, providing scaffolding or by obstruction of key physical or sequence-specific features of its target protein (Bridges and Moorhead, 2004). 14-3-3 proteins exist as either heterodimers in permutations of the seven 14-3-3 isomer families, or as homodimers of the same 14-3-3 family. X-ray crystallography has shown that each monomer of 14-3-3 can concurrently bind a target motif on either a single client protein or on two separate proteins (Gardino et al, 2006). Because of the phospho-dependent nature of 14-3-3 binding, these associations have been intimately linked to many of the key phospho-regulatory cascades that influence normal cell cycle progression and cell growth. Dysregulation of these pathways often lead to disease such as cancer and incriminate 14-3-3 in in the process (Morrison, 2009).

14-3-3 and apoptotic/survival signalling

The tug of war between apoptotic and survival signalling is at the heart of cell cycle control and the cell fate decision making process. 14-3-3 proteins are known to influence this fine balance by affecting the activity of proteins involved in proliferation and apoptosis. For example, 14-3-3 has been shown to localize the pro-apoptotic transcription factor FOXO1 to the cytoplasm by first

exposing its nuclear export sequence (NES) and then masking a nuclear important sequence (NLS). In this instance, apoptosis is inhibited by preventing the transactivation of pro-apoptotic genes by FOXO1. This inhibition of apoptosis is abolished when the FOXO1/14-3-3 complex is disrupted when stress signals result in the phosphorylation of FOXO1 by Jun-N-terminal kinase (JNK) (Donovan et al., 2002). 14-3-3 has also been shown to promote proliferation by influencing members of the mitogen activated protein kinase (MAPK) cascade. For example, maximal activity of C-Raf kinase depends on 14-3-3 mediated heterodimerization with B-Raf, resulting in the proliferative outcomes associated with the MAPK cascade (Rushworth et al., 2006). Mutations in *BRAF* have been found in human cancers, and are associated with constitutive 14-3-3 dependent heterodimerization of C-Raf and B-Raf proteins. It has been shown that 14-3-3 is therefore required for the transforming ability of B-Raf proteins (Wan et al, 2004).

14-3-3 and tumor suppression

The ability to supress cell-growth and cell-cycle progression in the event of DNA damage is an imperative step in tumor-suppression activity. 14-3-3 has been shown to be involved in this process. For example, upregulation of 14-3-3 by p53 and breast cancer type 1 susceptibility protein (BRCA1) results in the DNA-damage-induced cell-cycle checkpoint (Hermeking et al., 1997; Aprelikova et al., 2001). Expression of 14-3-3 by these tumor suppressor results in binding of the Cyclin-B1/Cdc2 complex and its cytoplasmic sequestration, leading to a halt of cell cycle progression thereby allowing DNA damage repair to take place (Chan et al., 1999). Loss of 14-3-3 expression has been associated with tumors of the epithelium, most notably in breast cancer (Lodygin and Hermeking, 2006). Loss of 14-3-3 activity can occur by numerous means, including targeted ubiquitin-mediated degradation and hypermethylation of the 14-3-3 promoter (Umbricht et al., 2001).

14-3-3 as a cancer therapeutic target

Epigenetic silencing of 14-3-3 is a phenomenon which takes place early in carcinogenesis and often occurs before any cancerous morphology is evident. This fact offers an opportunity for early detection of disease and recurrence in cancer patients by monitoring 14-3-3 methylation in various bodily fluids (Bhatia et al., 2003). This may prove to be a promising approach for cancer detection when considering that 14-3-3 downregulation via CpG hypermethylation has been detected in adenocarcinomas of the breast (96%), in hepatocellular carcinoma (89%), in lung cancer (83%) and endometroid endometrial adenocarcinoma (74%) (Ferguson et al., 2000; Moreira et al., 2004; Iwata et al., 2000).

A promising therapeutic approach relies on the leveraging of methylation inhibitors to reverse 14-3-3 silencing via CpG hypermethylation. The methyltransferase inhibitor 5-aza-2deoxycytidine (5-Azra) has been shown to reverse silencing of 14-3-3 via CpG hypermethylation and induce expression of 14-3-3 to pre-cancerous levels *in vivo*. Although different cell lines have exhibited unique sensitivities to 5-Azra, clinical trials focusing on cancer patients remain promising (Esteller, 2005).

In examples where 14-3-3 activity is implicated in cancer initiation and progression, such as in the case of B-Raf/*BRAF*, targeted inhibition of 14-3-3 may prove to be an effective treatment strategy. This has been achieved by down regulation of 14-3-3 via siRNA, increasing the sensitivity of lung carcinomas, head and neck cancers and diffuse large B cell lymphomas to ionizing radiation and other apoptosis-inducing treatments (Fan et al., 2007, Maxwell et al., 2009 and Matta et al., 2010).

In the almost half century since their discovery, 14-3-3 proteins have proven to play a crucial role in a wide array of cellular processes. These include apoptosis, cell growth and cell-cycle

progression. Although 14-3-3 proteins themselves posses no intrinsic catalytic activity, they serve as organizational nodes for signaling cascades that rely on serine/threonine kinases. An increased interest in epigenetics and methylation over the last ten years has broadened the scope of 14-3-3 function and influence. Advances in proteomics and the ongoing mapping of the proteome has revealed the far-reaching implications of 14-3-3 via its 200 plus binding partners. There is no doubt that our understanding of 14-3-3 function will continue to expand over the coming years, especially as analysis of patient tumors begin to reveal the penetrance of 14-3-3 in cancer initiation and progression. Arming ourselves with this information will allow us to better design treatment options for cancer patients and screening techniques for early disease detection.

What emerges from a study of 14-3-3 proteins is a recurring theme of bridging, or the bringing together of proteins that would otherwise not associate (Figure 3.1). In light of the fact that 14-3-3 often facilitates homodimerization, we have yet to show whether this is the case between monomers of CDCA7. To date we have shown that CDCA7 physically interacts as a heterodimer with both Myc and 14-3-3 proteins in a phospho-dependent manner which is mediated by the kinase Akt. It is also well known that DNA binding proteins, most notably transcription factors, utilize homo and heterodimerization to impart specificity and control over DNA binding (Amoutzias et al., 2008). This line of reasoning is of interest because the related protein JPO2 was shown to bind to SP1 sites of the MAOA gene via its C-terminal Zinc Finger domain (Ou et al., 2006). CDCA7 and JPO2 are 77% identical within this region, suggesting that CDCA7 may also bind to similar SP1 elements. In this chapter we ask the questions: does CDCA7 homodimerize with itself and if so, is this interaction dependent on 14-3-3 as bridging protein? Is there a possibility of a second 14-3-3 binding site within CDCA7?

Results

CDCA7 Co-association – coimmunoprecipitation approach

To investigate if CDCA7 homodimerizes, we first conducted a series of experiments using ectopically expressed proteins isolated from cells. Our initial approach was to express CDCA7 from two plasmids – one containing an N-terminal FLAG epitope and the second an HA epitope tag. This allowed us to distinguish the two CDCA7 proteins following co-immunoprecipitation and immunoblotting. Thus, we first expressed pCMV10-3xHA-CDCA7 together with either empty vector or pCMV10-3xFLAG-CDCA7 in HEK293 cells. Following immunoprecipitation with anti-FLAG bound agarose we resolved the proteins by SDS-PAGE and probed with anti-HA. Using this approach, we have shown that FLAG- tagged CDCA7 associates with HA- tagged CDCA7. Mutation of the T163 phosphorylation site or enforced/suppressed 14-3-3 binding (DE or KK R18 peptide substitution respectively) did not alter CDCA7 association (Figure 3.2A). Association is reduced upon deletion of the C-terminal 260-371 region (Figure 3.2B), suggesting that the C-terminal zinc-finger domain could play a role in in this protein-protein interaction. In contrast, deletion of the Myc-interacting region, Δ(156-187)-CDCA7, did not alter association with WT CDCA7 (Figure 3.3A). A surprising result of our work has been the consistent inhibition of Myc function by Δ(156-187)-CDCA7. The effect of this deletion on apoptosis and transformation is similar to the knockdown of endogenous CDCA7 expression by shRNA, suggesting that Δ(156-187)-CDCA7 may be acting as a dominant negative by associating with endogenous CDCA7, preventing it from binding Myc and inhibiting any influence CDCA7 may have on Myc function. Next, we assayed other internal deletions, N- and C-terminal truncations to further refine the area of CDCA7 co-association. Of the truncations and deletions shown in figure 3.3A, the N-terminal truncation of amino acids 1-234 showed the most notable reduction in HA-CDCA7 co-

immunoprecipitation. Figures 3.3 B and C further dissect the region flanked by amino acids 112 and 234 by assaying internal deletion mutants and their ability to co-precipitate HA WT-CDCA7. Evidence of complete loss of association can be difficult to ascertain from western blots, especially considering that internal deletions may not completely target the region of interaction and may result in proportional reductions of association. Therefore, this data needs to be quantified to reveal subtle but significant changes in association when compared to a HA WT-CDCA7/FLAG WT-CDCA7 interaction. This is achieved by quantifying the intensity of the HA WT-CDCA7 and FLAG CDCA7 signal in immunoprecipitation samples and calculating the HA:FLAG ratio of these signals. Specifically, this was accomplished using the Odyssey infrared scanner, which allows direct measurement of signal intensity which represents protein quantity. This data is then expressed as a percentage of HA WT-CDCA7/FLAG WT-CDCA7 association, which is defaulted to 100%. Figure 3.4 reveals that the internal deletions inclusive of amino acids 187-234 show a statistically significant reduction in association when compared to WT CDCA7. This data is summarized in a map illustrating the internal deletions responsible for a reduction in CDCA7 co-association (Figure 3.5).

CDCA7 Co-association – BioID approach

Although coimmunoprecipitations are a general indicator of protein-protein interactions, there are some caveats which can render the technique impractical. It is important to consider a) the possibility of interactions occurring post lysis, leading to false-positive results b) the general difficulty involved in working with a milieu of soluble and insoluble proteins c) forced interactions due to over expression of ectopic proteins or conversely the insensitivity of antibodies to endogenous proteins leading to weak signals that are difficult to interpret. A recently developed

technique known as BioID aims to resolve most of these issues, and has become a powerful tool used to investigate novel protein-protein interactions. The technique involves the fusion of a protein of interest with a mutated biotin ligase (known as BirA*) isolated from *Escherichia coli*. Mutation of arginine 118 to glycine reduces BirA* affinity for bioAMP, resulting in early release of bioAMP and promiscuous biotinylation of proteins within ~ 10 nm (Kim et al., 2014). Biotinylated proteins can then be efficiently purified with streptavidin-agarose beads and identified by mass spectrometry, allowing for identification of novel protein-protein interactions (Figure 3.6). This powerful approach has been used to identify the components of the mammalian nuclear lamina (Roux et al., 2012), cell junction complexes (Van Itallie et al., 2014) and constituents of centrosomes (Firat-Karalar et al., 2001). We have adapted this technique to study interactions between proteins of interest (POI) rather than unknown and novel interactions. In this case we have adapted the BioID protocol to further investigate CDCA7 co-association and to precisely map the area of interaction between CDCA7 monomers. Our protocol involves co-transfection of HEK293T cells with BirA*FLAG-WT-CDCA7 and a subset of FLAG-tagged CDCA7 mutants, biotin treatment followed by immunoprecipitation with FLAG-agarose beads and standard western blotting procedures (Figure 3.7). Samples transferred to membrane are probed with streptavidin-IR (streptavidin conjugated to an infrared sensitive dye) and scanned by the LiCOR infrared imager to reveal levels of biotinylation on FLAG-CDCA7 proteins. Biotinylation of FLAG-CDCA7 would suggest that protein-protein interactions have occurred, while loss of biotinylation due to truncation or deletions would reveal the location at which interactions are likely to take place.

Using the original BioID method described by Roux and colleagues, we have been able to show for the first time that endogenous CDCA7 interacts with the ectopically expressed BirA*FLAG-

WT-CDCA7 (Figure 3.8). This experiment also reveals that co-transfected FLAG-tagged CDCA7 was also biotinylated by BirA*FLAG-WT-CDCA7.

Next, as a proof of concept we employed our modified protocol as described above (Figure 3.7) to evaluate the extent to which an innocuous protein like GFP may interact with co-transfected FLAG-CDCA7. Figure 3.9 reveals that although co-transfected FLAG-CDCA7 was immunoprecipitated equally between BirA*GFP and BirA*FLAG-WT-CDCA7 co-transfections, only those transfected along with BirA*FLAG-WT-CDCA7 revealed any appreciable levels of biotinylation. These results indicate that promiscuous biotinylation by BirA* biotin ligase occurs at an acceptably low level.

We attempted to map the area of interaction between BirA*FLAG-WT-CDCA7 and FLAG-CDCA7 by repeating our modified protocol with a subset of FLAG-CDCA7 truncation and deletion mutants, similar to those used in figures 3.2 and 3.3 (Figure 3.10). Figure 3.11 reveals the quantified levels of biotinylation of these CDCA7 mutants and figure 3.12 illustrates these mutants on a binding map. As with our experiments investigating co-association via co-immunoprecipitation, we decided to probe the region flanked by amino acids 187 and 234 with various deletion mutants targeting this region. Figure 3.13 shows that the area of interaction between CDCA7 monomers is between amino acids 187-234. These results are consistent with those gathered by the classical co-immunoprecipitation technique outlined above. This putative area of interaction is of interest because of secondary structure prediction that points to the presence of a helix and enrichment of leucine residues (Jones, 1999), a combination which is indicative of the classical leucine zipper motif involved in protein-protein interactions (Figure 3.14) (Bridges and Moorhead, 2005).

Finally, we asked ourselves whether 14-3-3 binding with CDCA7 affects the co-association of CDCA7 monomers? We began this portion of our investigation by noting that the T163A mutation completely abolishes 14-3-3 association with CDCA7 but does not reduce CDCA7 co-association. The same is true of the KK CDCA7 substitution mutant, which relies on the mutated R18 peptide to replace T163 and to prevent 14-3-3 association (Figure 3.2). Using the internal deletion mutants within and proximal to the CDCA7 co-association domain, we performed coimmunoprecipitations of FLAG CDCA7, HA CDCA7 and endogenous 14-3-3. As with the T163A mutation and KK substitution, deletion of amino acids 138-167 within CDCA7 completed abolished any interaction with 14-3-3, without impacting CDCA7 co-association (Figure 3.16 A and B). This loss of 14-3-3 interaction is likely due to the loss of the T163 residue. However, in the case of deletion mutants targeting the putative CDCA7 co-association domain which keep T163 intact, there is a concurrent decrease between 14-3-3 association and CDCA7 co-association. This is statistically significant in the case of Δ187-204, Δ187-224 and Δ187-234 CDCA7 (Figure 3.16 A and B). In the case of deletions Δ187-194 and Δ187-214, although not statistically significant when quantified, there seems to be an objective restoration of 14-3-3 binding based on visual inspection of western blots. It remains to be seen whether 14-3-3 interaction and CDCA7 co-association are correlative or causative in nature.

Investigating a Second 14-3-3 Binding Site

It is well known that 14-3-3 exists as either homo or heterodimers involving combinations of the seven 14-3-3 family isoforms (Jones et al., 1995; Chaudhri et al., 2003). Although certain isomers prefer to either homo or heterodimerize, all 14-3-3 dimers have an affinity for a pair of pospho-serine/residues centered around consensus sites I (RSX(pS/T)XP) or II (RX(F/Y)X(pS)XP) (Gardino et al., 2006). Crystal structure solutions show that each 14-3-3 monomer contains an

amphipathic ligand binding channel, allowing for 14-3-3 dimers to a) bind two identical/different motifs on the same client protein (usually >15 amino acid residues apart), or b) two identical/different motifs, each of which appears once on two identical/different proteins (Zhu et al., 2005; Obsil et al., 2001). In the former scenario, a single protein containing two 14-3-3 binding sites results in 30-fold greater affinity for binding then a protein displaying only one 14-3-3 site (Yaffe et al., 1997). The later scenario facilitates the coming together of two client proteins that would otherwise not associate as in the example of 14-3-3 mediated dimerization of B-Raf and C-Raf (Figure 3.1) (Paul et al., 2012; Rushworth et al., 2006). This paradigm within which 14-3-3 must operate is known as the 'lynchpin' hypothesis. The theory proposes that the conservation of one of the phospho-serine/threonine binding sites (the lynchpin residue) allowed the second residue to evolve and perhaps become the target of a novel kinase (Johnson et al., 2011). The evidence for the conservation of the lynchpin residue can be found in pre-2R-WGD invertebrate chordates dating back to the two rounds of whole-genome duplication that occurred approximately 500 million years ago (Tinti et al., 2012; Huminiecki and Heldin, 2010). Due to the variable nature of the second site proposed by the lynchpin hypothesis, motifs outside of mode I and II must be considered when predicting 14-3-3 binding sites. Popular prediction tools such as Scansite or ELM (Eukaryotic linear motif database) do not take this into account and rely on a partial set of experimentally derived 14-3-3 binding sites (Obenauer, 2003; Puntervoll, 2003). Tinti and colleagues have recently developed an online tool known as '14-3-3 Pred' which includes not only modes I and II, but motifs which extend beyond the original predictors used by Scansite and ELM (Tinti et al., 2014; http://www.compbio.dundee.ac.uk/1433pred). Analysis of the human CDCA7 coding sequence by '14-3-3 Pred' (Figure 3.15A) suggests there may be four phospho-serine/threonine residues within proximity of the CDCA7 co-association domain (a.a.187-234):

S185, T213, S231 and T234 (Madeira et al., 2015). Sequence alignment of human CDCA7 with *Branchiostoma belcheri* or *Ciona intestinalis*, a pair of pre-2R-WGD organisms, reveals that four of these residues are in fact conserved (Figure 3.15B). In light of our data which suggests that the CDCA7 co-association domain is within amino acids 187-234 (Figure 3.4, 3.11 and 3.13) it would be prudent of us to investigate the existence of such a secondary 14-3-3 binding motif. Doing so would allow us to gain more insights into if and how 14-3-3 may play a role in CDCA7 co-association.

Next we generated a series of mutations targeting the four 14-3-3 consensus residues predicted by '14-3-3 Pred' to assay their affects on 14-3-3 binding and CDCA7's ability to co-associate with itself. As with earlier experiments these serine/threonine residues were mutated to an alanine to preclude any potential phosphorylation. These alanine mutations were then individually compounded with the T163A mutation. Transfection into HEK293 cells of these FLAG CDCA7 mutants followed by immunoprecipitation with α-FLAG agarose allowed us to focus on three parameters: i) affect on 14-3-3 association with FLAG CDCA7 mutants (14-3-3/FLAG), ii) affect on phosphorylation of T163 in these novel mutants (pT163/FLAG) and iii) the amount of 14-3-3 association as a product of any potential changes in T163 phosphorylation (14-3-3/pT163). Figure 3.17 shows that although not all of the results were statistically significant, none of the point mutations in question completely abolished 14-3-3 binding or T163 phosphorylation in the manner that the T163A mutation yields. In the case of the T213A mutation, there is a statistically significant ~20% reduction in 14-3-3 association. Predictably, the T163A compound mutations completely abolished 14-3-3 interaction in every case. Finally, phosphorylation of T163 remained unchanged in every case other then the S234A which may have produced a statistically significant increase of 30%. These results suggest that the S185, S231 and T234 consensus sites in question

do little to impact 14-3-3 binding to CDCA7. However, there was a marginal reduction in 14-3-3 binding observed in the T213A mutant, resulting in ~20% less 14-3-3 coprecipitating with CDCA7.

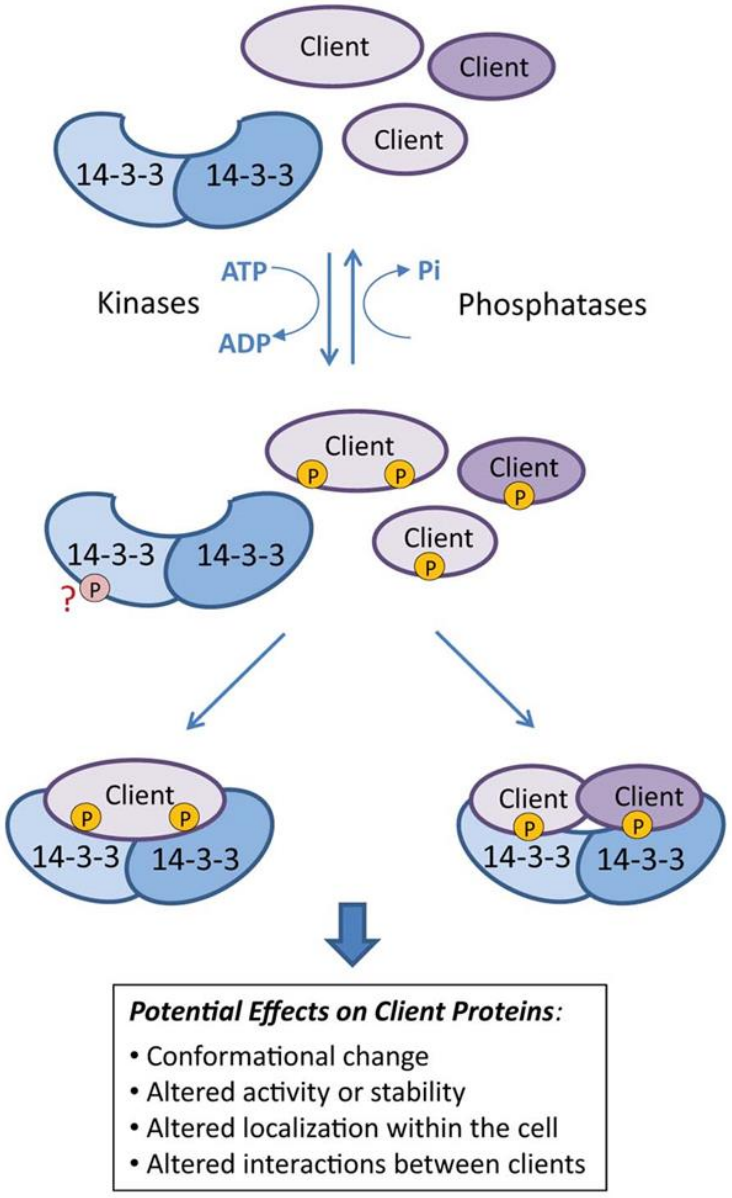

Figure 3.1. Modes of 14-3-3/client interactions. 14-3-3 exists as a dimer and interacts with its target protein at either: a) two separate phospho-14-3-3 sites on the same target protein or b) two identical phospho-14-3-3 sites on a pair of target proteins (Paul et al., 2012). Adapted from Paul et al., 2012.

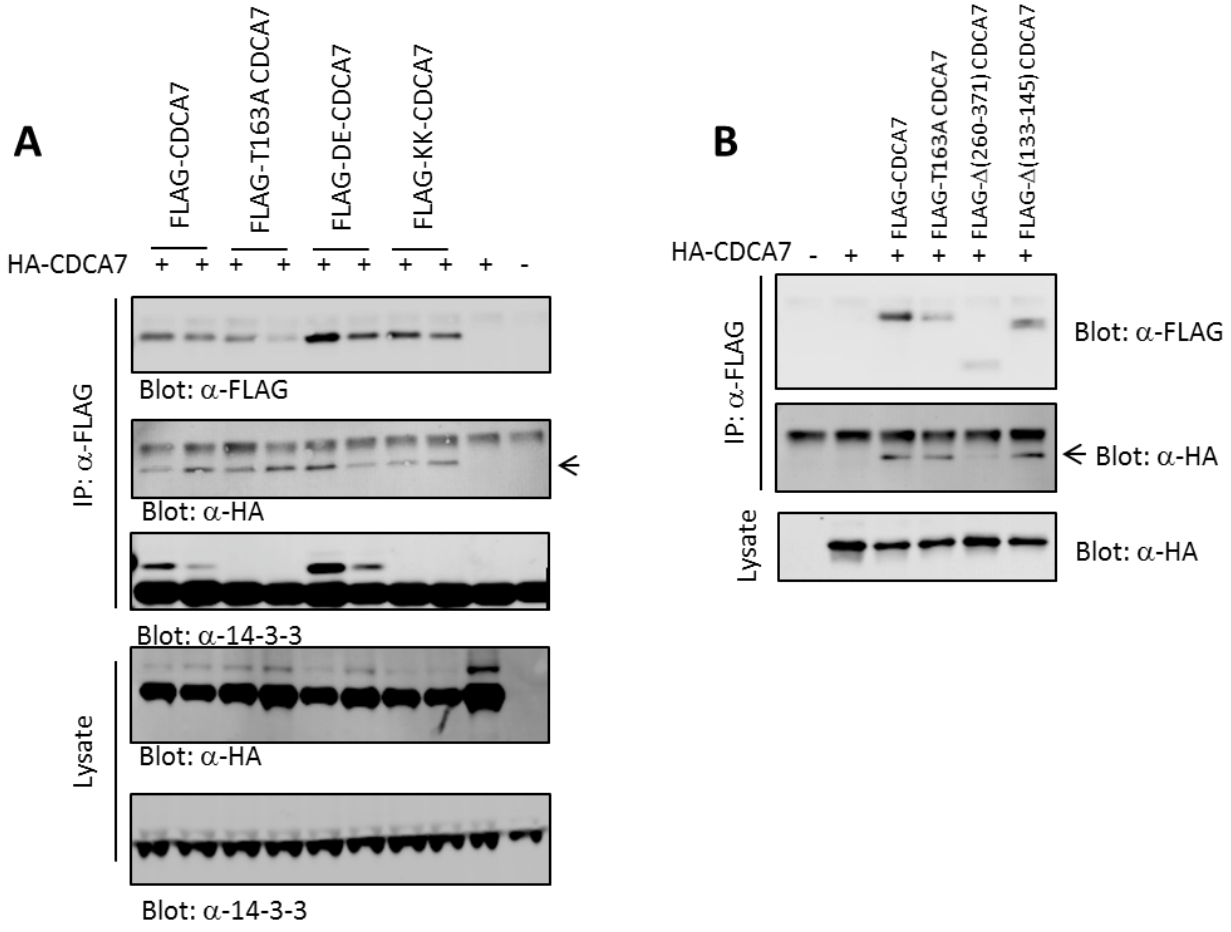

Figure 3.2. CDCA7 Co-association. **A**. HA-CDCA7 and FLAG-CDCA7 were co-transfected into HEK293 cells, and immunoprecipitated with α-FLAG agarose. Co-precipitating HA-CDCA7 was detected by HA immunoblotting. Mutation of the T163 phosphorylation site or enforced 14-3-3 binding (by substituting T163 with the DE or KK R18 peptide) did not alter co-association. Arrow indicates the position of HA-CDCA7. **B**. CDCA7 co-association was reduced by deletion of the C-terminal zinc finger domain at amino acids 260-371.

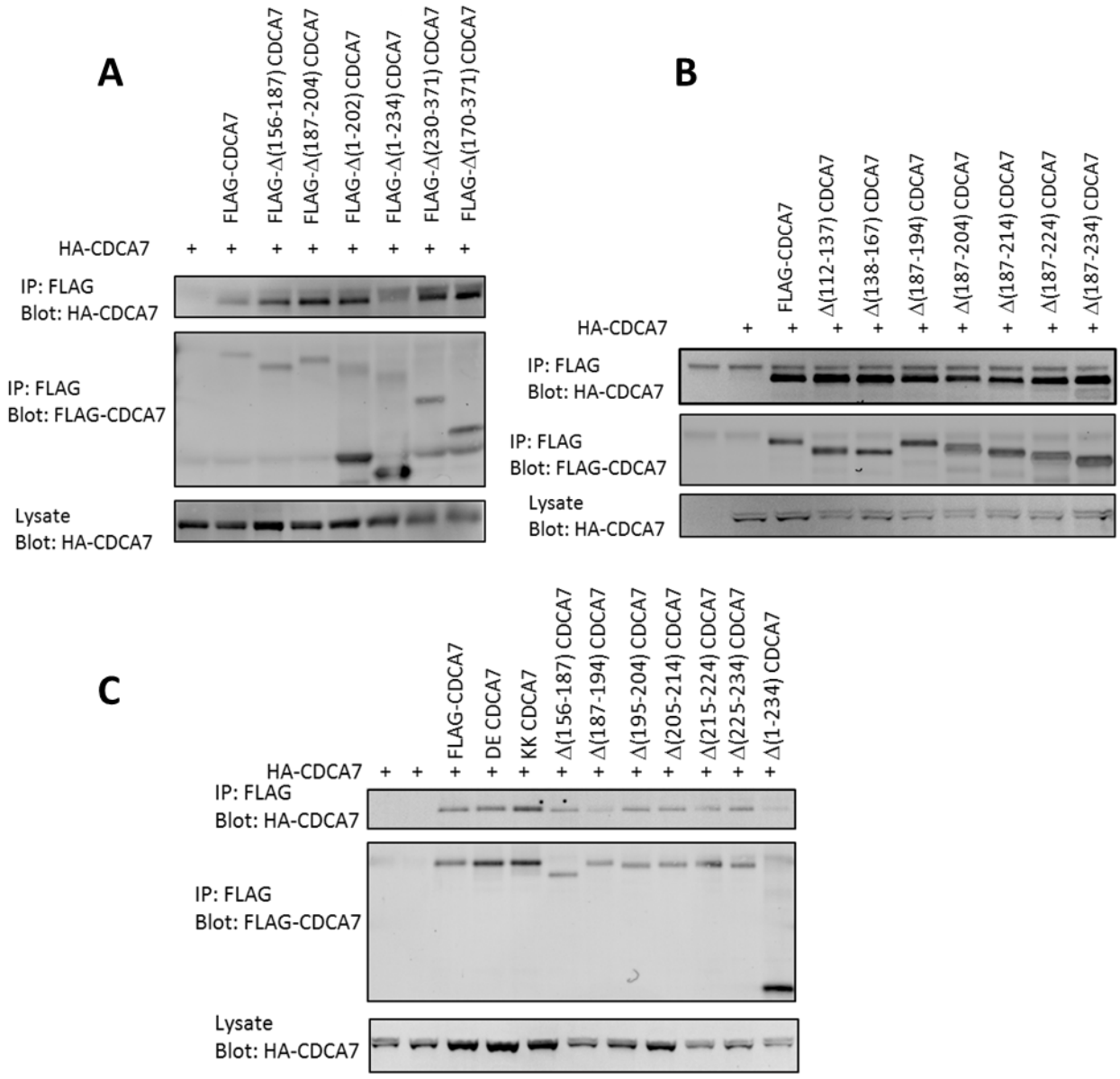

Figure 3.3. Refining the area of CDCA7 co-association. **A**. HA-CDCA7 and various internal, N- and C-terminal deletion mutants of FLAG-CDCA7 were co-transfected into HEK293 cells, and immunoprecipitated with α-FLAG agarose. Co-precipitating HA-CDCA7 was detected by HA immunoblotting. Co-association was reduced most notably by the N-terminal deletion of amino acids 1-234 **B**. Deletions of increasing length between amino acids 187-234 were tested for their ability to co-associate with WT CDCA7. **C.** In order to further refine the area of co-association, deletions of constant length were used to scan the region between amino acids 187-234 to assay their ability to coprecipitate with WT CDCA7.

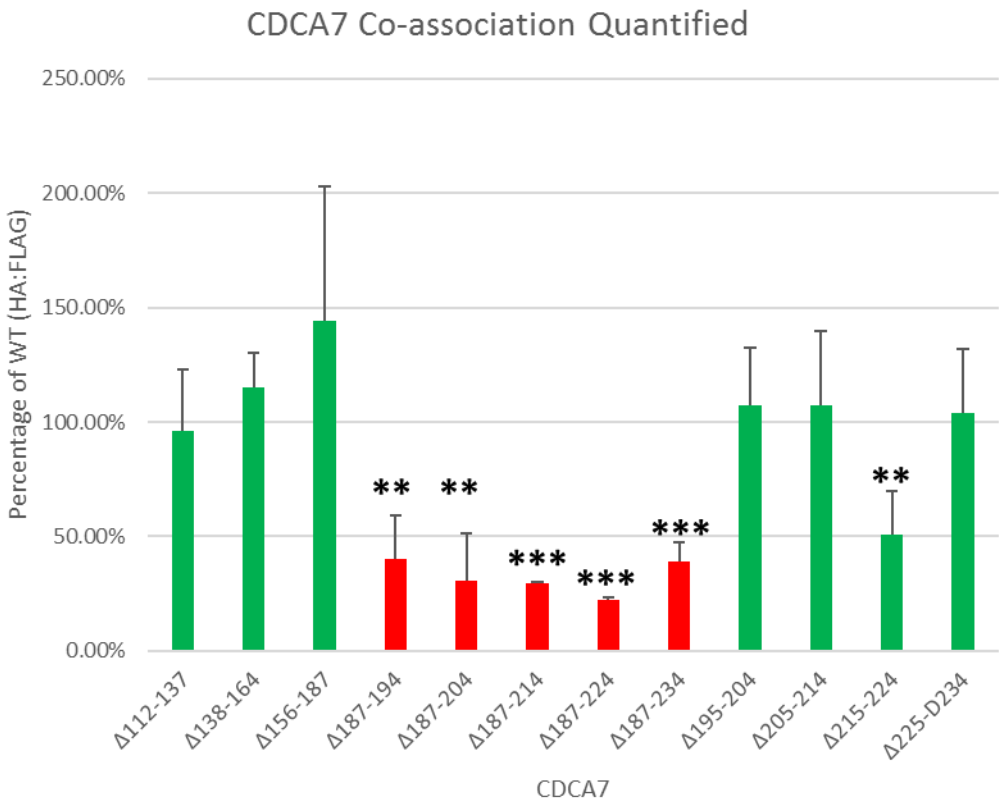

Figure 3.4. Quantification of CDCA7 co-association. Co-association of CDCA7 was quantified as a ratio of HA WT-CDCA7:FLAG CDCA7 in immunoprecipitated samples as visualized by western blots via the Odyssey LiCor scanner. Deletions within the region between amino acids 187-234 resulted a statistically significant reduction of coimmunoprecipitated HA WT-CDCA7. Red bars indicate ratios < 50% of WT, green bars indicate ratios ≥ 50% of WT. n=2 for all samples except Δ187-194 where n=3. ** = $P \leq 0.01$ and *** = $P \leq 0.001$. Error bars represent standard deviation.

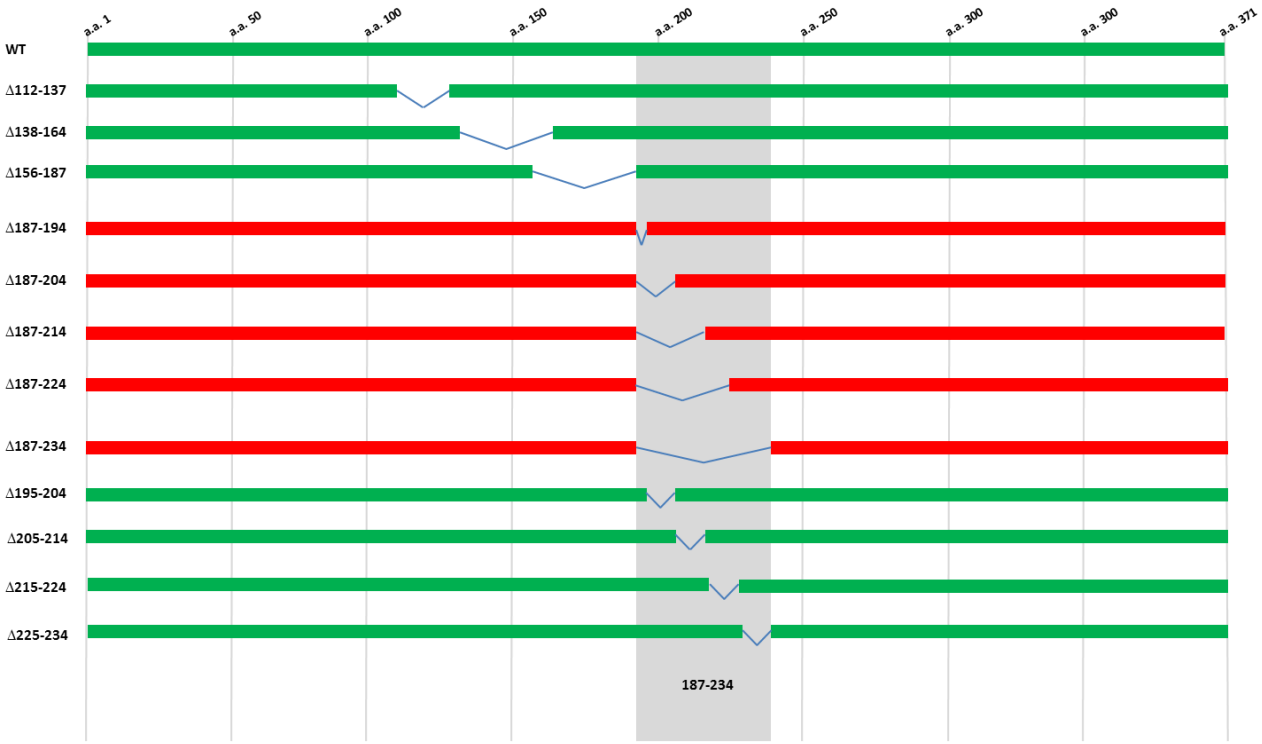

Figure 3.5. Mapping of CDCA7 co-association by immunoprecipitation. The area of responsible for CDCA7 co-association was mapped using the data in figure 3.4. Red bars indicate ratios < 50% of WT, green bars indicate ratios ≥ 50% of WT. Amino acid positions are indicated at top, while the grey area represents the area of interest between amino acids 187-234.

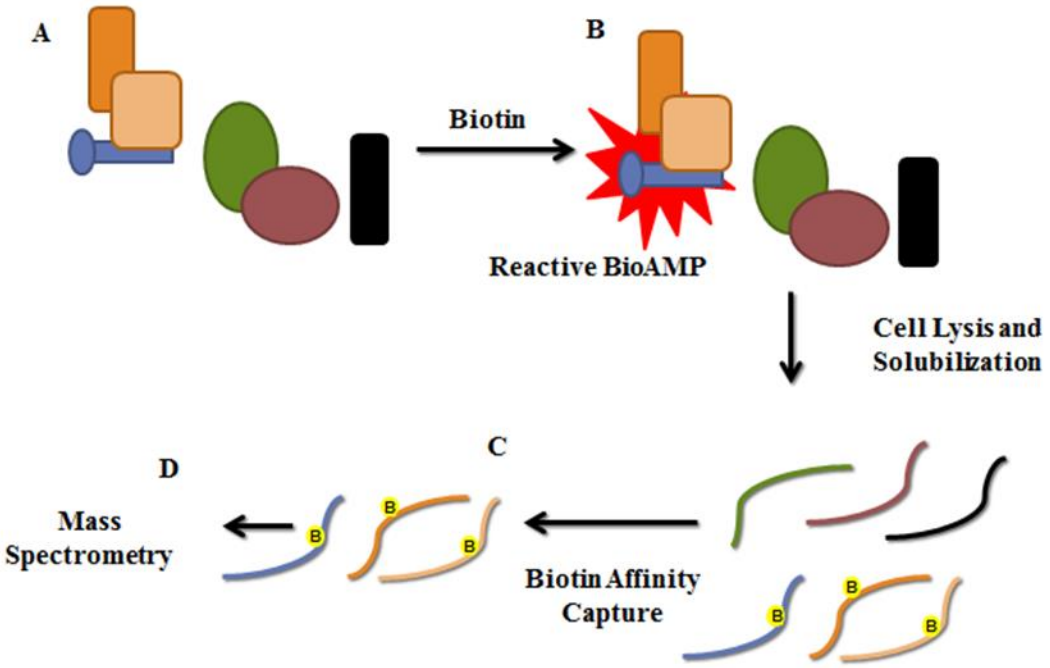

Figure 3.6. Summary of BioID. **A**) The BirA* fusion protein (blue) is transfected into HEK 293 cells, associates with proximal/interacting proteins (orange) but does not associate with distance/non-interacting proteins (green, gray and black). **B)** When biotin is supplemented for 24 hours, the BirA* fusion protein converts biotin into biotinyl-AMP (bioAMP) and prematurely releases it. The reactive bioAMP reacts with proximal/interacting proteins and tags them with biotin. **C)** Following cell lysis and solubilization, biotinylated proteins are captured on streptavidin conjugated beads and washed to purify out nonspecific interactors. **D)** Purified biotinylated proteins are then identified via mass spectrometric analysis. Modified from Roux et al. 2012.

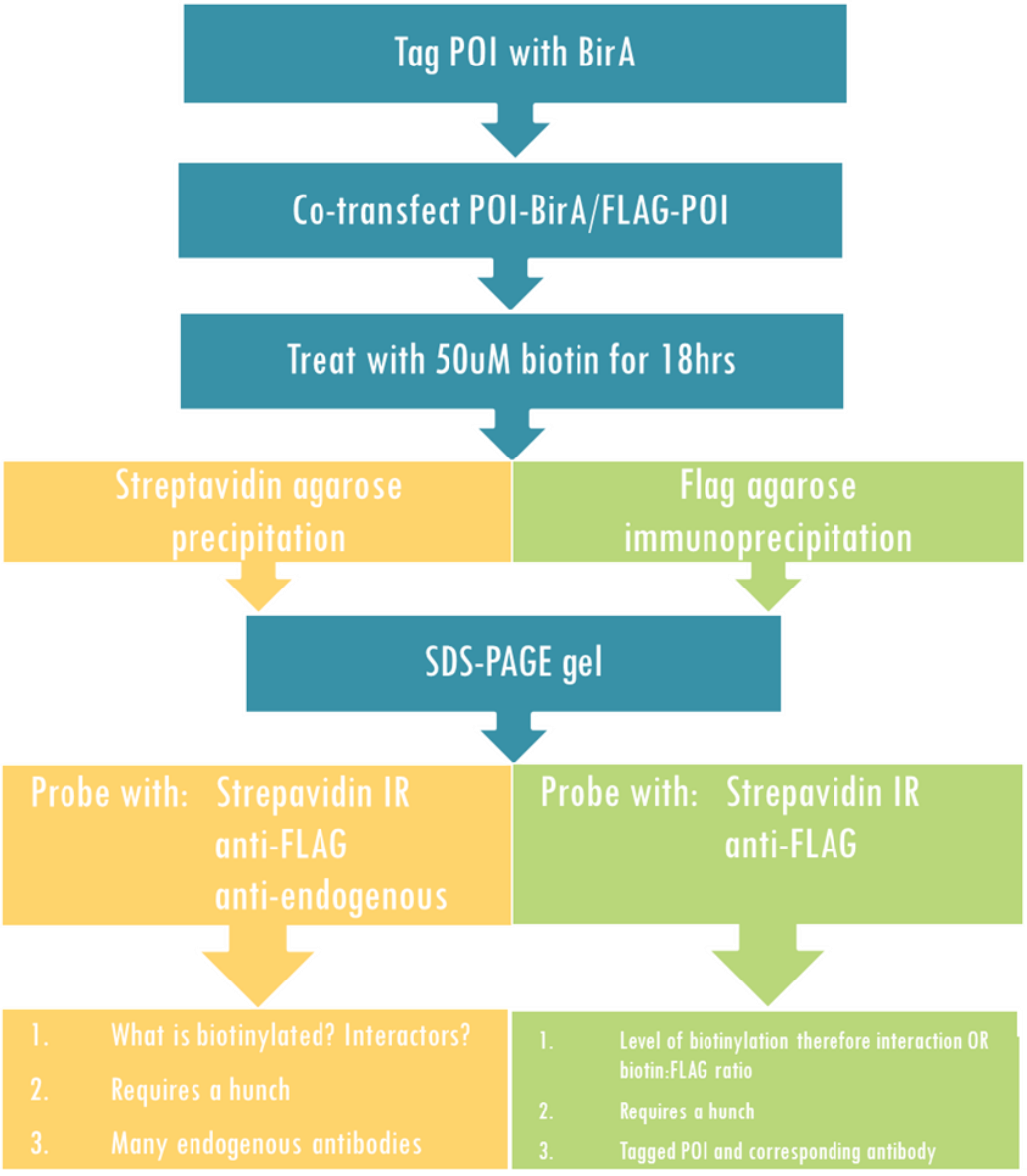

Figure 3.7. Summary of classical and adapted method of BioID. We have adapted the classical BioID method, in yellow, by following biotin treatment with immunoprecipitation of the FLAG tagged protein of interest (POI) with α-FLAG agarose rather then streptavidin capture. Western blotting and probing with α-FLAG antibody and streptavidinIR allows one to identify the level of biotinylation on the FLAG tagged POI, and therefore infer the ability of the POI to interact with the BirA fusion protein.

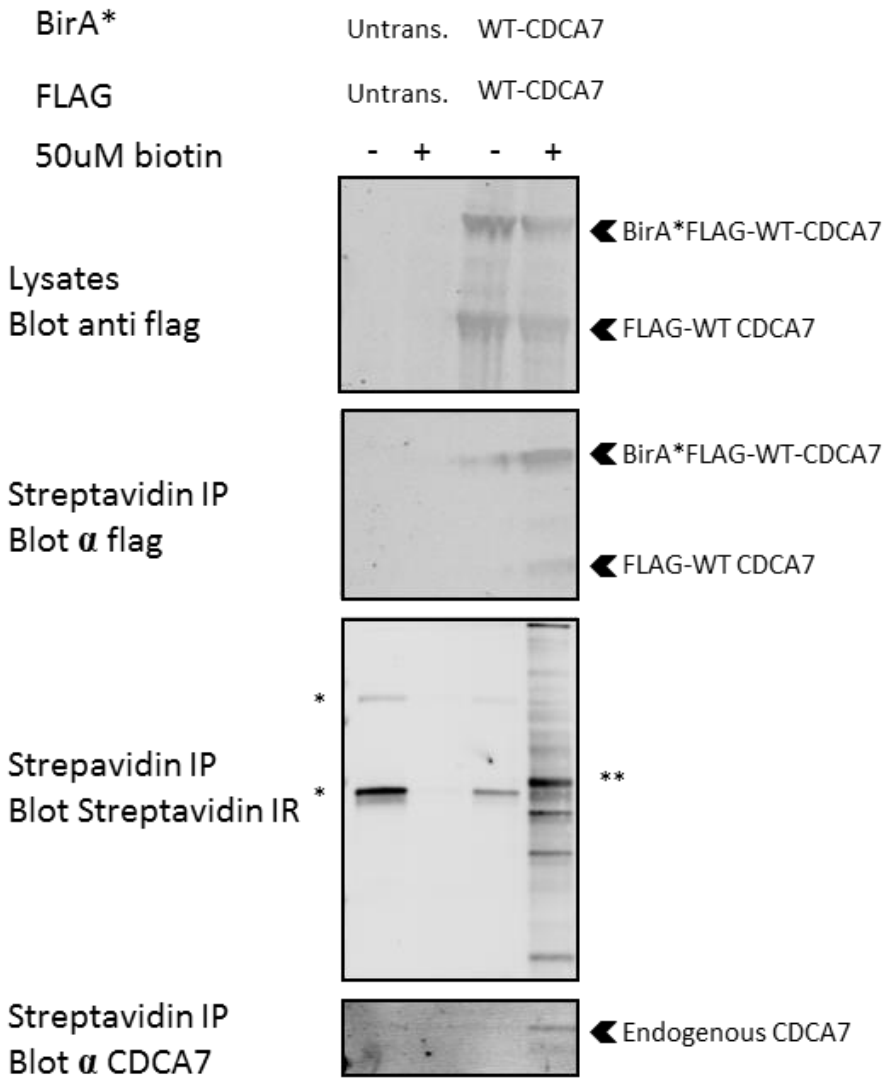

Figure 3.8. BioID proof of concept. HEK293T cells were co transfected with BirA-FLAG-WT-CDCA7 fusion protein and FLAG WT-CDCA7. Purification with streptavidin agarose followed by immunoblotting with α-FLAG and α-CDCA7 antibodies reveals that both ectopically expressed and endogenous CDCA7 are biotinylated by the BirA-FLAG-WT-CDCA7 fusion protein. * indicates possible endogenously biotinylated proteins. ** indicates a molecular weight of 55 kDa.

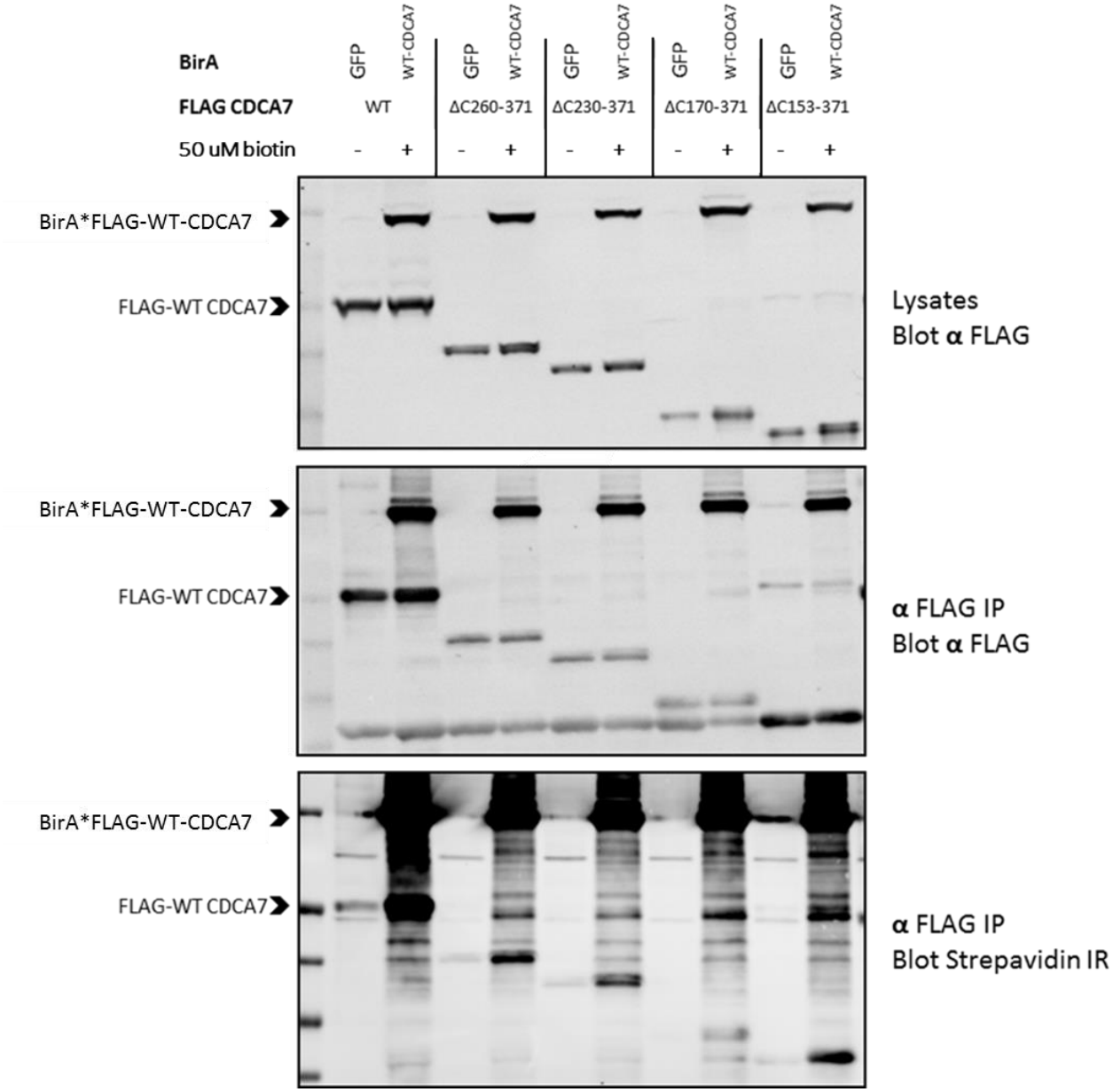

Figure 3.9. Adapted BioID protocol proof of concept. HEK293T cells were co-transfected with negative control BirA-GFP or BirA-FLAG-WT-CDCA7 fusion protein and one of several deletion mutants. Immunoprecipitation with α-FLAG agarose followed by western blotting and probing with streptavidinIR reveals the extent of FLAG-CDCA7 biotinylation by BirA fusion proteins.

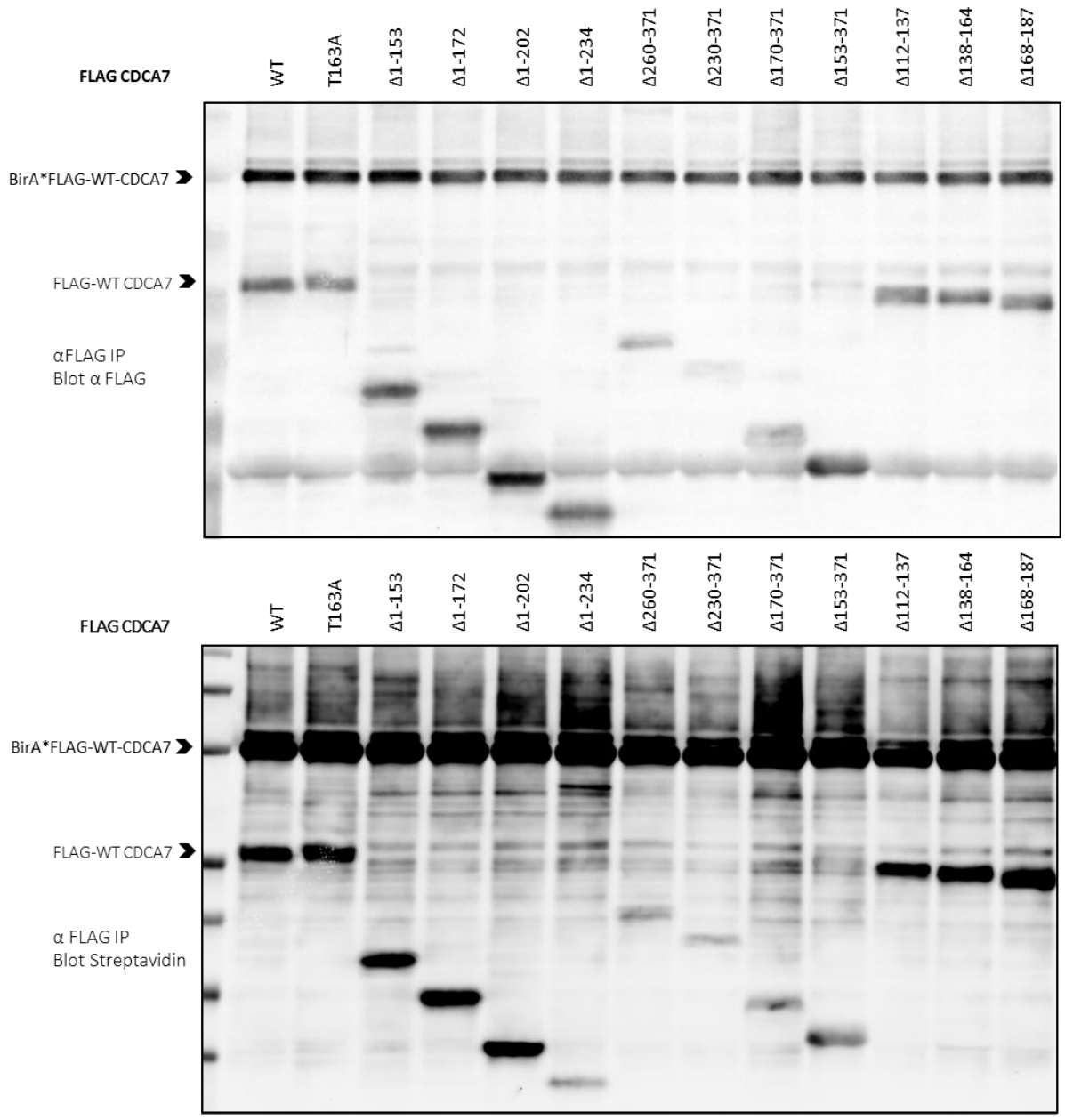

Figure 3.10. Biotinylation of wild type CDCA7 and deletion mutants. HEK293T cells were co-transfected with BirA-FLAG-WT-CDCA7 fusion protein and one of seven deletion mutants including internal, N- and C-terminal deletions. Immunoprecipitation with α-FLAG agarose followed by western blotting and probing with streptavidinIR reveals the extent of FLAG-CDCA7 biotinylation by BirA fusion proteins. Top and bottom results were obtained from scanning the same membrane which was probed with secondary antibodies bound to 700nm and 800nm infrared dyes.

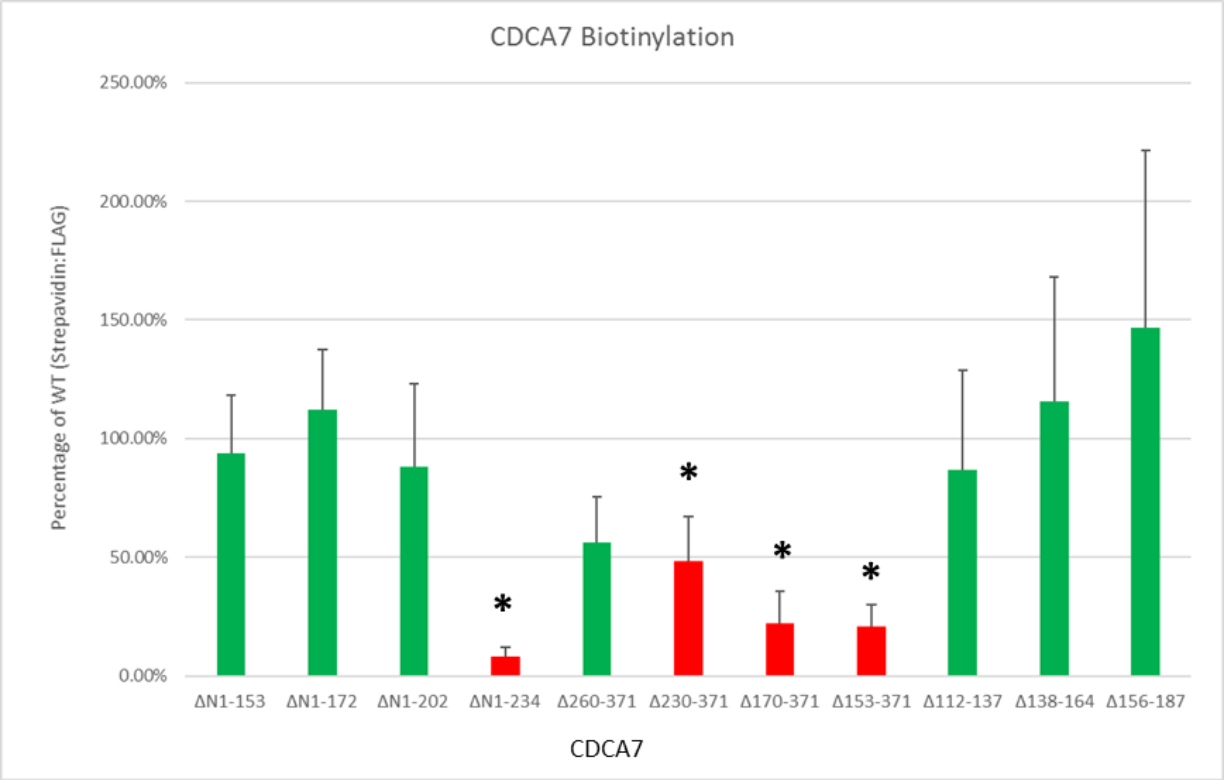

Figure 3.11. Quantification of FLAG CDCA7 biotinylation. Biotinylation of CDCA7 was quantified as a ratio of streptavidinIR:FLAG CDCA7 in immunoprecipitated samples as visualized by western blots via the Odyssey LiCor scanner. Red bars indicate ratios < 50% of WT, green bars indicate ratios ≥ 50% of WT. n=3 for all samples except Δ153-371, Δ112-137 and Δ138-164 where n=2. * = $P < 0.05$. Error bars represent standard deviation.

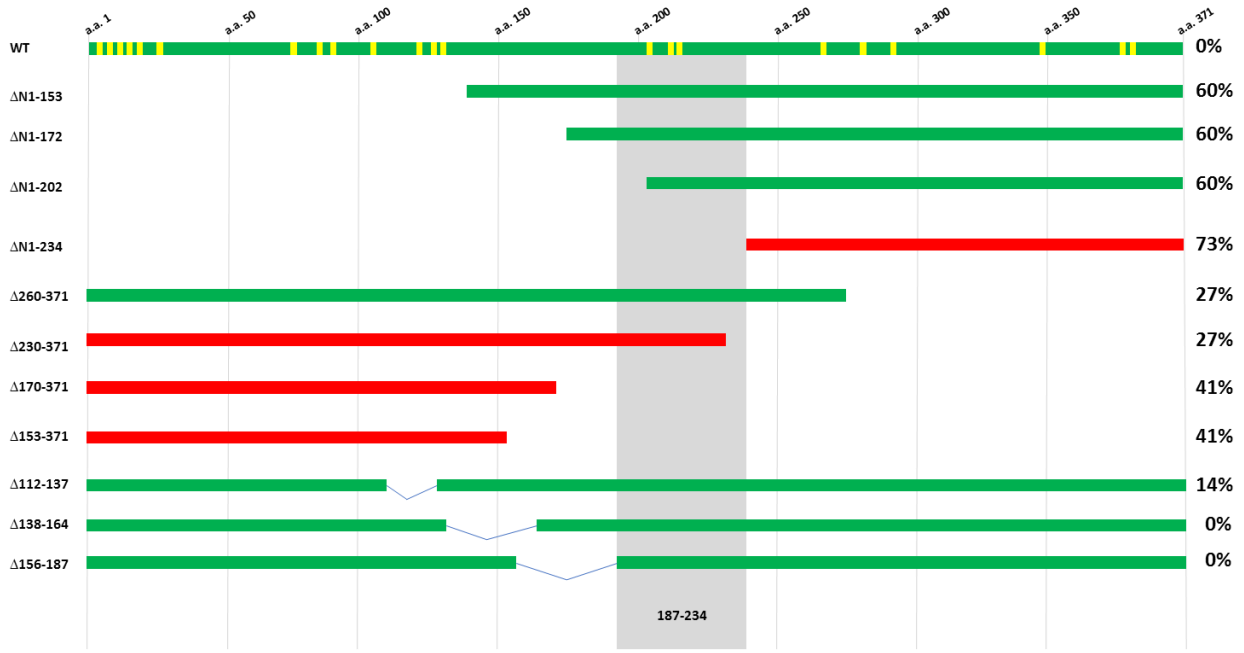

Figure 3.12. Mapping of CDCA7 co-association by biotinylation. The area of biotinylation on variations of FLAG CDCA7 was mapped using the data in figure 3.11. Red bars indicate ratios < 50% of WT, green bars indicate ratios ≥ 50% of WT. Amino acid positions are indicated at top, while the grey area represents the area of interest between amino acids 187-234. Yellow bars in WT CDCA7 indicate positions of all lysine residues with the percentage of missing lysine residues in truncation and deletion mutants indicated on the right.

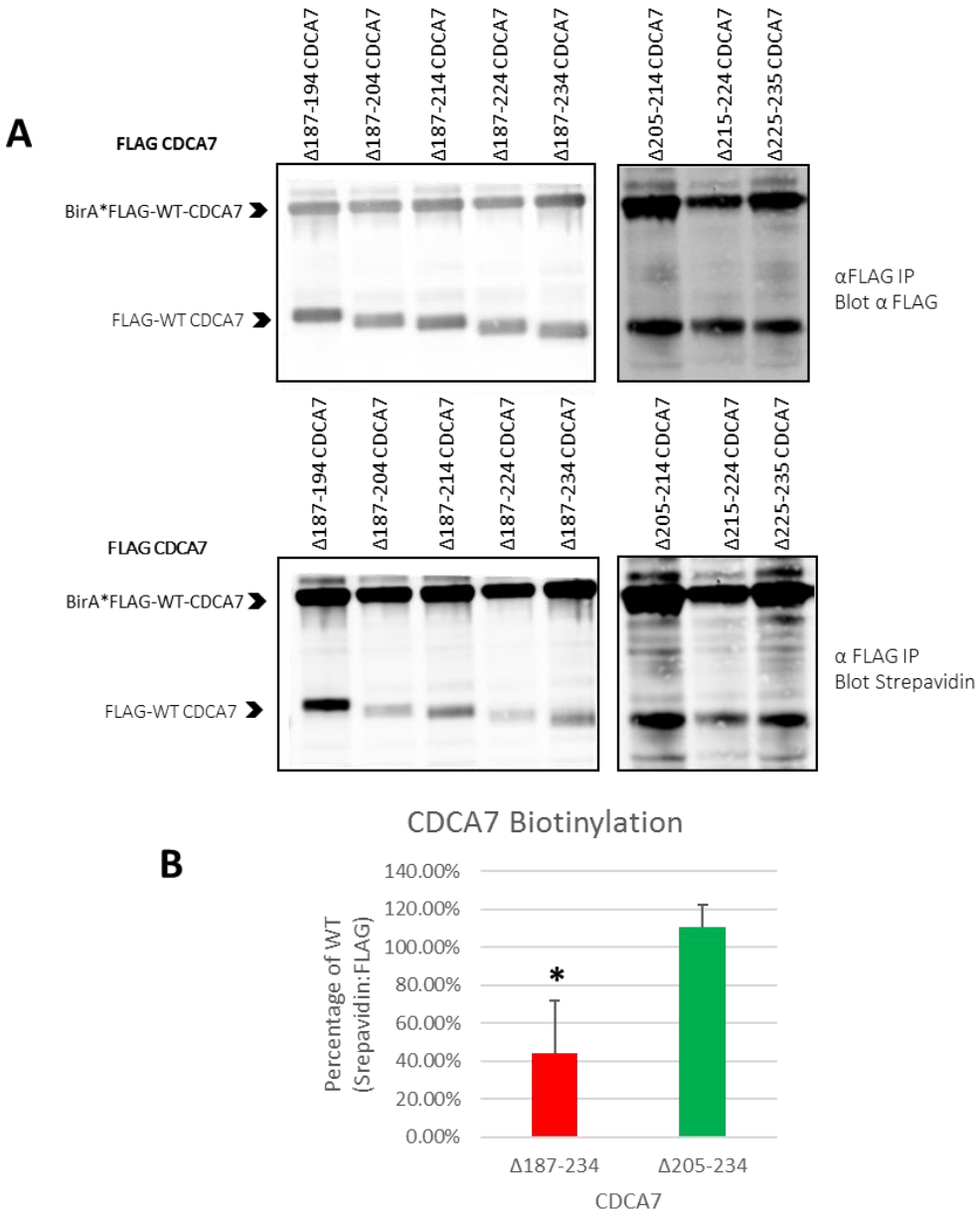

Figure 3.13. Refining the area of biotinylation between amino acids 187-234. A) Two sets of internal deletions within the amino acids 187-234 region were co-transfected with BirA-FLAG-WT-CDCA7 fusion protein into HEK293T cells. Biotinylation was visualized after western blotting by probing with streptavidinIR via the Odyssey LiCor scanner. **B)** Biotinylation of CDCA7 was quantified as a ratio of streptavidinIR:FLAG CDCA7 in immunoprecipitated samples seen in A). The data was grouped into deletions inclusive of a.a.187-234 and a.a.205-234. The Δ187-234 group is significantly less biotinylated then WT CDCA7. Red bar indicates ratios < 50% of WT, green bar indicates ratios ≥ 50% of WT. n=5 for Δ187-234 deletion group and n=3 for Δ205-234 deletion group. * = $P < 0.05$. Error bars represent standard deviation.

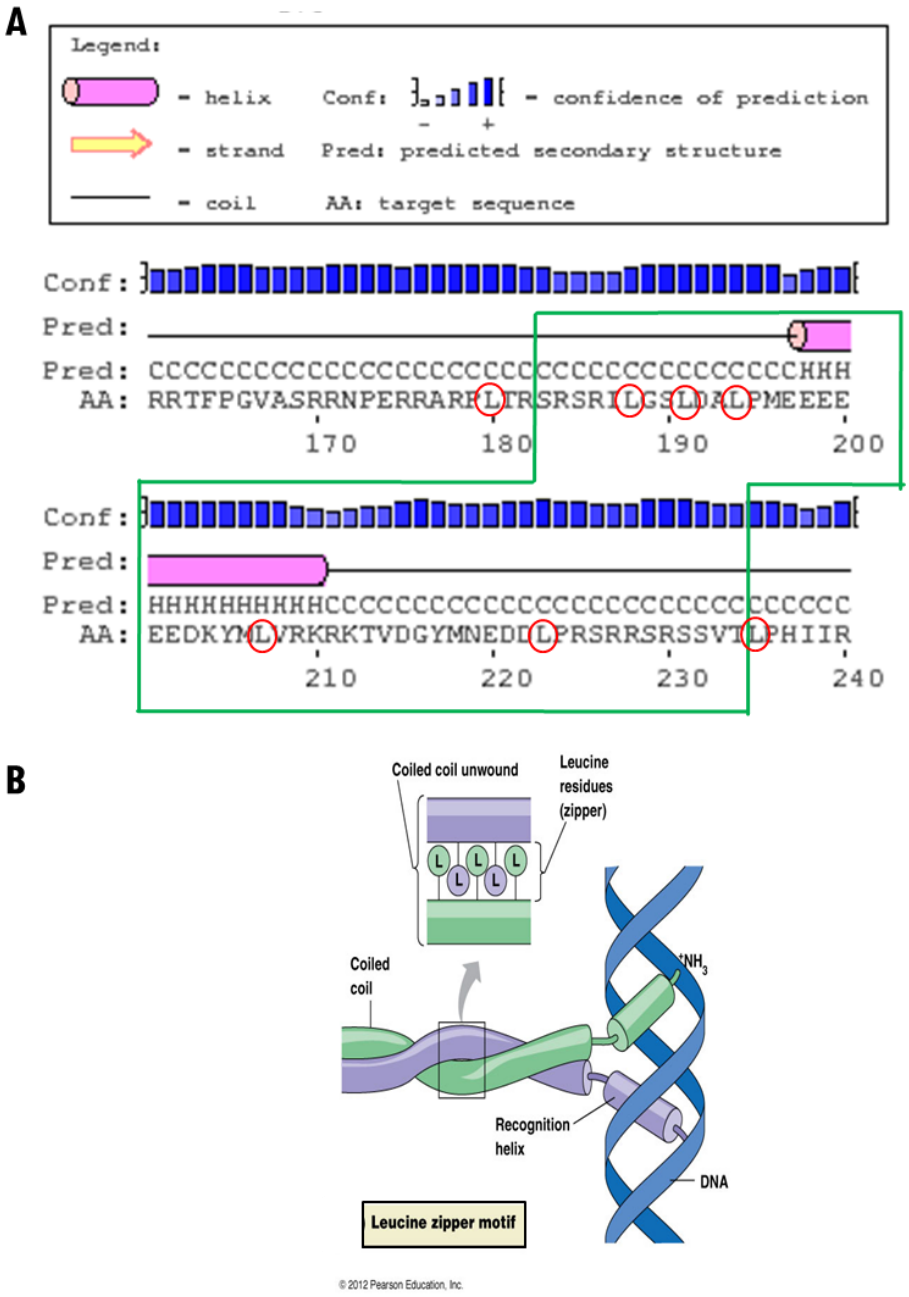

Figure 3.14. hCDCA7 secondary structure prediction. A) Prediction of hCDCA7 secondary structure by Psipred reveals a helix and a concentration of leucine residues (red circles) in the putative co-association domain (highlighted in green). http://bioinf.cs.ucl.ac.uk/psipred/. **B)** Leucine zipper motifs are known mechanism by which proteins can interact. Regularly spaced leucine residues within a helix interact with similar residues in the helix of the adjacent binding partner. (c)2012 Pearson Education Inc.

A

Position	Peptide [-6:4]	ANN	PSSM	SVM	Consensus	phosphoS/T
163	RRPRRR[T]FPGV	0.939	1.721	1.272	1.311	Yes
169	TFPGVA[S]RRNP	0.103	-0.245	-1.320	-0.487	-
181	RRARPL[T]RSRS	0.323	0.728	-0.295	0.252	-
183	ARPLTR[S]RSRI	0.078	-0.063	-1.583	-0.523	-
185	PLTRSR[S]RILG	0.795	1.115	0.822	0.911	-
190	RSRILG[S]LDAL	0.507	0.331	-0.077	0.254	Yes
213	LVRKRK[T]VDGY	0.829	0.538	0.740	0.702	-
226	EDDLPR[S]RRSR	0.028	-0.464	-1.830	-0.755	-
229	LPRSRR[S]RSSV	0.132	0.046	-1.337	-0.386	-
231	RSRRSR[S]SVTL	0.827	1.253	0.774	0.951	-
232	SRRSRS[S]VTLP	0.316	0.356	-0.611	0.020	-
234	RSRSSV[T]LPHI	0.953	0.962	1.546	1.154	-

Highly scored by three methods

Highly scored by two methods only

Highly scored by one method only

Legend

ANN - Artificial Neural Network (cut-off = 0.55)

PSSM - Position-Specific Scoring Matrix (cut-off = 0.80)

SVM - Support Vector Machine (cut-off = 0.25)

Consensus - Average of the scores provided by the three methods (cut-off = 0.50)

pSer/Thr sites are obtained from UniProt and PhosphoSitePlus

B

```
Human CDCA7                129  LAKLMSELESFPGSFRGRHPLPGSDS--QSRRPRRRTF--PGVASRRNPER-------RA  177
Branchiostoma belcheri     206  LKQALAELKSNP-----EFNIPLKKA--RKSPSRRRTMGDDNFVPRRNPKRLSYCSTRTS  258
Ciona intestinalis          73  LSQLMAELDKDPVFLKMKTSTPEQIKRFQTTKKLVRSP--P---RRYTQNI-------RG  120

Human CDCA7                178  RPLTRSRSRILGSL---DALPMEEEEEEDKYMLV-RKRKTVDG------YMNEDDLPRS-  226
Branchiostoma belcheri     259  PPMTRARGNDNNNT---PKLRFKF-----GFMFSSEKRQGSDGEDEDEIALEERELPQP-  309
Ciona intestinalis         121  PPLTRRRSSMVGNVEYPDGLNDDGADTIRSRLTV-RFTSMKRK------LSNDDPAERTP  173

Human CDCA7                227  -RRSRSSV--TLPHIIRPVEEITEEELENVCSNSREKIYNRSLGSTCHQCRQKTIDTKTN  283
Branchiostoma belcheri     310  -KRRRSGGYRAQPHRVVPVEEITEEDLELVADRVADKVYNSVHGTSCHQCRQKTADTKTT  368
Ciona intestinalis         174  KRRHVSSL--SQPHIIIPVEDVTQEMLDNIAEHSVGKTYDTINGTSCHQCRQKTIDTKSC  231
```

Figure 3.15. 14-3-3 pS/T motif prediction. A) Bioinformatic prediction of 14-3-3 pS/T motifs based on three different algorithms developed by Madeira et al., which are then cross referenced against confirmed sites in current literature and rated according to an average score of the three methods (Madeira et al., 2015). **B)** Protein conservation between human, *Branchiostoma belcheri* and *Ciona intestinalis*. T163, S185, S231 and T234 in human CDCA7 is conserved as possible targets of phosphorylation and may represent a second 14-3-3 phospho S/T site. Green arrow = T163 confirmed by our group (conserved), black arrow = conserved between humans and *Branchiostoma belcheri* or *Ciona intestinalis*, red = not conserved.

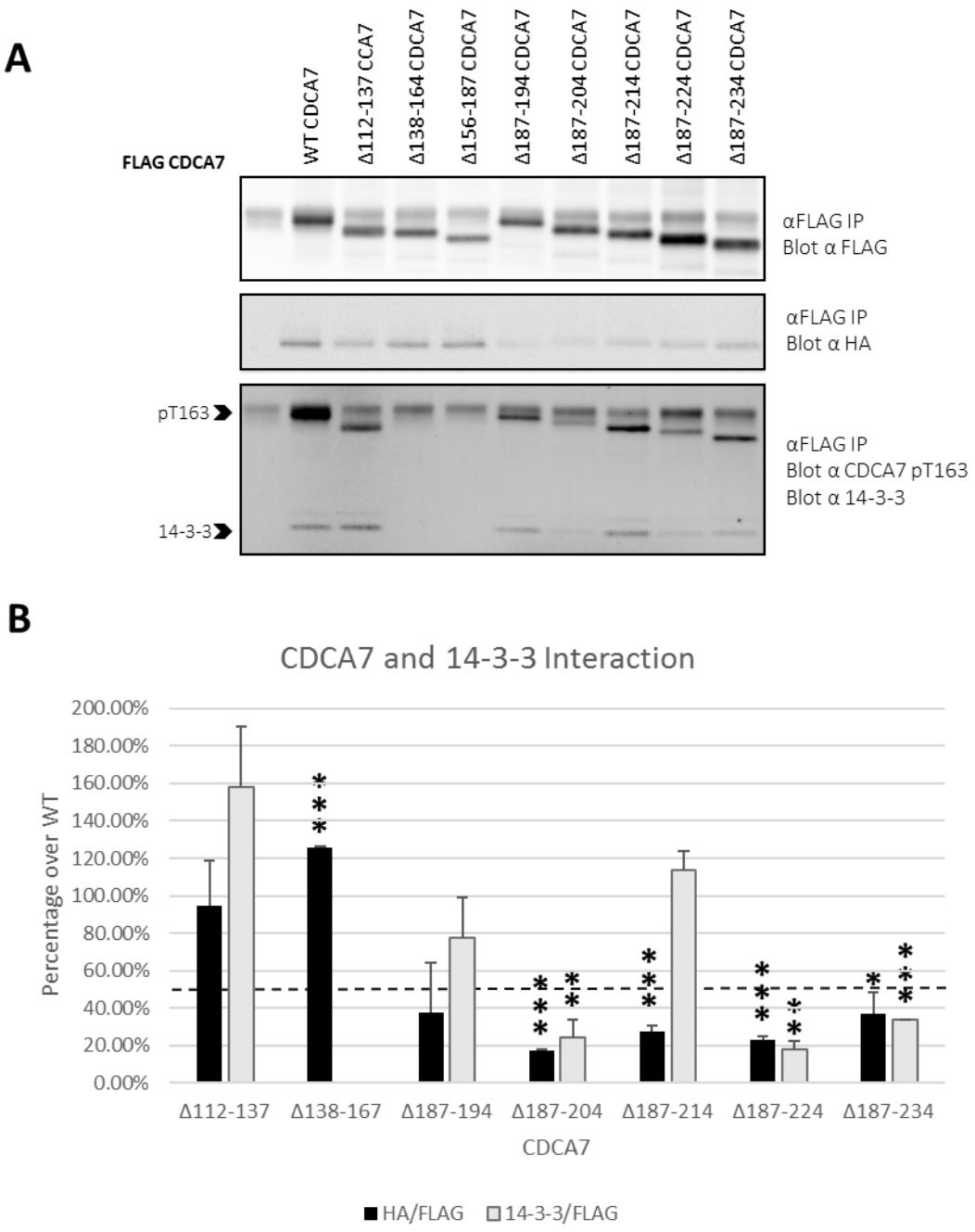

Figure 3.16. CDCA7 Co-association and 14-3-3 Interaction. A) HA-CDCA7 and FLAG-CDCA7 were co-transfected into HEK293 cells, and immunoprecipitated with α-FLAG agarose. Co-precipitating HA-CDCA7 and endogenous 14-3-3 were detected by immunoblotting. **B)** Quantification of HA CDCA7 and endogenous 14-3-3 coimmunoprecipitation shows that in the absence of 14-3-3, HA-CDCA7 still associates with FLAG CDCA7 (Δ138-167). However, in the case of Δ187-224 and Δ187-234 where both results are statistically significant, there is proportionate decrease in CDCA7 and 14-3-3 association. Dashed line indicates a 50% threshold. n=2 for all samples. * = P<0.05, ** = P ≤ 0.01 and *** = P ≤ 0.001. Error bars represent standard deviation.

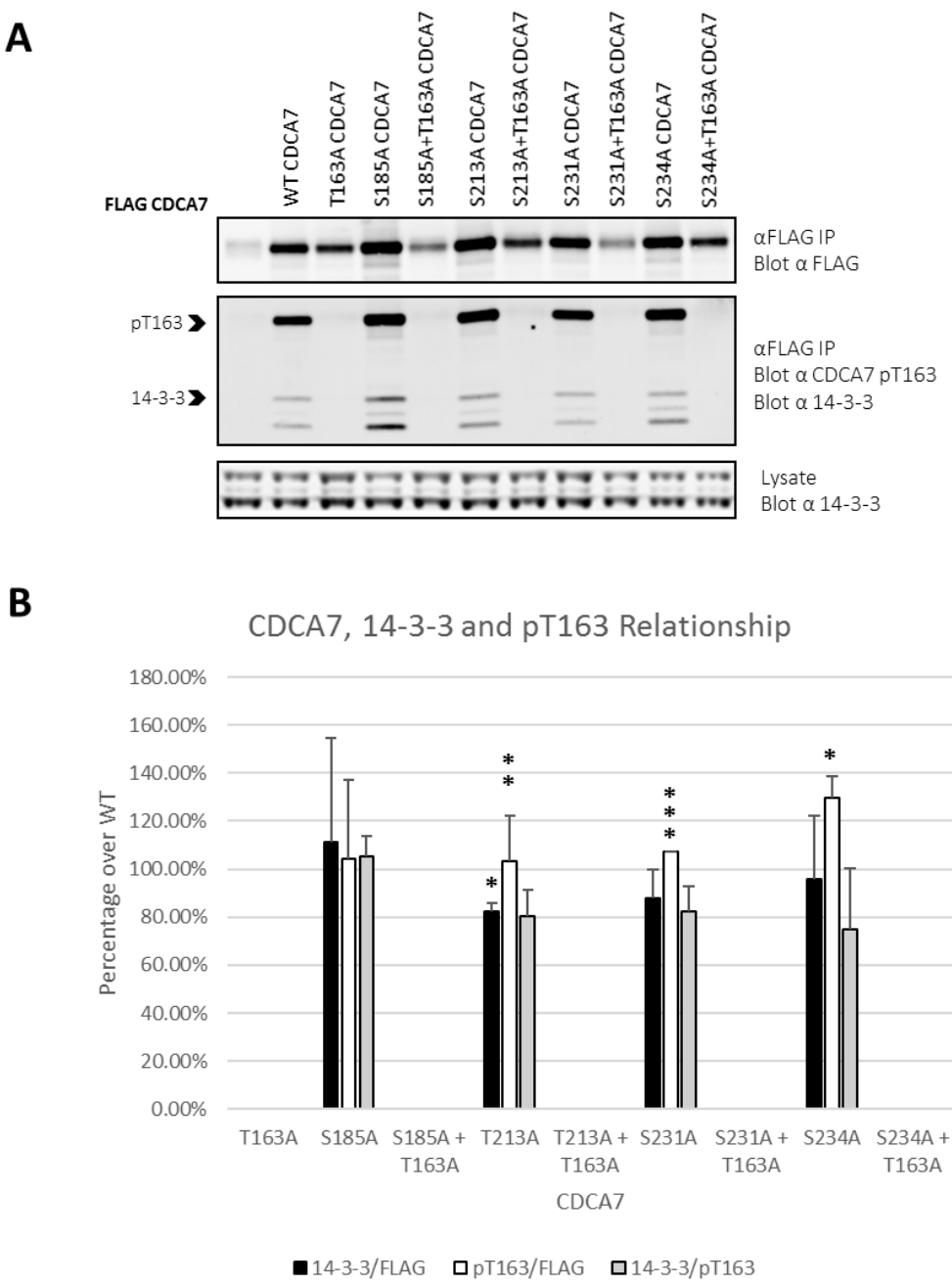

Figure 3.17. Investigating secondary 14-3-3 binding sites on CDCA7. A) FLAG-CDCA7 and various mutants of 14-3-3 consensus pS/T residues were transfected into HEK293 cells, and immunoprecipitated with α-FLAG agarose. Co-precipitating endogenous 14-3-3 was detected by immunoblotting. **B)** Quantification of endogenous 14-3-3/FLAG, pT163/FLAG and 14-3-3/pT163 in secondary site mutants reveals marginal decreases when compared to wild type. The single T163A and compound mutants completely abolishes 14-3-3 association with CDCA7 Dashed line indicates a 50% threshold. n=2 for all samples. * = $P<0.05$ and ** = $P \leq 0.01$. Error bars represent standard deviation.

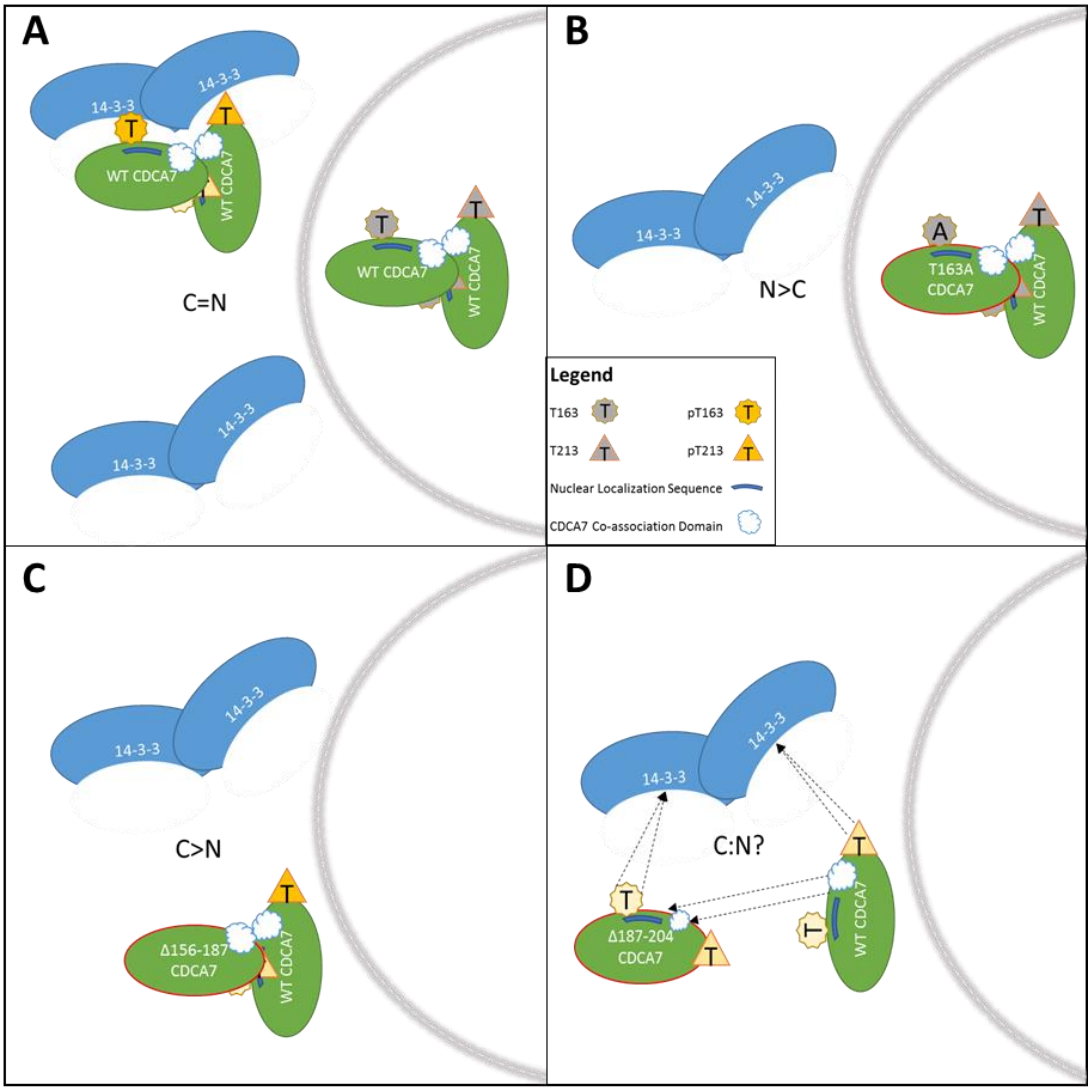

Figure 3.18. Hypothetical model of CDCA7 interactions and localization. CDCA7 monomers may associate in such a way that one monomer presents a T163 residue and nuclear localization signal (NLS), while masking the T163 residue and NLS on the opposing monomer, leaving only T213 exposed. For CDCA7 to bind 14-3-3, the exposed T163 residue must be phosphorylated. The sub-cellular localization of CDCA7 is then determined by the status of the exposed NLS. **A)** WT-WT CDCA7 complexes are distributed throughout the cell depending on the phosphorylation state of T163. When phosphorylated, WT CDCA7 complexes are bound to 14-3-3, which masks the exposed NLS and sequesters the complex to the cytoplasm. **B)** When T163A CDCA7 associates with WT CDCA7, 14-3-3 cannot associate with the alanine residue nor the T213 residue alone. The NLS is exposed and therefore shuttles the complex to the nucleus. **C)** Deletion of the NLS at residues 156-187 also removes the otherwise exposed T163, therefore the complex is isolated in the cytoplasm despite not binding to 14-3-3. Because both monomers have their co-association domains present, the complex remains intact, thereby continuing to mask the NLS in the WT CDCA7 monomer. **D)** When a portion of the co-association domain is removed, there is a concurrent reduction of 14-3-3 interaction and CDCA7 co-association. Subcellular localization is unknown.

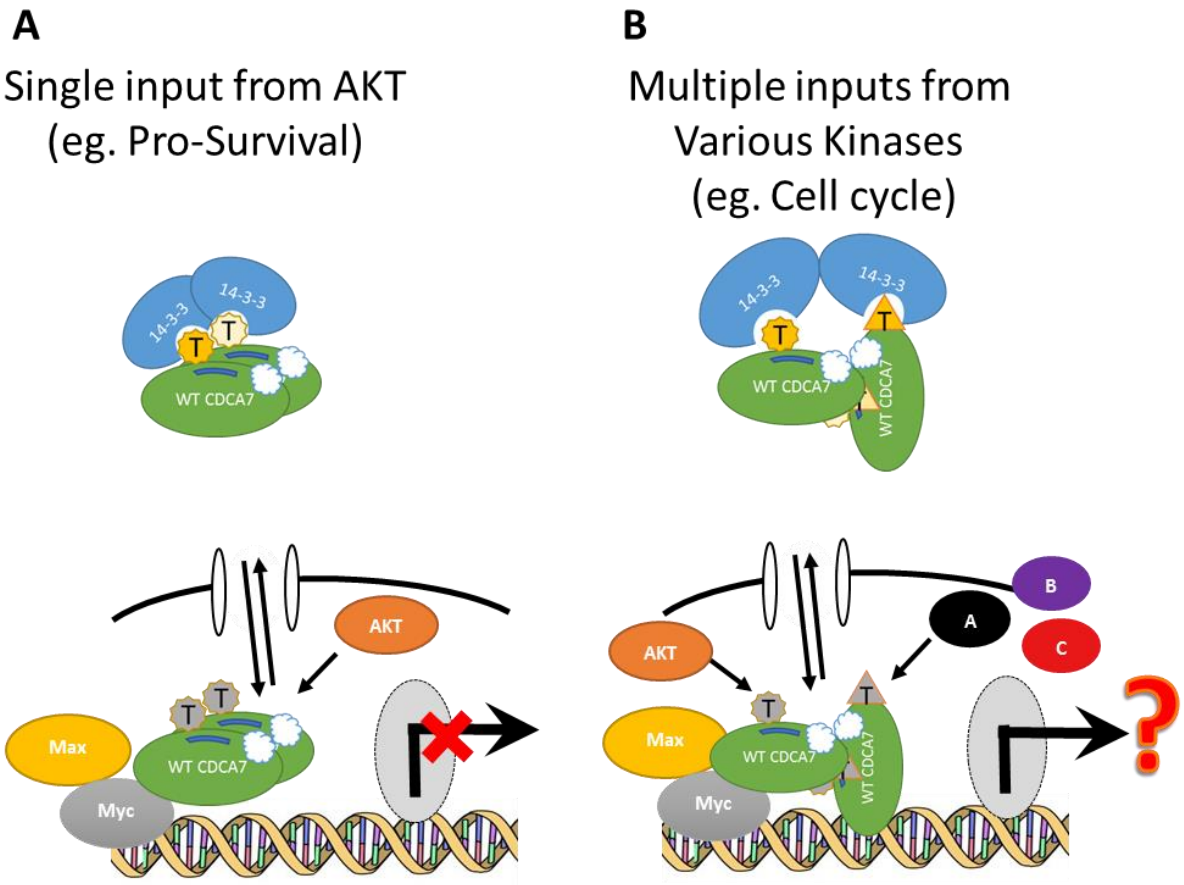

Figure 3.19. Hypothetical model of CDCA7 function mediated by Akt alone, or Akt and another kinase. 14-3-3 binding to CDCA7 can mediate its function by **A)** input from a single kinase such as Akt at T163, which is sufficient to disrupt CDCA7-Myc interaction and effect the activation of a subset of genes, or **B)** T163 and T213 need to be phosphorylated by different kinases to promote 14-3-3 binding and thus affecting various possible outcomes.

Discussion

Secondary structure predictions based on the CDCA7 primary sequence suggest that the area between amino acids 187-234 may contain a helix and is enriched for leucine residues (Figure 3.14 A). This prediction was obtained using PSIPRED, an online tool supplied by the Bioinformatics Group at the University College London. PSIPRED predicts secondary structures by first comparing input sequences with evolutionary related proteins in order to generate a position specific scoring matrix. This data is then processed by an artificial neural network that predicts secondary structure based on known crystal structures (Jones, 1999). Our results mentioned above (Figure 3.14 A) are of particular note because of the documented role that both helix structures and leucine residues play in protein-protein interactions (Jerome and Muller, 2001). We have used two complementary approaches to reveal that CDCA7 co-associates with itself. Using co-immunoprecipitations of exogenously expressed WT-CDCA7 and various internal, N- and C-terminal deletions we have mapped the region of this interaction to amino acids 187-234 (Figures 3.2-3.5). However, a criticism of this approach suggests that over expression of proteins *in vivo* often results in forced interactions (Nan et al., 2015). This could be a product of stoichiometry or interaction post-lysis and therefore not an accurate representation of naturally occurring complexes in terms of levels, sub-cellular localization or temporal variances. Therefore, a means of taking a snapshot of interactions as they occur in the cell is required to overcome this criticism. BioID can achieve this by identifying proximal proteins which are biotinylated by the promiscuous biotin-ligase BirA*. BirA* will only biotinylate proteins within a distance of ~10 nm (the average width of a protein) and only when cell culture media is supplemented with biotin. Washing away biotin prior to lysis prevents false-positives that may occur otherwise post lysis (Kim et al., 2014). Although biotinylation of proteins is not a direct indication of a protein-protein interaction, it can

at least suggest the presence of a complex of proteins which include the BirA* fusion protein and the protein of interest within ~10 nm. Using BioID we have replicated our co-immunoprecipitation study and confirmed that CDCA7 co-association in fact depends on the region between amino acids 187-234 (Figure 3.8-3.13). We have hesitated to use the term 'dimer' or 'dimerization' when describing this interaction simply because these studies do not preclude the possibility of two CDCA7 monomers exiting in a larger complex, yet still within the ~10 nm resolution of BioID. To be certain that a protein(s) can in fact form a dimer, it would have to be expressed in bacteria, purified and passed through a size exclusion column. The mass of the complex would indicate whether the protein exists as a monomer, or in a complex of multiples thereof. Alternatively, direct association can be assayed for by the same means we used to show a direct CDCA7-Myc interaction (Figure 2.1), that is to test for *in vitro* association of alternately tagged and purified proteins. These two methods generally rely on the expression and purification of the protein of interest in a bacterial host, which in most cases is an excellent means of producing large quantities of protein. However, our efforts using this approach yielded nominal levels of ectopically expressed CDCA7 in *E. coli.* This is can be explained by a phenomenon that results in inclusion bodies containing high concentrations of recombinant protein aggregates. A combination of high temperature, high concentration of induction compounds and expression via strong promoters can cause protein quality assurance mechanism to be overwhelmed. As a result, poorly folded proteins find themselves accumulating within inclusion bodies and are essentially of no use to researchers (Carrio and Villaverde, 2005). This setback forced us to rely on the methods described here, namely expression in HEK293 cells followed by co-immunoprecipitation studies and BioID.

With the knowledge that CDCA7 interacts with the bridging protein 14-3-3 and that CDCA7 monomers have the ability to associate, it was imperative for us to investigate whether 14-3-3 is

responsible for bringing CDCA7 together. The mechanism by which 14-3-3 can mediate such an interaction is outlined in figure 3.1 and is described above in detail. Our data reveals that CDCA7 co-association does not depend on 14-3-3 to act as a bridging molecule. This is well illustrated in the T163A point mutation which completely abolishes 14-3-3 binding but not CDCA7 co-association (Figure 3.2). However, when amino acids 187-234 are deleted from CDCA7 there is a significant drop in co-association and 14-3-3 binding despite T163 being intact (Figure 3.16 A and B). This result would suggest that either a) already existing complexes of CDCA7 (perhaps including other proteins) are acting as docking sites for 14-3-3, b) deletion of amino acids 187-234 alters conformation of the pT163 binding site or c) deletion of amino acids 187-234 removes an unidentified second 14-3-3 binding site. Bioinformatic scans for 14-3-3 consensus sites within CDCA7 reveal 4 potential residues in the a.a.187-234 region of interest, with three of the sites being conserved over 500 million years (Figure 3.15 A and B) (Madeira et al., 2015). Our results indicate that mutation of T213 to alanine results in ~20% less 14-3-3 co-immunoprecipitation with CDCA7, and a complete abolishment when the T163A mutant is compounded with T213A (Figure 3.17 A and B). This may suggest that T213 is a second, weaker site of 14-3-3 interaction which is not required for binding under our assay conditions. This makes way for the exciting potential that T213 could fall under the control of a kinase other than Akt (which phosphorylates T163). To that end, a Scansite search for consensus kinase sites at T213 suggests that Aurora B kinase may target that residue (Obenauer et al., 2003) which has been confirmed via mass spectrometry as being phosphorylated (Hornbeck et al., 2015). Aurora B kinase plays an important role during mitosis as part of the chromosomal passenger complex (CPC) which is required for cytokinesis to take place faithfully (Sampath et al., 2005). Confirmation of T213 phosphorylation by Aurora B kinase has yet to be established and would require a combination of: a) a custom antibody raised against

pT213, b) 2D-phosphotryptic mapping, c) *in vitro* kinase assays, d) experiments using Aurora B null cells and e) an Aurora B selective inhibitor such as AZD1152 (Bavetsias and Linardopoulos, 2015).

If 14-3-3 is not mediating the coming together of CDCA7 monomers, what other roles may it play in regulating CDCA7's function? In most cases, being under the direct control of Akt kinase would warrant serious consideration, as Akt is known to regulate many critical functions of the cell (Fresno et al., 2004). In our published work from 2013 we showed that CDCA7 not only binds 14-3-3 when T163 is phosphorylated by Akt, but that CDCA7 migrates to the cytoplasm in the process (Figure 2.5 and 2.6). We showed that T163 is in fact found within a nuclear localization sequence between amino acids 156-187 (Figure 2.4). Is it possible that 14-3-3 binding to CDCA7 is mediating subcellular localization by binding T163 and masking the NLS in the process? There is precedent for exactly this function of 14-3-3 in the cytoplasmic localization of Cdc25. It has been shown that mutation of serine 287 to an alanine in *Xenopus* Cdc25 completely abolishes 14-3-3 binding, resulting in nuclear accumulation of Cdc25 (Muslin and Xing, 2000). A threonine to alanine mutation at T163 of CDCA7 also causes nuclear accumulation and an inability to bind 14-3-3 (Figure 2.3). It is important to consider that any explanation of how CDCA7 functions should take into account that it exists in a complex with another monomer of itself. All of the data that we have gathered to that end is in the context of one of the monomers existing as a wildtype molecule (HA CDCA7) while its counterpart bares the mutations in question (various forms of FLAG CDCA7). Therefore, in the example of T163A CDCA7, the loss of 14-3-3 binding and subsequent nuclear localization cannot be reversed by the wildtype threonine and what should be a masked NLS presented by the WT monomer. This is especially evident when considering that the T163A mutation does not alter CDCA7 co-association. What is even more striking is the fact that deletion

of the NLS at a.a. 156-187 (and loss of T163) prevents 14-3-3 binding, maintains co-association but reverses the nuclear targeting seen in the case of the T163A mutant. In this case, the WT CDCA7 monomer maintains its T163 residue and NLS, which may otherwise either bind 14-3-3 or cause nuclear shuttling if the NLS is exposed. How is it that there is preference for one monomer of the CDCA7 complex to dictate 14-3-3 binding and sub-cellular localization? The answer may be found in a subtle variation in the way complexes of two proteins are generally depicted when a protein's crystal structure has yet to be solved, which is usually side by side like beads on a string. Figure 3.18A depicts an arrangement of a WT-WT CDCA7 complex in such a way where monomer A presents a T163 residue and its NLS while masking the same structures on monomer B. This results in monomer B presenting only a T213 residue (the putative second 14-3-3 binding site, Figure 3.17) while occluding T213 on monomer A. This paradigm is depicted in Figure 3.18 and elegantly allows for the four conflicting properties of CDCA7 to work in concert, that is 14-3-3 binding at T163, the presence of a nuclear localization signal, CDCA7 co-association and a second 14-3-3 binding site at T213.

The discovery that monomers of CDCA7 co-associate may reveal further insights into how Akt and potentially other kinases might mediate CDCA7 on a mechanistic level. Figure 3.19 outlines a hypothetical model whereby CDCA7 function is mediated through a single kinase (Akt) at T163, or by multiple kinases at T163 and T213. In the case of Akt acting alone, input from Akt is sufficient for 14-3-3 binding, shuttling to the cytoplasm and disruption of the CDCA7-Myc interaction. This results in a pro-survival outcome. CDCA7 function can also be mediated by phosphorylation via Akt at T163 and another kinase(s) at T213 to affect a variety of possible outcomes.

To date we have shown that CDCA7 not only interacts with another monomer of itself, but with Myc and 14-3-3 as well. The nexus of these interactions and understanding the conditions which determine their states are crucial to deciphering the exact means by which CDCA7 cooperates with its partners to affect proliferation, apoptosis or yet to be discovered processes. These conditions are myriad and should be explored further. For example, one must not overlook studying CDCA7 in the context of: a) different points of the cell cycle, b) cell density and contact inhibition, d) stimulation with a variety of growth factors or e) experiments in different cell types.

Materials and Methods

Cell lines and cell culture

HEK 293 and NIH 3T3 cells were obtained from the American Type Culture Collection and maintained in Dulbecco's modified Eagle's medium supplemented with 10% fetal bovine serum and antibiotics at 37°C and 5% CO_2.

Transfections

For transient expression of cDNA in HEK 293 cells, cells were plated onto 100-mm-diameter dishes at 80% confluency and transfected with 8 μg of total plasmid using polyethylenimine (PEI) (Sigma-Aldrich #408727). 8 μg of DNA was diluted with 1 mL of serum-free Opti-MEM (ThermoFisher Scientific #31985062). 24 μg of PEI was added to the diluted DNA mix for a final ratio of 3:1 μg PEI:μg DNA. The mix was vortexed 10x and allowed to incubate at room temperature for 30 minutes. 3 mL of Dulbecco's modified Eagle's medium supplemented with 10% fetal bovine serum was gently added to the transfection mix. The 4 mL total transfection mix

was then added to cells following aspiration. 7 hours later, transfection medium was removed and replaced with complete Dulbecco's modified Eagle's medium overnight.

Antibodies and Reagents

Mouse monoclonal M2 anti-flag (A2220), rabbit polyclonal anti-CDCA7 (HPA005565) and rat monoclonal anti-HA (3F10) and biotin (B4639) were purchased from Sigma-Aldrich. Streptavidin agarose (69203) was purchased from Millipore and StreptavidinIRdye 680 (926-68079) was purchased from Mandel. Mouse monoclonal anti-14-3-3β (SC-1657) was purchased from Santa Cruz. An anti-p-Thr163 CDCA7 rabbit polyclonal antibody was generated by Genscript Corporation (California).

Cloning

The CDCA7 coding region was ligated into the pCMV-HA-N mammalian expression vector (Clontech) to introduce an amino terminal HA epitope. The CDCA7coding region was ligated into the p3XFLAG-CMV10 mammalian expression vector (Sigma-Aldrich) to introduce an amino terminal FLAG epitope. Mutagenesis of p3XFLAG-CMV10-CDCA7 was performed using the QuikChange kit (Stratagene) and NEB Q5 Site Directed Mutagenesis Kit (E0554), and the various mutations were sequence-verified. Amino-terminal and internal deletions were created by introducing silent mutations coding for unique restriction sites, followed by digestion and re-ligation. Carboxyl terminal deletions were created by introducing stop codons. All deletions were sequence verified. CDCA7 containing the 14-3-3-binding R18-peptide PHCVPRDLSWLDLEANMCLP or the control non-14-3-3-binding peptide PHCVPRDLSWLKLKANMCLP were created by ligating a double-stranded oligonucleotide to replace amino acids 139-164 of CDCA7 in the 3XFLAG-CMV10 vector.

The coding region for green fluorescent protein (GFP) and CDCA7 were ligated into the pcDNA3.1 MCS-BirA(R118G)-HA vector which was a gift from Kyle Roux (Addgene plasmid # 36047)

BioID

HEK293 cells were plated at 50% confluency and transfected with the BirA* fusion proteins and p3XFLAG-CMV10-CDCA7 as per above. 18 hours later cell media was supplemented with 50 μM biotin and allowed to incubate at 37°C and 5% CO_2 for 24 hours.. Following 3x washes with PBS, cells were harvested in T-X100 lysis buffer on ice as bellow. Samples were incubated with either 50 μL of streptavidin agarose or anti FLAG agarose slurry and rotated overnight at 4°C. Samples where centrifuged and washed 3x with PBS prior to elution in sodium dodecyl sulfate sample buffer as per below. Lysates and immunoprecipitations were fractionated by SDS-PAGE, transferred to a PVDF membrane, blocked in Odyssey blocking buffer (Mandel, LIC-927-40100), and probed with a variety of primary antibodies or the streptavidinIR 700 dye. Primary antibodies were decorated with IR700 anti-mouse or rabbit and/or IR800 anti-mouse, rabbit or rat secondary antibodies (Li-Cor Biosciences) for 3 hours at room temperature and visualized using the infrared laser scanning (Odyssey, Li-Cor Biosciences).

Cell Lysis, Immunoprecipitation, and Immunoblotting

Cells were lysed in either RIPA lysis buffer (10mM NaPO4, pH 7.6, 150mMNaCl, 5mM EDTA, 0.1% sodium dodecyl sulphate, 0.25% deoxycholic acid, 1% triton X-100, plus protease (Roche #88666) and phosphatase inhibitors (Roche #88667) or Triton X-100 lysis buffer (50mMHepes, pH 7.9, 250mMNaCl, 0.1% Triton X-100, 10% glycerol, plus protease and phosphatase inhibitors). Ten μl of anti-FLAG M2 agarose conjugated beads (Sigma Aldrich) were added to lysates and

incubated overnight at 4°C. The beads were washed five times with lysis buffer, and proteins were eluted with 200 μl of sodium dodecyl sulfate sample buffer and heated to 99°C for 5 min. Portions of the lysates prior to immunoprecipitation were also reserved and boiled with sodium dodecyl sulfate-containing sample buffer. Lysates and immunoprecipitations were fractionated by SDS-PAGE, transferred to a PVDF membrane, blocked in Odyssey blocking buffer (Mandel, LIC-927-40100), and probed with the appropriate antibody overnight at room temperature. Primary antibodies were decorated with IR700 anti-mouse or rabbit and/or IR800 anti-mouse, rabbit or rat secondary antibodies (Li-Cor Biosciences) for 3 hours at room temperature and visualized using the infrared laser scanning (Odyssey, Li-Cor Biosciences).

Chapter 4: CDCA7, 14-3-3 Association and the Cell Cycle

Introduction

The most important requisite which separates the living world from the inanimate is the ability to self-replicate and faithfully pass on proprietary genetic information from one generation to the next. This process as a whole is known as the cell cycle, and although it is cyclical, the endgame of the process is one of four outcomes: quiescence, senescence, apoptosis or mitosis. In order for a cell to enter a round of the cell cycle, it must cross a threshold between G1 and S phase known as the restriction point. It is the transition through this point which commits a cell to a round of DNA duplication. Control of the decision to transition from one phase to another is of great interest to molecular biologists, as it has been shown to be dysregulated in many cancers and serves as potential point for medical intervention. The importance of this critical juncture in the cell cycle is obvious as perhaps the three most studied proteins, Myc, the retinoblastoma protein pRB and p53, converge to control the restriction point (Santoni-Rugiu et l., 2000). Therefore, an intimate understanding of cell cycle and its components can be invaluable when studying cell cycle progression, proliferation and aberrations which can lead to disease.

In previously published work we have identified cell division cycle associated protein 7 (CDCA7) as physically interacting with the transcription factor Myc (Gill et al., 2013). We have mapped the domains of CDCA7-Myc interaction and have discovered that Akt phosphorylates CDCA7 near this contact region, leading to loss of its association with Myc, binding to 14-3-3 proteins and exclusion from the nucleus. Co-expression of CDCA7 with Myc sensitized cells to serum-withdrawal induced apoptosis and this pro-apoptotic activity required the Myc-binding region. Short hairpin RNAi-mediated knockdown of CDCA7 rescued cells from MYC-dependent apoptosis following removal from serum. Although this data implicates cooperation between Myc,

CDCA7 and Akt as affecting apoptosis, it does not address the possibility of a concurrent affect on the cell cycle. It is important to note that CDCA7's (cell division cycle associated protein 7) name sake is derived from its periodic expression during the G1/S phase transition of the cell cycle (Osthus et al., 2005). Therefore, we have sought to investigate any possible affects CDCA7 may have on the cell cycle, and how if any influence Myc and Akt may have on that outcome. What follows is a review of the most pertinent information regarding the cell cycle, its progression, inhibition and how it may be altered in disease.

Cyclin-dependent kinases

The very term 'cell cycle' suggests the reoccurrence of a series of events in an orderly fashion, the control of which is commissioned to a set of serine/threonine kinases known as cyclin-dependent kinases (Cdks) (Morgan, 1995). Cdks were discovered in the early 1970's by Lee Hartwell, a milestone in molecular biology which would eventually earn him the Nobel Prize. Using early methods of genetic screening, Hartwell was able to isolate a family of genes which, when mutated, halted the cell cycle of the common baker's yeast when cultured at elevated temperatures (Hartwell et al., 1970). He termed these genes *cell division cycle,* or CDC genes, which were quickly shown to be conserved amongst eukaryotes and the driving force behind what is known as the cell cycle engine. CDC genes code for kinases known as cyclin-dependent kinase, of which there are five that are active during the cell cycle; during G1 (CDK4, CDK6 and CDK2), S (CDK 2), G2 and M (CDK1) and CDK7 during the entire cycle (Morgan, 1995). The activity of these kinases hinges on the availability of cyclins, which activate Cdks when the proteins form a heterodimeric complex (Hunt, 1991). Although Cdk levels do not fluctuate during the cell cycle, it is the periodic rise and fall in cyclin protein levels which are responsible for the cycle's division of phases. Phosphorylation of Cdks subunits can either positively or negatively modulate the activity of these

kinases (Arellano and Moreno, 1997). The exact set of Cdk targets has not been completely catalogued as the phosphorylation cascades initiated by these kinases bifurcate at many points. The most well-known Cdk target is the mammalian retinoblastoma susceptibility protein, pRB, which works to regulate progression from G1 to S and has been shown to be the central node of the restriction point. When in its underphosphorylated state, pRB exerts its function by binding the transcription factor E2F, preventing the transactivation of genes that are critical for S phase (see below) (Zhou and Elledge, 2000). Progression through the restriction point is highly dependent on cell type, environment and context; largely owing to the spectrum of requirement for homeostatic tissue renewal. Although entry into S phase may be initiated differently between cell types, one criteria must always be realized and that is the activation of Cdks (Massague, 2004).

Cyclins

Cyclins exert their influence on Cdks by forcing them into an active conformation upon binding, effectively establishing a binary system in which the Cdk is the inactive catalytic subunit that relies on the activating subunit that are cyclins. The periodic fluctuation of cyclin protein levels via programmed synthesis and degradation guarantees a finite window for Cdk activation. The irreversibility of ubiquitin mediated proteolysis of cyclins guarantees the one-way direction of the cell cycle. To date, sixteen mammalian cyclins have been discovered, A, B1, C, D1-3, E, F, G1 and 2, H, I, K, T1 and T2. Cyclin D activates Cdks 4/6 in early G1 while cyclin E activates Cdk 2 in mid G1. During mid S phase, cyclin A associates with Cdk2 but also activates Cdk1 in G2. Finally, cyclin B associates with Cdk1 while the cycle transitions to M phase (Johnson and Walker, 1999). Although the cell cycle is in theory a continuously revolving door, an opportunity for the cycle to initiate must exist. This is made possible by the fact that unlike other cyclins, cyclin D levels do not fluctuate during the cycle, but are constantly synthesized so long as growth factors

are present. This disconnect from the rhythm of the cell cycle allows cells to integrate information and growth cues from its environment. As growth factors activate receptor tyrosine kinases, the Ras/Raf/Mek/Erk cascade is initiated and results in the activation of downstream transcription factors such as c-Jun and c-Myc, which transactivate the cyclin D gene and thus provides a link between extracellular inputs and the initiation of the cell cycle (Kerkhoff and Rapp, 1998; Johnson et al., 1996). Cyclin D is responsible for activating Cdks 4 and 6 which promote the transition through the restriction point via the molecular switch that is the pRB node (in addition to Cyclin E/Cdk 2 hyperphosphorylation of pRb), committing the cell to a round of the cell cycle.

Cyclin-dependent kinase inhibitors

The forward progression of the cell cycle can be attributed to the cooperative nature of Cdks and cyclins, however in the event that the cell requires a halt in the cycle it turns to cyclin-dependent kinase inhibitors (CKIs) to complete this task. CKIs can be recruited in a number of situations such as in the event of DNA damage or when required to enter a state of post-mitotic terminal differentiation. Their exact mode of influence has been difficult to interpret because the inventory of CKIs remains constant between cells, however they are differentially regulated depending on the stimuli or cell type (Ekholm and Reed, 2000). CKIs are categorized into one of two families depending on their structure and affinity: the INK4 family consists of p15, p16, p18 and p19, and the Cip/Kip family is composed of p21, p27 and p57 (Carneo and Hannon, 1998).

INK4 CKIs are specific in their affinity, as they only inactivate G1 Cdks 4 and 6 by binding them *before* they complex with cyclin D, thus preventing activation of the kinase. INK4 binding of Cdks 4 and 6 occurs via a concave cleft in the CKI which is composed of ankryin repeats. This forces the Cdks into an inactive conformation, further inhibiting their catalytic function and a promotes arrest of the cycle in G1 (Russo et al., 1998, Brotherton et al., 1998). The best example of a INK4

inhibitor's effect on the cell cycle is the induction of p15 by the antiproliferative factor TGFβ, thereby preventing progression through G1 via inhibition of Cdks 4 and 6 (Massague and Wotton, 2000).

Cip/Kip inhibitors are considered to be broad spectrum CKIs as they inhibit both cyclin-Cdk 1 and cyclin-Cdk2. The ability to inhibit both cyclin-Cdk complexes establishes a unique mode of regulation known as *CKI exchange* (discussed below), that allows CKIs to be sequestered away from targets when cell cycle progression is required. Inhibition by Cip/Kip proteins is achieved by binding *both* units of the cyclin-Cdk heterodimeric complex and invasion of the kinases substrate binding pocket (Russo et al., 1996). p21 is arguably the most studied of the Cip/Kip family as it is integral to the DNA damage response mediated by p53 at the G1/S checkpoint. Upon DNA damage, the transcription factor p53 becomes stabilised and induces the expression of p21 and thus promotes G1 arrest by binding cyclin E-Cdk2, which is one of the critical kinases that promotes progression through the restriction point by phosphorylating pRB.

The pRB-E2F pathway

The induction of cyclin D by c-Jun and c-Myc via the Ras/Raf/Mek/Erk cascade is the first step in entering the cell cycle. Accumulation of cyclin D in G1 encourages the activation of Cdks 4 and 6, of which the primary target is the retinoblastoma susceptibility protein pRB. pRB plays a critical role in the progression of the cell cycle through G1 by being the central node in the molecular switch that is the restriction point. pRB is known to bind numerous proteins when in its active and underphosphorylated state, most notably the transcription factor E2F which is rendered ineffective by virtue of being in complex with pRB. E2F transcription factors are responsible for regulating the expression of key proteins that are essential for the progression of the cell cycle, most notably cyclin E. Upon phosphorylation and inactivation of pRB by cyclin D-Cdk 4/6, E2F dissociates

from pRB and is allowed to transactivate the cyclin E gene. Build up in cyclin E levels promotes association with and activation of Cdk2, whose primary substrate is also pRB (Johnson and Walker, 1999). By further phosphorylating pRB, cyclin E-Cdk2 works to maintain pRB in a hyperphosphorylated and inactive state, thereby establishing a positive feedback loop that allows E2F to transactivate other important genes for DNA replication; such as those coding for cyclin A or DNA polymerase. Cyclin E-Cdk 2 also phosphorylates histone H1, an important event in the rearrangement of chromatin during genome replication (Stevaux and Dyson, 2002). However, to suggest that progression through the restriction point is as simple as phosphorylating pRB would be overlooking the importance of c-Myc in the transition from G1 to S phase.

Myc and G1/S transition

The induction of the transcription factor c-Myc occurs rapidly in early G1 upon mitogen stimulation, with proteins levels reaching their peak in G1 but dropping to lower steady-state concentrations in proliferating cells (Campisi et al., 1984). Although Myc has been convincingly linked to promoting proliferation, the exact set of gene targets that link Myc to mitogen stimulation and the cell cycle apparatus is still being investigated. Despite this, it is now known that Myc promotes the transition through the restriction point by both indirect and direct means. As eluded to above, Myc induces the transcription of cyclin D through the Ras/Raf/Mek/Erk cascade, promoting progression in three ways: a) by activating Cdks 4 and 6, resulting in cyclin E induction, b) sequestration of the Cip/Kip inhibitors p21 and p27 by cyclin D-Cdk 4/6 away from cyclin E-Cdk 2, promoting the activation of Cdk2 and c) Myc transactivates the phosphatase cdc25, which relieves the inhibitory phosphorylation of Cdk2 on Thr 14/Tyr 15 (Bartek and Lukas, 2001). The former is made possible by the fact that Cip/Kip inhibitors can bind to pre-existing cyclin-Cdk complexes and have dual specificities for cyclin D-Cdk 4/6 and cyclin E-Cdk 2, unlike their INK4

counterparts. This mechanism is known as CKI exchange and is important in regulating the G1/S transition. The process relies on the accumulation of cyclin D-Cdk 4 which recruits Cip/Kip inhibitors (p27 for example) away from cyclin E-Cdk2, allowing for the activation of the liberated cyclin E-Cdk2 kinase. The freeing of cyclin E-Cdk 2 from Cip/Kip inhibition and relief of inhibitory phosphates on Cdk 2 by cdc25, allows for the ubiquitination and proteasome-mediated degradation of p27. This complex series of events commits the cell to enter S phase, which eventually results in the resetting of the molecular switch via the induction of INK4 inhibitors p16 and p15 (Ekholm and Reed, 2000).

The cell cycle and cancer

With increasing levels of cell cycle regulations comes many opportunities for dysregulation promoting unrestrained cell growth. Normal cells are receptive to their environmental cues and are able to integrate them such that internal checks and balances ensure the timely and accurate progression of the cell cycle. Cells that have stepped outside of these controls are able to bypass the G1 restriction point and proliferate in the absence of external growth cues. Over expression of the oncogene cyclin D promotes pRB phosphorylation and G1/S progression, while deletion or mutation of tumor suppressors such p53, pRB or CKIs results in unchecked cell growth resulting in an elevated risk of tumor formation.

There have been numerous examples of altered Cdk expression in cancer. For example, overexpression of Cdk4 by amplification has been identified in melanoma, sarcoma and glioma (Wolfel et al., 1995), while overexpressed Cdks 1 and 2 have been identified in a subset of colon adenomas (Yamamoto et al., 1998). Point mutations have also been reported to result in selective growth advantage in cells carrying the R24C mutation within CDK4, due to the mutant protein's inability to bind the INK4 inhibitor p16. This results in constitutive activation of CDK4 in certain

lung cancers, lymphomas and familial melanoma (Peyressatre et al., 2015).

Cyclin D seems to be the most frequently altered cyclin in human cancers, not surprisingly since cyclin D allows cells to integrate environmental cues in order to initiate the cell cycle. Translocation of the cyclin D gene next to the immunoglobulin heavy chain locus enhancer region causes cyclin D1 overexpression in centrocytic B-lymphocytes and is often a sign of poor prognosis (Weisenburger et al., 1987). Overexpression, amplification or both of Cyclin E has been identified in acute lymphoblastic and myeloid leukemias as well as in some cases of breast and colon cancer (Vermeulen et al., 2003).

Inhibitors of the cell cycle are also found to be dysregulated in cancer. CKIs are commissioned to restrain cell growth by preventing the phosphorylation of pRB, therefore they are considered to function as tumor suppressors. Due to the specificity of p16 for cyclin D, any alterations in function would have a severe impact on the restriction point's ability to modulate the cell cycle. p16 has indeed been found to be altered in cancers, by means of point mutations, deletions or silencing by hypermethylation (Kamb, 1998). Deletions are the most common alterations affecting p16 levels and are found in 20-30% of acute lymphoblastic leukemias, 40-60% of nasopharyngeal, biliary tract and pancreatic tumors as well as in 50% of gliomas and mesotheliomas (Hall and Peters, 1996).

Loss of gene expression may be a result of events other than gene deletion. In colorectal carcinomas, p27 loss has been attributed to an increased rate of proteasome dependent degradation (Pagano, 1997), while p21 expression is affected due to its transcriptional regulation by p53. Considering the fact that p53 is the most frequently mutated gene in human cancer, it is of no surprise that the p21 mediated DNA damage checkpoint is sidestepped when p53 is inactivated (Deng et al., 1995).

Although the components of the cell cycle machinery are often dysregulated in cancer, their substrates can also fall victim to molecular pathology. The restriction point governing the transition from G1 to S phase converges on pRB, the most important substrate of cyclin D-Cdk4/6. When pRB function is altered, cell cycle progression proceeds unchecked and results in uncontrolled cell growth. pRB is commonly mutated in lung cancer and retinoblastoma, the cancer from which it derives its name (Hall and Peters, 1996). Alterations in pRB can be a result of deletions or mis-sense mutations that cause absence of pRB, truncation or a non-functional protein. Inactivation of pRB can also result from binding of tumor virus proteins such as human papillomavirus E7, adenovirus E1A and simian virus 40 (Vermeulen et al., 2003).

The above examples demonstrate that studying cancer requires an intimate knowledge of the cell cycle and its regulators. It is estimated that approximately 90% of human cancers acquire alterations in at least one component of the pRB molecular switch, so it is of no surprise that current efforts in drug development seek to target components of the cell cycle machinery. New insights into cancer pathophysiology have shifted the focus of drug development from brutish attempts to kill tumor cells towards more sophisticated methods that target the cell cycle machinery. These approaches include induction of checkpoint mechanisms in hopes of encouraging cytostasis or apoptosis, or inducing arrest of cancerous cells in phases of the cell cycle that render them susceptible to other treatments.

The most attractive approach to date is the targeting of Cdks by either indirect or direct means. Cdk activity can be indirectly inhibited by focusing on Cdk regulators by either overexpressing CKIs, administrating synthetic peptides that mimic CKIs, decreasing cyclin levels, targeted degradation of Cdks and manipulating the phosphorylation states of Cdks and their regulators. However, the most successful strategy to date has been the direct targeting of Cdks by inhibiting

their kinase activity. These methods focus on the disruption of ATP binding sites rather than the inhibition of protein-protein interactions between Cdks and their activating cyclin cohorts (Senderowicz and Sausville, 2000; Mcdonald and el Deiry, 2000).

Flavopiridol is a first-generation pan-Cdk inhibitors which shows specificity for Cdk1, 2 and 4. The compound is a synthetic analogue of an alkaloid found in *Dysoxylumbinectariferum,* a plant native to India, and was discovered as a powerful growth inhibitor of lung and breast cancer cell lines. Flavopiridol has gone through numerous phase II and III clinical trials, but unfortunately has yet to live up to the early expectations placed in Cdk inhibitors (Byrd et al., 2007). Despite setbacks, second generation Cdk inhibitors are currently in either advanced pre-clinical testing or clinical trials. Three particular classes of Cdk inhibitors are showing promise, as they are more potent and/or drug-like then their predecessors: a) broad spectrum Cdk inhibitors targeting Cdks 1, 2, 4, 6, 7 and 9. b) inhibitors specific for cdk4/6 or cdk2 and c) inhibitors specific for Cdks in addition to off target kinases that may synergistically enhance anti-tumor activity (Malumbres et al, 2007). Most recently, Palbociclib became the first Cdk 4/6 specific inhibitor to be approved for cancer treatment (Rocca et al., 2017). Our understanding of the genetic nature of cancer and the cell cycle and the ability to genotype the tumours of patients will enhance our ability to develop drugs and insure the most effective treatment. For example, foreknowledge of the status of p53 or pRB would aid in the selection of therapies which take advantage of the cells ability to arrest the cell cycle.

The concept of the cell cycle has long fascinated biologists, and though the end product is blatantly obvious, the means by which one cell becomes two has only until recently, remained a mystery. Described here is only a distilled outline of the most important aspects of the pRB molecular switch and the DNA damage checkpoint that converges at the restriction point. Our growing

understanding of the mechanisms which regulate the cell cycle have expanded our insights into its dysregulation and the tenacious beast that is cancer. The restriction point between the G1/S transition and the mechanisms that control it have proven to be a crucial node in both tumorigenesis and cancer therapy. Although the basics behind the cell cycle have been solved, advances in high-throughput technologies and computing capabilities promise to broaden our knowledge to new levels. An expanding repertoire of cell cycle signalling networks means greater opportunities to intervene in tumorigenesis by rational drug design.

The following data reveals the implications of CDCA7 on cell cycle distribution and proliferation rates. We have investigated the links between these phenotypic profiles with the expression of key components of the cell cycle via qPCR, ChIP and promoter assays. We have shown that expression of CDCA7 in Rat1 and HEK293 cells results in the increase of the proportion of cells in the G2/M phase of the cell cycle (Figure 4.3-4.5). In addition, we have shown that Rat1 cells expressing various versions of CDCA7 results in different proliferation rates (Figure 4.6). Preliminary data suggests that CDCA7's effect on cell cycle distribution and growth rates may be attributed to alterations in expression of Cyclin D1, Cyclin B1, BAX and other known Myc targets (Figure 4.7 and 4.8). Finally, in light of CDCA7's physical interaction with Myc and cooperation in activating a Myc reporter (Figure 4.1 and 4.2), we hypothesize that CDCA7 directly cooperates with Myc in altering the expression of key Myc-dependent cell cycle components in a manner that is controlled by Akt. This may occur either directly by influencing Myc promoter occupancy or by competing for Myc binding with other known Myc binding partners.

Results

CDCA7 cooperates with Myc to activate a Myc E-Box reporter

We have identified CDCA7 as being a Myc binding partner (Gill et al., 2013). To answer whether CDCA7 alters Myc's ability to transactivate an E-box promoter, we transfected a Myc-luciferase reporter containing a canonical E-box (CACGTG) into HEK293 cells that stably expressed doxycycline-inducible CDCA7. Myc reporter activation was positively correlated with increasing amounts of doxycycline and CDCA7 expression. Activation was highest in cells expressing the KK variant of CDCA7, which does not bind the 14-3-3 adaptor protein and is localized in the nucleus. Conversely, the DE variant of CDCA7 that forces binding to 14-3-3 and sequestration in the cytoplasm away from Myc, resulted in the poorest activation of the Myc reporter (Figure 4.1A). To determine if this activity was dependent on CDCA7's ability to bind Myc, we infected Rat1 cells that were stably expressing Myc with a retrovirus containing an empty vector, CDCA7 or the non-Myc binding Δ(156-187)CDCA7. Western blots confirming this expression can be seen in figure 4.1B. Measurement of luciferase activity suggests that activation of the reporter was dependent on Myc's ability to bind CDCA7, as the non-Myc binding Δ(156-187) CDCA7 resulted in less activation then even native Rat1 cells (Figure 4.1C).

CDCA7 expression increases Myc occupancy at the BAX promoter

Next, we asked whether CDCA7 and Myc co-associate on chromatin to alter Myc-dependent gene expression. We have previously shown that expression of T163A CDCA7 results in significant increases in Myc-dependent apoptosis (Gill et al., 2013) and we have data indicating that CDCA7 expression causes an increase in BAX mRNA (Figure 4.9), which is a pro-apoptotic Myc target gene (Dang, 1999; Robson et al., 2011). Thus, we preformed chromatin immunoprecipitations from Rat1 clones stably expressing wildtype CDCA7 or T163A CDCA7. This showed that during

serum-starvation conditions, a condition which sensitizes CDCA7 expressing cells to apoptosis, CDCA7 expression elevates both Myc and RNAPII occupancy at the BAX promoter (Figure 4.2). These results were further enhanced when expressing T163A CDCA7, which is localized almost exclusively to the nucleus and undergoes greater amounts of Myc-dependent apoptosis. This data is the first to demonstrate that CDCA7 can associate with chromatin, and supports the hypothesis that CDCA7 modulates Myc-dependent gene expression.

CDCA7 expression alters cell cycle progression

Propidium iodide is a fluorescent molecule which can intercalate with DNA in a stoichiometric fashion and therefore alert users to DNA content as cells progress through the cell cycle. This principle is the basis for fluorescence based flow cytometry. The use of both propidium iodide and antibodies conjugated to fluorescent molecules is a powerful method that allows users to track protein content or post translational modifications (such as phosphorylation) as cells progress through the cell cycle. We have used flow cytometry to analyze the cell cycle distribution of Rat1 or Rat1-Myc cells expressing WT CDCA7 or Δ(156-187) CDCA7. Our results indicate that cells expressing CDCA7 in 10% serum conditions show larger population of cells occupying the G2/M phase of the cell cycle. This ratio is marginally increased with coexpression of ectopic Myc. Expression of the non-Myc binding Δ(156-187) CDCA7 abrogates this shift towards G2/M phase (Figure 4.3A). Expression of T163A CDCA7 in 0% serum also resulted in fewer cells within G2/M compared to WT CDCA7 (Figure 4.3B).

To further investigate the affects of CDCA7 on cell cycle progression, we synchronized HEK293 cells transiently expressing CDCA7 in G2/M phase with 100 ng/ml Nocodazole (a microtubule inhibitor) for 18 hours. These cells were then allowed to re-enter the cell cycle and were collected at various time points for cell cycle analysis via flow cytometry. Figure 4.4 shows that Nocodazole

did in fact synchronize a large portion of cells in G2/M (untransfected and transfected cells), however analysis of FLAG positive gated-cells indicates that expression of FLAG-CDCA7 prevents those cells from entering G2/M and may in fact result in a noticeable population of apoptotic cells (sub-G1 cells). What remains unknown is the status of T163 phosphorylation during progression through the cell cycle. To shed light on this we repeated cell synchronization in the same fashion, followed by staining with propidium iodide and α-pT163 CDCA7 prior to flow cytometry. Figure 4.5A indicates that T163 appears to be phosphorylated in those cells which are synchronized in G2/M. Upon release and progression through the cell cycle, phosphorylation of T163 becomes almost undetectable as the majority of cells progress back into G1 phase. This result was replicated at the protein level when lysates from the same cells used for flow cytometry were lysed and subjected to western blot analysis (Figure 4.5B). Finally, this result is reinforced when both negative and positive phospho-T163 cells are depicted on the same histogram (gathered via flow cytometry). In figure 4.5C cells negative for T163 phosphorylation are indicated by the left gate, while positive cells are bound by the right gate. Upon synchronization in G2/M with Nocodazole, there are two distinct populations of cells representing phospho-T163 negative and positive cells. However, upon 2 hour release into the cell cycle, the positive phospho-T163 signal is no longer detectable. Although the sensitivity of flow cytometry and infrared-based western blotting can differ (depending on the set of antibodies being employed), the results in both cases suggest that phosphorylation of T163 is occurring primarily during G2/M and drops considerably as cells cycle out of G2/M and into G1.

CDCA7 phosphorylation at T163 occurs in the nucleus

With the knowledge that T163 is phosphorylated during to G2/M phase, we sought to identify the subcellular localization of phospho-T163 CDCA7 upon G2/M synchronization. In our experience,

cell synchronization with nocodazole often resulted in cells which are far less adherent and amenable to microscopy. This could be attributed to the toxic nature of nocodazole, which can act as a pro-apoptotic agent during prolonged incubation. Therefore, we were forced to use RO-3306 as a substitute for nocodazole, with greater success in regard to cell adherence during fixing and mounting protocols. RO-3306 is a non-toxic reversible Cdk1 inhibitor with the ability to synchronize cells in G2/M in the μM range (Vassilev, 2006). Figure 4.6A shows that when HEK293 cells are synchronized in G2/M with RO-3306, there is a complete absence of T163 phosphorylation. However, 60 minutes after release from synchronization, T163 phosphorylation appears striking, and punctate within the nucleus. Next, we investigated the striking subcellular localization of pT163 CDCA7 and asked whether it correlated with similar, and typical localization of centrosomes during mitosis (Dahm et al., 2007). We repeated synchronization of HEK293 and HeLa cells with RO-3306 and visualized phospho-T163 CDCA7, endogenous CDCA7, the centrosomal marker protein γ-Tubulin and the Akt activation marker phospho-S473 Akt. Figure 4.6B shows that 60 minutes post release from RO-3306 synchronization, phospho-T163 CDCA7 colocalizes with γ-Tubulin at the same punctate regions in HEK293 cells as seen in figure 4.6A. In HeLa cells released from RO-3306 synchronization, endogenous CDCA7 also colocalize with γ-Tubulin (Figure 4.6C top). In these same cells, phospho-T163 CDCA7 was seen to colocalize with activated Akt as indicated by the presence of phospho-S473 Akt (Figure 4.6B bottom), in the same punctate manner seen in previous results. Finally, these results were recapitulated in HEK293 cells transfected with FLAG-CDCA7 as well as NIH3T3 cells stably expressing FLAG-CDCA7 (Figure 4.7).

CDCA7 alters proliferation rates

To evaluate whether CDCA7's effect on the cell cycle translates into altered growth rates, we have measured proliferation rates using a colorimetric assay based on the reduction of XTT (2,3-bis-(2-methoxy-4-nitro-5-sulfophenyl)-2H-tetrazolium-5-carboxanilide) via the membrane-electron transport chain. Color intensity of the reaction product is directly proportional to the quantity of cells being assayed. Therefore, cell proliferation rates can be tracked as a function of color intensity as cells are assayed over multiple time points. We employed this assay to test the proliferation rates of Rat1 cells stably expressing CDCA7 (Figure 4.8A). The most intriguing observation from these results is the differential growth rates produced by the various iterations of CDCA7, suggesting that CDCA7 may play a direct role in cell proliferation. More specifically, the gradient in growth rates may be a result of CDCA7's ability to bind 14-3-3, as we have shown that DE CDCA7 constitutively binds 14-3-3 while T163A and KK CDCA7 cannot bind 14-3-3. When cells were maintained in media supplemented with 2 % FBS for 6 days, only Rat1 cells expressing DE CDCA7 (constitutively bound to 14-3-3) showed a growth advantage over Rat1 control cells (Figure 4.8B). Conversely, WT CDCA7 and KK CDCA7 (cannot bind 14-3-3) exhibited the slowest growth rates. When cells were maintained in 5% FBS, cells expressing WT CDCA7 saw an improvement in growth rates over cells expressing KK and T163A CDCA7, indicating that perhaps only WT CDCA7 has an ability to affect growth rates in response to serum concentrations.

CDCA7 alters the expression of Myc target genes involved in the cell cycle

We have accumulated data which suggests that expression of CDCA7 affects Myc-dependent apoptosis, cell cycle distribution and proliferation, and therefore decided to probe the expression profiles of Myc target genes that are involved in these processes (Dang, 1999; Robson et al., 2011). After an initial screen of a large subset of genes via qPCR (data not shown), we identified INS,

BAX and CyclinB1 expression as being upregulated and INK4B as being suppressed in Rat1 cells stably expressing CDCA7 (Figure 4.9A). Induction of CDCA7 by doxycycline, resulted in similar upregulation of INS and suppression of INK4B expression (Figure 4.9B) while in cells stably expressing shRNA targeting CDCA7, the opposite trend was observed when compared to a scrambled shRNA control (Figure 4.9C). These results would indicate that the mRNA products of the INS and INK4B genes are positively and negatively (respectively) affected by CDCA7 expression. The INS gene encodes for the peptide hormone insulin which is crucial for the metabolism of carbohydrates, proteins and fats. Insulin exerts its function by initiating a signaling cascade which includes the activation of Akt (Lee et al., 2009), the same kinase which is responsible for phosphorylating CDCA7 at T163. The INK4B gene encodes a protein known as $p15^{INK4B}$ which is known to inhibit G1 progression by sequestering CDK4 or CDK6 away from cyclin D, thereby preventing CDK activation (Krimpenfort et al., 2007). It is possible that the compounded effects of increased INS expression and decreased INK4B expression are aiding in the transition of cells from G1 into G2/M as we see a larger population of cells in G2/M when expressing CDCA7.

Next, we probed the expression of cyclin D1 and B1. These genes were chosen because of their importance in the progression of the cell cycle. Cyclin D1 is responsible for allowing cells to transition through G1 phase by complexing with CDK4, phosphorylating the retinoblastoma protein (pRB) and thereby allowing the E2F transcription factor to transactivate genes required for transition into S phase (Matsushime et al., 1992). Cyclin B1 is known to be a positive regulator of mitosis as it complexes with CDK1 and encourages G2/M transition by phosphorylating and activating 13S condensin to promote chromosome condensation (Kimura et al., 1998). We asked if cells expressing CDCA7 show a shift in cell population towards G2/M, then how might these

genes be affected? We used qPCR with pools stably expressing CDCA7 that were synchronized by starvation for 18 hours and then stimulated with the addition of FBS. In the case of Cyclin D1 (Figure 4.10A), we observed a marginal increase in Cyclin D1 message in cells expressing WT CDCA7, while cells expressing T163A CDCA7 contained approximately 30% less Cyclin D1 mRNA compared to controls cells upon release from starvation conditions. qPCR for Cyclin B1 message resulted in a more pronounced affect upon release from starvation (Figure 4.10B). Expression of WT or T163A CDCA7 yielded approximately 40% and 50% (respectively) increases in Cyclin B1 mRNA. Whether CDCA7 is directly responsible for the changes in mRNA levels reported here is unknown, there is also the possibility that any affects might be indirect. For example, increased levels of cyclin B1 may simply be a product of the larger population of cells found in G2/M when CDCA7 is expressed (Figures 4.3-4.5). Finally, we decided to test CDCA7's ability to affect the activation of a Cyclin D1 promoter via luciferase assay (Figure 4.10C). In both cases where WT or T163A CDCA7 was stably expressed in Rat1 cells, activation of the Cyclin D1 reporter was approximately 50% lower when compared to control cells. The reduction of Cyclin D1 promoter activity seen in figure 4.10C may explain the reduction in mRNA levels seen in figure 4.9.

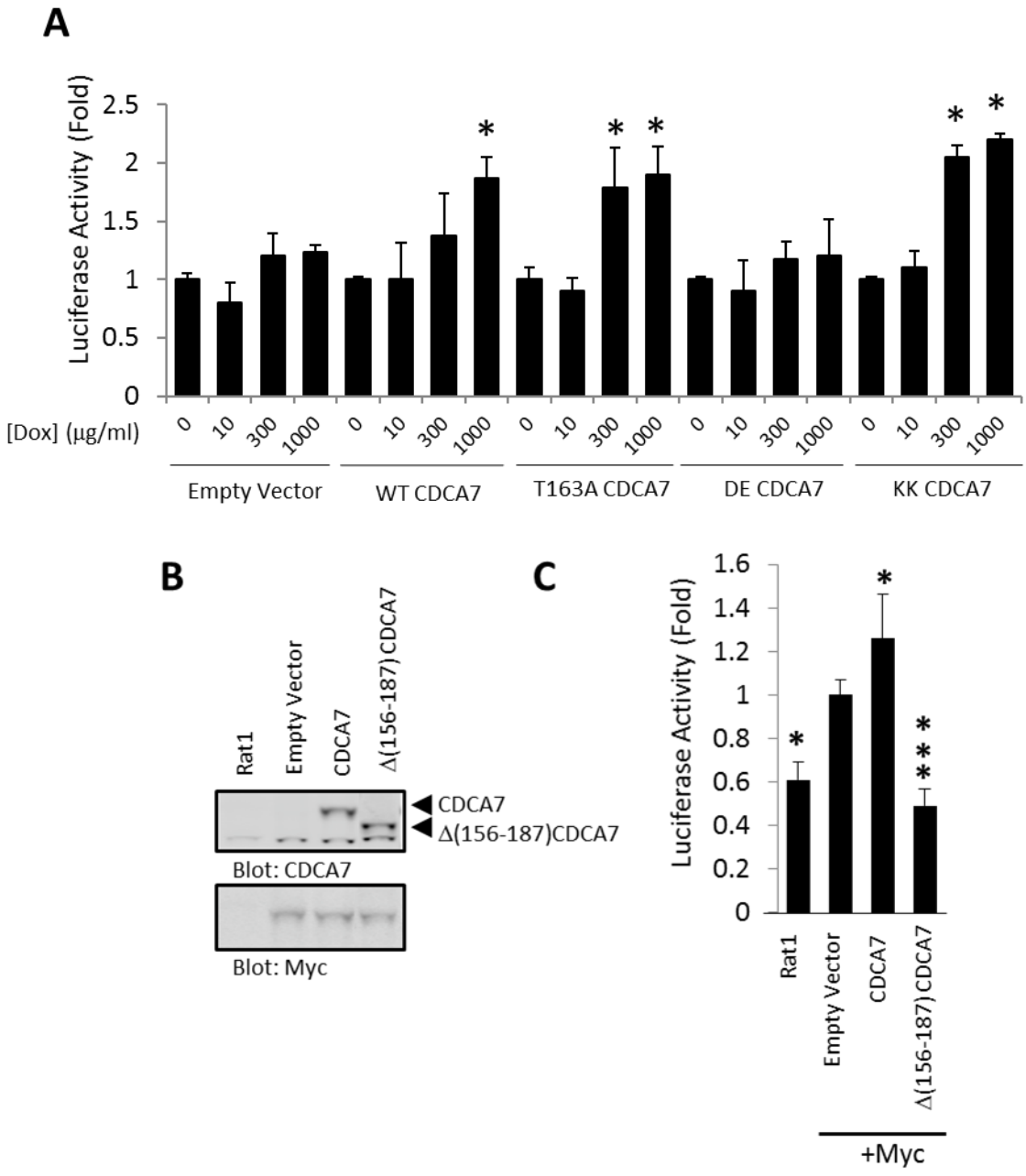

Figure 4.1. Myc activity is regulated by CDCA7. **A**. (n=3) HEK293 cells stably expressing doxycycline-inducible CDCA7 and the indicated mutations were transfected with a Myc-reporter plasmid and treated with doxycycline for 24 hours as indicated, and luciferase activity was determined after normalization with b-gal. P values were calculated using WT CDCA7 as the comparison population. **B**. Rat1 cells stably expressing Myc were infected with retrovirus containing empty vector, CDCA7 or Δ(156-187) CDCA7. **C**. (n=5) After selection for 6 days, a Myc-reporter plasmid was transfected and luciferase was measured after 24 hours. * = P<0.01 when compared to 0 µg/ml DOX for each transfection. Error bars represent standard deviation.

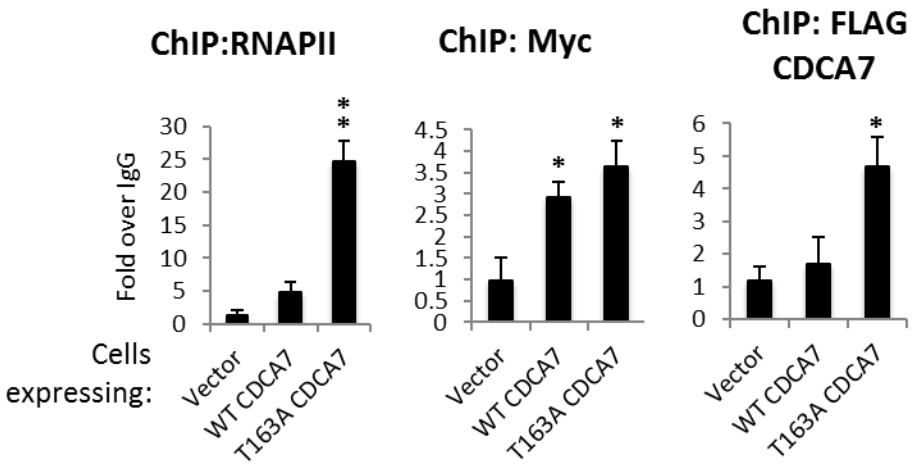

Figure 4.2. ChIP analysis of CDCA7 at the BAX promoter. A. Rat1-Myc cells stably expressing either empty vector, WT CDCA7 or T163A CDCA7 were cross-linked, lysed and chromatin sheared by sonication. Anti-RNAPII, anti-Myc or anti-FLAG-CDCA7 antibodies were used to precipitate protein-DNA complexes. Following reversal of cross-links, DNA was isolated using a commercial kit (Millipore) and quantified by qPCR. The amount of DNA precipitated was measured against DNA isolated by a non-specific IgG control. * = $P<0.05$, ** = $P\leq0.01$, N=3. Error bars represent standard deviation.

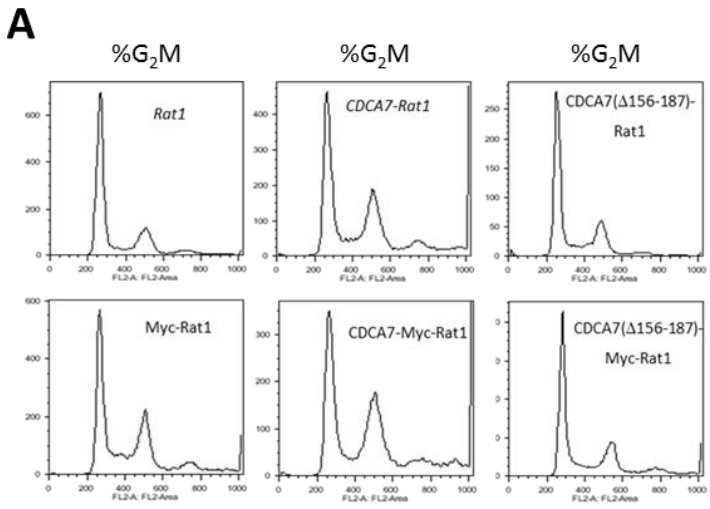

Cell Type	G2/M :G1 Fold over Rat1
Rat1 (n=5)	1.00
CDCA7-Rat1 (n=5)	2.36
CDCA7[Δ156-187)-Rat1 (n=5)	1.22
Myc-Rat1 (n=5)	1.44
CDCA7-Myc-Rat1 (n=3)	2.43
CDCA7[Δ156-187]-Myc-Rat1 (n=3)	1.12

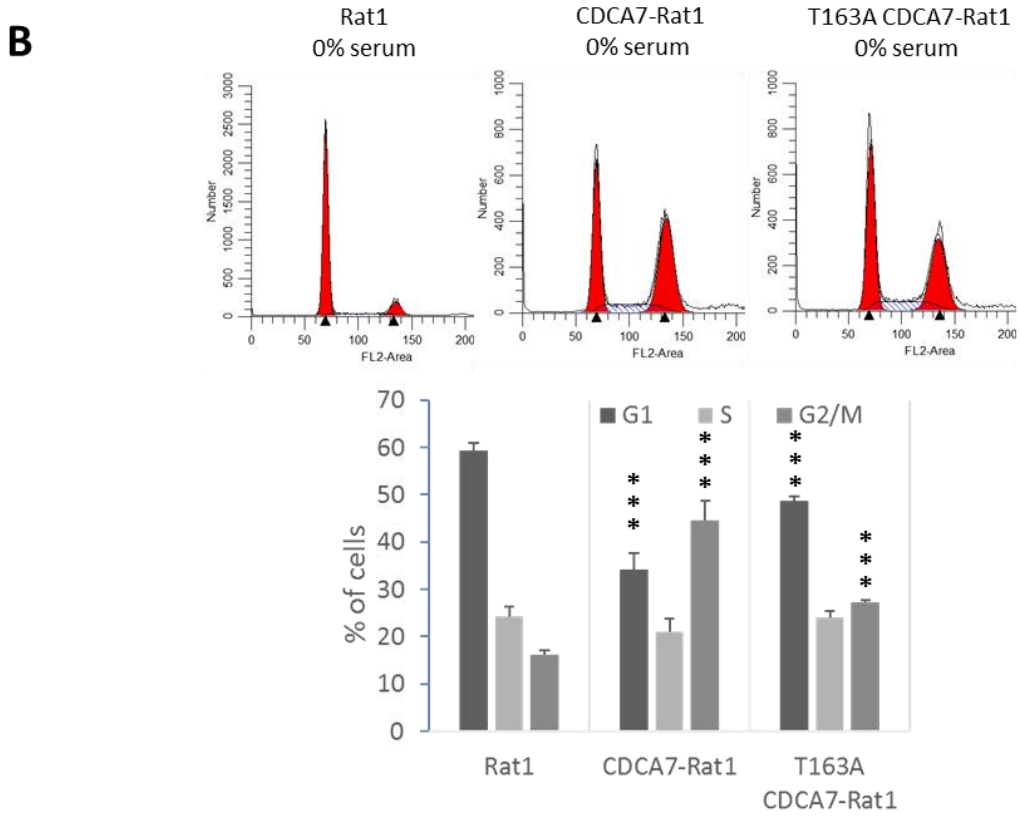

Figure 4.3. CDCA7 promotes G2/M transition. **A**. (left) Cell cycle distribution of Rat1 or Rat1-Myc cells stably expressing CDCA7 or Δ(156-187) CDCA7 maintained in media supplemented with 10% FBS. (right) G2/M:G1 Ratio summary for 3 – 5 independent experiments, normalized to the G2/M:G1 ratio of Rat1 cells. **B.** (top) Cell cycle distribution of Rat1 cells stably expressing CDCA7 and maintained in media containing 0% FBS for 18 hours. (bottom) Quantified cell cycle data over three experiments. Average cell population gated for G1, S and G2/M. * = $P<0.05$, ** = $P \leq 0.01$ and *** = $P \leq 0.001$. Error bars represent standard deviation.

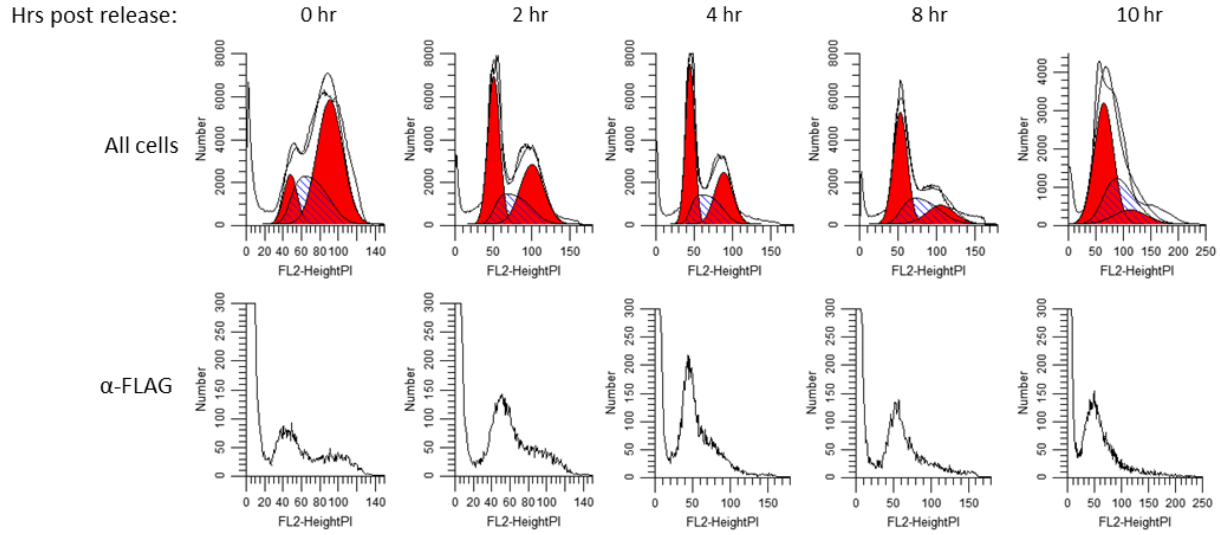

Figure 4.4. CDCA7 prevents cells from synchronizing in G2/M. HEK293 cells transiently expressing FLAG-CDCA7 were synchronized in G2/M with 100 ng/ml of Nocodazole for 18 hours and then released as indicated. Top row of histograms represents cell cycle profiles of all cells stained with propidium iodide, with red representing gating for G1 and G2/M cells by Modfit. Bottom row of histograms represents cell cycle profile of cells positively stained with α-FLAG antibody, as gated by Modfit.

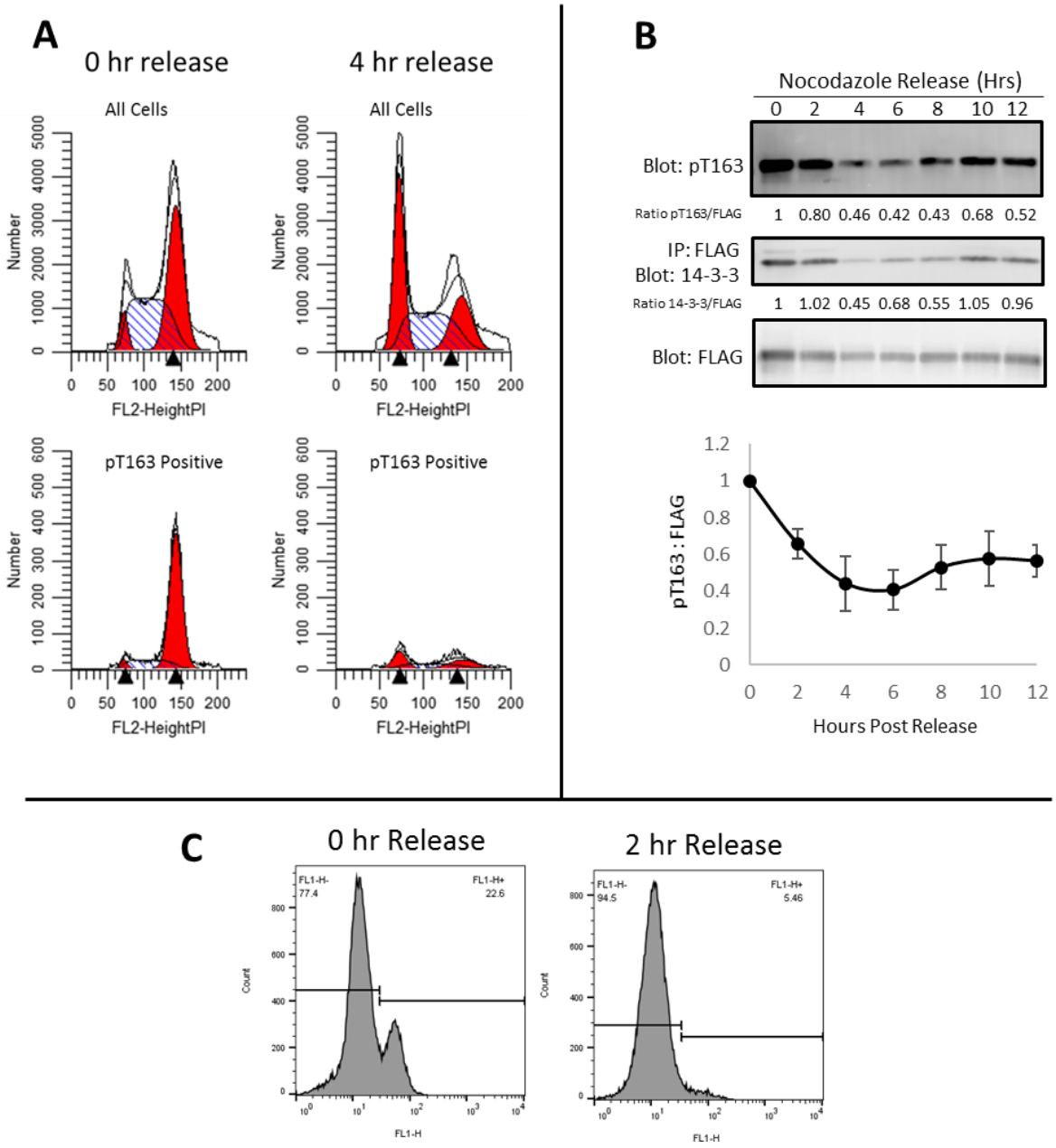

Figure 4.5. T163 CDCA7 is phosphorylated in G2/M. **A.** HEK293 cells transiently expressing FLAG-CDCA7 were synchronized in G2/M with 100 ng/ml of Nocodazole for 18 hours and then released as indicated. Top row of histograms represents cell cycle profiles of all cells stained with propidium iodide. Bottom row of histograms represents cell cycle profile of cells positively stained with α-pT163 CDCA7 antibody. **B.** Lysates and immunoprecipitations were generated from cells in A and subjected to western blotting. Membranes were probed with α-FLAG, α-14-3-3 and α-pT163 CDCA7 antibodies. This data was quantified via the Odyssey infrared scanner and is depicted below (averaged over 3 experiments). **C.** Total cell population distribution from A at 0 and 2 hours post release from Nocodazole synchronization. Left gate indicates phospho-T163 negative cells, right gate indicates phospho-T163 positive cells as per staining with α-pT163 CDCA7 antibody. Error bars represent standard deviation.

A

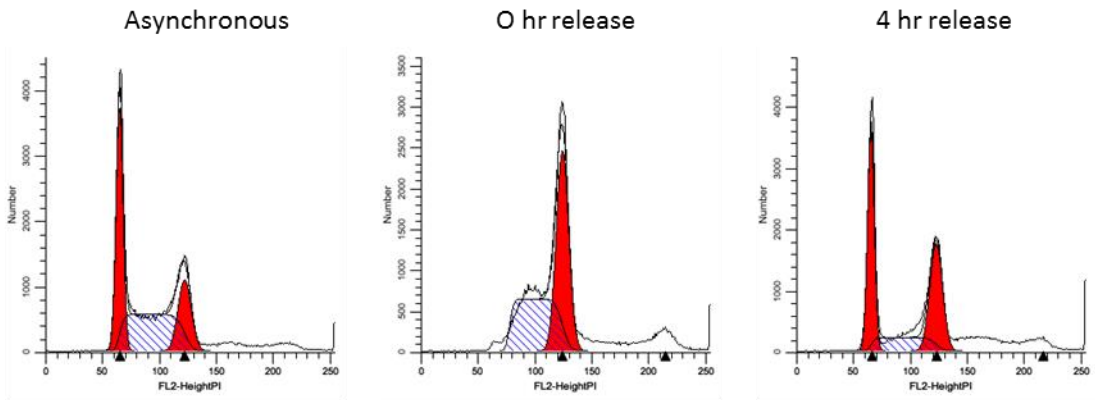
Asynchronous
O hr release
4 hr release
Number
FL2-HeightPI

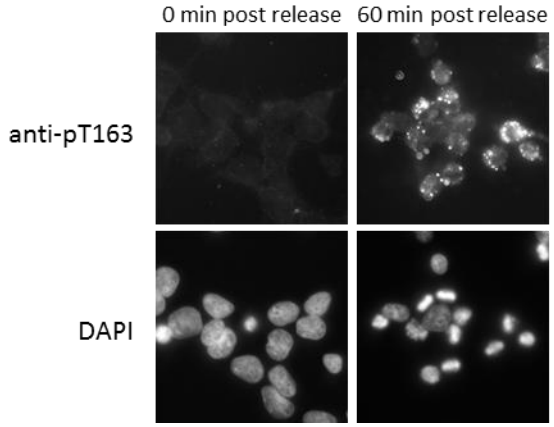
0 min post release
60 min post release
anti-pT163
DAPI

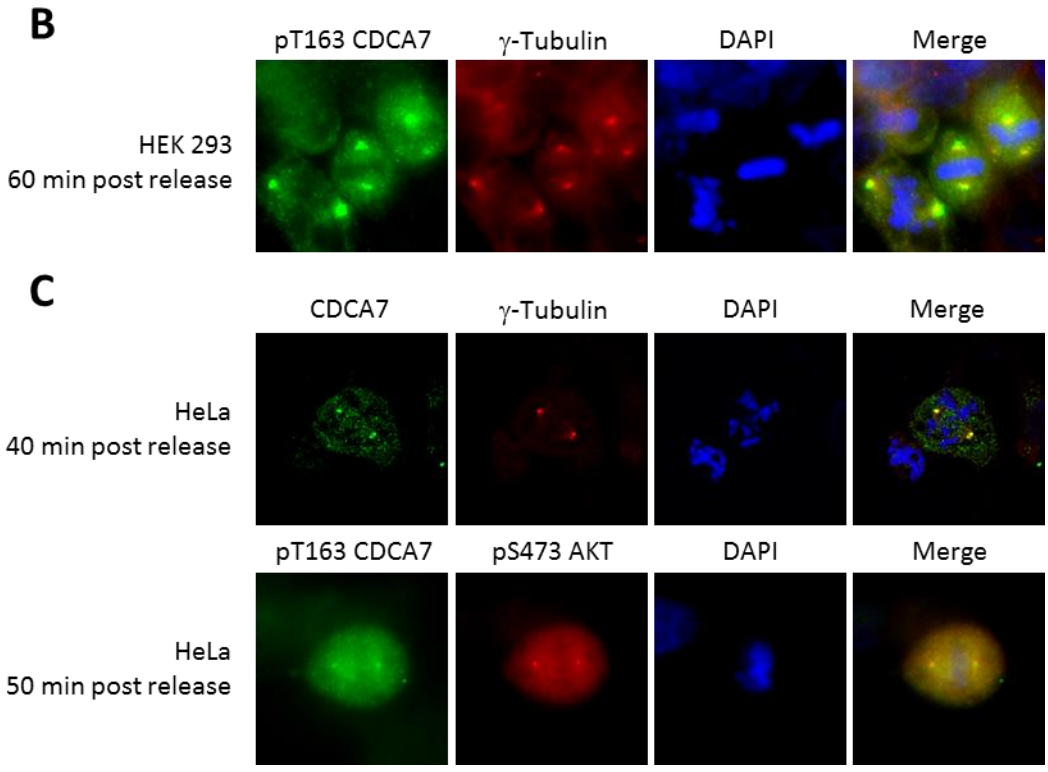

Figure 4.6 CDCA7 T163 phosphorylation is localized to centrosomes. HEK293 and HeLa cells were treated with 10 μM RO-3306 for a minimum of 18 hours in order to synchronize cells in G_2/M phase. Cells were washed three times with PBS and released in RO-3306 free media before being fixed and mounted for immunofluorescence microscopy or FLOW cytometry. **A.** HEK 293 cells synchronized with RO-3306 (top, cell cycle distribution) for 18 hours show no phosphorylation of endogenous T163 CDCA7 (bottom). Phosphorylation of T163 becomes evident at 60 minutes post release. **B.** pT163 CDCA7 is localized to centrosomes as indicated by the centrosomal marker protein γ-Tubulin (Dahm et al., 2007). **C.** Similar results were recapitulated in HeLa cells that were synchronized for 24 hours and released for 40 minutes (top) or synchronized for 20 hours and released for 50 minutes (bottom). Activated Akt (pS473) colocalizes with pT163 CDCA7.

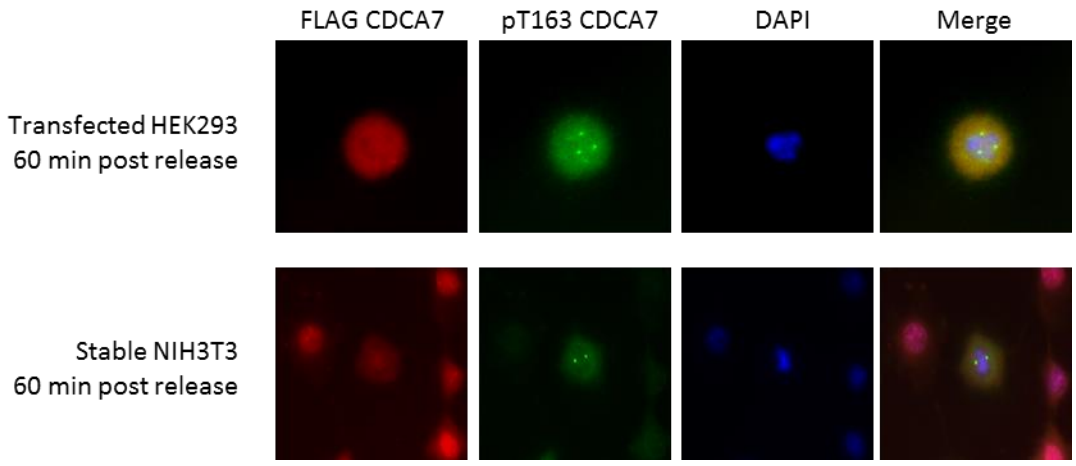

Figure 4.7 CDCA7 T163 phosphorylation in transfected cells is localized to specific areas of the nucleus. HEK293 and NIH3T3 cells were synchronized in G_2/M phase with 10 μM RO-3306 for 18 hours. Cells were washed three times with PBS and released in RO-3306 free media before being fixed and mounted for immunofluorescence microscopy. HEK293 cells were transiently transfected with FLAG-WT CDCA7. NIH3T3 cells are stably expressing FLAG-WT CDCA7. Although FLAG WT-CDCA7 is evenly distributed throughout the cell, pT163 appears punctate and localized to DNA, likely at centrosomes as in figure 4.6.

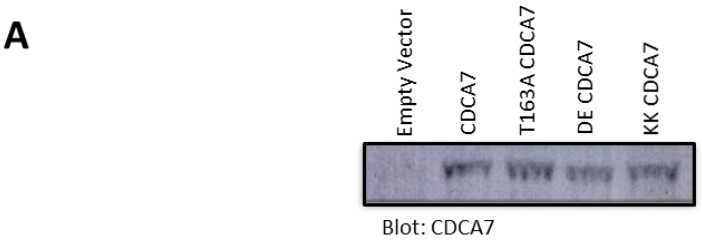

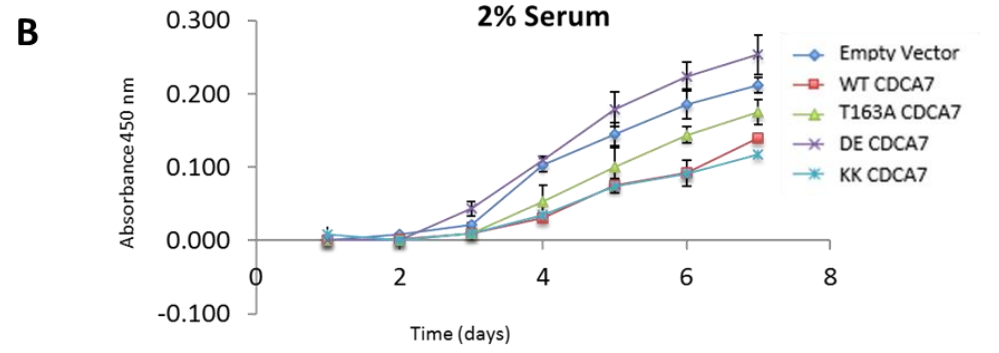

	Day 1	Day 2	Day 3	Day 4	Day 5	Day 6	Day 7
WT CDCA7	0.192567	0.165572	0.060834	0.004243	0.030000	0.021288	0.035452
T163A CDCA7	0.001328	0.067615	0.015193	0.011158	0.184473	0.061351	0.057281
DE CDCA7	0.002663	0.037905	0.037501	0.220638	0.011043	0.039475	0.211199
KK CDCA7	0.070251	0.006103	0.128974	0.010263	0.017433	0.014025	0.038377

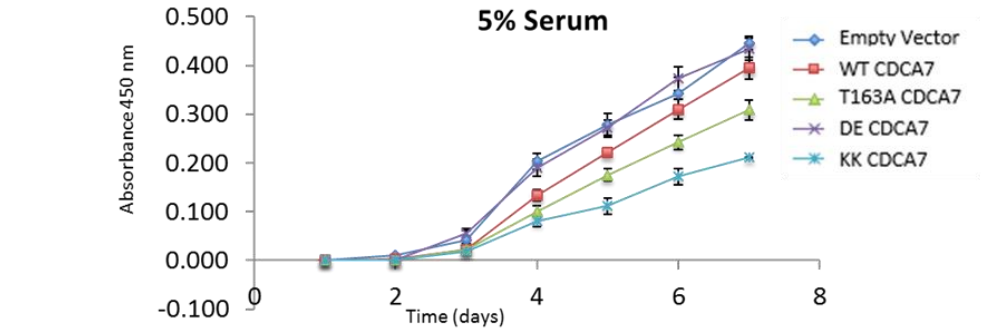

	Day 1	Day 2	Day 3	Day 4	Day 5	Day 6	Day 7
WT CDCA7	0.346619	0.027324	0.072083	0.021454	0.001718	0.120228	0.000323
T163A CDCA7	0.028429	0.000268	0.026775	0.011674	0.006282	0.003012	0.062914
DE CDCA7	0.218510	0.016106	0.260650	0.047461	0.379122	0.141214	0.076281
KK CDCA7	0.002194	0.005822	0.027026	0.003422	0.000241	0.003150	0.019682

Figure 4.8. Generation of Rat1 pools stably expressing CDCA7 and their XTT growth assays profiles. A. Rat1 cells were infected with retrovirus containing an antibiotic selection marker and cDNA of various forms of flag tagged CDCA7. After two weeks of selection, lysates were generated from antibiotic resistant pools and probed with anti-flag antibody to confirm expression of CDCA7. **B**. Cells from pools depicted in A. were plated in triplicate in 96-well plates at 2000 cells/well and were allowed to grow for 6 days in media containing 2% or 5% FBS. Samples were assayed each day at the same hour. P values for each time point are indicated below graphs, where $p<0.05$ is highlighted, N=3. Error bars represent standard deviation.

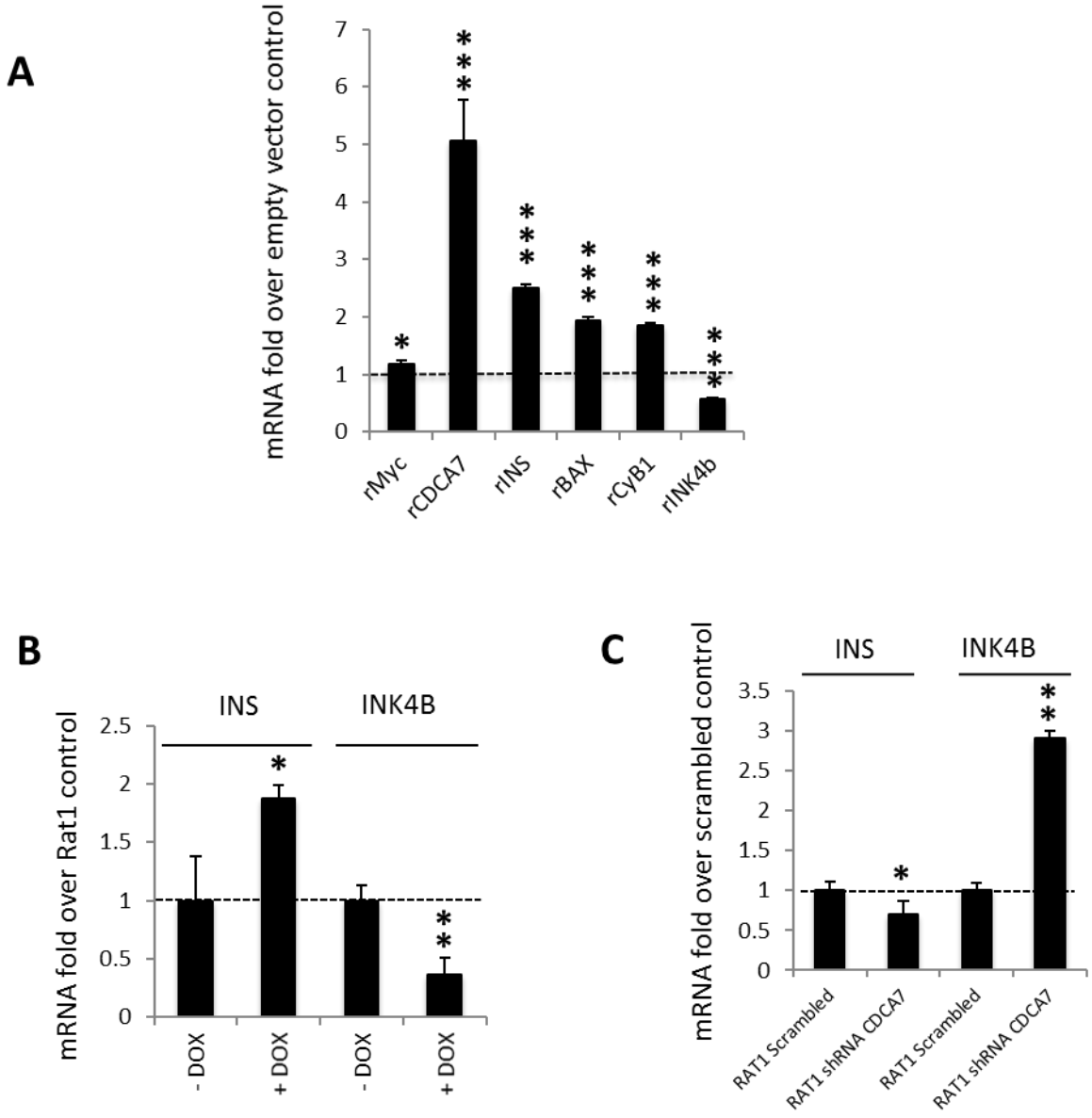

Figure 4.9. **qPCR analysis of Myc target genes**. **A**. mRNA was analyzed by qPCR in Rat1 cells stably expressing CDCA7 vs Rat1 expressing empty vector (Control). The primers for CDCA7 detected ectopic CDCA7, which was 5 fold above control Rat1 cells. **B.** Rat1 cells stably expressing doxycycline-inducible CDCA7 were treated with doxycycline for 18 hours and mRNA for INS and INK4B was measured by qPCR. **C**. Rat1 cells expressing either scrambled shRNA or CDCA7- targeted shRNA were isolated and mRNA for INS and INK4B was measured by qPCR. * = P<0.05, ** = P ≤ 0.01 and *** = P ≤ 0.001. Error bars represent standard deviation.

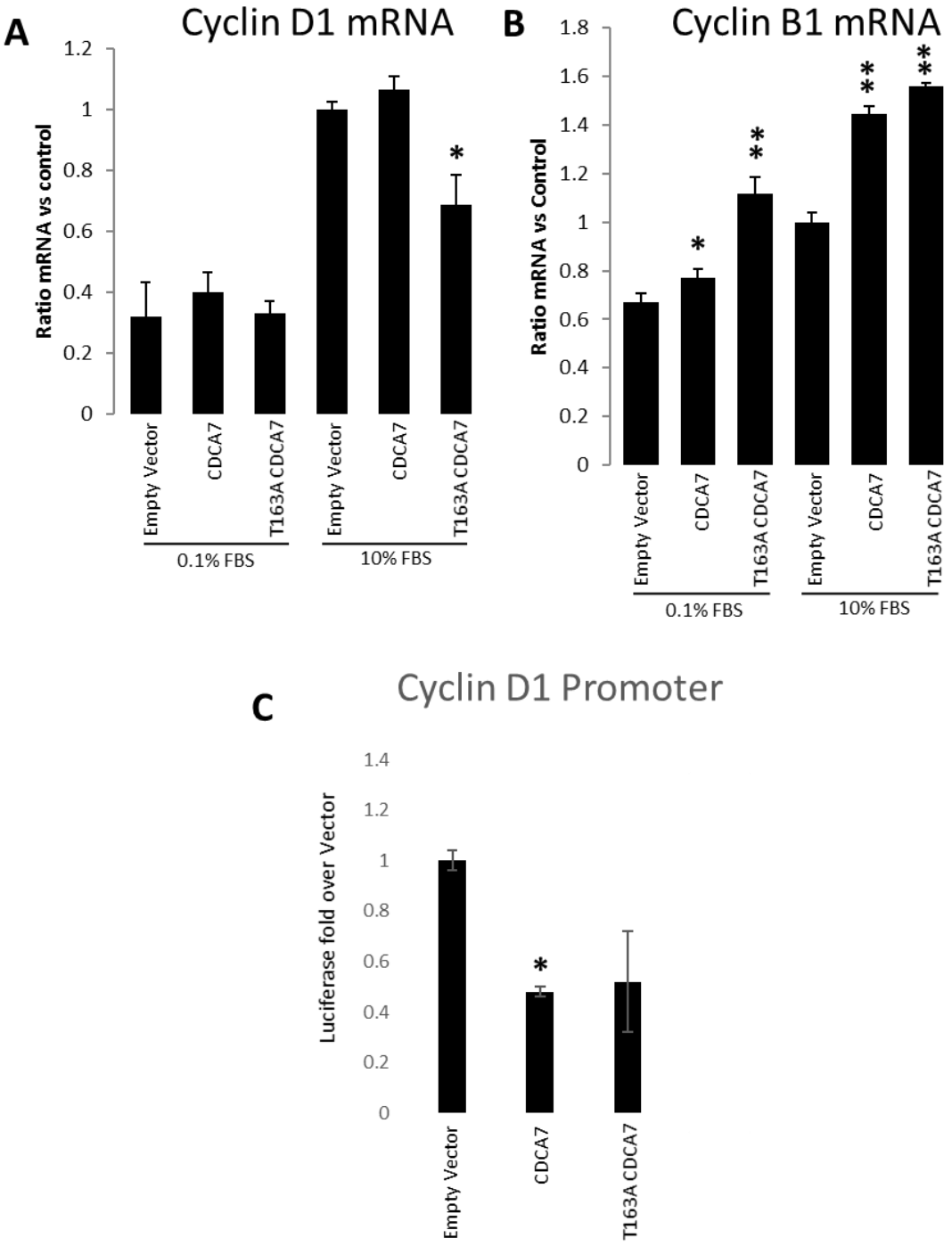

Figure 4.10. **qPCR analysis of Cyclin D1 and B1**. mRNA levels of Cyclin D1 **A.** and Cyclin B1 **B.** was analyzed by qPCR in Rat1 cells stably expressing CDCA7 vs Rat1 expressing empty vector (Control). Pools were starved in 0.1% FBS for 18 hours at which point 10% FBS was added back for 5 hours. **C.** Cyclin D1 promoter assay via a luciferase reporter was conducted with Rat1 cells stably expressing CDCA7 vs empty vector. Cells were plated at equal densities and kept in media supplemented with 10% FBS for 24 hours. * = $P<0.05$, ** = $P\leq0.01$, N=3 in A and B, N=2 in C. Error bars represent standard deviation.

Discussion

In the studies outlined above, we have shown that cooperation between CDCA7 and Myc results in altered cell cycle distribution with a shift of cell populations towards G2/M phase, while expression of WT CDCA7 prevents cells from synchronizing in G2/M. Cell cycle data also shows that phosphorylation of T163 occurs in G2/M and it likely occurs in proximity to centrosomes. Proliferation assays have revealed that growth rates vary depending on the form of CDCA7 that is expressed which results in growth rates which may be correlated with CDCA7's ability to bind 14-3-3. For example, forced binding of 14-3-3 resulted in the quickest proliferation rates, while lack of binding resulted in the slowest rates. The phenotypic results summarized here broadens the scope of CDCA7's influence on major cellular process including not only apoptosis, but cell cycle progression and proliferation. In this chapter, we have also sought to better understand the extent to which CDCA7 might be directly involved in Myc-mediated gene expression. We have shown that CDCA7 enhances Myc's ability to activate a reporter that contains a canonical E-box promoter element. ChIP experiments verify that CDCA7 binds to chromatin and promotes increased Myc occupancy of the BAX promoter, which is a proapoptotic Myc target gene. Finally, expression of CDCA7 alters the mRNA levels of Myc target genes that are involved in cell cycle progression, proliferation and apoptosis.

As our group reported in 2013, CDCA7 directly interacts with Myc and potentiates Myc-dependent apoptosis (Gill et al. 2013). What was unknown at the time was whether CDCA7 interacts with DNA directly or indirectly via its association with Myc. This scenario is likely as CDCA7 and JPO2 share a high degree of homology in their C-terminal cysteine rich regions, which in JPO2 has been shown to confer DNA binding ability (Goto, 2006). Here we have established that CDCA7 expression enhances the activation a Myc E-box reporter and that this activation is

dependent on CDCA7's interaction with Myc (Figure 4.1C). Based on these results, we surmised that CDCA7 may enhance the promoter occupancy of Myc at target genes involved in apoptosis. We chose to specifically focus on the BAX promoter, as this well-known pro-apoptotic Myc target gene has been shown to be involved in Myc-mediated apoptosis upon serum withdrawal (Mitchell et al., 2000). Activation of the PI3K pathway has also been shown to suppress the translocation of BAX to the mitochondria, and therefore promoting survival (Tsuruta et al., 2002). Using chromatin immunoprecipitation followed by qPCR, we have shown that expression of WT CDCA7 does in fact increase Myc occupancy of the BAX promoter (Figure 4.2). This is further enhanced by the expression of T163A CDCA7, which when co-expressed with Myc in Rat1 cells results in hypersensitivity to apoptosis upon serum withdrawal (Gill et al., 2013). Finally, expression of CDCA7 also increases BAX mRNA levels by approximately 2.5 times over empty vector expression alone, perhaps as a product of increased Myc occupancy at the BAX promoter. These results are the first to implicate CDCA7 in a known apoptotic pathway involving the Myc target gene BAX, and may shed light on how CDA7 is involved in Myc-mediated apoptosis.

The G2/M distribution of cells expressing CDCA7 (figure 4.3) may also be a reflection of Myc target genes influenced by CDCA7 (Figure 4.9 and 4.10). In particular, we have evidence showing that expression of CDCA7 increases mRNA levels of Cyclin B1 while decreasing mRNA levels of $p15^{INK4B}$. These two proteins are of considerable note because of their roles in G2/M progression and commitment to mitosis. Cyclin B1 is critical in initiating mitosis by promoting chromatin condensation and works by activating Cdk1, and in doing so forms the mitosis promoting factor (MPF) (Sciortino et al., 2001; Chang et al., 2003). The CDK inhibitor $p15^{INK4B}$ is known to arrest cells in G1 by inhibiting Cyclin D/Cdk 4/6 and are induced via the MAPK pathway (Carneo and Hannon, 1998). The simultaneous upregulation of Cyclin B1 and down regulation of $p15^{INK4B}$ may

explain the preponderance of CDCA7 expressing cells occupying G2/M phase. However, at this point one cannot rule out the possibility that this mRNA profile is simply a result of cells being encouraged into G2/M by some other means and is simply a normal reflection of cells in this state. This line of reasoning may also extend to the reduction of Cyclin D1 promoter activity seen upon CDCA7 expression (Figure 4.10C). Cyclin D1 is expressed via Myc during G1 and promotes G1/S transition. It is possible that the reduction of Cyclin D1 promoter activity is due to: a) CDCA7 expressing cells occupying G2/M or b) CDCA7's association with Myc represses Cyclin D1 expression directly or by altering Myc promoter occupancy and specificity to the Cyclin D1 promoter.

One of the most surprising results from our investigation into cell cycle progression is the fact that CDCA7 T163 phosphorylation occurs strictly in G2/M and in proximity to centrosomes (Figure 4.5-4.7). This is revealing in light of two recent publications that implicate mutations in CDCA7 as being correlated with immunodeficiency-centromeric-instability-facial anomalies syndrome (ICF) (Thijssen et al., 2015; Wu et al., 2016). CpG hypomethylation in juxtacentromeric DNA is a hallmark of ICF and is used as a diagnostic indicator for the syndrome. These hypomethylated sequence have been shown to correlate with chromosomal abnormalities in interphase as well as mitotic missegregation (Tuck-Muller et al., 2000; Gisselsson et al., 2005). It remains to be seen whether there is a relationship between ICF onset or progression and T163 phosphorylation at centrosomes. Interestingly, the four mutations within CDCA7 that are associated with ICF occur in the C-terminal zinc finger domain (Thijssen et al., 2015) which we believe may impart DNA binding ability on CDCA7. Could these mutations prevent CDCA7 from localizing to juxtacentromeric DNA, thus preventing methylation of juxtacentromeric DNA? Could phosphorylation of T163 in proximity to centrosomes play a part in mitotic missegregation seen

in ICF? Our lab is currently generating the mutations in question in order to investigate their effect on CDCA7 localization, T163 phosphorylation and DNA binding ability. We will also investigate how these mutations affect cell cycle progression, cell proliferation and apoptosis.

Materials and Methods

Cell lines and cell culture

HEK 293, Rat1 and 3T3 cells were obtained from the American Type Culture Collection and maintained in Dulbecco's modified Eagle's medium supplemented with 10% fetal bovine serum and antibiotics at 37°C and 5% CO_2. Rat1-MYC cells were obtained by stable transfection of Myc and selection in 600 μg/ml G418 and 20% fetal bovine serum. Clones expressing both wild-type and mutant CDCA7 were established using the Tet-ON advanced inducible gene expression system from Clontech. Specifically, stable clones expressing a tet-induced transactivator (rtTA) were obtained by stable transfection of Rat1 and Rat1-MYC cells, respectively, with pIREShyg3-rtTA, followed by selection in 200μg/ml hygromycin. Subsequently the rtTA-Rat1 and rtTA-Rat1-MYC cells were co-transfected with a 100:1 ratio of pTRE-tight-3xFLAG-CDCA7 plasmid and linearized puromycin plasmid, followed by selection in 2μg/ml puromycin. All Rat1-MYC derived inducible lines were maintained in 20% fetal bovine serum while Rat1-CDCA7 derived inducible lines were maintained in 10% fetal bovine serum. Rat1 pools stably expressing CDCA7 were generated via viral infection as per Clontech's protocol, followed by selection in 200μg/ml hygromycin.

Transfections

For transient expression of cDNA in HEK 293 and Rat1 cells, cells were plated onto 100-mm-diameter dishes at 80% confluency and transfected with 8 μg of total plasmid using

polyethylenimine (PEI) (Sigma-Aldrich #408727). 8 μg of DNA was diluted with 1 mL of serum-free Opti-MEM (ThermoFisher Scientific #31985062). 24 μg of PEI was added to the diluted DNA mix for a final ratio of 3:1 μg PEI:μg DNA. The mix was vortexed 10x and allowed to incubate at room temperature for 30 minutes. 3 mL of Dulbecco's modified Eagle's medium supplemented with 10% fetal bovine serum was gently added to the transfection mix. The 4 mL total transfection mix was then added to cells following aspiration. 7 hours later, transfection medium was removed and replaced with complete Dulbecco's modified Eagle's medium overnight.

Transfection of cDNA for stable integration and expression in Rat1 cells was accomplished using Lipofectamine 2000 (Life Technologies #11668019) and serum free Opti-MEM (ThermoFisher Scientific #31985062) according to manufacture's protocol. Briefly, Rat1 cells were plated onto 100-mm-diameter dishes at 80% confluency and transfected with 5 μg of plasmid using Lipofectamine 2000 (Invitrogen) following the manufacturer's protocol. Transfection medium was removed and replaced with complete Dulbecco's modified Eagle's medium overnight.

Virus Production and Infections

The ORF of CDCA7 was cloned into the Clontech retroviral vector set (Clontech #631516) and expressed in DH5α *E. coil*, from which cDNA was purified for use in transfections. This cDNA was transfected into Clontech Ecopack 2-293 cells (Clontech #631507) for virus production according to manufacture's protocols. Virus collected from Ecopack 2-293 was used in infections of Rat1 or 3T3 cells according to manufacture's protocols. Following 24-48 hour incubation periods, stable pools were selected using the appropriate antibiotic as dictated by the viral vector. Briefly, 3X-FLAG-CDCA7 or CDCA7 with various mutations were cloned into the pQCXIH retroviral vector (Clontech) upstream of an IRES sequence and the hygromycin resistance gene. Either empty pQCXIH or pQCXIH-CDCA7-IRES-Hygro retroviral vectors were transfected into

the ecotropic-envelope protein packaging cell line EcoPack 2-293 (Clontech). Viral particles were collected 48 hours later and concentrated using Retro-X concentrator (Clontech).

Antibodies and Reagents

Mouse monoclonal M2 anti-flag (A2220) and rabbit polyclonal anti-CDCA7 (HPA005565) were purchased from Sigma-Aldrich. Rabbit polyclonal anti-CDCA7 (Ab69609) was purchased from Abcam. Mouse monoclonal anti-14-3-3β (SC-1657) and 9E10 mouse monoclonal anti-MYC (SC-40) were purchased from Santa Cruz. Rabbit polyclonal anti-Myc (5605) was purchased from Cell Signaling Technologies. An anti-p-Thr163 CDCA7 rabbit polyclonal antibody was generated by Genscript Corporation (California).

qRTPCR

Total RNA was purified and cDNA synthesized using NEB's ProtoScript® M-MuLV First Strand cDNA Synthesis Kit. Up and down regulation of genes of interest were performed using SA Bioscience's RT² SYBR® Green qPCR Master mix and Applied Biosystems' 7500 Fast RT-PCR system.

Cloning

The CDCA7coding region was ligated into the p3XFLAG-CMV10 mammalian expression vector (Sigma-Aldrich) to introduce an amino terminal FLAG epitope. Mutagenesis of p3XFLAG-CMV10-CDCA7 was performed using the QuikChange kit (Stratagene) and NEB Q5 Site Directed Mutagenesis Kit (E0554), and the various mutations were sequence-verified. Amino-terminal and internal deletions were created by introducing silent mutations coding for unique restriction sites, followed by digestion and re-ligation. Carboxyl terminal deletions were created by introducing

stop codons. All deletions were sequence verified. CDCA7 containing the 14-3-3-binding R18-peptide PHCVPRDLSWLDLEANMCLP or the control non-14-3-3-binding peptide PHCVPRDLSWLKLKANMCLP were created by ligating a double-stranded oligonucleotide to replace amino acids 139-164 of CDCA7 in the 3XFLAG-CMV10 vector.

Cell Lysis, Immunoprecipitation, and Immunoblotting

Cells were lysed in either RIPA lysis buffer (10mM NaPO4, pH 7.6, 150mMNaCl, 5mM EDTA, 0.1% sodium dodecyl sulphate, 0.25% deoxycholic acid, 1% triton X-100, plus protease (Roche #88666) and phosphatase inhibitors (Roche #88667) or Triton X-100 lysis buffer (50mMHepes, pH 7.9, 250mMNaCl, 0.1% Triton X-100, 10% glycerol, plus protease and phosphatase inhibitors). Ten μl of anti-FLAG M2 agarose conjugated beads (Sigma Aldrich) were added to lysates and incubated overnight at 4°C. The beads were washed five times with lysis buffer, and proteins were eluted with 200 μl of sodium dodecyl sulfate sample buffer and heated to 99°C for 5 min. Portions of the lysates prior to immunoprecipitation were also reserved and boiled with sodium dodecyl sulfate-containing sample buffer. Lysates and immunoprecipitations were fractionated by SDS-PAGE, transferred to a PVDF membrane, blocked in Odyssey blocking buffer (Mandel, LIC-927-40100), and probed with the appropriate antibody overnight at room temperature. Primary antibodies were decorated with IR700 anti-mouse or rabbit and/or IR800 anti-mouse, rabbit or rat secondary antibodies (Li-Cor Biosciences) for 3 hours at room temperature and visualized using the infrared laser scanning (Odyssey, Li-Cor Biosciences).

Microscopy

Rat1, NIH3T3 or HEK 293cells were plated at 80% confluency on no. 1 glass coverslips. Following the desired treatment, the coverslips were washed twice in PBS and then fixed and

permeabilized in 3:1 methanol:acetic acid for 25 minutes. The coverslips were then washed three times in PBS followed by blocking in 1% BSA in PBS. Primary antibodies at varying concentrations were applied for 1.5 hours in a humidified chamber at room temperature. Coverslips were washed three times in PBS prior to applying secondary antibodies for 2 hours in a humidified chamber at room temperature and in the dark. The slips were washed three times in PBS before mounting with Invitrogen's ProLong Gold antifade reagent with DAPI. The slides were viewed on an Olympus microscope and images were taken via a QImaging 2000R camera and Q-Capture pro software.

XTT Proliferation Assay

Cells were plated at 2000 cells/well in triplicate within a 96 well plate for 24-48 hours. 10 mg of XTT (Sigma Aldrich #X4626) was dissolved in 20 ml of PBS containing 2 ml of DMEM (containing 10% fetal bovine serum). A 1/10 dilution of 10 mM PMS (N-methyl dibenzopyrazine methyl sulfate, Sigma Aldrich #P13401) was made in the 0.5 mg/ml XTT solution. Cells were washed three times with 37°C PBS, followed by addition of 100 µl of the XTT/PMS solution, including addition to blank wells as a control. Cells are incubated for 2 hours at 37°C and 5% CO_2 and then read at 490 nm using a spectrophotometer. This is repeated every day, making an effort to keep all actions and volumes constant.

Cell Synchronization and Flow analysis

Synchronization of cells was accomplished with either 50 ng/ml Nocodazole (Sigma Aldrich #M1404) or 10 µM RO-3306 (Sigma Aldrich #SML0569) in DMEM containing 10% FBS for 18 hours. Cells were then washed three times with PBS and either collected for analysis or released to progress through the cell cycle by add back of DMEM containing 10% FBS for a predetermined

length of time. Cells were collected by trypsinization, centrifuged at 2000g and washed three times with PBS. 70% ethanol was prechilled to -20°C and added dropwise while vortexing to 300 µl, and then incubated at -20°C for 20 minutes. Cells were centrifuged at 2000g for 10 minutes followed by decanting of supernatant. Cells were resuspended by vortexing in 350 µl of PBS containing 500 µg/ml RNase A (ThermoFisher #12091021) and 40 µg/ml propidium iodide (ThermoFisher #P3566) and incubated at 37°C for 30 minutes. Counter staining with α-FLAG M2 (1/1000) and α-pT163 (1/1000) antibodies was performed prior to propidium iodide staining and followed immediately by staining with IR700 anti-mouse or rabbit and/or IR800 anti-mouse or rabbit secondary antibodies (As per Cell Signalling Technology https://www.cellsignal.com/contents/resources-protocols/flow-cytometry-protocol-(flow)/flow). Data was gathered with the BDFacscalibur system coupled with BD CellQuest Pro software and analyzed with ModFit LT.

Reporter Assay

The MYC and D1 promoters were cloned into vectors supplied by Promega (#E6661) and transfected into HEK293 and Rat1 cells. 24 hour-48 hours cells were collected and processed through Promega's Luciferase Assay System (#E4030) as per the supplied protocol.

ChIP

Genomic DNA was isolated from Rat1 cells stably expressing Myc and variants of CDCA7 using Millipore EX-ChIP (#17-371) and used as sample for immunoprecipitations as per manufacture's protocols. Mouse monoclonal M2 anti-flag (Sigma Aldrich #A2220), 9E10 mouse monoclonal anti-MYC (Santa Cruz #SC-40) and anti-RNA polII (Abcam #ab26721) were used for immunoprecipitation from sheared genomic DNA samples.

Chapter 5: Concluding Discussion and Future Directions

Discussion

At the onset of this research project, our goal was to learn as much as we could about CDCA7 and how it may be involved in processes mediated by the transcription factor Myc. We were optimistic in this regard because prior to our investigation others had shown that JPO2, a protein closely related to CDCA7, directly interacts with Myc (Huang et al., 2005) and has DNA binding abilities (Goto et al., 2006). To that end, our initial bioinformatic analysis indicated that CDCA7 may be a target of Akt phosphorylation at T163 and may associate with 14-3-3. This piqued our interest because our lab was uniquely positioned to investigate 14-3-3 and the PI3K pathway as this was the subject of previous projects produced by our group (Matitau and Scheid, 2008; Moon et al., 2008; Sephton et al., 2009). Of particular interest was the possibility that CDCA7 may be involved in Myc-mediated apoptosis because it had been shown that activation of the PI3K pathway could suppress Myc-mediated apoptosis upon serum withdrawal (Kauffmann-Zeh et al., 1997). Therefore, if CDCA7 was in fact a target of Akt and did associate with Myc, we might be able to shed some light on the paradox of Myc-mediated apoptosis. The specifics behind the dual signal model of Myc function has evaded researchers since Evan and colleagues first described this paradox in 1992. The model proposes that Myc drives proliferation while simultaneously priming cells for apoptosis. Cell death is kept at bay in the presence of growth factors, which promotes survival via the PI3K pathway among others. Upon growth factor withdrawal, the priming of apoptosis is realized and cell death is initiated (Evan et al., 1992). Investigating if and how CDCA7 is implicated in this model would be the foundation of this research project (chapter II), which would ultimately bifurcate into many unexpected lines of questioning (chapters III and IV).

Our publication in 2013 confirmed that CDCA7 associated with Myc and was in fact phosphorylated by Akt to regulate Myc-dependent apoptosis and tumorigenesis (Gill et al., 2013). Phosphorylation of T163 by Akt results in binding of 14-3-3 and masking of a nuclear localization signal, thus sequestering CDCA7 in the cytoplasm and away from nuclear-Myc. Although this model affords us a general and valuable understanding of CDCA7 on a molecular level, it does not explain how CDCA7's relationship with Myc can affect apoptosis or tumorigenesis. The data presented in chapter IV attempts to elucidate these unknown mechanisms. We have added the following to our understanding of CDCA7 and its relationship to Myc: CDCA7 potentiates the activation of an E-box element, enhances Myc's occupancy of the BAX promoter and can enhance or repress Myc target gene expression. These results suggest that CDCA7 confers DNA binding specificity or selectivity to Myc and can drive the expression of genes involved in apoptosis. We have for the first time not only implicated CDCA7 in Myc-dependent apoptosis, but we have revealed the means by which CDCA7 sensitizes cells to apoptosis in the absence of growth factors. CDCA7 is therefore a prime candidate for being involved in the dual signal model of Myc function proposed by Evan in 1992. According to this model, Myc would drive proliferation in the presence of growth factors, which has the effect of stimulating the PI3K pathway. Subsequent activation of Akt would result in phosphorylation of CDCA7 at T163, 14-3-3 binding and sequestering of CDCA7 in the cytoplasm. In its 14-3-3 bound state, CDCA7 would be prevented from interacting with Myc and therefore decrease Myc driven expression of BAX by reducing occupancy at the BAX promoter. Withdrawal of serum would result in a reduction of CDCA7 phosphorylation at T163, dissociation from 14-3-3 and shuttling to the nucleus where CDCA7 and Myc can cooperate to express proapoptotic genes such as BAX. This hypothesis is strengthened by the fact that the

T163A CDCA7 mutant cannot be phosphorylated, does not bind 14-3-3, is primarily nuclear and sensitizes cells to apoptosis greater than WT CDCA7.

In addition to affecting Myc-dependent apoptosis, our research indicates that CDCA7 may also influence cell cycle progression and proliferation rates. As with apoptosis, CDCA7's influence on these processes might be a product of targeted gene expression. We have shown that expression of CDCA7 results in an increase of cells in G2/M phase. This shift is further exaggerated by coexpression of CDCA7 and Myc while being abolished with the expression of the non-Myc binding mutant Δ(156-187) CDCA7. This cell cycle profile may be a result of the simultaneous increase in Cyclin B1 mRNA and decrease in $p15^{INK4B}$ mRNA levels upon expression of CDCA7. Expression of Cyclin B1 is known to be required for chromatin condensation during mitosis while the CDK inhibitor $p15^{INK4B}$ promotes arrest in G1 (Sciortino et al., 2001; Chang et al., 2003; Carneo and Hannon, 1998). It is important to note that Cyclin B1 is a confirmed target of Myc transactivation, while $p15^{INK4B}$ is known to be actively repressed by Myc (Menssen and Hermeking, 2002; Wiese et al., 2013). It is possible that expression of CDCA7 is shifting cell cycle distribution towards G2/M by influencing Myc's role in the expression of Cyclin B1 and $p15^{INK4B}$. This is supported by the fact that the non Myc binding mutant Δ(156-187) CDCA7 is insulated from changes in cell cycle distribution. What remains unknown is if and how this mutant affects the expression of Cyclin B1 and $p15^{INK4B}$. While it is possible that the cell cycle distribution seen here is a product of the up and down regulation of Cyclin B1 and $p15^{INK4B}$ respectively, the inverse may also be true. The mRNA profiles of these two genes may simply be a product of cells predominantly occupying G2/M. If the latter is the case, then CDCA7 is still likely to be responsible for the change in cell cycle distribution upon its expression. Careful consideration

should be placed into selecting other possible Myc target genes which are involved in G2/M transition and assay them for changes in expression.

We have shown that phosphorylation of CDCA7 at T163 is a critical event in regulating its subcellular localization and availability to Myc. This knowledge extends from our research published in 2013, which probed the nature of T163 phosphorylation in asynchronous cells treated by various means which activate the PI3K pathway. In chapter IV of this thesis, we relied on the synchronization of cells by either nocodazole or RO-3306 in G2/M phase as a means of not only studying cell cycle progression but to accentuate various effects of CDCA7 expression. This broadened the scope of our knowledge regarding the spatial and temporal nature of T163 phosphorylation. Using flow cytometry after synchronization in G2/M, we have established that CDCA7 is phosphorylated at T163 exclusively in G2/M. We have also established that phospho-T163 CDCA7 colocalizes with the centrosomal protein marker γ-Tubulin and activated Akt (phospho-S473) to produce a pronounced punctate topography. This colocalization is presumably in the vicinity of centrosomes. The spatial and temporal nature of T163 phosphorylation should be of interest to those studying immunodeficiency-centromeric-instability-facial anomalies syndrome (ICF). Thijssen, Wu and colleagues have recently identified four mutations within CDCA7's C-terminal zinc finger as being directly correlated with ICF (Thijssen et al., 2015; Wu et al., 2016). Molecular hallmarks of ICF include hypomethylation of juxtacentromeric DNA which can result in chromosomal abnormalities in interphase as well as mitotic missegregation leading to chromosomal instability (CIN) (Tuck-Muller et al., 2000; Gisselsson et al., 2005). It is well known that CIN can be a result of improper mitotic spindle formation arising from centrosome dysfunction, improper centrosomal biogenesis or abnormal centrosome number (Vitre and Cleveland, 2012). The fact that phosphorylation of CDCA7 at T163 occurs during mitosis and

within the vicinity of centrosomes may warrant further investigation as it pertains to CIN and ICF. It is also worth noting that centromeric aberrations and CIN are indicative of various types of cancer, including chronic myeloid leukemia (CML) which Osthus and colleagues identified as harboring elevated CDCA7 mRNA levels (Giehl et al., 2005; Osthus et al., 2005). Finally, Nam and colleagues have recently shown that activation of the PI3K-Akt pathway via oncogenic hepatocyte growth factor receptor signaling induces centrosome amplification and CIN (Nam et al., 2010). These data points suggest that CDCA7 may play a role in disease development which extends beyond the reach of Myc's influence.

Chapter III of this thesis focused on dissecting the details behind CDCA7 co-association. Using a complement of experiments including co-immunoprecipitations of endogenous and ectopic protein as well as BioID, we have identified that CDCA7 co-associates at amino acids 187-234. We have also investigated the possibility that CDCA7 contains a second 14-3-3 binding site which may be involved in mediating co-association of CDCA7. Bioinformatics suggest that four phospho-serine/threonine residues within proximity of the CDCA7 co-association domain (a.a.187-234) conform to predicted 14-3-3 binding sites. These residues are S185, T213, S231 and T234 (Madeira et al., 2015). Sequence alignment of human CDCA7 with *Branchiostoma belcheri* or *Ciona intestinalis* reveals that 3 of the 4 predicted sites are in fact conserved and may lend credence to the lynchpin hypothesis of 14-3-3 binding. The theory proposes that the conservation of one of the phospho-serine/threonine binding sites (the lynchpin residue) allowed the second residue to evolve and perhaps become the target of a novel kinase (Johnson et al., 2011). The data outlined in chapter III identifies T213 as a potential second 14-3-3 binding site, as mutation of threonine 213 to alanine resulted in approximately 20% less 14-3-3 co-immunoprecipitating with CDCA7. Deletion of the a.a. 187-224 region (inclusive of T213) resulted in approximately 80% less 14-3-

3- binding and CDCA7 co-association. However, the T213A point mutation's effect on co-association is currently unknown and needs to be assayed. At present, we are certain that CDCA7 co-associates either via a larger complex or perhaps directly via protein-protein interactions between monomers of CDCA7. What role CDCA7 co-association or dimerization may play in its function or regulation thereof remains a mystery. However, this should not be overlooked as there is precedent for Akt mediated homodimerization in regulating the function of proteins (Kolliputi and Waxman, 2009; Han et al., 2013).

In chapter I, we identified seven research objectives that served as a framework for our investigation into CDCA7. We have successfully addressed these objectives, and in doing so raised new questions based on our broadened understanding of CDAC7. The following is a summary of those objectives and our findings:

Research Objective 1 - *Investigate Consensus Sites within CDCA7's Amino Acid Sequence*

We have confirmed the existence of an Akt phosphorylation site, 14-3-3 binding site and nuclear localization signal within CDCA7.

Research Objective 2 - *Does CDCA7 Interact with the Oncogene Myc?*

CDCA7 interacts with Myc at a.a. 156-187 in CDCA7.

Research Objective 3 - *Map the Subcellular Localization of CDCA7*

CDCA7 subcellular localization is dynamic and depends on T163 phosphorylation and 14-3-3 binding. Phosphorylation of CDCA7 at T163 enforces 14-3-3 binding, masking of the nuclear localization signal and results in cytoplasmic sequestration of CDCA7.

Research Objective 4 - *How Does CDCA7 Affect Apoptosis and Proliferation?*

CDCA7 potentiates Myc dependent apoptosis and reduces proliferation rates.

Research Objective 5 - *Does CDCA7 Exist as a Monomer or a Homodimer?*

CDCA7 has the ability to co-associate either via larger complexes containing other proteins or directly via protein-protein interactions between monomers.

Research Objective 6 - *How Does CDCA7 Affect Gene Expression?*

CDCA7 activates an E-box promoter in a Myc-binding dependent manner. CDCA7 can enhance or repress the expression of Myc target genes and increases Myc occupancy at the BAX promoter.

Research Objective 7 - *How Does CDCA7 Affect the Cell Cycle?*

CDCA7 causes cells to shift towards G2/M phase and phosphorylation of CDCA7 at T163 was observed exclusively in G2/M. Finally, phosphorylation of CDCA7 at T163 was observed in mitotic cells, colocalized with the centrosomal marker protein γ-Tubulin and activated Akt (phospho-S473) near centrosomes.

The research outlined in this thesis solidifies CDCA7 as an important node in PI3K pathway convergence on Myc-mediated apoptosis and tumorigenesis. CDCA7 functions by influencing Myc target gene expression and has the ability to influence the cell cycle, albeit by an unknown mechanism. Figure 5.1 summarizes our findings and outlines our current understanding of CDCA7's involvement in the dual-signalling model of Myc dependent apoptosis It is our hope that the data presented here will serve those who continue to research CDCA7 and diseases such as cancer and immunodeficiency-centromeric-instability-facial anomalies syndrome.

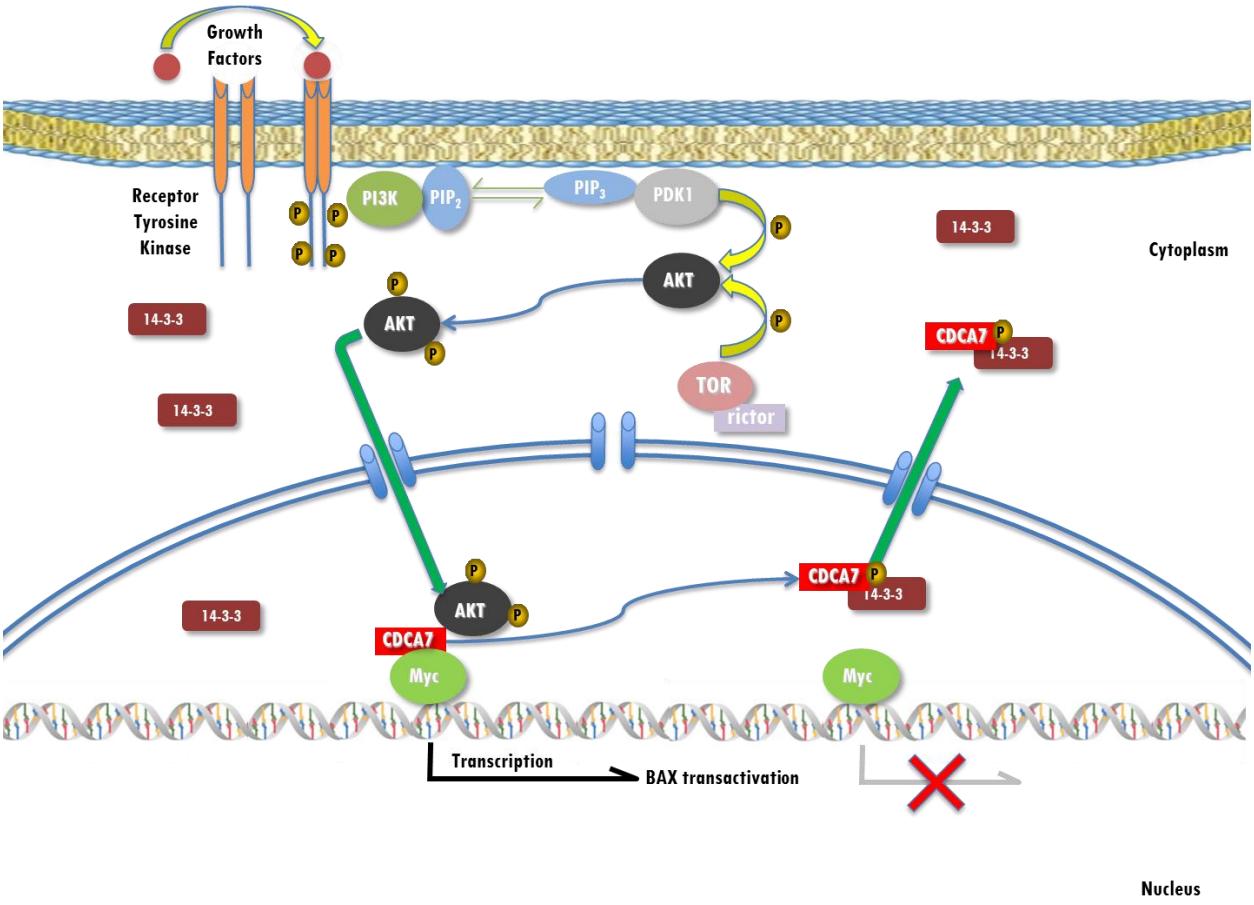

Figure 5.1. **Hypothetical model of CDCA7's contribution to the dual signal model of Myc mediated apoptosis**. In the presence of growth factors, such as the tissue culture media supplemented with serum, receptor tyrosine kinases initiate the activation of the PI3K/Akt pathway. This allows activated Akt to phosphorylate CDCA7 in the nucleus, resulting in the disassociation of CDCA7 from Myc, binding of 14-3-3 at pT163 and subsequent localization to the cytoplasm. This event results in Myc's inability to drive the transactivation of the pro-apoptotic BAX gene, and therefore proliferation in favored. CDCA7 and 14-3-3 are both depicted as monomers for simplicity.

Future Directions

The following is a list of unanswered questions and future directions which will aid in understanding the function and regulation of CDCA7:

1. CDCA7 and regulation of Myc-target genes – we have presented a limited scope of CDCA7's influence on Myc target genes. We opted to probe Myc target genes which are known to be involved in apoptosis and proliferation. The results we obtained were satisfactory, however employing high throughput qPCR arrays on a large number of Myc target genes would be far more informative. This data could subsequently be used to select promoters for ChIP analysis. Finally, qPCR and ChIP should be performed using various mutants of CDCA7 not included in this study. These include the co-association mutant Δ(187-234) CDCA7 and the proapoptotic T163A CDCA7 mutant.

2. Is CDCA7 co-association direct or via a complex? Direct protein-protein interactions between monomers of CDCA7 can be assayed *in vitro* using purified proteins either from a bacterial or mammalian host. Although we have attempted this strategy, quantities of purified proteins must be substantially improved before one can draw any conclusions.

3. What causes CDCA7 to shift cells towards G2/M? Our study has revealed that CDCA7 causes a shift towards G2/M phase, while upregulating expression of Cyclin B1 and downregulating expression of $p15^{INK4B}$. What remains unknown is whether this mRNA profile causes the reported change in cell cycle distribution or is simply a product as such. Investigating means by which CDCA7 affects the cell cycle could prove to be important as deregulated cell cycle progression is a common theme in cancer onset and progression.

4. Use BioID to identify novel binding partners of CDCA7 – We have successfully employed BioID as a means of assaying association of CDCA7 monomers. It would be tremendously valuable to employ this technique in conjunction with mass spectrometry to identify novel binding partners of CDCA7. The initial stages of this investigation have begun in our lab, and will continue to be a focus going forward.

5. Investigate the CDCA7 mutations reported in immunodeficiency-centromeric-instability-facial anomalies syndrome (ICF) – Thijssen and colleagues have identified 4 homozygous variants of CDCA7 in ICF patients, each containing missense mutations within the c-terminal z-finger domain. These include R274C, R274H, G294V and R304H (Thijssen et al., 2015). It would be prudent of us to generate these mutations in and test their affect on various properties of CDCA7 including but not limited to: T163 phosphorylation, DNA binding ability, subcellular localization, apoptosis and proliferation. It would also be of interest to obtain ICF B-cells that are commonly used when investigating ICF and to use these a model for experiments focusing on ICF.

Bibliography

Albihn, A., J. I. Johnsen, and M. A. Henriksson. 2010. MYC in oncogenesis and as a target for cancer therapies. Adv Cancer Res 107:163-224.

Alessi DR, Andjelkovic M, Caudwell B, Cron P, Morrice N, Cohen P, Hemmings BA. Mechanism of activation of protein kinase B by insulin and IGF-1. EMBO J. 1996 Dec 2;15(23):6541-51.

Allan LA, Clarke PR. Apoptosis and autophagy: Regulation of caspase-9 by phosphorylation. FEBS J. 2009 Nov;276(21):6063-73

Altomare DA, Testa JR. Perturbations of the AKT signaling pathway in human cancer. Oncogene. 2005 Nov 14;24(50):7455-64.

Amati, B., T. D. Littlewood, G. I. Evan, and H. Land. 1993. The c-Myc protein induces cell cycle progression and apoptosis through dimerization with Max. Embo J 12:5083-5087.

Amanullah A, Liebermann DA, Hoffman B. p53-independent apoptosis associated with c-Myc-mediated block in myeloid cell differentiation. Oncogene. 2000 Jun 15;19(26):2967-77.

Amoutzias GD, Robertson DL, Van de Peer Y, Oliver SG. Choose your partners: dimerization in eukaryotic transcription factors. Trends Biochem Sci. 2008 May;33(5):220-9.

Anderson K.E., Coadwell J., Stephens L.R., Hawkins P.T., Translocation of PDK-1 to the plasma membrane is important in allowing PDK-1 to activate protein kinase B, Curr. Biol., 8: 684-691, 1998

Andjelkovic M., Alessi D.R., Meier R., Fernandez A., Lamb N.J., Frech M., Cron P., Cohen P., Lucocq J.M., Hemmings B.A., Role of translocation in the activation and function of protein kinase B, J. Biol. Chem., 272: 31515- 31524, 1997

Aprelikova O, Pace AJ, Fang B, Koller BH, Liu ET. BRCA1 is a selective co-activator of 14-3-3 sigma gene transcription in mouse embryonic stem cells. J Biol Chem. 2001 Jul 13;276(28):25647-50

Arellano M, Moreno S. (1997). Regulation of CDK/cyclin complexes during the cell cycle. Int. J. Biochem. Cell Biol. 29:559–73

Askew, D. S., R. A. Ashmun, B. C. Simmons, and J. L. Cleveland. 1991. Constitutive c-myc expression in an IL-3-dependent myeloid cell line suppresses cell cycle arrest and accelerates apoptosis. Oncogene 6:1915-1922.

Ayer DE, Kretzner L, Eisenman RN. Mad: a heterodimeric partner for Max that antagonizes Myc transcriptional activity. Cell. 1993 Jan 29;72(2):211-22.

Bartek J and Lukas J (2001) Pathways governing G1/S transition and their response to DNA damage.FEBS Lett490:117-122.

Balendran A., Casamayor A., Deak M., Paterson A., Gaffney P., Currie R., Downes C.P., Alessi D.R., PDK1 acquires PDK2 activity in the presence of a synthetic peptide derived from the carboxyl terminus of PRK2, Curr. Biol., 9: 393-404, 1999

Baudino TA, McKay C, Pendeville-Samain H, Nilsson JA, Maclean KH, White EL, Davis AC, Ihle JN, Cleveland JL. c-Myc is essential for vasculogenesis and angiogenesis during development and tumor progression. Genes Dev. 2002 Oct 1;16(19):2530-43.

Bavetsias, V., & Linardopoulos, S. (2015). Aurora Kinase Inhibitors: Current Status and Outlook. Frontiers in Oncology, 5, 278.

Bellacosa A, de Feo D, Godwin AK, Bell DW, Cheng JQ, Altomare DA, Wan M, Dubeau L, Scambia G, Masciullo V, Ferrandina G, Benedetti Panici P, Mancuso S, Neri G, Testa JR. Molecular alterations of the AKT2 oncogene in ovarian and breast carcinomas. Int J Cancer. 1995 Aug 22;64(4):280-5.

Bellacosa A, Kumar CC, Di Cristofano A, Testa JR. Activation of AKT kinases in cancer: implications for therapeutic targeting. Adv Cancer Res. 2005;94:29-86

Berger R, Flexor M, Le Coniat M, Larsen CJ. 1996. Presence of three recurrent chromosomal reaarrangements, t(2;3) (p12;q37), del(8)(q24), and t(14;18), in an acute lymphoblastic leukemia. Cancer Genet Cytogenet 86: 76–79.

Bhatia K, Huppi K, Spangler G, Siwarski D, Iyer R, Magrath I. Point mutations in the c-Myc transactivation domain are common in Burkitt's lymphoma and mouse plasmacytomas. Nat Genet. 1993 Sep;5(1):56-61.

Bhatia K, Siraj AK, Hussain A, Bu R, Gutierrez MI. The tumor suppressor gene 14-3-3σ is commonly methylated in normal and malignant lymphoid cells. Cancer Epidemiol Biomarkers Prev 2003; 12:165-9

Bissonnette, R. P., F. Echeverri, A. Mahboubi, and D. R. Green. 1992. Apoptotic cell death induced by c-myc is inhibited by bcl-2. Nature 359:552-554.

Blackwood EM, Lugo TG, Kretzner L, King MW, Street AJ, Witte ON, Eisenman RN. Functional analysis of the AUG- and CUG-initiated forms of the c-Myc protein. Mol Biol Cell. 1994 May;5(5):597-609.

Born, T. L., J. A. Frost, A. Schonthal, G. C. Prendergast, and J. R. Feramisco. 1994. c-Myc cooperates with activated Ras to induce the cdc2 promoter. Mol Cell Biol 14:5710-5718.

Bouchard, C., J. Marquardt, A. Bras, R. H. Medema, and M. Eilers. 2004. Myc-induced proliferation and transformation require Akt-mediated phosphorylation of FoxO proteins. Embo J 23:2830-2840.

Bozulic L, Surucu B, Hynx D, Hemmings BA. PKBalpha/Akt1 acts downstream of DNA-PK in the DNA double-strand break response and promotes survival. Mol Cell. 2008 Apr 25;30(2):203-13.

Bretones G, Delgado MD, León J. Myc and cell cycle control. Biochim Biophys Acta. 2015 May;1849(5):506-16.

Bridges D, Moorhead GB: 14-3-3 proteins: a number of functions for a numbered protein.Sci STKE 2004, 2004(242):re10.

Brodbeck D., Cron P., Hemmings B.A., A human protein kinase B with regulatory phosphorylation sites in the activation loop and in the C-terminal hydrophobic domain, J. Biol. Chem., 274: 9133-9136, 1999

Brotherton DH, Dhanaraj V, Wick S, Brizuela L, Domaille PJ, Volyanik E, Xu X, Parisini E, Smith BO, Archer SJ, Serrano M, Brenner SL, Blundell TL, Laue ED. Crystal structure of the complex of the cyclin D-dependent kinase Cdk6 bound to the cell-cycle inhibitor p19INK4d. Nature. 1998 Sep 17;395(6699):244-50. Erratum in: Nature 1998 Nov 26;396(6709):390.

Brunet, A., A. Bonni, M. J. Zigmond, M. Z. Lin, P. Juo, L. S. Hu, M. J. Anderson, K. C. Arden, J. Blenis, and M. E. Greenberg. 1999. Akt Promotes Cell Survival by Phosphorylating and Inhibiting a Forkhead Transcription Factor. Cell 96:857-868.

Brunet, A., F. Kanai, J. Stehn, J. Xu, D. Sarbassova, J. V. Frangioni, S. N. Dalal, J. A. DeCaprio, M. E. Greenberg, and M. B. Yaffe. 2002. 14-3-3 transits to the nucleus and participates in dynamic nucleocytoplasmic transport. The Journal of cell biology 156:817-828.

Burgering BM, Medema RH. Decisions on life and death: FOXO Forkhead transcription factors are in command when PKB/Akt is off duty. J Leukoc Biol. 2003 Jun;73(6):689-701.

Byrd JC, Lin TS, Dalton JT, Wu D, Phelps MA, Fischer B, Moran M, Blum KA, Rovin B, Brooker-McEldowney M, Broering S, Schaaf LJ, Johnson AJ, Lucas DM, Heerema NA, Lozanski G, Young DC, Suarez JR, Colevas AD, Grever MR. Flavopiridol administered using a pharmacologically derived schedule is associated with marked clinical efficacy in refractory, genetically high-risk chronic lymphocytic leukemia. Blood. 2007 Jan 15;109(2):399-404. Epub 2006 Sep 26.

Campisi J, Gray HE, Pardee AB, Dean M, Sonenshein GE. (1984) Cell cycle control of c-myc but not c-ras expression is lost following chemical transformation.Cell.36:241

Cardone MH, Roy N, Stennicke HR, Salvesen GS, Franke TF, Stanbridge E, Frisch S, Reed JC. Regulation of cell death protease caspase-9 by phosphorylation. Science. 1998 Nov 13;282(5392):1318-21.

Carnero A, Hannon GJ (1998) The INK4 family of CDK inhibitors. Curr. Top. Microbiol. Immunol. 227, 43

Carrió MM, Villaverde A. Localization of chaperones DnaK and GroEL in bacterial inclusion bodies. J Bacteriol. 2005 May;187(10):3599-601.

Cavalieri F, Goldfarb M. Growth factor-deprived BALB/c 3T3 murine fibroblasts can enter the S phase after induction of c-myc gene expression. Mol Cell Biol. 1987 Oct;7(10):3554-60.

Chan TA, Hermeking H, Lengauer C, Kinzler KW, Vogelstein B. 14-3-3Sigma is required to prevent mitotic catastrophe after DNA damage. Nature. 1999 Oct 7;401(6753):616-20.

Chang DC, Xu N, Luo KQ. Degradation of cyclin B is required for the onset of anaphase in Mammalian cells. J Biol Chem. 2003 Sep 26;278(39):37865-73.

Chaudhri M, Scarabel M, Aitken A. Mammalian and yeast 14-3-3 isoforms form distinct patterns of dimers in vivo. Biochem Biophys Res Commun. 2003 Jan 17;300(3):679-85

Cheng JQ, Godwin AK, Bellacosa A, Taguchi T, Franke TF, Hamilton TC, Tsichlis PN, Testa JR. AKT2, a putative oncogene encoding a member of a subfamily of protein-serine/threonine kinases, is amplified in human ovarian carcinomas. Proc Natl Acad Sci U S A. 1992 Oct 1;89(19):9267-71.

Cheng JQ, Ruggeri B, Klein WM, Sonoda G, Altomare DA, Watson DK, Testa JR. Amplification of AKT2 in human pancreatic cells and inhibition of AKT2 expression and tumorigenicity by antisense RNA. Proc Natl Acad Sci U S A. 1996 Apr 16;93(8):3636-41.

Cheng JQ, Altomare DA, Klein MA, Lee WC, Kruh GD, Lissy NA, Testa JR. Transforming activity and mitosis-related expression of the AKT2 oncogene: evidence suggesting a link between cell cycle regulation and oncogenesis. Oncogene. 1997 Jun 12;14(23):2793-801.

Choi SM, Tucker DF, Gross DN, Easton RM, DiPilato LM, Dean AS, Monks BR, Birnbaum MJ. Insulin regulates adipocyte lipolysis via an Akt-independent signaling pathway. Mol Cell Biol. 2010 Nov;30(21):5009-20.

Chugh P, Bradel-Tretheway B, Monteiro-Filho CM, Planelles V, Maggirwar SB, Dewhurst S, Kim B. Akt inhibitors as an HIV-1 infected macrophage-specific anti-viral therapy. Retrovirology. 2008 Jan 31;5:11.

Coller, H. A., C. Grandori, P. Tamayo, T. Colbert, E. S. Lander, R. N. Eisenman, and T. R. Golub. 2000. Expression analysis with oligonucleotide microarrays reveals that MYC regulates genes involved in growth, cell cycle, signaling, and adhesion. Proceedings of the National Academy of Sciences of the United States of America 97:3260-3265.

Cowling VH, Chandriani S, Whitfield ML, Cole Michael D. (2006) A conserved Myc protein domain, MBIV, regulates DNA binding, apoptosis, transformation, and G2 arrest. Mol. And Cell Bio. 26(11): 4226-4239.

Dahia, P. L., R. C. Aguiar, J. Alberta, J. B. Kum, S. Caron, H. Sill, D. J. Marsh, J. Ritz, A. Freedman, C. Stiles, and C. Eng. 1999. PTEN is inversely correlated with the cell survival factor Akt/PKB and is inactivated via multiple mechanismsin haematological malignancies. Hum Mol Genet 8:185-193.

Dang, C. V., McGuire, M., Buckmire, M. & Lee, W. M. Involvement of the 'leucine zipper' region in the oligomerization and transforming activity of human c-myc protein. Nature. 1989. 337, 664–666.

Dang CV (1999) c-Myc Target Genes Involved in Cell Growth, Apoptosis, and Metabolism. Mol Cell Biol. 19(1): 1–11.

Datta, S. R., H. Dudek, X. Tao, S. Masters, H. Fu, Y. Gotoh, and M. E. Greenberg. 1997. Akt phosphorylation of BAD couples survival signals to the cell-intrinsic death machinery. Cell 91:231-241.

Davis AC, Wims M, Spotts GD, Hann SR, Bradley A. A null c-myc mutation causes lethality before 10.5 days of gestation in homozygotes and reduced fertility in heterozygous female mice. Genes Dev. 1993 Apr;7(4):671-82.

del Peso, L., M. Gonzalez-Garcia, C. Page, R. Herrera, and G. Nunez. 1997. Interleukin-3-induced phosphorylation of BAD through the protein kinase Akt. Science 278:687-689.

Delpuech, O., B. Griffiths, P. East, A. Essafi, E. W. Lam, B. Burgering, J. Downward, and A. Schulze. 2007. Induction of Mxi1-SR alpha by FOXO3a contributes to repression of Myc-dependent gene expression. Mol Cell Biol 27:4917-4930.

Deng C, Zhang P, Harper JW, Elledge SJ, Leder P (1995) Mice lacking p21CIP1/WAF1 undergo normal development, but are defective in G1 checkpoint control. Cell 82, 675.

Desjeux P. The increase in risk factors for leishmaniasis worldwide. Trans R Soc Trop Med Hyg. 2001 May-Jun;95(3):239-43.

Di Cristofano, A., and P. P. Pandolfi. 2000. The multiple roles of PTEN in tumor suppression. Cell 100:387-390.

Donovan N, Becker EB, Konishi Y, Bonni A. JNK phosphorylation and activation of BAD couples the stress-activated signaling pathway to the cell death machinery. J Biol Chem. 2002 Oct 25;277(43):40944-9.

Dorlo TP, Balasegaram M, Beijnen JH, de Vries PJ. Miltefosine: a review of its pharmacology and therapeutic efficacy in the treatment of leishmaniasis. J Antimicrob Chemother. 2012 Nov;67(11):2576-97.

Du K, Montminy M. CREB is a regulatory target for the protein kinase Akt/PKB. J Biol Chem. 1998 Dec 4;273(49):32377-9.

Dudek, H., S. R. Datta, T. F. Franke, M. J. Birnbaum, R. Yao, G. M. Cooper, R. A. Segal, D. R. Kaplan, and M. E. Greenberg. 1997. Regulation of neuronal survival by the serine-threonine protein kinase Akt. Science 275:661-665.

Dygas A, Baranska J. (2001). Lipids and signal transduction in the nucleus. Acta Biochim Pol 48:541–549.

Efthymiadis, A., H. Shao, S. Hubner, and D. A. Jans. 1997. Kinetic characterization of the human retinoblastoma protein bipartite nuclear localization sequence (NLS) in vivo and in vitro. A comparison with the SV40 large T-antigen NLS. J Biol Chem 272:22134-22139.

Eischen CM, Weber JD, Roussel MF, Sherr CJ, Cleveland JL. Disruption of the ARF-Mdm2-p53 tumor suppressor pathway in Myc-induced lymphomagenesis. Genes Dev. 1999 Oct 15;13(20):2658-69.

Eischen, C. M., M. F. Roussel, S. J. Korsmeyer, and J. L. Cleveland. 2001. Bax loss impairs Myc-induced apoptosis and circumvents the selection of p53 mutations during Myc-mediated lymphomagenesis. Mol Cell Biol 21:7653-7662.

Ekholm SV, Reed SI (2000) Regulation of G1 cyclin-dependent kinases in the mammalian cell cycle. Cur. Op. In Cel Biol 12:678-684

Esteller M. DNA methylation and cancer therapy: new developments and expectations. Curr Opin Oncol 2005; 17:55-60.

Evan, G. I., A. H. Wyllie, C. S. Gilbert, T. D. Littlewood, H. Land, M. Brooks, C. M. Waters, L. Z. Penn, and D. C. Hancock. 1992. Induction of apoptosis in fibroblasts by c-myc protein. Cell 69:119-128.

Fan T, Li R, Todd NW, Qiu Q, Fang HB, Wang H, Shen J, Zhao RY, Caraway NP, Katz RL, Stass SA, Jiang F. Up-regulation of 14-3-3zeta in lung cancer and its implication as prognostic and therapeutic target. Cancer Res. 2007 Aug 15;67(16):7901-6.

Fanidi, A., E. A. Harrington, and G. I. Evan. 1992. Cooperative interaction between c-myc and bcl-2 proto-oncogenes. Nature 359:554-556.

Ferguson AT, Evron E, Umbricht CB, Pandita TK, Chan TA, Hermeking H, Marks JR, Lambers AR, Futreal PA, Stampfer MR, Sukumar S. High frequency of hypermethylation at the 14-3-3 sigma locus leads to gene silencing in breast cancer. Proc Natl Acad Sci U S A. 2000 May 23;97(11):6049-54.

Fernandez, P.C., Frank, S.R., Wang, L., Schroeder, M., Liu, S., Greene, J., Cocito, A., and Amati, B. (2003). Genomic targets of the human c-Myc protein. Genes Dev. 17, 1115–1129.

Firat-Karalar EN, Rauniyar N, Yates JR 3rd, Stearns T. Proximity interactions among centrosome components identify regulators of centriole duplication. Curr Biol. 2014 Mar 17;24(6):664-70.

Frank, S. R., M. Schroeder, P. Fernandez, S. Taubert, and B. Amati. 2001. Binding of c-Myc to chromatin mediates mitogen-induced acetylation of histone H4 and gene activation. Genes Dev 15:2069-2082.

Freeman, A. K., and D. K. Morrison. 2011. 14-3-3 Proteins: Diverse functions in cell proliferation and cancer progression. Semin Cell Dev Biol.

Fresno Vara, J. A., E. Casado, J. de Castro, P. Cejas, C. Belda-Iniesta, and M. Gonzalez-Baron. (2004). PI3K/Akt signalling pathway and cancer. Cancer Treat. Rev. 30:193–204.

Fukuda M, Gotoh I, Gotoh Y, Nishida E. (1996) Cytoplasmic Localization of Mitogen-activated Protein Kinase Kinase Directed by Its NH2-terminal, Leucine-rich Short Amino Acid Sequence, Which Acts as a Nuclear Export Signal. BJC 271:33. 20024-20028.

Garcia-Echeverria C, Sellers WR. (2008) Drug discovery approaches targeting the PI3K/Akt pathway in cancer. Oncogene. Sep 18 27(41):5511-26.

Gardino AK, Smerdon SJ, Yaffe MB. Structural determinants of 14-3-3 binding specificities and regulation of subcellular localization of 14-3-3-ligand complexes: a comparison of the X-ray crystal structures of all human 14-3-3 isoforms. Semin Cancer Biol. 2006 Jun;16(3):173-82.

Gearhart J, Pashos EE, Prasad MK. (2007) Pluripotency Redux – Advances in Stem-Cell Research. N Engl J Med; 367:15. 1479-1472.

Giehl M, Fabarius A, Frank O, Hochhaus A, Hafner M, Hehlmann R, Seifarth W. Centrosome aberrations in chronic myeloid leukemia correlate with stage of disease and chromosomal instability. Leukemia. 2005 Jul;19(7):1192-7.

Gill RM, Gabor T, Couzens A, Scheid MP (2013). The MYC-associated protein CDCA7 is phosphorylated by AKT to regulate MYC-dependent apoptosis and transformation. Mol Cell Biol 33(3):498-513.

Gisselsson D, Shao C, Tuck-Muller CM, Sogorovic S, Pålsson E, Smeets D, Ehrlich M. Interphase chromosomal abnormalities and mitotic missegregation of hypomethylated sequences in ICF syndrome cells. Chromosoma. 2005 Jul;114(2):118-26.

Goto, Y., R. Hayashi, T. Muramatsu, H. Ogawa, I. Eguchi, Y. Oshida, K. Ohtani, and K. Yoshida. 2006. JPO1/CDCA7, a novel transcription factor E2F1-induced protein, possesses intrinsic transcriptional regulator activity. Biochim Biophys Acta 1759:60-68.

Gottlieb T.M., Leal J.F., Seger R., Taya Y., Oren M., Cross-talk between Akt, p53 and Mdm2: possible implications for the regulation of apoptosis, Oncogene, 21: 1299- 1303, 2002

Grandori, C., S. M. Cowley, L. P. James, and R. N. Eisenman. 2000. The Myc/Max/Mad network and the transcriptional control of cell behavior. Annu Rev Cell Dev Biol 16:653-699.

Guiu J, Bergen DJ, De Pater E, Islam AB, Ayllón V, Gama-Norton L, Ruiz-Herguido C, González J, López-Bigas N, Menendez P, Dzierzak E, Espinosa L, Bigas A. Identification of Cdca7 as a novel Notch transcriptional target involved in hematopoietic stem cell emergence. J Exp Med. 2014 Nov 17;211(12):2411-23.

Haas-Kogan, D., Shalev, N., Wong, M., Mills, G., Yount, G., and Stokoe, D. (1998) AKT/Akt Activity is Increased in Glioblastoma Cell Lines due to Mutation of PTEN. Curr Biol 8, 1195-1198

Hall M, Peters G (1996) Genetic alterations of cyclins, cyclin-dependent kinases, and CDK inhibitors in human cancer. Adv. Cancer Res. 68, 67.

Hann, S. R., and R. N. Eisenman. 1984. Proteins encoded by the human c-myc oncogene: differential expression in neoplastic cells. Mol. Cell. Biol. 4:2486-2497.

Harrington EA, Bennett MR, Fanidi A, Evan GI.(1994) c-Myc-induced apoptosis in fibroblasts is inhibited by specific cytokines. EMBO J 13(14):3286–95.

Harris AW, Pinkert CA, Crawford M, Langdon WY, Brinster RL, Adams JM. The E mu-myc transgenic mouse. A model for high-incidence spontaneous lymphoma and leukemia of early B cells. J Exp Med. 1988 Feb 1;167(2):353-71.

Harris MH, Thompson CB. The role of the Bcl-2 family in the regulation of outer mitochondrial membrane permeability. Cell Death Differ. 2000 Dec;7(12):1182-91.

Hartwell LH, Culotti J, and Reid B (1970). Genetic Control of the Cell-Division Cycle in Yeast, I. Detection of Mutants PNAS 66: 352-359

Han X, Liu D, Zhang Y, Li Y, Lu W, Chen J, Songyang Z. Akt regulates TPP1 homodimerization and telomere protection. Aging Cell. 2013 Dec;12(6):1091-9

Hanson, K. D., M. Shichiri, M. R. Follansbee, and J. M. Sedivy. 1994. Effects of c-myc expression on cell cycle progression. Mol Cell Biol 14:5748-5755.

Haupt Y, Rowan S, Shaulian E, Kazaz A, Vousden K, Oren M. p53 mediated apoptosis in HeLa cells: transcription dependent and independent mechanisms. Leukemia. 1997 Apr;11 Suppl 3:337-9.

Heikkila R, Schwab G, Wickstrom E, Loke SL, Pluznik DH, Watt R, Neckers LM. A c-myc antisense oligodeoxynucleotide inhibits entry into S phase but not progress from G0 to G1. Nature. 1987 Jul 30-Aug 5;328(6129):445-9.

Hemann, M. T., A. Bric, J. Teruya-Feldstein, A. Herbst, J. A. Nilsson, C. Cordon-Cardo, J. L. Cleveland, W. P. Tansey, and S. W. Lowe. 2005. Evasion of the p53 tumour surveillance network by tumour-derived MYC mutants. Nature 436:807-811.

Hermeking, H., and D. Eick. 1994. Mediation of c-Myc-induced apoptosis by p53. Science 265:2091-2093.

Hermeking H, Lengauer C, Polyak K, He TC, Zhang L, Thiagalingam S, Kinzler KW, Vogelstein B. 14-3-3sigma is a p53-regulated inhibitor of G2/M progression. Mol Cell. 1997 Dec;1(1):3-11

Hill MM, Andjelkovic M, Brazil DP, Ferrari S, Fabbro D, Hemmings BA. Insulin-stimulated protein kinase B phosphorylation on Ser-473 is independent of its activity and occurs through a staurosporine-insensitive kinase. J Biol Chem. 2001 Jul 13;276(28):25643-6.

Hornbeck PV, Zhang B, Murray B, Kornhauser JM, Latham V, Skrzypek E. PhosphoSitePlus, 2014: mutations, PTMs and recalibrations. Nucleic Acids Res. 2015 Jan;43(Database issue):D512-20

Huang, A., C. S. Ho, R. Ponzielli, D. Barsyte-Lovejoy, E. Bouffet, D. Picard, C. E. Hawkins, and L. Z. Penn. 2005. Identification of a novel c-Myc protein interactor, JPO2, with transforming activity in medulloblastoma cells. Cancer Res 65:5607-5619.

Huang Y-T, Mason JO, Price DJ. Lateral cortical Cdca7 expression levels are regulated by Pax6 and influence the production of intermediate progenitors. BMC Neuroscience. 2017;18:47.

Huminiecki L, Heldin CH. 2R and remodeling of vertebrate signal transduction engine. BMC Biol. 2010 Dec 13;8:146. doi: 10.1186/1741-7007-8-146.

Hunt T (1993) Cyclins and their partners: from a simple idea to a complicated reality. Semin Cell Biol 2:213-222

Iwata N, Yamamoto H, Sasaki S, Itoh F, Suzuki H, Kikuchi T, Kaneto H, Iku S, Ozeki I, Karino Y, Satoh T, Toyota J, Satoh M, Endo T, Imai K. Frequent hypermethylation of CpG islands and loss of expression of the 14-3-3 sigma gene in human hepatocellular carcinoma. Oncogene. 2000 Nov 2;19(46):5298-302.

Jain M, Arvanitis C, Chu K, Dewey W, Leonhardt E, Trinh M, Sundberg CD, Bishop JM, Felsher DW. Sustained loss of a neoplastic phenotype by brief inactivation of MYC. Science. 2002 Jul 5;297(5578):102-4.

Jérôme V, Müller R. A synthetic leucine zipper-based dimerization system for combining multiple promoter specificities. Gene Ther. 2001 May;8(9):725-9.

Johnson C, Tinti M, Wood NT, Campbell DG, Toth R, Dubois F, Geraghty KM, Wong BH, Brown LJ, Tyler J, Gernez A, Chen S, Synowsky S, MacKintosh C. Visualization and biochemical analyses of the emerging mammalian 14-3-3-phosphoproteome. Mol Cell Proteomics. 2011 Oct;10(10):M110.005751.

Johnson DG, Walker CL (1999). Cyclins and cell cycle checkpoints. Ann Rev Pharmacol Toxicol 39:295-312.

Jones PF, Jakubowicz T, Hemmings BA. Molecular cloning of a second form of rac protein kinase. Cell Regul. 1991 Dec;2(12):1001-9.

Jones DH, Ley S, Aitken A. Isoforms of 14-3-3 protein can form homo- and heterodimers in vivo and in vitro: implications for function as adapter proteins. FEBS Lett. 1995 Jul 10;368(1):55-8

Jones DT. Protein secondary structure prediction based on position-specific scoring matrices. J Mol Biol. 1999 Sep 17;292(2):195-202.

Jücker M, Südel K, Horn S, Sickel M, Wegner W, Fiedler W, Feldman RA. Expression of a mutated form of the p85alpha regulatory subunit of phosphatidylinositol 3-kinase in a Hodgkin's lymphoma-derived cell line (CO). Leukemia. 2002 May;16(5):894-901.

Juin P, Hueber AO, Littlewood T, Evan G. c-Myc-induced sensitization to apoptosis is mediated through cytochrome c release. Genes Dev. 1999 Jun 1;13(11):1367-81.

Kamb A (1998) Cyclin-dependent kinase inhibitors and human cancer. Curr. Top. Microbiol. Immunol. 227, 139

Kauffmann-Zeh, A., P. Rodriguez-Viciana, E. Ulrich, C. Gilbert, P. Coffer, J. Downward, and G. Evan. 1997. Suppression of c-Myc-induced apoptosis by Ras signalling through PI(3)K and PKB. Nature 385:544-548.

Kelly, K., Cochran, B.H., Stiles, C.D., and Leder, P. (1983). Cell-specific regulation of the c-myc gene by lymphocyte mitogens and platelet-derived growth factor. Cell 35, 603–610.

Kennedy, S. G., A. J. Wagner, S. D. Conzen, J. Jordan, A. Bellacosa, P. N. Tsichlis, and N. Hay. 1997. The PI 3-kinase/Akt signaling pathway delivers an anti-apoptotic signal. Genes Dev 11:701-713.

Kerkhoff E and Rapp UR (1998) Cell cycle targets of Ras/Raf signalling, Oncogene, 17, 1457–1462

Khan M, Pelengaris S (2007) 'c-myc apoptosis and disordered tissue growth', in Apoptosis, Cell Signaling, and Human Diseases, 137- 178, Editors: Srivastava R, Humana

Khwaja, A., P. Rodriguez-Viciana, S. Wennstrom, P. H. Warne, and J. Downward. 1997. Matrix adhesion and Ras transformation both activate a phosphoinositide 3-OH kinase and protein kinase B/Akt cellular survival pathway. Embo J 16:2783-2793.

Kim DI, Birendra KC, Zhu W, Motamedchaboki K, Doye V, Roux KJ. Probing nuclear pore complex architecture with proximity-dependent biotinylation. Proc Natl Acad Sci U S A. 2014 Jun 17;111(24):E2453-61

Kimura K, Hirano M, Kobayashi R, Hirano T. Phosphorylation and activation of 13S condensin by Cdc2 in vitro. Science. 1998 Oct 16;282(5388):487-90.

Knobbe, C. B. and Reifenberger, G. (2003), Genetic Alterations and Aberrant Expression of Genes Related to the Phosphatidyl-lnositol-3′-Kinase/Protein Kinase B (Akt) Signal Transduction Pathway in Glioblastomas. Brain Pathology, 13: 507–518.

Kolliputi N, Waxman AB. IL-6 cytoprotection in hyperoxic acute lung injury occurs via PI3K/Akt-mediated Bax phosphorylation. Am J Physiol Lung Cell Mol Physiol. 2009 Jul;297(1):L6-16.

Krimpenfort P, Ijpenberg A, Song JY, van der Valk M, Nawijn M, Zevenhoven J, Berns A. p15Ink4b is a critical tumour suppressor in the absence of p16Ink4a. Nature. 2007 Aug 23;448(7156):943-6.

Laplante M, Sabatini DM. mTOR signaling in growth control and disease. Cell. 2012 Apr 13;149(2):274-93.

Lee HK, Kumar P, Fu Q, Rosen KM, Querfurth HW. The insulin/Akt signaling pathway is targeted by intracellular beta-amyloid. Mol Biol Cell. 2009 Mar;20(5):1533-44.

Leonard R, Hardy J, van Tienhoven G, Houston S, Simmonds P, David M, Mansi J. Randomized, double-blind, placebo-controlled, multicenter trial of 6% miltefosine solution, a topical chemotherapy in cutaneous metastases from breast cancer. J Clin Oncol. 2001 Nov 1;19(21):4150-9.

Letai A, Sorcinelli MD, Beard C, Korsmeyer SJ. 2004. Antiapoptotic BCL-2 is required for maintenance of a model leukemia. Cancer Cell 6: 241 –249.

Levine AJ, Oren M. The first 30 years of p53: growing ever more complex. Nat Rev Cancer. 2009 Oct;9(10):749-58. doi: 10.1038/nrc2723. Review.

Levens, D. (2010). You don’t muck with MYC. Genes Cancer 1, 547–554.

Li, J., L. Simpson, M. Takahashi, C. Miliaresis, M. P. Myers, N. Tonks, and R. Parsons. 1998. The PTEN/MMAC1 tumor suppressor induces cell death that is rescued by the AKT/protein kinase B oncogene. Cancer Res 58:5667-5672.

Lietzke SE, Bose S, Cronin T, Klarlund J, Chawla A, Czech MP, Lambright DG. Structural basis of 3-phosphoinositide recognition by pleckstrin homology domains. Mol Cell. 2000 Aug;6(2):385-94.

Lin, H., Bondy, M. L., Langford, L. A., Hess, K. R., Delclos, G. L., Wu, X., Chan, W., Pershouse, M. A., Yung, W. K., and Steck, P. A. (1998) Allelic deletion analyses of MMAC/PTEN and DMBT1 loci in gliomas: Relationship to prognostic significance. Clin Cancer Res 4, 2447-2454

Lodygin D, Hermeking H. Epigenetic silencing of 14-3-3sigma in cancer. Semin Cancer Biol. 2006 Jun;16(3):214-24.

Lowe SW, Cepero E, Evan G. 2004. Intrinsic tumour suppression. Nature 432: 307–315.

Madeira, F., Tinti, M., Murugesan, G., Berrett, E., Stafford, M., Toth, R., Cole, C., MacKintosh, C. and Barton, G.J. (2015) 14-3-3-Pred: Improved methods to predict 14-3-3-binding phosphopeptides. Bioinformatics, 2015 Mar 3, btv133

Maehama, T., and Dixon, J. E. (1998) The tumor suppressor, PTEN/MMAC1, dephosphorylates the lipid second messenger, phosphatidylinositol 3,4,5-trisphosphate. J Biol Chem 273, 13375-13378

Malumbres, M., Pevarello, P., Barbacid, M., and Bischoff, J.R. (2008). CDK inhibitors in cancer therapy: what is next? Trends in pharmacological sciences 29, 16-21.

Martelli AM, Chiarini F, Evangelisti C, Cappellini A, Buontempo F, Bressanin D, Fini M, McCubrey JA. Two hits are better than one: targeting both phosphatidylinositol 3-kinase and mammalian target of rapamycin as a therapeutic strategy for acute leukemia treatment. Oncotarget. 2012 Apr;3(4):371-94.

Martini M, Ciraolo E, Gulluni F, Hirsch E. Targeting PI3K in Cancer: Any Good News? Front Oncol. 2013 May 8;3:108

Martin-Subero JI, Odero MD, Hernandez R, Cigudosa JC, Agirre X, Saez B, Sanz-Garcia E, Ardanaz MT, Novo FJ, Gascoyne RD, et al. 2005. Amplification of IGH/MYC fusion in clinically aggressive IGH/BCL-2-positive germinal center B-cell lymphomas. Genes Chromosomes Cancer 43: 414 –423.

Mateyak, M. K., A. J. Obaya, S. Adachi, and J. M. Sedivy. 1997. Phenotypes of c-Myc-deficient rat fibroblasts isolated by targeted homologous recombination. Cell Growth Differ 8:1039-1048.

Matitau AE, Scheid MP. Phosphorylation of MEKK3 at threonine 294 promotes 14-3-3 association to inhibit nuclear factor kappaB activation. J Biol Chem. 2008 May 9;283(19):13261-8.

Maruyama K, Schiavi SC, Huse W, Johnson GL, Ruley HE. myc and E1A oncogenes alter the responses of PC12 cells to nerve growth factor and block differentiation. Oncogene. 1987;1(4):361-7.

Massague J (2004). G1 cell-cycle control and cancer. Nature 432: 298-306.

Massague J, Wotton D (2000) Transcriptional control by the TGF beta/Smad signaling system. EMBO J 19:1745-1754

Matitau, A. E., and M. P. Scheid. 2008. Phosphorylation of MEKK3 at threonine 294 promotes 14-3-3 association to inhibit nuclear factor kappaB activation. J Biol Chem 283:13261-13268.

Matsushime H, Ewen ME, Strom DK, Kato JY, Hanks SK, Roussel MF, Sherr CJ. Identification and properties of an atypical catalytic subunit (p34PSK-J3/cdk4) for mammalian D type G1 cyclins. Cell. 1992 Oct 16;71(2):323-34.

Matta A, DeSouza LV, Ralhan R, Siu KW. Small interfering RNA targeting 14-3-3zeta increases efficacy of chemotherapeutic agents in head and neck cancer cells. Mol Cancer Ther. 2010; 9:2676–88.

Mauro, V. P., & Chappell, S. A. (2014). A critical analysis of codon optimization in human therapeutics. Trends in Molecular Medicine, 20(11), 604–613.

Mayo L.D., Donner D.B., A phosphatidylinositol 3- kinase/Akt pathway promotes translocation of Mdm2 from the cytoplasm to the nucleus, Proc. Natl. Acad. Sci. USA., 98: 11598-11603, 2001

Maxwell SA, Li Z, Jaye D, Ballard S, Ferrell J, Fu H. 14-3-3zeta mediates resistance of diffuse large B cell lymphoma to an anthracycline-based chemotherapeutic regimen. J Biol Chem. 2009; 284:22379–89.

McDonald ER III, el Deiry WS (2000) Cell cycle control as a basis for cancer drug development. Int. J. Oncol. 16, 871.

Menssen A, Hermeking H. Characterization of the c-MYC-regulated transcriptome by SAGE: identification and analysis of c-MYC target genes. Proc Natl Acad Sci U S A. 2002 Apr 30;99(9):6274-9.

Mertz JA, Conery AR, Bryant BM, Sandy P, Balasubramanian S, Mele DA, Bergeron L, Sims RJ 3rd. Targeting MYC dependence in cancer by inhibiting BET bromodomains. Proc Natl Acad Sci U S A. 2011 Oct 4;108(40):16669-74.

Meyer, N., S. S. Kim, and L. Z. Penn. 2006. The Oscar-worthy role of Myc in apoptosis. Semin Cancer Biol 16:275-287.

Meyer, N., and L. Z. Penn. 2008. Reflecting on 25 years with MYC. Nat Rev Cancer 8:976-990.

Mhawech P. (2005) 14-3-3 proteins – an update. Cell Research 15(4). 228-236.

Mitchell KO, Ricci MS, Miyashita T, Dicker DT, Jin Z, Reed JC, El-Deiry WS. Bax is a transcriptional target and mediator of c-myc-induced apoptosis. Cancer Res. 2000 Nov 15;60(22):6318-25.

Moll, T., G. Tebb, U. Surana, H. Robitsch, and K. Nasmyth. 1991. The role of phosphorylation and the CDC28 protein kinase in cell cycle-regulated nuclear import of the S. cerevisiae transcription factor SWI5. Cell 66:743-758.

Moon Z, Wang Y, Aryan N, Mousseau DD, Scheid MP. Serine 396 of PDK1 is required for maximal PKB activation. Cell Signal. 2008 Nov;20(11):2038-49.

Moreira JM, Gromov P, Celis JE. Expression of the tumor suppressor protein 14-3-3σ is down-regulated in invasive transitional cell carcinomas of the urinary bladder undergoing epithelial-to-mesenchymal transition. Mol Cell Proteomics 2004; 3: 410-9

Morrison DK. The 14-3-3 proteins: integrators of diverse signaling cues that impact cell fate and cancer development. Trends Cell Biol. 2009 Jan;19(1):16-23

Murphy DJ, Junttila MR, Pouyet L, Karnezis A, Shchors K, Bui DA, Brown-Swigart L, Johnson L, Evan GI. 2008. Distinct thresholds govern Myc's biological output in vivo. Cancer Cell 14: 447–457.

Muslin AJ, Xing H. 14-3-3 proteins: regulation of subcellular localization by molecular interference. Cell Signal. 2000 Dec;12(11-12):703-9.

Mymryk, J. S., K. Shire, and S. T. Bayley. 1994. Induction of apoptosis by adenovirus type 5 E1A in rat cells requires a proliferation block. Oncogene 9:1187-1193.

Morgan DO (1995) Principles of CDK regulation. Nature 374, 131.

Nam HJ, Chae S, Jang SH, Cho H, Lee JH. The PI3K-Akt mediates oncogenic Met-induced centrosome amplification and chromosome instability. Carcinogenesis. 2010 Sep;31(9):1531-40.

Nan X, Tamgüney TM, Collisson EA, Lin LJ, Pitt C, Galeas J, Lewis S, Gray JW, McCormick F, Chu S. Ras-GTP dimers activate the Mitogen-Activated Protein Kinase (MAPK) pathway. Proc Natl Acad Sci U S A. 2015 Jun 30;112(26):7996-8001

Neiman PE, Thomas SJ, Loring G. 1991. Induction of apoptosis during normal and neoplastic B-cell development in the bursa of Fabricius. Proc Natl Acad Sci 88: 5857– 5861.

Nilsson, J. A., and J. L. Cleveland. 2003. Myc pathways provoking cell suicide and cancer. Oncogene 22:9007-9021.

Obenauer JC, Cantley LC, Yaffe MB. (2003) Scansite 2.0: Proteome-wide prediction of cell signalling interactions using short sequence motifs. Nucleic Acids Res. 31(13).3635-41.

Obsil, T., Ghirlando, R., Klein, D. C., Ganguly, S. and Dyda, F. (2001). Crystal structure of the 14-3-3zeta:serotonin N-acetyltransferase complex. a role for scaffolding in enzyme regulation. Cell 105, 257-267.

Obsilova V, Vecer J, Herman P, Pabianova A, Sulc M, Teisinger J, Boura E, Obsil T. 14-3-3 Protein interacts with nuclear localization sequence of forkhead transcription factor FoxO4. Biochemistry. 2005 Aug 30;44(34):11608-17.

Oster, S. K., C. S. W. Ho, E. L. Soucie, and L. Z. Penn. 2002. The myc Oncogene: omplex, p. 81-154, Adv Cancer Res, vol. Volume 84. Academic Press.

Osthus, R. C., B. Karim, J. E. Prescott, B. D. Smith, M. McDevitt, D. L. Huso, and C. V. Dang. 2005. The Myc target gene JPO1/CDCA7 is frequently overexpressed in human tumors and has limited transforming activity in vivo. Cancer Res 65:5620-5627.

Ou, X. M., K. Chen, and J. C. Shih. 2006. Monoamine oxidase A and repressor R1 are involved in apoptotic signaling pathway. Proc Natl Acad Sci U S A 103:10923-10928.

Ozdek A, Sarac S, Akyol MU, Sungur A, Yilmaz T. 2004. c-myc and bcl-2 expression in supraglottic squamous cell carcinoma of the larynx. Otolaryngol Head Neck Surg 131: 77–83.

Pagano M (1997) Cell cycle regulation by the ubiquitin pathway. FASEB J. 11, 1067.

Pal SK, Reckamp K, Yu H, Figlin RA. Akt inhibitors in clinical development for the treatment of cancer. Expert Opin Investig Drugs. 2010 Nov;19(11):1355-66

Parisi, F., P. Wirapati, and F. Naef. 2007. Identifying synergistic regulation involving c-Myc and sp1 in human tissues. Nucleic Acids Res 35:1098-1107.

Park S, Chung S, Kim KM, Jung KC, Park C, Hahm ER, Yang CH. Determination of binding constant of transcription factor myc-max/max-max and E-box DNA: the effect of inhibitors on the binding. Biochim Biophys Acta. 2004 Feb 24;1670(3):217-28.

Paul A-L, Denison FC, Schultz ER, Zupanska AK, Ferl RJ (2012) 14-3-3 phosphoprotein interaction networks – does isoform diversity present functional interaction specification? Frontiers in Plant Science 3: 190

Pemberton LF, Paschal BM.(2005). Mechanisms of receptormediated nuclear import and nuclear export. Traffic 6: 187–198.

Peterson R.T., Schreiber S.L., Kinase phosphorylation: keeping it all in the family, Curr. Biol., 9: R521-524, 1999

Peyressatre M, Prével C, Pellerano M, Morris MC. Targeting cyclin-dependent kinases in human cancers: from small molecules to Peptide inhibitors. Cancers (Basel). 2015 Jan 23;7(1):179-237

Philp AJ, Campbell IG, Leet C, Vincan E, Rockman SP, Whitehead RH, Thomas RJ, Phillips WA. The phosphatidylinositol 3'-kinase p85alpha gene is an oncogene in human ovarian and colon tumors. Cancer Res. 2001 Oct 15;61(20):7426-9

Porta C, Figlin RA. Phosphatidylinositol-3-kinase/Akt signaling pathway and kidney cancer, and the therapeutic potential of phosphatidylinositol-3-kinase/Akt inhibitors. J Urol. 2009 Dec;182(6):2569-77.

Prendergast GC. (1999) Mechanisms of apoptosis by c-Myc. Oncogene. May 13;18(19):2967-87.

Prescott, J. E., R. C. Osthus, L. A. Lee, B. C. Lewis, H. Shim, J. F. Barrett, Q. Guo, A. L. Hawkins, C. A. Griffin, and C. V. Dang. 2001. A novel c-Myc-responsive gene, JPO1, participates in neoplastic transformation. J Biol Chem 276:48276-48284.

Puntervoll P, Linding R, Gemünd C, Chabanis-Davidson S, Mattingsdal M, Cameron S, Martin DM, Ausiello G, Brannetti B, Costantini A, Ferrè F, Maselli V, Via A, Cesareni G, Diella F,

Superti-Furga G, Wyrwicz L, Ramu C, McGuigan C, Gudavalli R, Letunic I, Bork P, Rychlewski L, Küster B, Helmer-Citterich M, Hunter WN, Aasland R, Gibson TJ. ELM server: A new resource for investigating short functional sites in modular eukaryotic proteins. Nucleic Acids Res. 2003 Jul 1;31(13):3625-30.

Pusapati, R. V., R. J. Rounbehler, S. Hong, J. T. Powers, M. Yan, K. Kiguchi, M. J. McArthur, P. K. Wong, and D. G. Johnson. 2006. ATM promotes apoptosis and suppresses tumorigenesis in response to Myc. Proceedings of the National Academy of Sciences of the United States of America 103:1446-1451.

Robson SC, Ward L, Brown H, Turner H, Hunter E, Pelengaris S, Khan M. Deciphering c-MYC-regulated genes in two distinct tissues. BMC Genomics. 2011 Sep 30;12:476.

Rocca A, Schirone A, Maltoni R, Bravaccini S, Cecconetto L, Farolfi A, Bronte G, Andreis D. Progress with palbociclib in breast cancer: latest evidence and clinical considerations. Ther Adv Med Oncol. 2017 Feb;9(2):83-105

Roux KJ, Kim DI, Raida M, Burke B. 2012. A promiscuous biotin ligase fusion protein identifies proximal and interacting proteins in mammalian cells. J Cell Biol.196(6):801-810.

Qi, Y., M. A. Gregory, Z. Li, J. P. Brousal, K. West, and S. R. Hann. 2004. p19ARF directly and differentially controls the functions of c-Myc independently of p53. Nature 431:712-717.

Qin, X. Q., D. M. Livingston, W. G. Kaelin, Jr., and P. D. Adams. 1994. Deregulated transcription factor E2F-1 expression leads to S-phase entry and p53-mediated apoptosis. Proceedings of the National Academy of Sciences of the United States of America 91:10918-10922.

Rabbitts PH, Watson JV, Lamond A, Forster A, Stinson MA, Evan G, Fischer W, Atherton E, Sheppard R, Rabbitts TH. Metabolism of c-myc gene products: c-myc mRNA and protein expression in the cell cycle. EMBO J. 1985 Aug;4(8):2009-15.

Rao, L., M. Debbas, P. Sabbatini, D. Hockenbery, S. Korsmeyer, and E. White. 1992. The adenovirus E1A proteins induce apoptosis, which is inhibited by the E1B 19-kDa and Bcl-2 proteins. Proceedings of the National Academy of Sciences of the United States of America 89:7742-7746.

Rohn JL, Hueber AO, McCarthy NJ, Lyon D, Navarro P, Burgering BM, Evan GI. The opposing roles of the Akt and c-Myc signalling pathways in survival from CD95-mediated apoptosis. Oncogene. 1998 Dec 3;17(22):2811-8.

Rottman S, Luscher B. (2006). The mad side of the max network: antagonizing the function of myc and more. Curr Top Microbiol Immunol 302: 63–122.

Rudolph, B., R. Saffrich, J. Zwicker, B. Henglein, R. Muller, W. Ansorge, and M. Eilers. 1996. Activation of cyclin-dependent kinases by Myc mediates induction of cyclin A, but not apoptosis. Embo J 15:3065-3076.

Rushworth LK, Hindley AD, O'Neill E, Kolch W. Regulation and role of Raf-1/B-Raf heterodimerization. Mol Cell Biol. 2006 Mar;26(6):2262-72

Russo AA, Tong L, Lee JO, Jeffrey PD, Pavletich NP (1998) Structural basis of inhibition of the cyclin-dependent kinase Cdk6 by the tumour suppressor p16INK4a. Nature 395:237-243

Sampath SC, Ohi R, Leismann O, Salic A, Pozniakovski A, Funabiki H. The chromosomal passenger complex is required for chromatin-induced microtubule stabilization and spindle assembly. Cell (2004) 118:187–202.

Santoni-Rugiu E, Falck J, Mailand N, Bartek J, Lukas J. Involvement of Myc activity in a G(1)/S-promoting mechanism parallel to the pRb/E2F pathway. Mol Cell Biol. 2000 May;20(10):3497-509.

Sarbassov DD, Guertin DA, Ali SM, Sabatini DM. Phosphorylation and regulation of Akt/PKB by the rictor-mTOR complex. Science. 2005 Feb 18;307(5712):1098-101.

Schmid P, Schulz WA, Hameister H. (1989) Dynamic expression pattern of the myc protooncogene in midgestation mouse embryos. Science 243(4888):226–229

Schmitt CA, Fridman JS, Yang M, Baranov E, Hoffman RM and Lowe SW. (2002). Cancer Cell, 1, 289–298.

Schmitz R, Ceribelli M, Pittaluga S, Wright G, Staudt LM. 2014. Oncogenic mechanisms in Burkitt lymphoma. Cold Spring Harb Perspect Med 4: 014282.

Sciortino S, Gurtner A, Manni I, Fontemaggi G, Dey A, Sacchi A, Ozato K, Piaggio G. The cyclin B1 gene is actively transcribed during mitosis in HeLa cells. EMBO Rep. 2001 Nov;2(11):1018-23.

Sears R, Leone G, DeGregori J, Nevins JR. Ras enhances Myc protein stability. Mol Cell. 1999 Feb;3(2):169-79.

Senderowicz AM, Sausville EA. Preclinical and clinical development of cyclin-dependent kinase modulators. J Natl Cancer Inst. 2000 Mar 1;92(5):376-87.

Sephton CF, Zhang D, Lehmann TM, Pennington PR, Scheid MP, Mousseau DD. The nuclear localization of 3'-phosphoinositide-dependent kinase-1 is dependent on its association with the protein tyrosine phosphatase SHP-1. Cell Signal. 2009 Nov;21(11):1634-44.

She, Q. B., D. B. Solit, Q. Ye, K. E. O'Reilly, J. Lobo, and N. Rosen. 2005. The BAD protein integrates survival signaling by EGFR/MAPK and PI3K/Akt kinase pathways in PTEN-deficient tumor cells. Cancer Cell 8:287-297.

Shiio Y, Suh KS, Lee H, Yuspa SH, Eisenman RN, Aebersold R. Quantitative proteomic analysis of myc-induced apoptosis: a direct role for Myc induction of the mitochondrial chloride ion channel, mtCLIC/CLIC4. J Biol Chem. 2006 Feb 3;281(5):2750-6.

Singh, A., M. Ye, O. Bucur, S. Zhu, M. Tanya Santos, I. Rabinovitz, W. Wei, D. Gao, W. C. Hahn, and R. Khosravi-Far. Protein phosphatase 2A reactivates FOXO3a through a dynamic interplay with 14-3-3 and AKT. Molecular biology of the cell 21:1140-1152.

Simpson L., Parsons R., PTEN: life as a tumor suppressor, Exp. Cell. Res, 264: 29-41, 2001

Skeen, J. E., P. T. Bhaskar, C. C. Chen, W. S. Chen, X. D. Peng, V. Nogueira, A. Hahn-Windgassen, H. Kiyokawa, and N. Hay. 2006. Akt deficiency impairs normal cell proliferation and suppresses oncogenesis in a p53-independent and mTORC1-dependent manner. Cancer Cell 10:269-280.

Skorski T, Bellacosa A, Nieborowska-Skorska M, Majewski M, Martinez R, Choi JK, Trotta R, Wlodarski P, Perrotti D, Chan TO, Wasik MA, Tsichlis PN, Calabretta B. Transformation of hematopoietic cells by BCR/ABL requires activation of a PI-3k/Akt-dependent pathway. EMBO J. 1997 Oct 15;16(20):6151-61.

Smith AJ, Daut J, Schwappach B. Membrane proteins as 14-3-3 clients in functional regulation and intracellular transport. Physiology (Bethesda). 2011 Jun;26(3):181-91.

Song G, Ouyang G, Bao S. The activation of Akt/PKB signaling pathway and cell survival. J Cell Mol Med. 2005 Jan-Mar;9(1):59-71.

Sordella R, Bell DW, Haber DA, Settleman J. Gefitinib-sensitizing EGFR mutations in lung cancer activate anti-apoptotic pathways. Science. 2004 Aug 20;305(5687):1163-7.

Soucek, L., and G. I. Evan. 2010. The ups and downs of Myc biology. Curr Opin Genet Dev 20:91-95.

Soucie EL, Annis MG, Sedivy J, Filmus J, Leber B, Andrews DW, Penn LZ. Myc potentiates apoptosis by stimulating Bax activity at the mitochondria. Mol Cell Biol. 2001 Jul;21(14):4725-36.

Spencer CA, Groudine M. (1991) Control of c-myc regulation in normal and neoplastic cells. Adv Cancer Res 6:1–48.

Staal SP. Molecular cloning of the akt oncogene and its human homologues AKT1 and AKT2: amplification of AKT1 in a primary human gastric adenocarcinoma. Proc Natl Acad Sci U S A. 1987 Jul;84(14):5034-7.

Stål O, Pérez-Tenorio G, Akerberg L, Olsson B, Nordenskjöld B, Skoog L, Rutqvist LE. Akt kinases in breast cancer and the results of adjuvant therapy. Breast Cancer Res. 2003;5(2):R37-44.

Stambolic, V., A. Suzuki, J. L. de la Pompa, G. M. Brothers, C. Mirtsos, T. Sasaki, J. Ruland, J. M. Penninger, D. P. Siderovski, and T. W. Mak. 1998. Negative regulation of PKB/Akt-dependent cell survival by the tumor suppressor PTEN. Cell 95:29-39.

Stanton BR, Reid SW, Parada LF. Germ line transmission of an inactive N-myc allele generated by homologous recombination in mouse embryonic stem cells. Mol Cell Biol. 1990 Dec;10(12):6755-8.

Stephens L, Anderson K, Stokoe D, Erdjument-Bromage H, Painter GF, Holmes AB, Gaffney PR, Reese CB, McCormick F, Tempst P, Coadwell J, Hawkins PT. Protein kinase B kinases that mediate phosphatidylinositol 3,4,5-trisphosphate-dependent activation of protein kinase B. Science. 1998 Jan 30;279(5351):710-4.

Stevaux, O. & Dyson, N. J (2002).A revised picture of the E2F transcriptional network and RB function.Curr.Opin. Cell Biol. 14, 684–691

Stone J, de Lange T, Ramsay G, Jakobovits E, Bishop JM, Varmus H, Lee W. Definition of regions in human c-myc that are involved in transformation and nuclear localization. Mol Cell Biol. 1987 May;7(5):1697-709.

StrasserA, HarrisAW,BathML,CoryS.1990.Novel primitive lymphoid tumours induced in transgenic mice by cooperation between myc and bcl-2. Nature 348: 331–333.

Sun M, Wang G, Paciga JE, Feldman RI, Yuan ZQ, Ma XL, Shelley SA, Jove R, Tsichlis PN, Nicosia SV, Cheng JQ. AKT1/PKBalpha kinase is frequently elevated in human cancers and its constitutive activation is required for oncogenic transformation in NIH3T3 cells. Am J Pathol. 2001 Aug;159(2):431-7.

Takahashi K, Yamanaka S. Induction of pluripotent stem cells from mouse embryonic and adult fibroblast cultures by defined factors. Cell. 2006 Aug 25;126(4):663-76.

Takayama S, Sato T, Krajewski S, Kochel K, Irie S, Millan JA, Reed JC. 1995. Cloning and functional analysis of BAG-1: A novel Bcl-2-binding protein with anti-cell death activity. Cell 80: 279–284.

Tan J, Yu Q. Molecular mechanisms of tumor resistance to PI3K-mTOR-targeted therapy. Chin J Cancer. 2013 Jul;32(7):376-9. doi: 10.5732/cjc.012.10287.

Terakawa N, Kanamori Y, Yoshida S. Loss of PTEN expression followed by Akt phosphorylation is a poor prognostic factor for patients with endometrial cancer. Endocr Relat Cancer. 2003 Jun;10(2):203-8.

Thijssen PE, Ito Y, Grillo G, Wang J, Velasco G, Nitta H, Unoki M, Yoshihara M, Suyama M, Sun Y, Lemmers RJ, de Greef JC, Gennery A, Picco P, Kloeckener-Gruissem B, Güngör T, Reisli I, Picard C, Kebaili K, Roquelaure B, Iwai T, Kondo I, Kubota T, van Ostaijen-Ten Dam MM, van Tol MJ, Weemaes C, Francastel C, van der Maarel SM, Sasaki H. Mutations in CDCA7 and HELLS cause immunodeficiency-centromeric instability-facial anomalies syndrome. Nat Commun. 2015 Jul 28;6:7870.

Thompson CB, Challoner PB, Neiman PE, Groudine M. Levels of c-myc oncogene mRNA are invariant throughout the cell cycle. Nature. 1985 Mar 28-Apr 3;314(6009):363-6.

Thorpe LM, Yuzugullu H, Zhao JJ. PI3K in cancer: divergent roles of isoforms, modes of activation and therapeutic targeting. Nat Rev Cancer. 2015 Jan;15(1):7-24.

Tinti M, Johnson C, Toth R, Ferrier DEK, MacKintosh C. Evolution of signal multiplexing by 14-3-3-binding 2R-ohnologue protein families in the vertebrates. Open Biology. 2012;2(7):120103. doi:10.1098/rsob.120103.

Tinti M, Madeira F, Murugesan G, Hoxhaj G, Toth R, MacKintosh C. ANIA: ANnotation and Integrated Analysis of the 14-3-3 interactome. Database: The Journal of Biological Databases and Curation. 2014;2014:bat085.

Toker A, Newton AC. Akt/protein kinase B is regulated by autophosphorylation at the hypothetical PDK-2 site. J Biol Chem. 2000 Mar 24;275(12):8271-4.

Tsao AS, McDonnell T, Lam S, Putnam JB, Bekele N, Hong WK, Kurie JM. Increased phospho-AKT (Ser(473)) expression in bronchial dysplasia: implications for lung cancer prevention studies. Cancer Epidemiol Biomarkers Prev. 2003 Jul;12(7):660-4.

Tse C, Shoemaker AR, Adickes J, Anderson MG, Chen J, Jin S, Johnson EF, Marsh KC, Mitten MJ, Nimmer P, Roberts L, Tahir SK, Xiao Y, Yang X, Zhang H, Fesik S, Rosenberg SH, Elmore SW. ABT-263: a potent and orally bioavailable Bcl-2 family inhibitor. Cancer Res. 2008 May 1;68(9):3421-8.

Tsuruta F, Masuyama N, Gotoh Y. The phosphatidylinositol 3-kinase (PI3K)-Akt pathway suppresses Bax translocation to mitochondria. J Biol Chem. 2002 Apr 19;277(16):14040-7.

Tuck-Muller CM, Narayan A, Tsien F, Smeets DF, Sawyer J, Fiala ES, Sohn OS, Ehrlich M. DNA hypomethylation and unusual chromosome instability in cell lines from ICF syndrome patients. Cytogenet Cell Genet. 2000;89(1-2):121-8.

Tyers M, Rachubinski RA, Stewart MI, Varrichio AM, Shorr RG, Haslam RJ, Harley CB. Molecular cloning and expression of the major protein kinase C substrate of platelets. Nature. 1988 Jun 2;333(6172):470-3.

Umbricht CB, Evron E, Gabrielson E, Ferguson A, Marks J, Sukumar S. Hypermethylation of 14-3-3 sigma (stratifin) is an early event in breast cancer. Oncogene. 2001 Jun 7;20(26):3348-53.

Van Itallie CM, Tietgens AJ, Aponte A, Fredriksson K, Fanning AS, Gucek M, Anderson JM. Biotin ligase tagging identifies proteins proximal to E-cadherin, including lipoma preferred partner, a regulator of epithelial cell-cell and cell-substrate adhesion. J Cell Sci. 2014 Feb 15;127(Pt 4):885-95.

Vassilev LT. 2004. Small-molecule antagonists of p53- MDM2 binding: Research tools and potential therapeutics. Cell Cycle 3: 419–421.

Vassilev LT. Cell cycle synchronization at the G2/M phase border by reversible inhibition of CDK1. Cell Cycle. 2006 Nov;5(22):2555-6.

Vaux, D. L., S. Cory, and J. M. Adams. 1988. Bcl-2 gene promotes haemopoietic cell survival and cooperates with c-myc to immortalize pre-B cells. Nature 335:440-442.

Vermeulen, Katrien, Dirk R. Van Bockstaele, and Zwi N. Berneman (2003) The Cell Cycle: A Review of Regulation, Deregulation and Therapeutic Targets in Cancer. Cell Proliferation 36 131-49.

Vitre BD, Cleveland DW. Centrosomes, chromosome instability (CIN) and aneuploidy. Curr Opin Cell Biol. 2012 Dec;24(6):809-15.

Vivanco, I., Sawyers, C.L. (2002). The Phosphoinositol-3-Kinase-AKT Pathway in Human Cancer. Nature Reviews. 2: 489-494

Wan PT, Garnett MJ, Roe SM, Lee S, Niculescu-Duvaz D, Good VM, Jones CM, Marshall CJ, Springer CJ, Barford D, Marais R; Cancer Genome Project.. Mechanism of activation of the RAF-ERK signaling pathway by oncogenic mutations of B-RAF. Cell. 2004 Mar 19;116(6):855-67.

Wang, B., H. Yang, Y. C. Liu, T. Jelinek, L. Zhang, E. Ruoslahti, and H. Fu. 1999. Isolation of high-affinity peptide antagonists of 14-3-3 proteins by phage display. Biochemistry 38:12499-12504.

Wasylishen, A. R., and L. Z. Penn. 2010. Myc: the beauty and the beast. Genes Cancer 1:532-541.

Welcker, M., Orian, A., Jin, J., Grim, J. A., Harper, J. W., Eisenman, R. N., and Clurman, B. E. (2004) The Fbw7 tumor suppressor regulates glycogen synthase kinase 3 phosphorylation-dependent c-Myc protein degradation. Proceedings of the National Academy of Sciences of the United States of America 101, 9085-9090

Weisenburger DD, Sanger WG, Armitage JO, Purtilo DT (1987) Intermediate lymphocytic lymphoma: immunophenotypic and cytogenetic findings. Blood 69, 1617.

Whitfield ML, Sherlock G, Saldanha AJ, Murray JI, Ball CA, Alexander KE, Matese JC, Perou CM, Hurt MM, Brown PO, Botstein D. (2002) Identification of genes periodically expressed in the human cell cycle and their expression in tumors. Mol Biol Cell. Jun;13(6):1977-2000.

Wiese KE, Walz S, von Eyss B, Wolf E, Athineos D, Sansom O, Eilers M. The role of MIZ-1 in MYC-dependent tumorigenesis. Cold Spring Harb Perspect Med. 2013 Dec 1;3(12):a014290.

Williams MR, Arthur JS, Balendran A, van der Kaay J, Poli V, Cohen P, Alessi DR. The role of 3-phosphoinositide-dependent protein kinase 1 in activating AGC kinases defined in embryonic stem cells. Curr Biol. 2000 Apr 20;10(8):439-48.

Wolfel T, Hauer M, Schneider J, Serrano M, Wolfel C, Klehmann HE, De Plaen E, Hankeln T, Meyerzum- Buschenfelde KH, Beach D (1995) A p16INK4a-insensitive CDK4 mutant targeted by cytolytic T lymphocytes in a human melanoma. Science 269, 1281.

Wolfer, A., and S. Ramaswamy. 2011. MYC and metastasis. Cancer Res 71:2034-2037.

Wolfer, A., B. S. Wittner, D. Irimia, R. J. Flavin, M. Lupien, R. N. Gunawardane, C. A. Meyer, E. S. Lightcap, P. Tamayo, J. P. Mesirov, X. S. Liu, T. Shioda, M. Toner, M. Loda, M. Brown, J. S. Brugge, and S. Ramaswamy. 2010. MYC regulation of a "poor-prognosis" metastatic cancer cell state. Proceedings of the National Academy of Sciences 107:3698-3703.

Wu, X., and A. J. Levine. 1994. p53 and E2F-1 cooperate to mediate apoptosis. Proceedings of the National Academy of Sciences of the United States of America 91:3602-3606.

Wu H, Thijssen PE, de Klerk E, Vonk KK, Wang J, den Hamer B, Aytekin C, van der Maarel SM, Daxinger L. Converging disease genes in ICF syndrome: ZBTB24 controls expression of CDCA7 in mammals. Hum Mol Genet. 2016 Sep 15;25(18):4041-4051

Wyllie AH, Rose KA, Morris RG, Steel CM, Foster E, Spandidos DA. Rodent fibroblast tumours expressing human myc and ras genes: growth, metastasis and endogenous oncogene expression. British Journal of Cancer. 1987;56(3):251-259.

Wymann M.P., Zvelebil M., Laffargue M., Phosphoinositide 3-kinase signaling-which way to target?, Trends Pharmacol. Sci., 24: 366-376, 2003

Yaffe MB, Rittinger K, Volinia S, Caron PR, Aitken A, Leffers H, Gamblin SJ, Smerdon SJ, Cantley LC. The structural basis for 14-3-3:phosphopeptide binding specificity. Cell. 1997 Dec 26;91(7):961-71.

Yamamoto H, Monden T, Miyoshi H, Izawa H, Ikeda K, Tsujie M, Ohnishi T, Sekimoto M, Tomita N, Monden M (1998) Cdk2/cdc2 expression in colon carcinogenesis and effects of cdk2/cdc2 inhibitor in colon cancer cells. Int. J. Oncol. 13, 233.

Yao R, Cooper GM. Requirement for phosphatidylinositol-3 kinase in the prevention of apoptosis by nerve growth factor. Science. 1995 Mar 31;267(5206):2003-6.

Yeh E, Cunningham M, Arnold H, Chasse D, Monteith T, Ivaldi G, Hahn WC, Stukenberg PT, Shenolikar S, Uchida T, Counter CM, Nevins JR, Means AR, Sears R. (2004) A signalling pathway controlling c-Myc degradation that impacts oncogenic transformation of human cells. Nat Cell Biol. Apr;6(4):308-18

Zhang XY, Pfeiffer HK, Mellert HS, Stanek TJ, Sussman RT, Kumari A, Yu D, Rigoutsos I, Thomas-Tikhonenko A, Seidel HE, et al. 2011. Inhibition of the single downstream target BAG-1 activates the latent apoptotic potential of MYC. Mol Cell Biol 31: 5037– 5045.

Zhou, B.-B. S. & Elledge, S. J. (2000) The DNA damage response: putting checkpoints in perspective. Nature 408, 433-439

Zhu,G. (2005) Exceptional disfavor for proline at the Pþ1 position among AGC and CAMK kinases establishes reciprocal specificity between them and the proline-directed kinases. J. Biol. Chem., 280, 10743–10748.

Zhu J, Blenis J, Yuan J. Activation of PI3K/Akt and MAPK pathways regulates Myc-mediated transcription by phosphorylating and promoting the degradation of Mad1. Proc Natl Acad Sci U S A. 2008 May 6;105(18):6584-9.

Zindy, F., C. M. Eischen, D. H. Randle, T. Kamijo, J. L. Cleveland, C. J. Sherr, and M. F. Roussel. 1998. Myc signaling via the ARF tumor suppressor regulates p53-dependent apoptosis and immortalization. Genes Dev 12:2424-2433.

Zundel, W., and A. Giaccia. 1998. Inhibition of the anti-apoptotic PI(3)K/Akt/Bad pathway by stress. Genes Dev 12:1941-1946.